

**Copyright**

**by**

**Aaron Paul Woods**

**2012**

The Thesis Committee for **Aaron Paul Woods**  
Certifies that this is the approved version of the following thesis:

**Double-Punch Test for Evaluating the Performance of  
Steel Fiber-Reinforced Concrete**

**APPROVED BY  
SUPERVISING COMMITTEE:**

---

James O. Jirsa, Supervisor

---

Richard E. Klingner

---

Oguzhan Bayrak

**Double-Punch Test for Evaluating the Performance of  
Steel Fiber-Reinforced Concrete**

by

**Aaron Paul Woods, B.S.C.E., B.S. Physics**

**Thesis**

Presented to the Faculty of the Graduate School of

The University of Texas at Austin

in Partial Fulfillment

of the Requirements

for the Degree of

**Master of Science in Engineering**

**The University of Texas at Austin**

**May 2012**

## **DEDICATION**

To my Lord and Savior Jesus Christ and to the glory of His name: For I am confident of this very thing, that He who began a good work in me will perfect it until the day of Christ Jesus

*Philippians 1:6*

## ACKNOWLEDGEMENTS

I would like to thank God for purchasing eternal life by sacrificing his only son Jesus Christ, saving me by his grace, and equipping me for every good work. Thank you Lord for granting me the opportunity to study at the esteemed University of Texas at Austin and for providing for my family spiritually, emotionally, and financially during this season.

My deepest thanks to my reinforcing system: To my beautiful wife (Tania) and incredible son (Elijah) for your patience, love, and support which motivated and comforted me in the most challenging moments. Tania, thank you for sharpening me, praying for me, and taking wonderful care of our home; you give me such an unfair advantage.

To my parents (Mom and Dad) and grandparents for teaching me what I could never learn in school: character and integrity; Thank you. To my brothers and sisters (Angela, Danielle, Joshua, Amanda, Timothy, and Johanna) for sharing me with others, and being understanding of the effects my studies have had on our relationships and time together.

To my Project 6348 teammates (Kiyeon, Umid), professors (Dr. Jirsa, Dr. Klingner, Dr. Bayrak), lab technicians (Eric, Blake, Dennis, Andrew), administrative staff (Barbara), and all the wonderful students who worked alongside me at the Ferguson Structural Engineering Laboratory as well as 18-B: Thank you. Dr. Jirsa, thank you for your mentorship, friendship, and kindness; it has been an honor to serve as one of your students. Thanks to TxDOT and the American Concrete Institute for your support of my endeavors.

I would like to extend a special thanks to my dear friend and brother in the Lord, Trevor Walker, for his commitment to the building of my faith while in graduate school together. Thank you for consistently reminding me of my purpose, investing in my spirit, and challenging me in the study of the Gospel. To those not mentioned formally: Thanks.

## ABSTRACT

### Double-Punch Test for Evaluating the Performance of Steel Fiber-Reinforced Concrete

Aaron Paul Woods, M.S.E.

The University of Texas at Austin, 2012

Supervisor: James O. Jirsa

The objective of this study is to develop test protocols for comparing the effectiveness of fiber-reinforced concrete (FRC) mixtures with high-performance steel fibers. Steel fibers can be added to fresh concrete to increase the tensile strength, ductility, and durability of concrete structures. In order to quantify steel fiber-reinforced concrete (SFRC) mixtures for field applications, a material test capable of predicting the performance of SFRC for field loading conditions is required. However, current test methods used to evaluate the structural properties of FRC (such as residual strength and toughness) are widely regarded as inadequate; a simple, accurate, and consistent test method is needed.

It was determined that the Double-Punch Test (DPT), originally introduced by Chen in 1970 for *plain concrete*, could be extended to *fiber-reinforced concrete* to satisfy this industry need. In the DPT, a concrete cylinder is placed vertically between the loading platens of the test machine and compressed by two steel punches located concentrically on the top and bottom surfaces of the cylinder. It is hypothesized that the Double-Punch Test is capable of comparing future fiber-reinforcement design options for use in structural applications, and is suitable for evaluating FRC in general.

The DPT Research and Testing Program was administered to produce sufficient within-laboratory data to make conclusions and recommendations regarding the simplicity, reliability, and reproducibility of the DPT for evaluating the performance of SFRC. Several variables (including fiber manufacturer, fiber content, and testing equipment) were evaluated to verify the relevance of the DPT for FRC. In this thesis, the results of 120 Double-Punch Tests are summarized and protocols for its effective application to fiber-reinforced concrete are recommended. Also, fundamental data is provided that indicates the DPT could be standardized by national and international agencies, such as the American Society of Testing and Materials (ASTM), as a method to evaluate the mechanical behavior of FRC.

This project is sponsored by the Texas Department of Transportation (TxDOT) through TxDOT Project 6348, *“Controlling Cracking in Prestressed Concrete Panels and Optimizing Bridge Deck Reinforcing Steel,”* which is aimed at improving bridge deck construction through developments in design details, durability, and quality control procedures.

## TABLE OF CONTENTS

<b>CHAPTER 1   INTRODUCTION</b>	<b>1</b>
1.1 Project Background .....	1
1.2 Motivation for Current Study .....	3
1.3 Research Objectives and Scope .....	6
1.4 Organization .....	7
<b>CHAPTER 2   LITERATURE REVIEW</b>	<b>8</b>
2.1 Composite Materials .....	8
2.1.1 History of Composites .....	8
2.2 Composite Structure .....	9
2.2.1 Matrix .....	13
2.2.2 Fibers .....	14
2.2.2.1 Fiber Types (Materials) .....	14
2.2.2.2 Fiber Geometry .....	15
2.2.2.3 Fiber Distribution & Orientation .....	17
2.2.2.4 Fiber Performance & Efficiency .....	18
2.2.3 Fiber-Matrix Interface .....	23
2.3 Fiber-Reinforced Concrete (FRC) .....	26
2.3.1 Overview of FRC .....	26
2.3.2 Production Technologies for FRC .....	27
2.3.3 Fracture Mechanics of FRC .....	28
2.3.4 Applications of FRC .....	29
2.3.4.1 Non-Structural Applications of FRC .....	30
2.3.4.2 Structural Applications of FRC .....	30
2.3.4.3 Repair & Rehabilitation Applications of FRC .....	32
2.3.5 Test Methods for FRC .....	33



<b>CHAPTER 3   STANDARD TEST METHODS FOR FRC</b>	<b>34</b>
3.1 Overview .....	34
3.1.1 ASTM C496: Standard Test Method for Splitting Tensile Strength of Cylindrical Concrete Specimens .....	36
3.1.2 ASTM C1609: Standard Test Method for Flexural Performance of Fiber-Reinforced Concrete (Using Beam with Third-Point Loading) .....	38
3.1.3 ASTM C1399: Standard Test Method for Obtaining Average Residual Strength of Fiber-Reinforced Concrete.....	44
3.1.4 ASTM C1550: Standard Test Method for Flexural Toughness of Fiber Reinforced Concrete (Using Centrally Loaded Round Panel) .....	50
3.1.5 Other Test Methods Proposed for Determination of the Toughness of FRC.....	56
3.1.5.1 EFNARC Panel Tests (Using Square Panel).....	56
3.1.5.2 Uniaxial Direct Tensile Test .....	57
3.2 Summary of Limitations of Existing Test Methods for FRC .....	61
3.2.1 Simplicity.....	61
3.2.2 Reliability.....	61
3.2.3 Reproducibility.....	62
3.3 Side-by-Side Comparison of Current Test Methods .....	62
3.4 Research Significance .....	65
<b>CHAPTER 4   DOUBLE-PUNCH TEST (DPT)</b>	<b>66</b>
4.1 Introduction.....	66
4.1.1 Theory and Mechanics of the Double-Punch Test .....	67
4.2 Extension of the Double-Punch Test to Evaluate the Mechanical Properties of FRC .....	71
4.2.1 Test Setup & Procedure.....	71
4.2.2 Cracking & Damage .....	72
4.2.3 Correlation with FRC Structure .....	75
4.3 Summary.....	77

<b>CHAPTER 5   DPT RESEARCH AND TESTING PROGRAM OUTLINE</b>	<b>78</b>
5.1 Introduction.....	78
5.2 DPT Program Organization.....	78
5.2.1 Nomenclature used to Identify Test Specimens .....	79
5.3 DPT Program Materials.....	80
5.3.1 Steel Fibers.....	80
5.3.2 Concrete Mix Design & Procedure.....	82
5.3.3 Specimen Preparation .....	87
5.4 DPT Program Testing.....	92
5.4.1 Test Setup & Equipment.....	92
5.4.2 Testing Procedure for DPT .....	95
5.4.3 Calculation of Key Test Parameters .....	98
<b>CHAPTER 6   DPT RESEARCH AND TESTING PROGRAM RESULTS</b>	<b>101</b>
6.1 Overview of Results .....	101
6.2 DPT Phase 1 Results.....	101
6.2.1 Discussion of Results .....	103
6.3 DPT Phase 2 Results.....	104
6.3.1 Discussion of Results .....	106
6.4 Combined Results.....	106
6.4.1 Discussion of Results .....	109
6.5 DPT Statistical Analysis .....	110
6.5.1 Analyzing the Effects of Fiber Type & Volume Fraction.....	111
6.5.1.1 Analysis Summary .....	114
6.5.2 Analyzing the Effects of Surface Preparation .....	116
6.5.2.1 Analysis Summary .....	118
6.5.3 Analyzing the Effects of Test Machine.....	121
6.5.3.1 Analysis Summary .....	126
6.5.4 Analyzing the Effects of Cylinder Portion (Casting).....	127

6.5.4.1	Analysis Summary .....	130
<b>CHAPTER 7</b>	<b>  CONCLUSIONS &amp; RECOMMENDATIONS</b>	<b>133</b>
7.1	Research Summary.....	133
7.2	Conclusions.....	133
7.2.1	Simplicity of the DPT .....	134
7.2.2	Reliability of the DPT .....	134
7.2.3	Reproducibility of the DPT .....	135
7.3	Recommendations .....	137
7.3.1	Recommended DPT Protocols for Effective Application to FRC.....	137
7.3.2	Recommendations for Future Research.....	138
<b>APPENDIX A</b>	<b>  DPT PERFORMANCE CURVES</b>	<b>139</b>
A.1	DPT Performance Curves for Phase 1 Testing.....	139
A.2	DPT Performance Curves for Phase 2 Testing.....	146
<b>APPENDIX B</b>	<b>  STATISTICAL ANALYSIS OF KEY DPT PARAMETERS</b>	<b>153</b>
B.1	Analyzing the Effects of Fiber Type & Volume Fraction .....	153
B.2	Analyzing the Effects of Specimen Surface Preparation .....	160
B.3	Analyzing the Effects of Test Machine .....	167
B.4	Analyzing the Effects of Cylinder Portion (Casting).....	174
<b>APPENDIX C</b>	<b>  ASTM STANDARDIZATION OF DOUBLE-PUNCH TEST</b>	<b>181</b>
C.1	ASTM Standardization Process .....	181
C.2	ASTM Draft Ballot for Standardization of Double-Punch Test .....	182
	<b>REFERENCES</b>	<b>189</b>
	<b>VITA</b>	<b>193</b>

## LIST OF TABLES

Table 2-1: Typical Fiber Types and Properties (Bentur and Mindess 2007) .....	15
Table 2-2: Pull-out Bond Stresses for Steel Fibers with Different Aspect Ratios and Deformed Geometries – modified from (Maage 1978).....	16
Table 3-1: Test Specimens Required for Current FRC Testing Procedures .....	63
Table 3-2: Simplicity, Reliability, and Reproducibility of Current FRC Testing Procedures..	64
Table 4-1: Tensile Strength Computed from Double-Punch Tests on Plain Concrete Cylinders – modified from (W. Chen 1970).....	70
Table 4-2: Comparison of the Specific Failure Surface of Test Specimens for Current FRC Test Methods vs. Double-Punch Test .....	76
Table 5-1: Concrete Mixture Proportions .....	82
Table 5-2: (a) Batch Quantities and (b) Fresh and Hardened Concrete Properties of SFRC Mixtures used in DPT Experiments.....	87
Table 6-1: Phase 1 – Royal Fibers .....	102
Table 6-2: Phase 2 – Bekaert Fibers .....	104
Table 6-3: Comparison between Initial Slopes from DPT and Calibration Test .....	125
Table 7-1: Simplicity, Reliability, and Reproducibility of Current FRC Testing Procedures vs. Double-Punch Test.....	136
Table B-1: Analyzing the Effects of Fiber Type & Volume Fraction on the Initial Slope ...	154
Table B-2: Analyzing the Effects of Fiber Type & Volume Fraction on the Peak Load.....	156
Table B-3: Analyzing the Effects of Fiber Type & Volume Fraction on the Residual Strength.....	158
Table B-4: Analyzing the Effects of Surface Preparation on the Initial Slope.....	161
Table B-5: Analyzing the Effects of Surface Preparation on the Peak Load.....	163
Table B-6: Analyzing the Effects of Surface Preparation on the Residual Strength.....	165
Table B-7: Analyzing the Effects of Test Machine on the Initial Slope .....	168

Table B-8: Analyzing the Effects of Test Machine on the Peak Load.....	170
Table B-9: Analyzing the Effects of Test Machine on the Residual Strength.....	172
Table B-10: Analyzing the Effects of Cylinder Portion (Casting) on the Initial Slope.....	175
Table B-11: Analyzing the Effects of Cylinder Portion (Casting) on the Peak Load .....	177
Table B-12: Analyzing the Effects of Cylinder Portion (Casting) on the Residual Strength.....	179

## LIST OF FIGURES

Figure 1-1: Tensile Stress Rings in Concrete (Tepfers 1973).....	2
Figure 1-2: Schematic of Double-Punch Test (W. Chen 1970) .....	4
Figure 1-3: Similarity between Loading Conditions at (a) End of PCPs (Tepfers 1973) and (b) Double-Punch Test [specimen rotated on its side] (W. Chen 1970).....	5
Figure 2-1: Hill and Ziggurat at Aqar-Quf (MKTJ 2009) .....	8
Figure 2-2: Schematic of Continuous and Aligned Fiber Orientation with Longitudinal and Transverse Loading Directions .....	11
Figure 2-3: Rule of Mixtures Approach for Estimating the Modulus of Elasticity of a Composite – modified from (Callister 2003).....	12
Figure 2-4: Fiber Orientations in Fiber-Reinforced Composites.....	13
Figure 2-5: Commonly Available Deformed Steel Fiber (Bentur and Mindess 2007).....	16
Figure 2-6: Non-uniform Distribution and “Balling” of Steel Fibers in Cement Matrix as Observed by X-ray (not to scale) – modified from (Stroeven and Shah 1978)....	17
Figure 2-7: Stress-Position Profiles when Fiber Length is (a) less than, (b) equal to, and (c) greater than the Critical Length for a FRC Composite that is Subjected to a Tensile Stress Equal to the Fiber Tensile Strength, $\sigma_f^*$ (Callister 2003) .....	20
Figure 2-8: The Intersection of an Oriented Fiber with a Crack Assuming (a) Uniform Fiber Orientation across the crack, and (b) Local Fiber Bending Around the Crack (Bentur and Mindess 2007).....	21
Figure 2-9: Effect of Fiber Orientation on the Pull-out Strength of Ductile Fibers (polypropylene and steel) and Brittle Carbon Fibers (De Vekey and Majumdar 1968).....	22
Figure 2-10: Idealized Representation of an Advancing Crack in Fiber-Reinforced Concrete (Wecharatana and Shah 1983).....	23
Figure 2-11: Deformation Pattern in the Matrix Surrounding a Fiber Subjected to Tensile Load – modified from (Callister 2003).....	24
Figure 2-12: Schematic of Cracking and Debonding in the Porous Layer of the ITZ for a SFRC – modified from (Bentur and Mindess 1985) .....	24

Figure 2-13: Interfacial Shear Stress Distribution along a Fiber Intersecting a Crack Immediately After Cracking: (a) Debonding Preceded Cracking, Weak Bond; (b) No Debonding Prior to Cracking, Strong Bond – modified from (Bentur and Mindess 2007).....	25
Figure 2-14: Comparison of Typical Stress-Strain Response in Tension of (a) Conventional FRC and (b) High Performance FRC (Bentur and Mindess 2007).....	29
Figure 2-15: Schematic of (a) Stand Alone, (b) Combination, and (c) Repair Applications for HPFRCC (Ramakrishnan 1987).....	31
Figure 2-16: Stress-Deflection Response of SIFCON, Conventional FRC, and Plain Concrete (A. Naaman 1992).....	32
Figure 3-1: Test Specimen Positioned in (a) Jig for Aligning Cylinder and Bearing Strips and (b) in Testing Machine for Determination of Splitting Tensile Strength (ASTM C496 2011).....	36
Figure 3-2: Beam with Three-Point Loading Test Setup (ASTM C1609 2010).....	39
Figure 3-3: Schematic of Japanese Yoke Loading System (Chen and Mindess 1995).....	39
Figure 3-4: Test Arrangement to Obtain Net Deflection via Japanese Yoke Loading System (ASTM C1609 2010).....	40
Figure 3-5: Variability of ASTM C1609 for Replicate Specimens in the (a) Load vs. Deflection Curves and (b) Location of Major Cracks (S.-H. Chao 2011).....	43
Figure 3-6: Schematic of Apparatus with Stainless Steel Plate and Suitable Support Frame (ASTM C1399 2010).....	44
Figure 3-7: Typical Load-Deflection Curve (ASTM C1399 2010).....	45
Figure 3-8: Schematic of Specimen Cross Sections to Indicate Permitted Flexural Tensile Surfaces during Testing (ASTM C1399 2010).....	48
Figure 3-9: Effect of Steel Plate on Determining Performance Immediately After First Crack – adapted from (ASTM C1399 2010).....	49
Figure 3-10: Testing Arrangement using Suggested Round Panel Support Fixture (ASTM C1550 2010).....	51
Figure 3-11: Rolling Steel Form after Molded Specimen Has Gained Sufficient Strength (ASTM C1550 2010).....	51
Figure 3-12: Manual Spraying of Shotcrete Panels (ASTM C1550 2010).....	52

Figure 3-13: (a) Profile and (b) Plan Views of Suggested Method of Deflection Measurement to Exclude Load-Train Deformations Using an LVDT .....	53
Figure 3-14: View from (a) Below and (b) Above Tested Round Panel Specimen Showing Location of Major Cracks (S.-H. Chao 2011) .....	54
Figure 3-15: View of Underside of ASTM C1550 Test Specimen showing Crack Width vs. LVDT Probe Width at Location of LVDT (S.-H. Chao 2011).....	55
Figure 3-16: Setup for EFNARC Panel Test (EFNARC 1996).....	57
Figure 3-17: Uniaxial Direct Tensile Test Specimen Dimensions (S.-H. Chao 2011) .....	58
Figure 3-18: Uniaxial Direct Tensile Test (a) Mold and (b) Testing Arrangement (S.-H. Chao 2011) .....	59
Figure 3-19: Replicate Specimen Results for Uniaxial Direct Tensile Test (S.-H. Chao 2011).....	60
Figure 3-20: Variability of Uniaxial Tensile Test in Location of Major Cracks for Four Replicate Specimens with 1.5% Fiber Content (S.-H. Chao 2011).....	60
Figure 3-21: Graphical Comparison of Specimen Weights for Current FRC Testing Procedures .....	63
Figure 4-1: Apparatus (W. Chen 1970) and Loading Schematic (Marti 1989) for the Double-Punch Test .....	67
Figure 4-2: Modified Mohr-Coulomb Criterion for Concrete (W. Chen 1970) .....	68
Figure 4-3: Bearing Capacity of a Double-Punch Test (W. Chen 1970).....	69
Figure 4-4: Two Possible DPT Collapse Mechanisms with (a) Three and (b) Four Radial Fracture Planes (Pros, Diez and Molins 2010) .....	73
Figure 4-5: Damage Profiles for (a) Split-Cylinder Test and (b) Double-Punch Test Loading on Plain Concrete Cylinders (Pros, Diez and Molins 2010) .....	74
Figure 4-6: Comparison of Test Specimen Weights for Current FRC Testing Procedures vs. Double-Punch Test .....	77
Figure 5-1: Testing Matrix for DPT Research and Testing Program.....	79
Figure 5-2: Nomenclature used to Identify Specimens for DPT Research and Testing Program.....	80



Figure 5-3: Royal™ Steel Fibers .....	80
Figure 5-4: Bekaert Dramix® Steel Fibers .....	81
Figure 5-5: Royal vs. Bekaert Fiber Type .....	81
Figure 5-6: SFRC Mixing Sequence, Step 2.....	83
Figure 5-7: SFRC Mixing Sequence, Step 3.....	84
Figure 5-8: SFRC Mixing Sequence, Step 4.....	84
Figure 5-9: SFRC Mixing Sequence, Step 5.....	85
Figure 5-10: Example of “Clumping” and “Balling” of Fibers Observed During Mixing .....	85
Figure 5-11: SFRC Mixing Sequence, Step 6 .....	85
Figure 5-12: SFRC Mixing Sequence, Step 7 .....	86
Figure 5-13: SFRC Mixing Sequence, Step 8 .....	86
Figure 5-14: Using Wet-Saw to Cut 6 x 12-in. Cylinder in Half .....	88
Figure 5-15: Schematic showing Surface Roughness on Top and Bottom Surfaces of Cylinder due to Mold .....	89
Figure 5-16: Surface-Grinding (SG) Uneven Faces of Test Specimens.....	90
Figure 5-17: Process of Applying Hydro-Stone to Rough Faces of Test Specimen.....	91
Figure 5-18: Schematic of DPT Arrangement on 60-kip Baldwin UTM (Hydraulic) .....	93
Figure 5-19: DPT Setup on 60-kip Baldwin UTM (Hydraulic).....	93
Figure 5-20: Schematic of DPT Arrangement on 120-kip Olsen UTM (Screw-Type).....	94
Figure 5-21: DPT Setup on 120-kip Olsen UTM (Screw-Type).....	94
Figure 5-22: Effect of Misaligned Steel Punches in DPT shown (a) Schematically and (b) for Trial Specimen .....	95
Figure 5-23: Steel Punch Centering Guide and Masking Tape Used to Secure Against Eccentric Loading Effects .....	96
Figure 5-24: Schematic of Shakedown Procedure for DPT Experiments .....	97

Figure 5-25: Typical DPT Performance Curve showing Key Test Parameters .....	99
Figure 6-1: Phase 1 - Selected DPT Performance Curves for Royal Fibers on Baldwin Machine .....	102
Figure 6-2: Phase 1 - Selected DPT Performance Curves for Royal Fibers on Olsen Machine .....	103
Figure 6-3: Phase 1 - Typical Damage and Cracking Pattern of DPT Specimens with Royal Fibers .....	103
Figure 6-4: Phase 2 - Selected DPT Performance Curves for Bekaert Fibers on Baldwin Machine .....	105
Figure 6-5: Phase 2 - Selected DPT Performance Curves for Bekaert Fibers on Olsen Machine .....	105
Figure 6-6: Phase 2 - Typical Damage and Cracking Pattern of DPT Specimens with Bekaert Fibers .....	106
Figure 6-7: Combined Results - Selected DPT Performance Curves showing Effect of Fiber Type and Volume Fraction at 0.75% Fiber Content.....	107
Figure 6-8: Combined Results - Selected DPT Performance Curves showing Effect of Fiber Type and Volume Fraction at 1.00% Fiber Content.....	107
Figure 6-9: Combined Results - Selected DPT Performance Curves showing Effect of Fiber Type and Volume Fraction at 1.50% Fiber Content.....	108
Figure 6-10: Effect of Fiber Type and Volume Fraction on Crack Widths and Cracking Pattern .....	109
Figure 6-11: Effect of Fiber Type and Volume Fraction on (a) Coefficient of Variation and (b) Average Value of Initial Slope .....	112
Figure 6-12: Effect of Fiber Type and Volume Fraction on (a) Coefficient of Variation and (b) Average Value of Peak Load.....	113
Figure 6-13: Effect of Fiber Type and Volume Fraction on (a) Coefficient of Variation and (b) Average Value of Residual Strength.....	114
Figure 6-14: Effect of Surface Preparation on (a) Coefficient of Variation and (b) Average Value of Initial Slope for Royal Fiber Type.....	116
Figure 6-15: Effect of Surface Preparation on (a) Coefficient of Variation and (b) Average Value of Peak Load for Royal Fiber Type .....	117

Figure 6-16: Effect of Surface Preparation on (a) Coefficient of Variation and (b) Average Value of Residual Strength for Royal Fiber Type.....	118
Figure 6-17: DPT Performance Curves showing Effect of Surface Preparation on Initial Slope Parameter.....	119
Figure 6-18: Effect of Test Machine on (a) Coefficient of Variation and (b) Average Value of Initial Slope for Bekaert Fiber Type .....	121
Figure 6-19: Effect of Test Machine on (a) Coefficient of Variation and (b) Average Value of Peak Load for Bekaert Fiber Type.....	122
Figure 6-20: Effect of Test Machine on (a) Coefficient of Variation and (b) Average Value of Residual Strength for Bekaert Fiber Type.....	123
Figure 6-21: Calibration Setup for Baldwin (left) and Olsen (right) UTMs .....	124
Figure 6-22: Tangent Stiffness Calibration Curves .....	125
Figure 6-23: Effect of Cylinder Portion (Casting) on (a) Coefficient of Variation and (b) Average Value of Initial Slope for Bekaert Fiber Type.....	128
Figure 6-24: Effect of Cylinder Portion (Casting) on (a) Coefficient of Variation and (b) Average Value of Peak Load for Bekaert Fiber Type .....	129
Figure 6-25: Effect of Cylinder Portion (Casting) on (a) Coefficient of Variation and (b) Average Value of Residual Strength for Bekaert Fiber Type.....	130
Figure 6-26: Effect of Casting on (a) the Fiber Distribution and (b) the Number of Fibers Crossing Crack Planes in Top and Bottom Test Specimens.....	132
Figure A-1: DPT Performance Curves for Phase 1 - Royal Fibers @ 0.75% Fiber Volume Fraction Tested on Baldwin Machine.....	140
Figure A-2: DPT Performance Curves for Phase 1 - Royal Fibers @ 0.75% Fiber Volume Fraction Tested on Olsen Machine.....	141
Figure A-3: DPT Performance Curves for Phase 1 - Royal Fibers @ 1.00% Fiber Volume Fraction Tested on Baldwin Machine.....	142
Figure A-4: DPT Performance Curves for Phase 1 - Royal Fibers @ 1.00% Fiber Volume Fraction Tested on Olsen Machine.....	143
Figure A-5: DPT Performance Curves for Phase 1 - Royal Fibers @ 1.50% Fiber Volume Fraction Tested on Baldwin Machine.....	144

Figure A-6: DPT Performance Curves for Phase 1 - Royal Fibers @ 1.50% Fiber Volume Fraction Tested on Olsen Machine.....	145
Figure A-7: DPT Performance Curves for Phase 2 – Bekaert Fibers @ 0.75% Fiber Volume Fraction Tested on Baldwin Machine.....	147
Figure A-8: DPT Performance Curves for Phase 2 – Bekaert Fibers @ 0.75% Fiber Volume Fraction Tested on Olsen Machine.....	148
Figure A-9: DPT Performance Curves for Phase 2 – Bekaert Fibers @ 1.00% Fiber Volume Fraction Tested on Baldwin Machine.....	149
Figure A-10: DPT Performance Curves for Phase 2 – Bekaert Fibers @ 1.00% Fiber Volume Fraction Tested on Olsen Machine.....	150
Figure A-11: DPT Performance Curves for Phase 2 – Bekaert Fibers @ 1.50% Fiber Volume Fraction Tested on Baldwin Machine.....	151
Figure A-12: DPT Performance Curves for Phase 2 – Bekaert Fibers @ 1.50% Fiber Volume Fraction Tested on Olsen Machine.....	152
Figure B-1: Effect of Fiber Type & Volume Fraction on the Coefficient of Variation and Average Value of Initial Slope.....	155
Figure B-2: Effect of Fiber Type & Volume Fraction on the Coefficient of Variation and Average Value of Peak Load .....	157
Figure B-3: Effect of Fiber Type & Volume Fraction on the Coefficient of Variation and Average Value of Residual Strength.....	159
Figure B-4: Effect of Surface Preparation on the Coefficient of Variation and Average Value of Initial Slope .....	162
Figure B-5: Effect of Surface Preparation on the Coefficient of Variation and Average Value of Peak Load.....	164
Figure B-6: Effect of Surface Preparation on the Coefficient of Variation and Average Value of Residual Strength .....	166
Figure B-7: Effect of Test Machine on the Coefficient of Variation and Average Value of Initial Slope .....	169
Figure B-8: Effect of Test Machine on the Coefficient of Variation and Average Value of Peak Load.....	171

Figure B-9: Effect of Test Machine on the Coefficient of Variation and Average Value of Residual Strength.....	173
Figure B-10: Effect of Cylinder Portion (Casting) on the Coefficient of Variation and Average Value of Initial Slope.....	176
Figure B-11: Effect of Cylinder Portion (Casting) on the Coefficient of Variation and Average Value of Peak Load .....	178
Figure B-12: Effect of Cylinder Portion (Casting) on the Coefficient of Variation and Average Value of Residual Strength.....	180

# CHAPTER 1

## INTRODUCTION

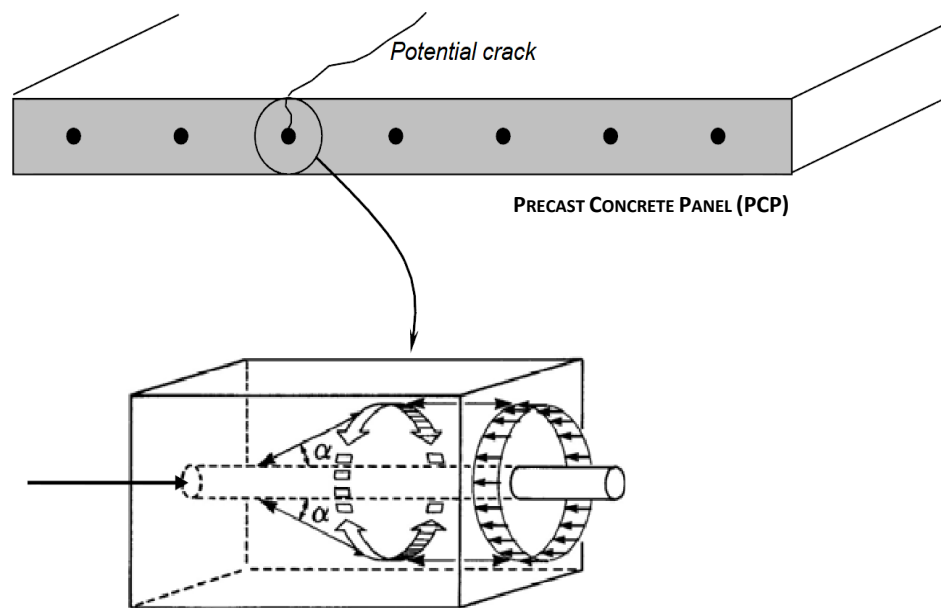
### 1.1 PROJECT BACKGROUND

The objective of this study was to develop test protocols for comparing the effectiveness of fiber-reinforced concrete (FRC) mixtures with high-performance steel fibers. Steel fibers can be added to the fresh concrete during mixing and, upon hardening, can increase the tensile strength, ductility, and durability of concrete. The current study is part of a larger research project conducted at the University of Texas at Austin (UT Austin) and the University of Texas at Arlington (UT Arlington) under the sponsorship of the Texas Department of Transportation (TxDOT) through TxDOT Project 6348, *“Controlling Cracking in Prestressed Concrete Panels and Optimizing Bridge Deck Reinforcing Steel.”* The project is aimed at improving construction and reducing the cost of bridge decks through developments in design details, durability, and quality control procedures.

For example, precast concrete panels (PCPs) are used in approximately 85% of all bridges in Texas (Merrill 2002). Bridge decks containing PCPs can be built very efficiently, because the panels act as stay-in-place formwork and serve as the bottom portion of the final bridge deck. However, nearly 200,000 square feet of PCPs are rejected every year due to cracking, which can result from a combination of tensile stresses at release, handling at the precast yard, or transportation to the job site (Foreman 2010). One research objective is to reduce collinear cracking (cracking parallel to the prestressed strands) in PCPs.

As shown in Figure 1-1, at prestress transfer, the concrete surrounding the strands is placed in circumferential (hoop) tension as the highly tensioned strands transfer the prestressing force into the concrete (Tepfers 1973). As the concrete is compressed along the

strands, bursting effects are being resisted by circumferential tension in the concrete. This is particularly critical at the ends of the panels due to the Hoyer effect (decrease in diameter of the strands due to Poisson's ratio), and over the transfer length of the strands due to the complex nature of the stress state there. In order to reduce the bursting effect and cracking potential of PCPs, various reinforcement alternatives were evaluated to provide TxDOT with optimized bridge deck design details.



*Figure 1-1: Tensile Stress Rings in Concrete (Tepfers 1973)*

Previous research indicated that actual prestress losses in PCPs are considerably less than losses estimated by code equations. Thus, it was suggested that a lower initial prestress force could be used to compensate for the overestimation of losses, and directly reduce the tensile stress transferred to the panel ends (Foreman 2010). This recommendation was employed for the first reinforcement option, in which the initial prestress force is reduced from 16.1 to 14.4 kips per strand. Secondly, because significant bursting and cracking have

been observed at the ends of PCPs, a reinforcement detail that included additional transverse rebar at the panel ends was also evaluated. PCPs fabricated at two Texas precast plants (with these reinforcement options) were instrumented in the field and transported to the Ferguson Structural Engineering Laboratory (FSEL). Multiple sets of PCPs were monitored at FSEL to determine long-term prestress losses and cracking potential (Foreman 2010, Azimov 2012).

## **1.2 MOTIVATION FOR CURRENT STUDY**

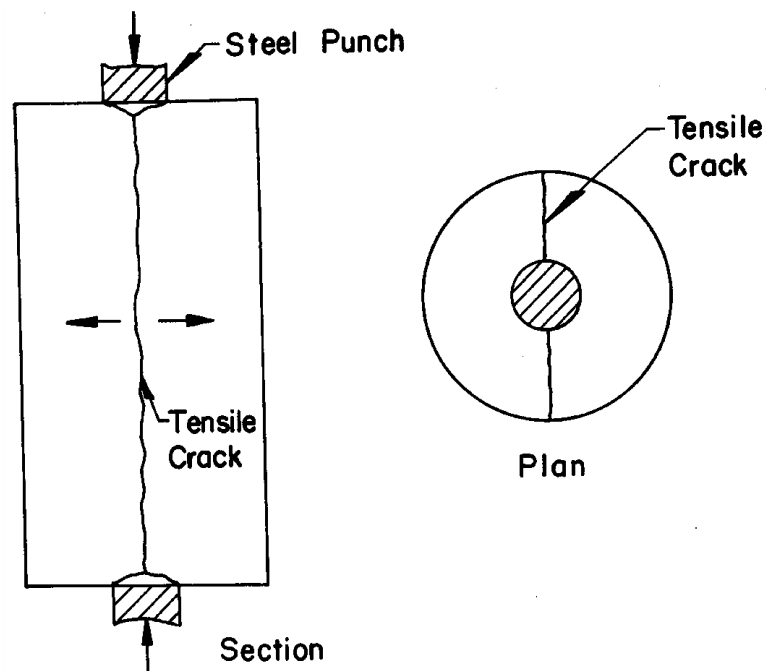
In addition to PCP experiments, reinforcement options for the cast-in-place (CIP) portion of the bridge deck were also evaluated. These “top-mat” reinforcement options included: (1) reductions in deformed-bar reinforcement; and (2) complete replacement of deformed-bar reinforcement with welded-wire fabric (Foster 2010). These designs were considered due to their potential to reduce the cost and expedite the construction of bridge decks. In addition to options with budget and labor incentives, a series of material tests on steel fiber-reinforced concrete (SFRC) specimens were proposed by UT Austin and UT Arlington to determine the feasibility of using SFRC in bridge deck applications. The purpose was to quantify the mix compositions, fiber types, and fiber dosages that could be used to enhance the durability and extend the service life of bridge decks by controlling cracking.

However, in order to quantify steel fiber-reinforced concrete mixtures for both CIP and PCP bridge deck applications, a material test capable of predicting the performance of SFRC for field loading conditions is first necessary. As previously stated, the PCPs are subjected to end bursting stresses while the CIP topping is typically stressed in tension resulting from temperature changes in the concrete, concrete shrinkage, and loading from self-weight and traffic (Foster 2010). Many standardized and non-standard material tests are



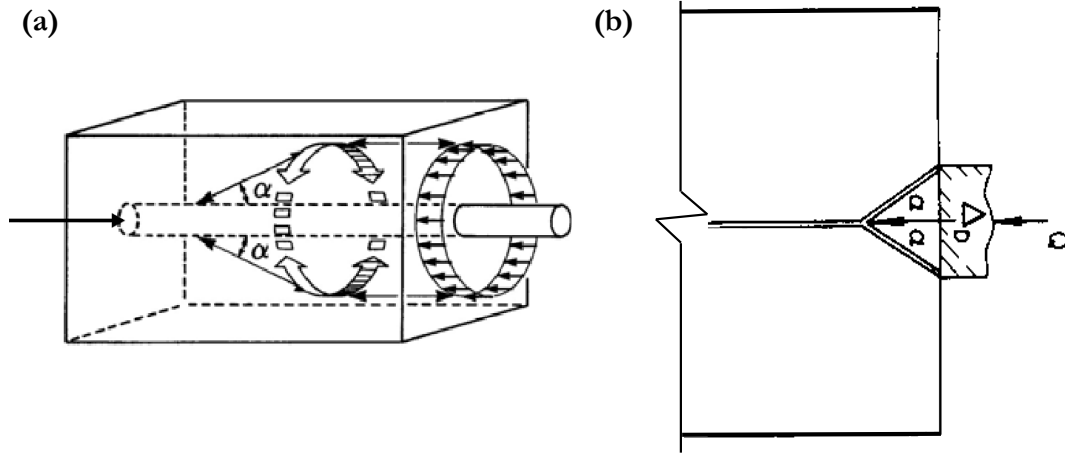
currently in place to evaluate the performance characteristics of fiber-reinforced concrete composites. However, these methods are not only unrepresentative of the loading conditions observed in bridge decks, but also widely regarded as inadequate (Bentur and Mindess 2007). Various attempts have been made to quantify load-deflection curves for FRC in terms of a parameter that could be used to compare different fiber types, as well as for specifications and quality control.

Following an extensive literature review of test methods used for concrete, it was determined that the Double-Punch Test (DPT), originally introduced by Chen in 1970 for *plain concrete*, could be extended to evaluate the behavior of *fiber-reinforced concrete* composites. As shown in Figure 1-2, in the Double-Punch Test, a concrete cylinder is placed vertically between the loading platens of the test machine and compressed by two steel punches located concentrically on the top and bottom surfaces of the cylinder (W. Chen 1970).



*Figure 1-2: Schematic of Double-Punch Test (W. Chen 1970)*

The DPT loading results in indirect tension along radial planes of the cylinder specimen. As seen in Figure 1-3 this stress state closely resembles the loading conditions observed at the ends of PCPs and within the CIP topping. This observation led Study 6348 researchers to investigate the validity of the Double-Punch Test for evaluating fiber-reinforced concrete.



**Figure 1-3: Similarity between Loading Conditions at (a) End of PCPs (Tepfers 1973) and (b) Double-Punch Test [specimen rotated on its side] (W. Chen 1970)**

Studies at two laboratories, UT Austin and UT Arlington, demonstrated that the DPT was repeatable within a laboratory and reproducible from one laboratory to another. The results from these tests indicated that the DPT is a quick and effective way to compare the behavior of FRC with different types of high-performance steel fibers. This led to further interest in the DPT and the factors that both positively and negatively impact its application to FRC. Research at UT Austin is focused on evaluating several variables (including fiber manufacturer, fiber volume fraction, specimen surface preparation, and testing equipment) to verify the relevance of the DPT for FRC.

### 1.3 RESEARCH OBJECTIVES AND SCOPE

It is hypothesized that the DPT is capable of comparing future fiber-reinforcement options for use in bridge deck construction. Moreover, it is believed that the DPT is an appropriate test method for evaluating FRC in general. It is possible that the Double-Punch Test may characterize the elastic and inelastic behavior (toughness) of fiber-reinforced concrete composites better than current testing procedures for FRC. The objectives of this portion of Study 6348 that are related to FRC are to:

1. Quantify the influence of mix compositions, fiber types, and fiber volume fractions on the mechanical characteristics of FRC;
2. Develop test protocols for comparing the effectiveness of steel fiber-reinforced concrete mixtures with different fiber types and volume fractions;
3. Supply intra- and inter-laboratory data and observations useful for comparing the Double-Punch Test with current test methods for FRC.

The central focus of the experiments described here is to produce sufficient within-batch, intra-laboratory data to make conclusions and recommendations regarding the simplicity, reliability, and reproducibility of the Double-Punch Test for evaluating the performance of steel fiber-reinforced concrete. In this thesis, trends in the Double-Punch Test are summarized, and protocols for its effective application to FRC are recommended. This report also provides fundamental data indicating that the DPT could be standardized by national and international agencies, such as the American Society of Testing and Materials (ASTM), as a method to evaluate the mechanical behavior of steel fiber-reinforced concrete.

Additional DPT experiments were conducted by researchers at UT Arlington, but are not summarized in this thesis.

## 1.4 ORGANIZATION

The details of the work completed in this two-year study are presented in the following chapters. A literature review of composite materials and fiber-reinforced concrete is provided in Chapter 2. The advantages and disadvantages of standardized (and non-standard) test methods currently used to evaluate the behavior of FRC are summarized in Chapter 3. Additional background regarding the theory and mechanics of the Double-Punch Test is given in Chapter 4. The two-phase DPT Research and Testing Program is described in detail in Chapter 5. Individual phase and combined results from the experimental program are presented in Chapter 6. Finally, conclusions and recommendations summarizing the findings of this research are stated in Chapter 7.

*Note 1-1: The DPT Research and Testing Program is meant to evaluate the DPT method. It is **not intended** to compare the performance of the different fibers used in this study. Royal™ and Bekaert Dramix® fibers were chosen arbitrarily to determine the ability of the Double-Punch Test to distinguish between FRC composed of different fiber types and volume fractions.*

## CHAPTER 2

### LITERATURE REVIEW

#### 2.1 COMPOSITE MATERIALS

##### 2.1.1 History of Composites

The earliest engineers and material scientists discovered, developed, and industrialized composite materials. The use of fibers to strengthen materials that are significantly weaker in tension than in compression can be traced back to ancient times. Possibly the oldest written account of such a composite material, composed of clay bricks reinforced with straw, is recorded in the Bible:

*<sup>6</sup>That same day Pharaoh sent this order to the Egyptian slave drivers and the Israelite foremen:*

*<sup>7</sup>“Do not supply any more straw for making bricks. Make the people get it themselves!”*

*Exodus 5:6-7 (Zondervan 2002)*

At about that same time, approximately 3500 years ago, sunbaked bricks reinforced with straw were used to build the 170-ft high hill of Aqar-Quf near present day Bagdad (MKTJ 2009). The ziggurat, which still stands today, is pictured in Figure 2-1.



*Figure 2-1: Hill and Ziggurat at Aqar-Quf (MKTJ 2009)*

Historical structures like the ziggurat inspired the use of other composite materials. The first widely used manufactured composite in modern times was asbestos cement, which was developed in about 1900 with the invention of the Hatschek process (Bentur and Mindess 2007). Ludwig Hatschek made the first asbestos reinforced cement products, using a paper-making sieve cylinder machine. The machine took a diluted slurry of about 10% asbestos fibers and 90% ordinary Portland cement (by weight of solids), and dewatered it into thin films of about 0.3 mm. The films were then wound up to a desired thickness (typically 3-6 mm) on a roll, and the resultant cylindrical sheet was cut and flattened to form a flat laminated sheet. Finally, the sheet was cut into rectangular pieces of the desired size (Frangky 2010, Cooke 2002).

For over 100 years, this form of fiber cement found extensive use for roofing, pipe, and cladding products. Due to its great thermal stability, asbestos cement was also used in many applications requiring high fire resistance (Frangky 2010). Now, fibers of various kinds are used to reinforce a number of different materials, such as epoxies, plastics, and ceramics. This thesis focuses on the use of fiber reinforcement in materials made with hydraulic cement binders.

## **2.2 COMPOSITE STRUCTURE**

Generally speaking, a composite is defined as any solid material system consisting of two or more phases, with macroscopically distinguishable phase boundaries, which achieves properties not attainable by any single component or by simple summation (Bentur and Mindess 2007). Many of our modern-day technologies require materials with unique combinations of properties achievable, for particular applications, only through the use of composite materials. In designing composite materials, scientists and engineers have cleverly combined various metals, ceramics, and polymers to produce a new generation of materials

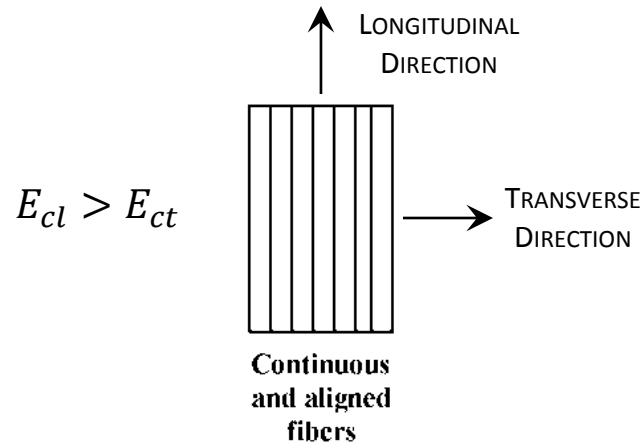
that improve one or more mechanical characteristics such as stiffness, toughness, or high-temperature strength.

The vast majority of composites are composed of two phases: the *matrix phase*, which is generally soft and ductile; and the *fiber* or *dispersed phase*, which is generally strong and brittle. In certain composites, such as fiber-reinforced concrete (FRC), the matrix and fiber phases have the opposite roles. In any case, the overall properties of the composite are most dependent on the following (Bentur and Mindess 2007):

1. Individual properties of the phases
2. Relative amount and distribution of each phase
3. Geometry of the dispersed phase

Composites are commonly categorized as particle-reinforced, fiber-reinforced, or structural composites. For example, concrete is a large-particle-reinforced composite that consists of cement (the matrix) and sand and gravel (the particulates) which serve as reinforcement. Similarly, fiber-reinforced concrete is composed of a cement matrix, and reinforcement consisting of aggregates of various sizes, along with discrete, discontinuous fibers.

The “Rule of Mixtures” approach has been used extensively to model the combined elastic behavior of composites (Callister 2003). This method provides an estimate of the elastic composite properties based on the relative volume fraction (%) and stiffness of the fiber and matrix phases. Fibers are anisotropic and are stronger when loaded in the longitudinal direction than when loaded in the transverse direction (Figure 2-2). Thus, two mathematical expressions have been formulated to provide upper and lower-bound estimates of the elastic modulus of composites with continuous and aligned fibers.



*Figure 2-2: Schematic of Continuous and Aligned Fiber Orientation with Longitudinal and Transverse Loading Directions*

The effective composite modulus for a composite loaded in the longitudinal direction can be expressed as (Callister 2003):

$$E_{cl} = E_f V_f + E_m V_m \quad \text{Equation 2-1}$$

Where:

$E_{cl}$  = modulus of elasticity of the composite loaded in longitudinal direction

$E_f$  = modulus of elasticity of the fiber

$V_f$  = volume content of the fiber phase (%)

$E_m$  = modulus of elasticity of the matrix

$V_m$  = volume content of the fiber phase (%)

Similarly for transverse loading:

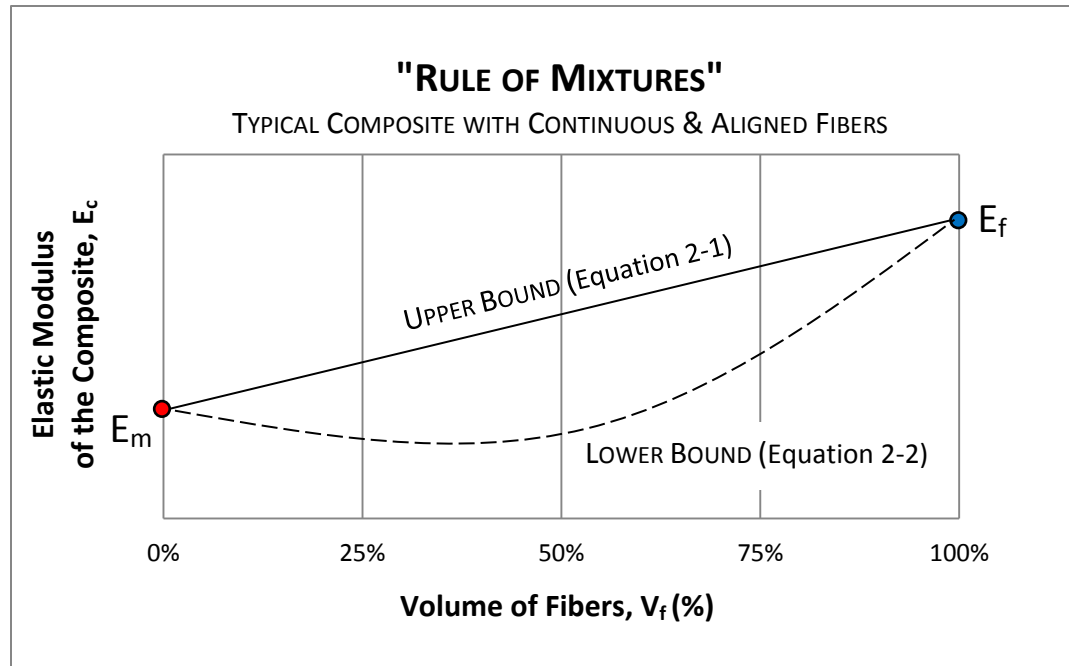
$$E_{ct} = \frac{E_m E_f}{E_f V_m + E_m V_f} \quad \text{Equation 2-2}$$

Where:

$E_{ct}$  = modulus of elasticity of the composite loaded in the transverse direction



As shown in Figure 2-3, the elastic modulus of the composite could typically be expected to fall somewhere between these limits when the fibers are continuous and aligned (Callister 2003).



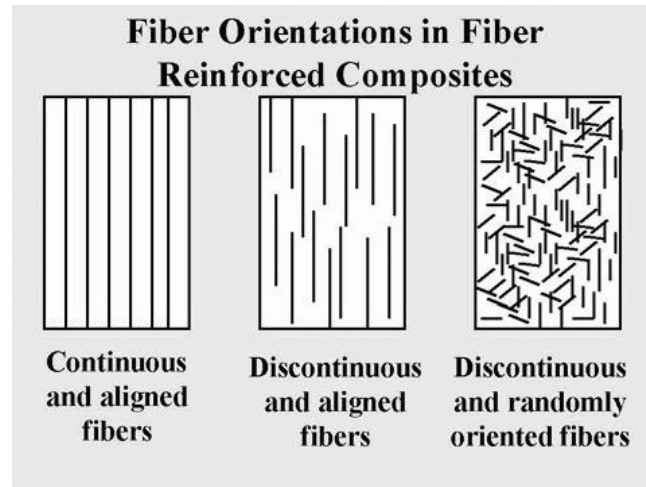
*Figure 2-3: Rule of Mixtures Approach for Estimating the Modulus of Elasticity of a Composite – modified from (Callister 2003)*

However, continuous and aligned fibers are not typically found in fiber-reinforced composites due to production, processing, and placement methods. Particularly for fiber-reinforced concrete, short and discontinuous fibers are normally used, and the fiber orientation is random. Under these circumstances, the following equation is a more appropriate expression for the elastic modulus of the composite:

$$E_{cd} = KE_fV_f + E_mV_m \quad \text{Equation 2-3}$$

In this expression, K is a fiber efficiency parameter, which depends on  $V_f$  and the  $E_f/E_m$  ratio. The K-factor is also influenced by the properties and geometry of the fiber. Its

magnitude is always less than unity, and is usually in the range of 0.1 to 0.6 (Callister 2003). The various fiber orientations or combination of orientations that may exist within a composite are shown in Figure 2-4.



*Figure 2-4: Fiber Orientations in Fiber-Reinforced Composites*

The mechanical properties and behavior of fiber-reinforced concrete composites depend on the individual constituents and their interaction with one another. This includes the structure of the matrix, shape and distribution of the fibers, and the fiber-matrix interface. Each of these components influences the behavior of the composite, and will be considered separately.

### **2.2.1 Matrix**

The bulk cementitious matrix is similar to other cement-based materials, and can be classified into two types based on the particulate filler it contains: (1) a *mortar matrix*, which denotes a cement-sand-water mixture; or (2) a *concrete matrix*, which denotes a cement-sand-coarse aggregate-water mixture. Fiber-reinforced cement pastes or mortars are usually applied in thin-sheet components, such as cellulose and glass fiber-reinforced cements used

mainly for cladding. In these applications the fibers act as the primary reinforcement and their content is usually in the range of 5% to 15% by volume. On the other hand, in fiber-reinforced concretes, the fiber volume is much lower (less than 2%); and the fibers act as secondary reinforcement, mainly for crack control. Higher contents of fibers can be incorporated using advanced matrix formulations which are based on sophisticated control of the rheology and microstructure of the mix. The dense microstructure of these composites enables the incorporation and fairly uniform dispersion of short fibers in volume fractions of 2% to 6%.

Whether mortar or concrete is used, it is important to understand how the matrix responds under loading. Tensile load is transferred through bond stresses and frictional resistance from the fiber to the matrix. As the load increases, matrix cracks develop when the tensile strength of the matrix is exceeded. With further increase in load, additional matrix cracks form. This is known as "multiple-matrix cracking" and is the desirable mode of failure for FRC and other brittle-matrix, ductile-fiber composites. *Multiple matrix cracking* suggests there is a significant bond between the fibers and the matrix; fibers are aligned so that they intersect crack planes; and fibers are of sufficient length to carry and transfer stresses (Callister 2003). Eventually, when one of these conditions no longer exists, no new cracks can form. Instead cracks increase in depth and width, and failure shifts to the fibers, which either pull out or fracture.

## **2.2.2 Fibers**

### ***2.2.2.1 Fiber Types (Materials)***

A broad range of fibers with different material and mechanical properties are used as reinforcement within cementitious matrices. Fiber types include steel, glass, and synthetic (polymer) fibers, each which vary considerably in strength, stiffness, toughness, and cost.

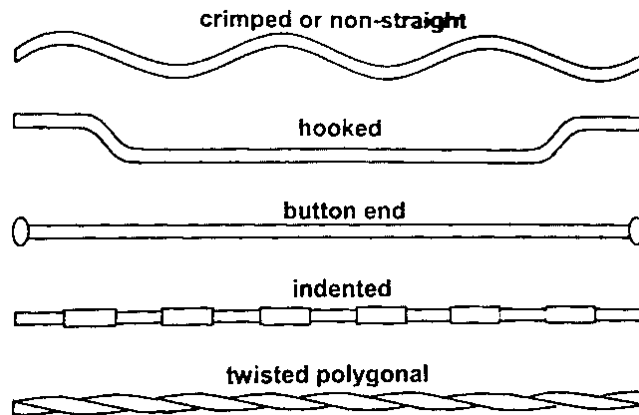
Early theoretical studies of FRC in the 1960s dealt primarily with the behavior of steel fiber-reinforced concrete (SFRC) (Romualdi and Batson 1963). Since then, SFRC has become the most commonly used fiber concrete, though synthetic fibers are becoming increasingly popular. Some common fibers types and their general properties are listed in Table 2-1.

*Table 2-1: Typical Fiber Types and Properties (Bentur and Mindess 2007)*

<b>Fiber Material</b>	<b>Diameter (μm)</b>	<b>Specific Gravity</b>	<b>Modulus of Elasticity (GPa)</b>	<b>Tensile Strength (GPa)</b>	<b>Elongation at Break (%)</b>
Steel	5 – 500	7.84	200	0.5 – 2.0	0.5 – 3.5
Glass	9 – 15	2.6	70 – 80	2 – 4	2 – 3.5
Polypropylene	20 – 400	0.9 – 0.95	3.5 – 10	0.45 – 0.76	15 – 25
Carbon	8 – 9	1.6 – 1.7	230 – 380	2.5 – 4.0	0.5 – 1.5
Cement matrix (for comparison)	---	1.5 – 2.5	10 – 45	0.003 – 0.007	0.02

#### **2.2.2.2 Fiber Geometry**

The individual fibers can be classified into two groups: (1) discrete monofilaments and (2) fiber assemblies. Discrete monofilaments are separated one from the other, and are frequently used in FRC. Fiber assemblies are made up of bundles of filaments which maintain their bundled nature in the composite itself, and do not disperse into individual filaments upon mixing or placement. The former, monofilament fibers, are cylinder-shaped and deformed into various configurations to improve the fiber-matrix interaction via mechanical anchorage. Different fiber geometries and end treatments are used to ensure that the fiber is anchored into the matrix so that load can be transferred and the full capacity of the fiber can be utilized. Figure 2-5 shows some of the more commonly available deformed shapes for steel fibers, including hooked, crimped, and twisted (Bentur and Mindess 2007).



*Figure 2-5: Commonly Available Deformed Steel Fiber (Bentur and Mindess 2007)*

In addition to their deformed shape, fibers are characterized by their aspect ratio: ratio of the length to the diameter. Pull-out tests can be performed on individual fibers to determine how the fiber aspect ratio affects the stress-strain behavior and bond strength. Fiber efficiency (resistance to pull-out) increases with increasing aspect ratio, and is influenced by the deformed shape (Maage 1978). Some of the trends resulting from fiber geometry are shown in Table 2-2.

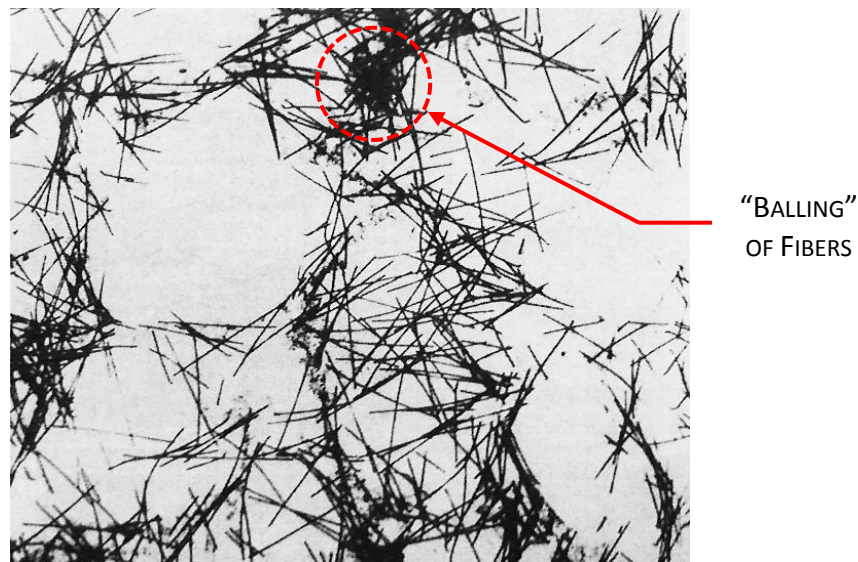
*Table 2-2: Pull-out Bond Stresses for Steel Fibers with Different Aspect Ratios and Deformed Geometries – modified from (Maage 1978)*

Fiber Type & Deformed Shape	Diameter (μm)	Length (mm)	Aspect Ratio	Fiber Strength (MPa)	Mean Bond Stress (MPa)
Plain, straight	0.30	Various	Various	1205	4.17
Indentations, straight	0.50	30	60	955	8.10
Plain, hooked ends	0.40	40	100	1355	4.93
Plain, weak crimped	0.35	30	86	1295	5.25
Plain, heavy crimped	0.40	25	63	1615	13.40
Plain, enlarged ends	0.3 x 0.4	14.5	36	510	7.27

### **2.2.2.3 Fiber Distribution & Orientation**

Distribution and orientation are two distinct characteristics of the fiber profile. As mentioned previously, fibers can be distributed uniformly or non-uniformly within the composite, and may assume various orientations. The fiber distribution is a measure of how well dispersed the fibers are in the composite, whereas the fiber orientation refers to the fiber alignment: the angle of a fiber (or fibers) with respect to a fixed 2-D plane. Both are used to describe the overall fiber profile.

The uniformity and orientation of the fibers is very sensitive to the mixing and consolidation process. In practice a uniform distribution is rarely achieved. Fibers are most commonly randomly distributed (non-uniform) once added to the matrix and solidified in the composite. Figure 2-6 is an example of non-uniform distribution of steel fibers in fiber-reinforced concrete as observed by x-ray (Stroeven and Shah 1978).



***Figure 2-6: Non-uniform Distribution and “Balling” of Steel Fibers in Cement Matrix as Observed by X-ray (not to scale) – modified from (Stroeven and Shah 1978)***

In FRC, fibers often "clump" or "ball" during mixing, consolidation, or placement; Clumping or balling is essentially a grouping of the fibers that restricts dispersion. This is also observed in the x-ray image provided in Figure 2-6. In addition to decreasing dispersion, clumped fibers can also create additional porous voids in the concrete, which weaken the interfacial transition zone in the microstructure of the composite (Bentur and Mindess 2007). This is a common phenomenon in FRC particularly when high fiber contents (greater than 2% by volume) are introduced into the mix, when high aspect ratio fibers are used, or when a large quantity of coarse aggregate is used in an FRC mixture (Chao 2009).

Some standard test protocols also make reference to “preferential fiber alignment” which has been observed after placing FRC into formwork or molds; these testing procedures specify that certain faces of the test specimens be used to avoid the effects of non-uniform distribution (ASTM C1609 2010, ASTM C1399 2010). Mixtures incorporating fibers with smaller diameters and high content of fine aggregate achieve a more uniform distribution during mixing and placement. In addition, there is less clumping and balling, but a completely uniform distribution is never accomplished when using discrete, discontinuous fibers (Bentur and Mindess 2007).

#### ***2.2.2.4 Fiber Performance & Efficiency***

Fiber type, geometry, distribution, and orientation are all factors that affect the performance and efficiency of the fibers in fiber-reinforced composites. The most obvious of these is the material, since different materials perform differently under static, dynamic, impact, and thermal loading. Other factors are less intuitive, but should not be neglected when selecting fibers, because they can significantly affect both the fresh and hardened composite properties of FRC.

Of the various factors affecting performance and efficiency, fiber length is most important. A critical length,  $l_c$ , can be defined as the minimum fiber length required to transfer stress (or load) from the concrete to the fiber to develop its ultimate tensile strength (or failure load). This is similar to the development requirements for conventional reinforcing bars set forth in Chapter 12 of ACI 318-11, *Building Code for Structural Concrete* (ACI 2011). The critical fiber length ( $l_c$ ) can be calculated for a given fiber according to Equation 2-4 (Callister 2003):

$$l_c = \sigma_f^* d / 2\tau_c \qquad \text{Equation 2-4}$$

Where:

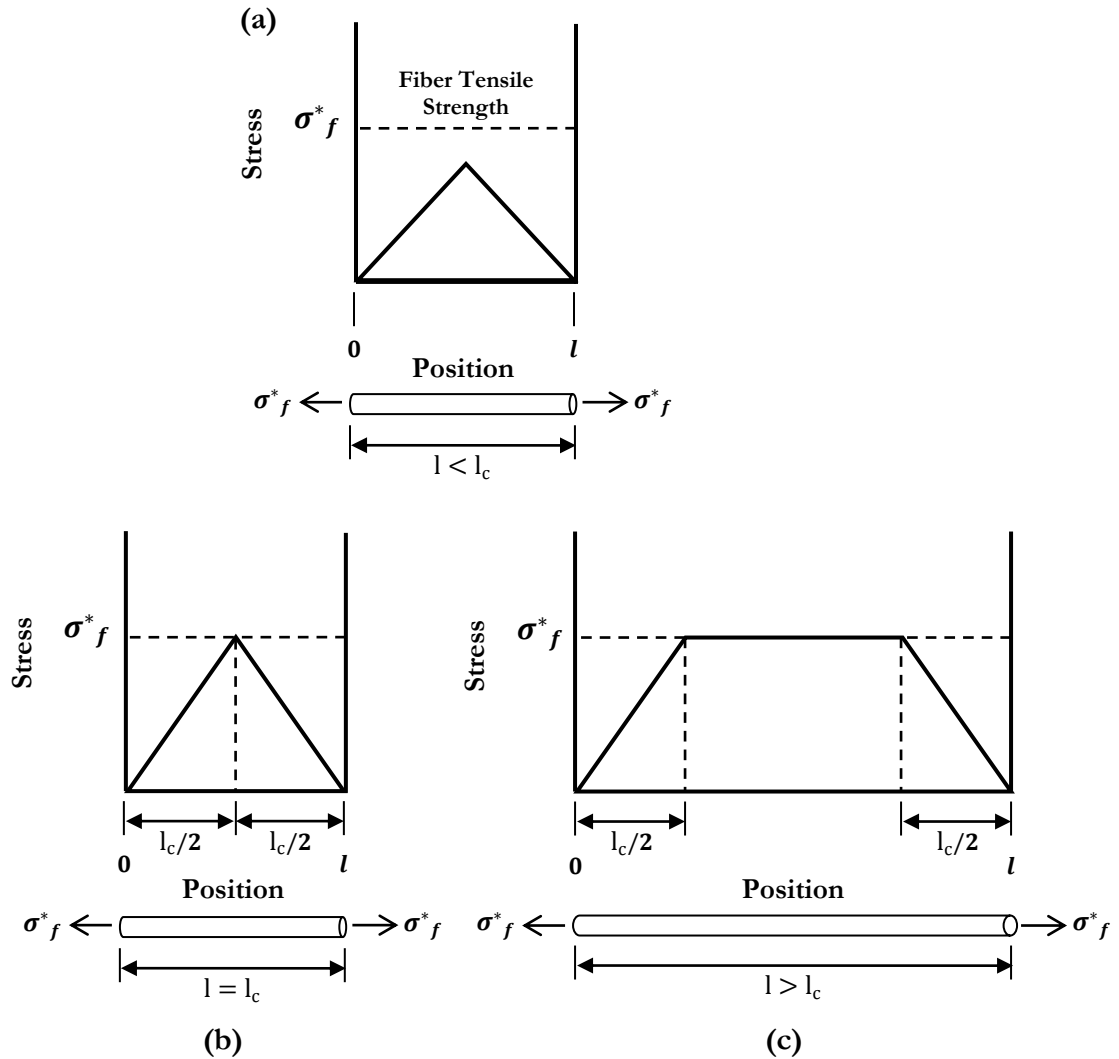
$l_c$  = critical length

$\sigma_f^*$  = fiber tensile strength

$d$  = fiber diameter

$\tau_c$  = shear strength of the matrix



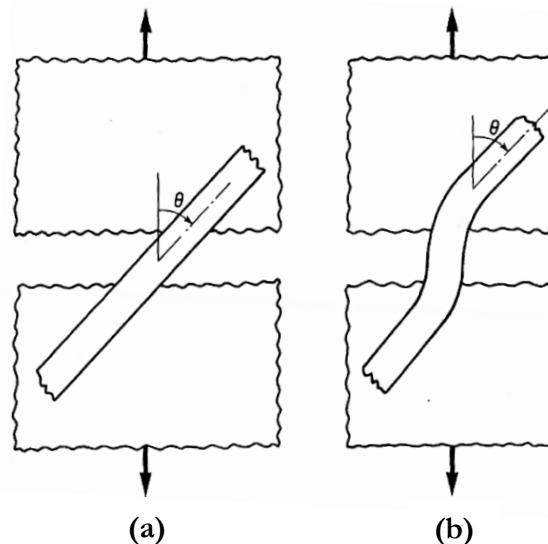


**Figure 2-7: Stress-Position Profiles when Fiber Length is (a) less than, (b) equal to, and (c) greater than the Critical Length for a FRC Composite that is Subjected to a Tensile Stress Equal to the Fiber Tensile Strength  $\sigma_f^*$  (Callister 2003)**

As shown in Figure 2-7 (a), when a stress equal to  $\sigma_f^*$  is applied to a fiber with less than the critical length, there is insufficient embedded length to generate a tensile stress equal to the fiber strength, and the fiber is not utilized efficiently. Only if the length of the fiber (b) equals or (c) considerably exceeds  $l_c$  does the fiber reach its yield or tensile strength, thus maximizing the contribution of the fiber reinforcement (Callister 2003). An

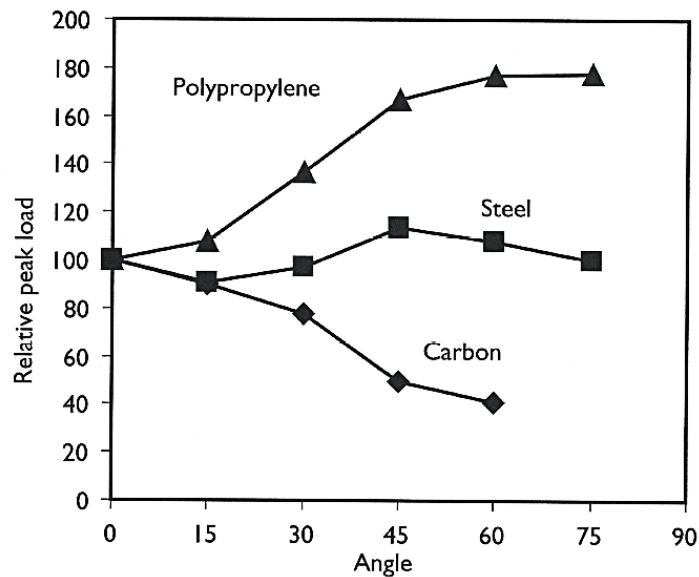
ideal fiber shape and length will maintain adequate workability of the fresh concrete mix, while providing effective anchorage in the hardened concrete composite. Longer fibers with smaller diameters (high aspect ratio) will be most efficient in the hardened FRC, but will make the fresh FRC more difficult to mix, consolidate, and place (Bentur and Mindess 2007).

Because fibers are strongest when loaded axially, the angle of inclination also plays a major role in fiber efficiency. When analyzing the contribution of fibers oriented at an angle  $\theta$  with respect to the load direction, two different geometrical details must be considered: Figure 2-8 (a) fibers maintaining a uniform angle along their length, and Figure 2-8 (b) fibers bending at the crack surface due to geometrical constraints. The assumption of a uniform angle is valid primarily before cracking, while the assumption of local bending is valid primarily after cracking. In each situation, the angle of inclination may increase or decrease the performance of the fiber depending on the fiber type (material) and the degree of cracking in the composite (Bentur and Mindess 2007).



**Figure 2-8: The Intersection of an Oriented Fiber with a Crack Assuming (a) Uniform Fiber Orientation across the crack, and (b) Local Fiber Bending Around the Crack (Bentur and Mindess 2007)**

For fibers with a uniform orientation sloped at an angle of  $45^\circ$ , the pull-out resistance was found to be 0.25 that of aligned fibers (Krenchel 1964). The effects of fiber orientation can also increase the pull-out resistance for fibers made of certain materials at particular angles (De Vekey and Majumdar 1968). As shown in Figure 2-9, for a composite with brittle fibers, an increase in the fiber orientation angle results in a reduction of pull-out resistance; However, for ductile, low-modulus fibers, pull-out resistance increases with orientation angle.



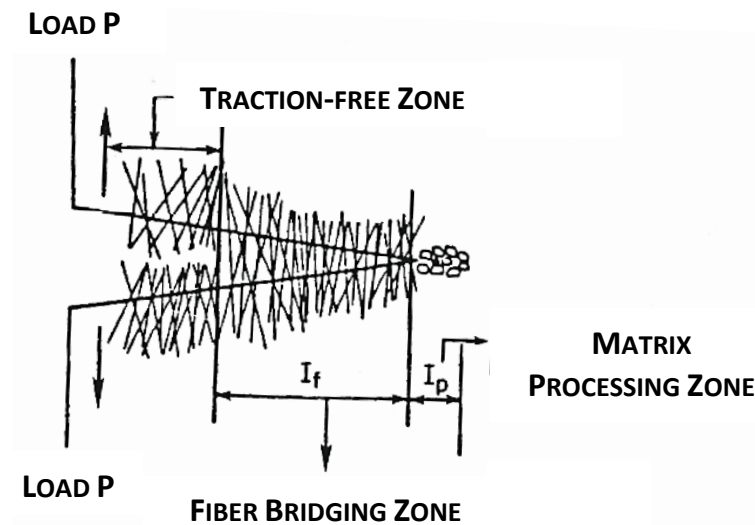
**Figure 2-9: Effect of Fiber Orientation on the Pull-out Strength of Ductile Fibers (polypropylene and steel) and Brittle Carbon Fibers (De Vekey and Majumdar 1968)**

The angle of fiber orientation is particularly important at a crack, where the size and propagation of the crack depend on the number of fibers crossing the crack. As illustrated in Figure 2-10, at the crack surface, three different zones can be identified (Wecharatana and Shah 1983):

1. *Traction-free zone*, where fibers are misaligned or fractured and no aggregate interlock is available to resist stress;

2. *Fiber bridging zone*, in which stress is transferred by frictional slip and yielding of the fibers;
3. *Matrix processing zone*, where enough continuity and aggregate interlock are available to transfer some stress in the matrix itself.

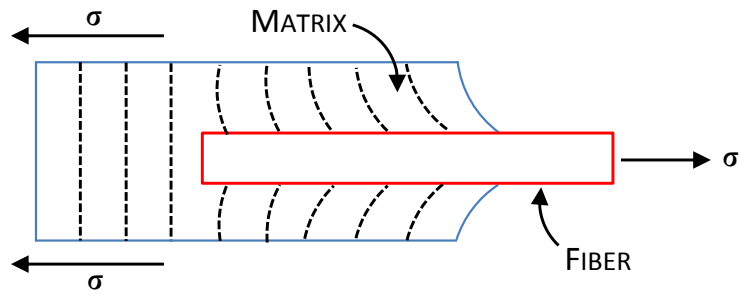
Once the first cracking has taken place in the brittle concrete matrix, the bridging fibers are most effective in providing the closing pressure required to arrest the crack (Wecharatana and Shah 1983).



*Figure 2-10: Idealized Representation of an Advancing Crack in Fiber-Reinforced Concrete (Wecharatana and Shah 1983)*

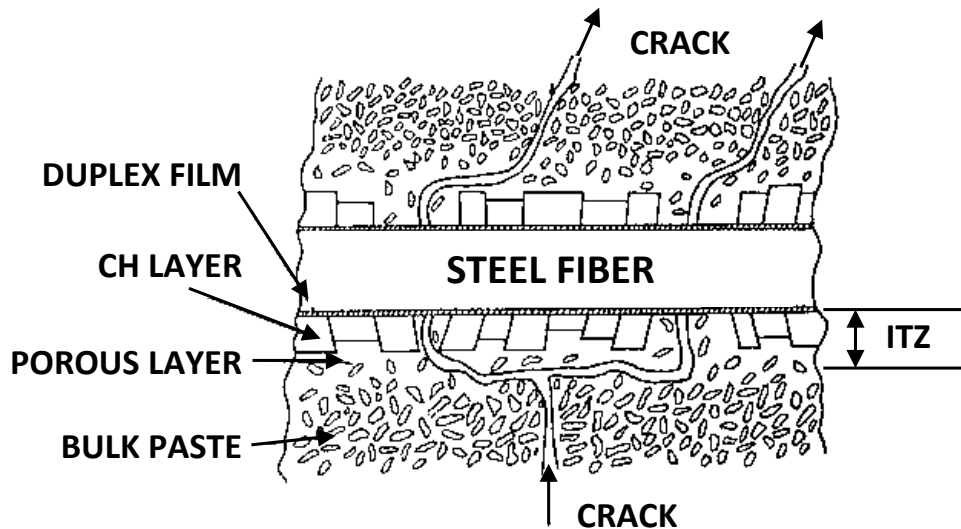
### 2.2.3 Fiber-Matrix Interface

The mechanical characteristics of an FRC composite depend not only on the properties of the fiber, but also on the degree to which an applied load is transmitted to the fibers by the matrix phase. Thus, the magnitude of the interfacial bond between the fiber and matrix phases becomes extremely important. Under an applied stress, this fiber-matrix bond ceases at the fiber ends, giving the matrix deformation pattern shown in Figure 2-11. In other words, there is no load transmitted from the matrix at each fiber extremity.



*Figure 2-11: Deformation Pattern in the Matrix Surrounding a Fiber Subjected to Tensile Load – modified from (Callister 2003)*

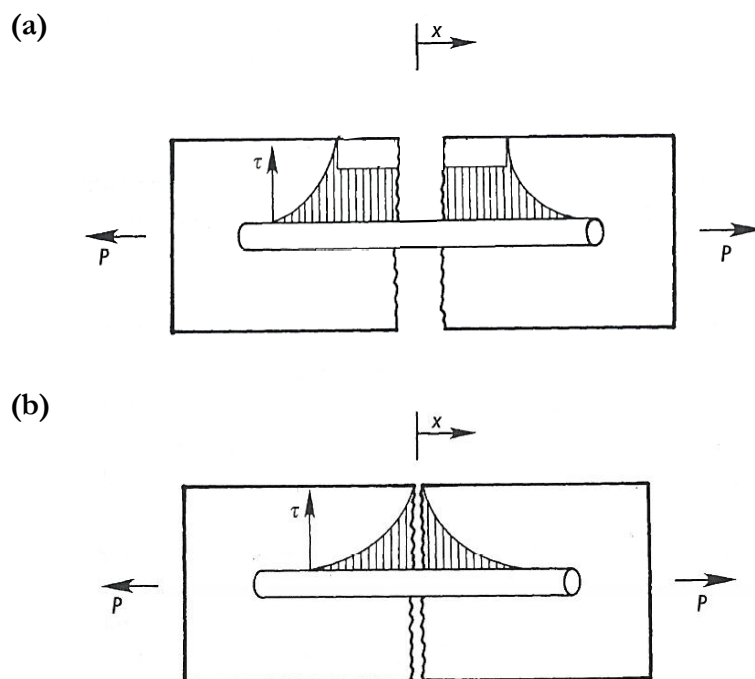
The weak link between the fiber and the matrix is not necessarily at the actual fiber-matrix interface; it can also be in the porous layer which extends to a distance of 10 to 40  $\mu\text{m}$  from the interface (Bentur and Mindess 1985). Cementitious composites are characterized by an interfacial transition zone (ITZ) in the vicinity of the reinforcing inclusion, in which the microstructure of the paste matrix differs considerably from that of the bulk paste away from the interface. As shown in Figure 2-12, cracking in the ITZ reduces the benefits gained by a strong fiber-matrix bond.



*Figure 2-12: Schematic of Cracking and Debonding in the Porous Layer of the ITZ for a SFRC – modified from (Bentur and Mindess 1985)*

The nature and size of the ITZ depend on the type of fiber, production technology, and the particulate nature of the matrix. Intensive processing, which involves higher shear stresses in the fresh mix, results in a denser and smaller ITZ. If the matrix is made of a well-graded mix, with fine fillers, and the fiber cross-section is sufficiently small, the transition zone can be almost eliminated, resulting in a high-bond matrix (Igarashi and Bentur 1996).

The differences between composites with weak and strong fiber-matrix bonds are illustrated in Figure 2-13 (a) and (b). Notice that for a high bond matrix, case (b), the fibers are more efficient, as indicated by the distribution of shear stress and the smaller crack width.



**Figure 2-13: Interfacial Shear Stress Distribution along a Fiber Intersecting a Crack Immediately After Cracking: (a) Debonding Preceded Cracking, Weak Bond; (b) No Debonding Prior to Cracking, Strong Bond – modified from (Bentur and Mindess 2007)**

## **2.3 FIBER-REINFORCED CONCRETE (FRC)**

### **2.3.1 Overview of FRC**

Fiber-reinforced concrete is made with hydraulic cement and aggregates of various sizes, incorporating discrete, discontinuous fibers. Most of the developments with FRC involve the use of ordinary Portland cements. However, high alumina cement, gypsum and a variety of special cements have also been used to produce FRC, generally to improve the durability of the composite, or to minimize chemical interactions between the fibers and the matrix. Recent developments also include specially formulated mortar and concrete matrices with controlled particle-size distributions (Bentur and Mindess 2007).

Plain, unreinforced concrete is characterized by low tensile strengths and tensile strain capacities, because concrete is a brittle material. Reinforcement is required before it can be used extensively as a construction material. Historically, this reinforcement has been in the form of continuous reinforcing steel bars or prestressing strands, which can be placed in the structure at the locations and orientations required to resist the applied tensile stresses. In contrast, fibers are most commonly distributed and oriented randomly throughout the matrix (Stroeven and Shah 1978). Fibers are therefore not as efficient at withstanding tensile stresses, because the required volume of fibers and their orientation cannot be guaranteed to coincide with the location and orientation of the expected tensile stresses.

However, since the fibers tend to be more closely spaced than conventional reinforcing bars, they are better at controlling crack widths. Thus, steel rebar or prestressing tendons are used to increase the load-carrying capacity of concrete whereas fibers are more effective for crack control. A wide variety of fibers have been used to reinforce cement matrices including asbestos, steel, glass, carbon, Kevlar, and low-modulus polypropylene fibers (Bentur and Mindess 2007).

### 2.3.2 Production Technologies for FRC

There are currently a number of available production technologies for FRC. These can be classified as one of the following processes (Bentur and Mindess 2007):

1. *Premix Process* – In this method, the fibers are combined with the cementitious matrix in a mixer. They are treated simply as an extra ingredient, and are usually added near the end of the mixing sequence. However, because fibers reduce the workability, only up to about 2% fibers by volume can be introduced in the mix by this method.
2. *Spray-Up Process* – This technique is used primarily with glass fibers. Chopped glass fibers and cement slurry are sprayed simultaneously onto a forming surface to produce thin sheets. With this technique, substantially higher fiber volume fractions (up to about 6%) can be achieved.
3. *Shotcreting* – Using a modification of normal shotcreting techniques, it is possible to produce steel and polypropylene fiber shotcretes. This method is used primarily for tunnel linings and for stabilization of rock slopes.
4. *Pulp-Type Processes* – The fibers are dispersed in a cement slurry, which is then dewatered to produce thin sheet materials. These can be built up to the required thickness by layering.
5. *Hand Lay-Up* – Layers of fibers in the form of mats or fabrics can be placed in molds, saturated with a cement slurry, and then vibrated or compressed to produce dense materials with very high fiber contents.
6. *Continuous Production* – Continuous production of a composite mix using special machinery with the output being a continuous composite with a thin-shaped geometry.



### 2.3.3 Fracture Mechanics of FRC

Similar to the behavior of plain concrete, composite failure of FRC under most types of loading is initiated by tensile cracking of the matrix along planes where normal tensile strains exceed permissible values (Gopalaratnam and Shah 1987). This may be followed by extensive cracking in the matrix prior to composite fracture if the fibers are sufficiently long, continuous, or high-performance (Bentur and Mindess 2007). However, when short fibers such as steel, polypropylene, or glass are used to reinforce brittle matrices, once the matrix has cracked, one of the following types of failures will occur (Gopalaratnam and Shah 1987):

- a) The composite fractures immediately after matrix cracking. This results from inadequate fiber content at the critical section, or insufficient fiber lengths to transfer tensile stresses across the matrix crack.
- b) The composite continues to carry additional load at a decreasing rate (strain-softening) after the peak. The post-cracking resistance is primarily provided by the pulling out of fibers from the cracked surfaces. Although no increase in composite tensile strength is observed, there is an increase in toughness.
- c) Even after matrix cracking, the composite continues to carry increasing tensile stresses; the peak stress and corresponding deformation are greater than those of the matrix alone. This behavior in the inelastic range is due to progressive de-bonding and frictional slip at the fiber-matrix interface, and some additional matrix cracking occurs.

It is clear that failure mode (c) results in improved performance of both the fibers and the matrix. This corresponds to the composite behavior of high-performance, fiber-reinforced composites (HPFRCC) shown in Figure 2-14 (b). These failure modes are important as they determine the limits of FRC applications.

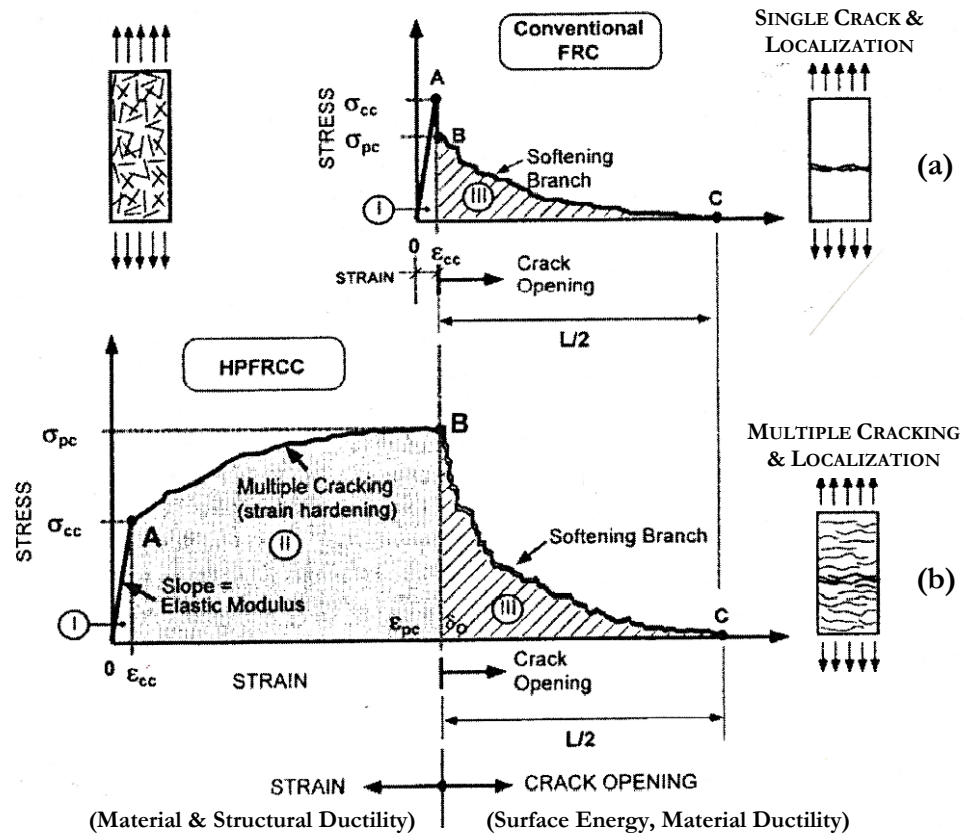


Figure 2-14: Comparison of Typical Stress-Strain Response in Tension of (a) Conventional FRC and (b) High Performance FRC (Bentur and Mindess 2007)

### 2.3.4 Applications of FRC

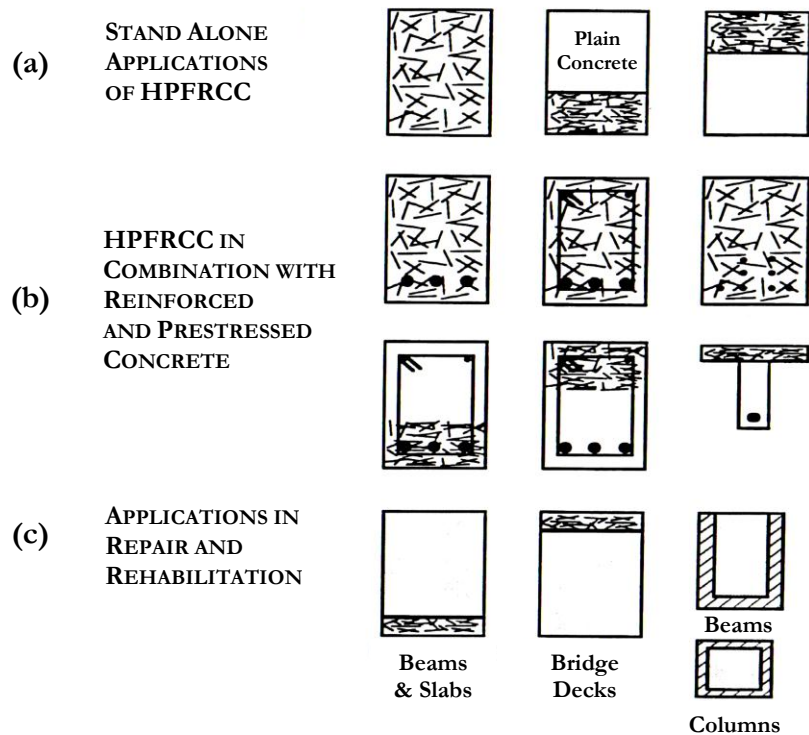
Since its introduction into the marketplace in the late 1960s, the use of fiber-reinforced concrete has increased steadily. Based on data from 2001, approximately 80 million cubic meters of FRC are produced annually, with the principal applications being slabs on grade (60%), fiber-shotcrete (25%), and precast members (5%), with the remainder of the production distributed among a number of other specialty products and structural forms (Bentur and Mindess 2007). A number of non-structural, structural, and repair applications exist.

#### ***2.3.4.1 Non-Structural Applications of FRC***

Fibers are used extensively in thin members such as bridge deck overlays, floor slabs, thin shells, and tunnel linings to reduce cracking and improve fatigue strength. In an evaluation of alternative materials to control drying shrinkage cracking in concrete bridge decks, fibers were effective in delaying early age cracking and limiting crack width (Folliard, Smith and Breen 2003). The fibers behave as a second line of defense to limit crack propagation because they help to distribute the stresses in the concrete around existing cracks so that the cracks stay relatively small. It was also shown that polypropylene fibers can eliminate plastic shrinkage. Thus, the addition of fibers improves concrete durability by preventing the ingress of harmful substances such as water, sulfates, and chlorides (Folliard, Smith and Breen 2003).

#### ***2.3.4.2 Structural Applications of FRC***

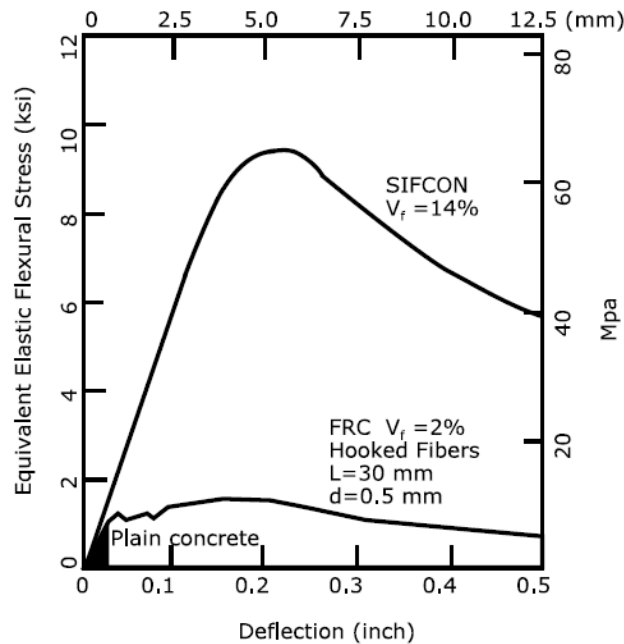
Although HPFRCCs have occasionally been used in stand-alone applications, fiber reinforcement is generally not a *substitute* for conventional reinforcement. Fibers and steel reinforcing bars play different roles in modern concrete technology, and there are many applications in which fibers and continuous reinforcing bars can be used together. Fibers have been used in this way to improve the static flexural strength, flexural fatigue strength, and post-cracking energy absorption capacity of structural members (Ramakrishnan 1987). Figure 2-15 provides some basic schematics of (a) stand-alone, (b) combined, and (c) repair applications for HPFRCC.



*Figure 2-15: Schematic of (a) Stand Alone, (b) Combination, and (c) Repair Applications for HPFRCC (Ramakrishnan 1987)*

HPFRCC come in a variety of forms, and have proven successful in a number of structural applications. One method for producing high-volume, high-aspect-ratio, fiber-cement composites was developed based on preparation of a preplaced steel fiber bed which is infiltrated with cement slurry (Lankard 1985). In this system, called SIFCON (Slurry Infiltrated Fiber Concrete), the fibers are placed by hand or using fiber-dispensing units. Fiber volume fractions of up to 20% can be achieved by vibrating the bed during slurry infiltration. With such high fiber volume fractions, it is possible to increase the toughness and flexural strength by more than an order of magnitude compared with the unreinforced matrix, or with a matrix reinforced with low fiber volume fractions (Bentur and Mindess

2007). Figure 2-16 compares the flexural performance of SIFCON, standard FRC, and plain (unreinforced) concrete.



*Figure 2-16: Stress-Deflection Response of SIFCON, Conventional FRC, and Plain Concrete (A. Naaman 1992)*

### **2.3.4.3 Repair & Rehabilitation Applications of FRC**

SIFCON and other high-performance fiber-reinforced concrete technologies lend themselves to repair and rehabilitation applications. The greatest interests have been retrofit designs for earthquake-resistant components and blast-resistant structures (Krstulovic and LaFave 2000, Coskun 2002). Each of these applications requires high energy absorption and ductility for adequate performance, and thus HPRCCs are great options because of their high toughness induced by their high fiber content. One repair and rehabilitation application for SIFCON is column jacketing, a widely used method for increasing the flexural, axial, and shear strength of existing columns.

### **2.3.5 Test Methods for FRC**

Fibers are still rarely used in purely structural concrete applications, despite their effectiveness under static and dynamic loading, their ability to control crack widths, and improved toughness behavior. This is due largely to the fact that fibers have yet to be widely integrated into structural design codes such as ACI 318 (ACI 2011). Part of the hesitation to implementing FRC into codes is due to the lack of a widely agreed upon body of standards for testing and quality control of FRC.

Many test methods can evaluate the performance of fibers with respect to plastic shrinkage, anchorage, and pull-out strength. However, test methods used to evaluate the composite properties of FRC that are of structural significance (such as toughness and residual strength) are inadequate and inconsistent (Bentur and Mindess 2007). This is unfortunate since research shows fiber-reinforced concrete has the potential to be used more commonly for structural purposes. Before FRC can be used extensively in practice, it is critical that simple, accurate, and consistent testing procedures be developed to evaluate the behavior of FRC composites.

## CHAPTER 3

# STANDARD TEST METHODS FOR FIBER-REINFORCED CONCRETE

### 3.1 OVERVIEW

The evaluation of the properties of fiber-reinforced concrete (FRC) composites is essential to the effective and economical use of these materials in design and construction practice. Some properties, such as compressive strength and freeze-thaw resistance, are largely matrix-dependent, and can be measured by methods commonly used for conventional concrete mixtures. However, the properties of the composite are much more dependent on the presence, proportion, and properties of the fiber phase as well as the fiber-matrix interactions. It is the *composite properties* that are of greatest interest for FRC materials and engineering purposes, because they can be used to quantify the effectiveness of fibers, the ductility of the composite, and the resistance offered by the material against crack propagation. These characteristics are generally undetectable by methods intended for standard concrete mix designs, and must be evaluated by test methods sensitive to the addition of fibers and capable of reflecting the composite behavior. It has been recommended that such processes used to describe key parameters of FRC should ideally satisfy the following criteria (Mindess, Young and Darwin 2003):

- i. It should have a physical meaning that is both understandable and of fundamental significance if it is to be used for the specification or quality control of FRC.

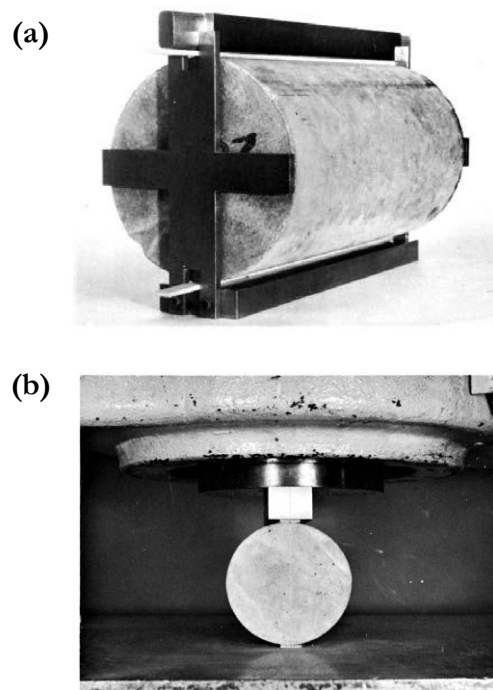
- ii. The “end-point” used in the calculation of the toughness parameters should reflect the most severe serviceability conditions anticipated for the particular application.
- iii. The variability inherent in any measurement of concrete properties should be low enough to give acceptable levels of both within-batch and between-laboratory precision.
- iv. It should be able to quantify at least one important aspect of FRC behavior such as tensile strength, toughness (residual strength), and crack resistance; and reflect some characteristics of the load-deflection curve.
- v. It should be as independent as possible of the specimen size and geometry.

Various test methods exist to evaluate the performance characteristics of FRC in a way that satisfies the above criteria. Most are used privately by fiber producers or in research fields, but a select minority have been refined and published by national and international agencies such as the American Society for Testing and Materials (ASTM), the European Federation of National Associations of Specialist Representing Concrete (EFNARC), the Japan Society of Civil Engineers (JSCE), and the International Union of Laboratories and Experts in Construction Materials, Systems, and Structures (RILEM). Several attempts have been made over the years to quantify the behavior of FRC in terms of parameters that can be used for comparing different fiber types and contents, as well as for specifications and quality control. The test methods presented in this chapter represent those most commonly used to achieve this result. The general scope, significance, and use of these methods are summarized, followed by a discussion of their limitations that are of particular importance to this research.



### 3.1.1 ASTM C496: Standard Test Method for Splitting Tensile Strength of Cylindrical Concrete Specimens

This test method is used to determine the splitting tensile strength of cylindrical concrete specimens, such as molded cylinders and drilled cores (ASTM C496 2011). The *Splitting Tensile Test*, as it is commonly called, consists of applying a compressive force along the diametrical length of a 4 x 8-in. [100 x 200-mm] cylindrical concrete specimen until failure occurs due to indirect tension.



***Figure 3-1: Test Specimen Positioned in (a) Jig for Aligning Cylinder and Bearing Strips and (b) in Testing Machine for Determination of Splitting Tensile Strength (ASTM C496 2011)***

Failure occurs in tension rather than compression because the areas of load application are in a state of tri-axial compression, thereby allowing them to withstand much higher compressive stress than a uniaxial compressive stress state. As shown in Figure 3-1, thin plywood bearing strips are used to distribute the load applied along the length of the

cylinder. The maximum sustained load is divided by the appropriate geometrical factors in Equation 3-1 to obtain the splitting tensile strength (ASTM C496 2011).

$$T = 2P/\pi ld \qquad \text{Equation 3-1}$$

Where:

$T$  = splitting tensile strength, psi [MPa]

$P$  = maximum applied load indicated by the testing machine, lbf [N]

$l$  = length, in. [mm]

$d$  = diameter, in. [mm]

Traditionally, the splitting tensile strength obtained from this test method is used in the design of structural concrete members to evaluate the shear resistance provided by concrete and to determine the required development length of reinforcement. Although less frequently utilized for fiber-reinforced concrete, some researchers have also used ASTM C496 as an indicator of the tensile capacity of FRC (Folliard and Smith 2003).

The Splitting Tensile Test is reliable and gives consistent results for both in-batch and inter-laboratory tests. Available research data suggests that the within-batch coefficient of variation is 5% for 6 x 12-in. [150 x 300-mm] cylindrical specimens with an average splitting tensile strength of 405 psi [2.8 MPa]. This test uses commonly available equipment, relatively small specimens, and a simple test setup and procedure. Splitting tensile strength is a good indicator of tensile capacity, and correlates well with the performance of conventional concrete structures stressed in tension (ASTM C496 2011).

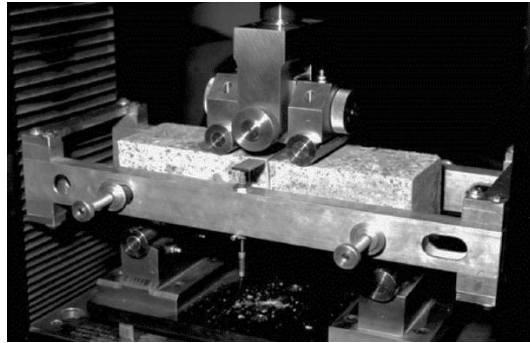
However, when this test method is extended to FRC, some limitations arise. ASTM C496 concentrates the loading along the diameter of the cylinder, and forces failure to occur along a single, pre-determined plane. This type of loading does not favor fiber-reinforced concrete mixtures. Since fibers are randomly distributed within a given concrete specimen,

forcing failure to a single, pre-determined plane reduces the probability that the crack plane will coincide with a plane containing fibers. Moreover, should the crack plane coincide with a plane containing a representative sample of the particular fiber content, there is no guarantee that the fibers will be oriented perpendicular to the crack plane, where they would be most effective.

Also, based on the test arrangement, procedure, and calculations, one is unable to determine the post-cracking behavior which is of greatest concern for FRC composites. ASTM C496 does not provide a means of obtaining the load-deflection curve, and cannot be used to measure or compare the performance of different fiber types and volume fractions except in terms of ultimate tensile capacity.

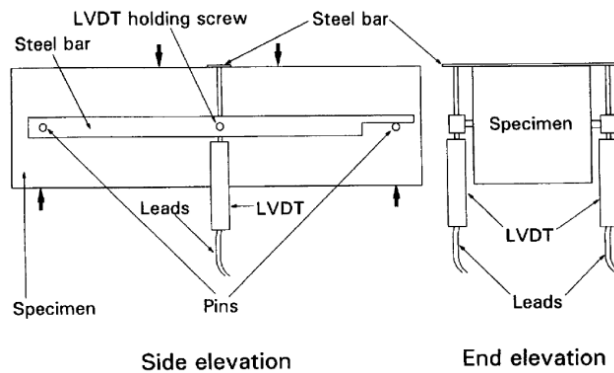
### **3.1.2 ASTM C1609: Standard Test Method for Flexural Performance of Fiber-Reinforced Concrete (Using Beam with Third-Point Loading)**

This test method evaluates the flexural performance of FRC using parameters derived from the load-deflection curve obtained by testing a simply supported beam using a closed-loop, servo-controlled testing system. Molded or sawn beam specimens having a square cross-section are tested in flexure using a third-point loading arrangement as shown in Figure 3-2. Preferred specimen sizes include 4 x 4 x 14-in. [100 x 100 x 350-mm] beam tested on a 12-in. [300-mm] span, or 6 x 6 x 20-in. [150 x 150 x 500-mm] beam tested on an 18-in. [450-mm] span. In this method, the first-peak and the peak loads are determined and the corresponding stresses calculated using the provided formulas. Residual strengths at specified deflections can be calculated similarly. Additionally, ASTM C1609 provides for determination of specimen toughness based on the area under the load-deflection curve up to a prescribed deflection (ASTM C1609 2010).

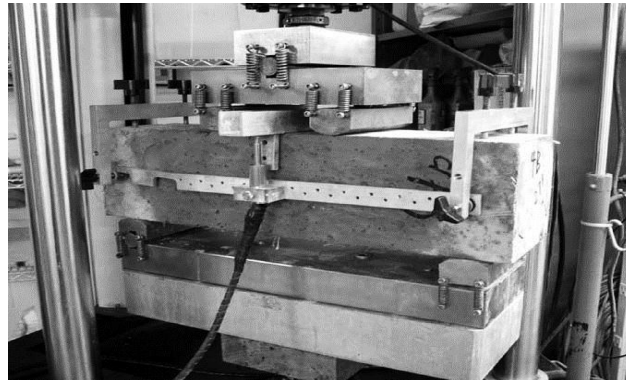


**Figure 3-2: Beam with Three-Point Loading Test Setup (ASTM C1609 2010)**

Previously denoted as ASTM C1018, and now as ASTM C1609, this test has evolved over the years to address its potential errors and complications. The most prevalent complication is accounting for extraneous deflections that occur due to machine deformations and seating and twisting of the specimen on the supports (Johnston 1995). Currently, testing laboratories can address this complication as they choose (ASTM C1609 2010). One acceptable technique, known as the “Japanese Yoke,” was introduced in the mid-90s by the JSCE, and is widely used for this test method (Chen and Mindess 1995). A schematic of this arrangement and its application is provided in Figure 3-3 and Figure 3-4.



**Figure 3-3: Schematic of Japanese Yoke Loading System (Chen and Mindess 1995)**



***Figure 3-4: Test Arrangement to Obtain Net Deflection via Japanese Yoke Loading System (ASTM C1609 2010)***

ASTM C1609 provides an advantage over ASTM C496 (Splitting Tensile Test) in that it is useful for describing post-peak behavior of FRC. The experimental results may be used for comparing the performance of various fiber-reinforced concrete mixtures or in research and development work. They may also be used to monitor concrete quality, to verify compliance with construction specifications, to obtain flexural strength data on fiber-reinforced concrete members subject to pure bending, or to evaluate the quality of concrete in service (ASTM C1609 2010).

Although ASTM C1609 can be used for several purposes, it has many disadvantages. For one, although the preferred specimen dimensions result in manageable size test samples, the test method depends on the specimen dimensions. Note (5) of the standard specification clearly states:

*“The results obtained from using one size of molded specimen may not correspond to the performance of larger or smaller molded specimens, concrete in large structural units, or specimens sawn from such units (ASTM C1609 2010).”*

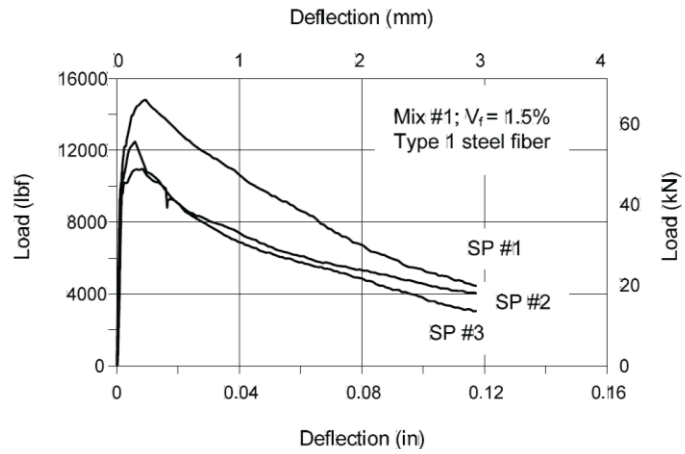
Variations in results may occur due to the degree of preferential fiber alignment within different specimens, but this random orientation is to be expected and should be accounted for in an adequate test method. Similar to the limitations of the Splitting Tensile Test, the random fiber distribution and orientation is unaccounted for due to the failure mechanism

inherent in the test. In ASTM C1609, failure of the specimen is also dominated by a *single large crack* in a *well-defined plane*. In fact, if the fracture occurs outside of the middle third of the span, the results are required to be discarded (ASTM C1609 2010). Again, because the fibers are randomly distributed and oriented, the effects that they produce are not well represented by a test in which the failure location is constrained.

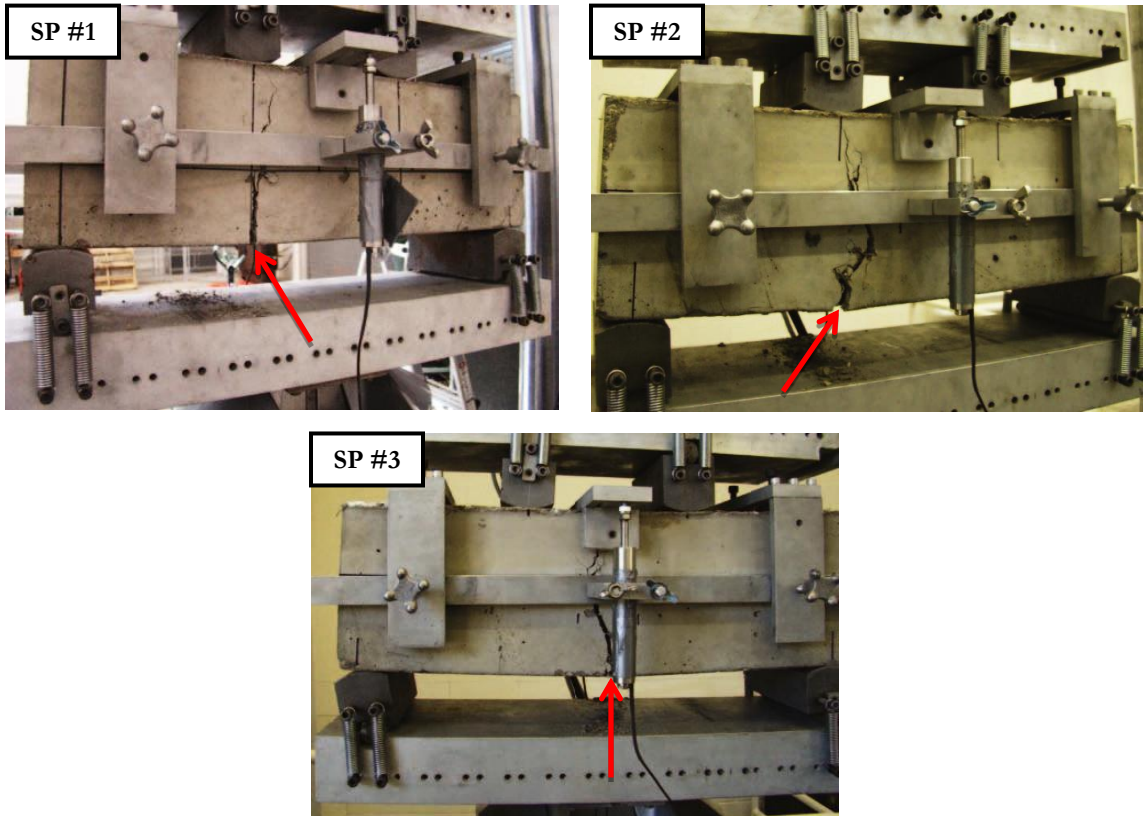
Secondly, the calculated toughness parameters greatly depend on how the point of “first crack” is defined. Thus it is important to determine the load vs. deflection curve very precisely. As a result, a number of difficulties arise (Bentur and Mindess 2007):

1. It is essential to correct for the “extraneous” deflections that occur due to seating of the specimen on the supports and machine deformations. Different laboratories may make these corrections differently, and hence may report different results (Chen and Mindess 1995, ASTM C1609 2010).
2. Because some micro-cracking begins almost immediately upon loading, it is difficult to define the point of first cracking unambiguously.
3. An *instability* often occurs in the measured load vs. deflection curve immediately after the first significant crack, particularly for low toughness FRC, and a servo-controlled operation is required to control the rate of increase of deflection. Closed-loop testing equipment is not always available, and different loading systems can result in quite different calculated toughness values.
4. Due to the uncertainty in determining the point of first cracking and difficulties introduced by the instability previously mentioned, toughness and residual strength parameters are sometimes insensitive to different fiber types or geometries.

Due to these and other factors, toughness and residual strength parameters show considerable scatter. The within-batch coefficient of variation (COV) has been reported from 15% to greater than 20% (ASTM C1609 2010, Bernard 2002, S.-H. Chao 2011). Moreover, reproducibility has yet to be determined (ASTM C1609 2010). Experimental evidence indicated that the high variability is due to the lack of control over the position of the cracks, as well as fiber orientation relative to the major crack plane (S.-H. Chao 2011). The effect of non-uniform fiber distribution on the variation in the load-deflection curves and crack location for replicate specimens can be seen in Figure 3-5 (a) and (b), respectively.



(a) Replicate Specimen P- $\delta$  Curves



(b) Location of Major Cracks

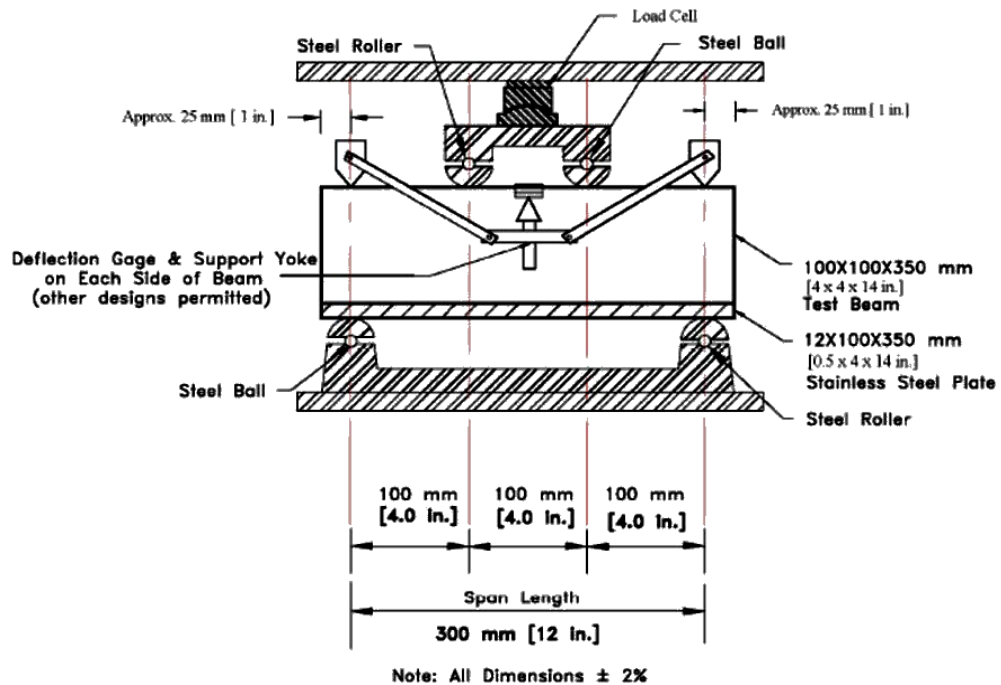
*Figure 3-5: Variability of ASTM C1609 for Replicate Specimens in the (a) Load vs. Deflection Curves and (b) Location of Major Cracks (S.-H. Chao 2011)*



Despite the considerable improvements that have been made in ASTM C1609 over the years, this testing procedure still presents major difficulties in accurately describing the behavior of FRC.

### 3.1.3 ASTM C1399: Standard Test Method for Obtaining Average Residual Strength of Fiber-Reinforced Concrete

This test method covers the determination of the residual strength of a fiber-reinforced concrete test beam. The average residual strength is computed using specified beam deflections that are obtained from the load-deflection curve of a beam that has been cracked in a standard manner (ASTM C1399 2010). Cast or sawed FRC beams having dimensions of 4 x 4 x 14-in. [100 x 100 x 350-mm] are cracked using a third-point loading apparatus similar to that described ASTM C1609, but modified by a steel plate used to support the concrete beam during the initial loading cycle (Figure 3-6).



*Figure 3-6: Schematic of Apparatus with Stainless Steel Plate and Suitable Support Frame (ASTM C1399 2010)*

As mentioned previously, for low-toughness FRC composites, an unstable condition often occurs in the load-deflection curve after the first major crack forms and begins to open. The steel plate is used in this method to help control the rate of deflection when the beam cracks, thereby eliminating the need for a servo-controlled operation as required by ASTM C1609. After the beam is cracked in the specified manner, the steel plate is removed and the cracked specimen is reloaded to obtain data and plot a reloading load-deflection curve. Load values at specified deflection values on the reloading curve (Figure 3-7) are averaged and used to calculate the average residual strength of the beam by Equation 3-2 (ASTM C1399 2010).

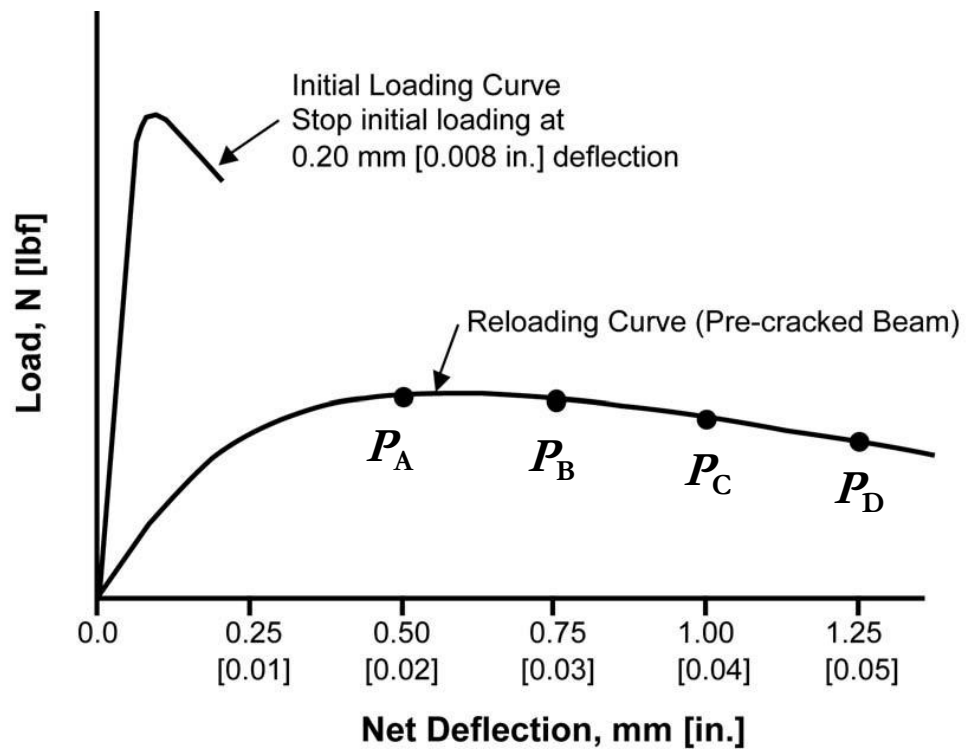


Figure 3-7: Typical Load-Deflection Curve (ASTM C1399 2010)

$$ARS = \left( \frac{P_A + P_B + P_C + P_D}{4} \right) * k \quad \text{Equation 3-2}$$

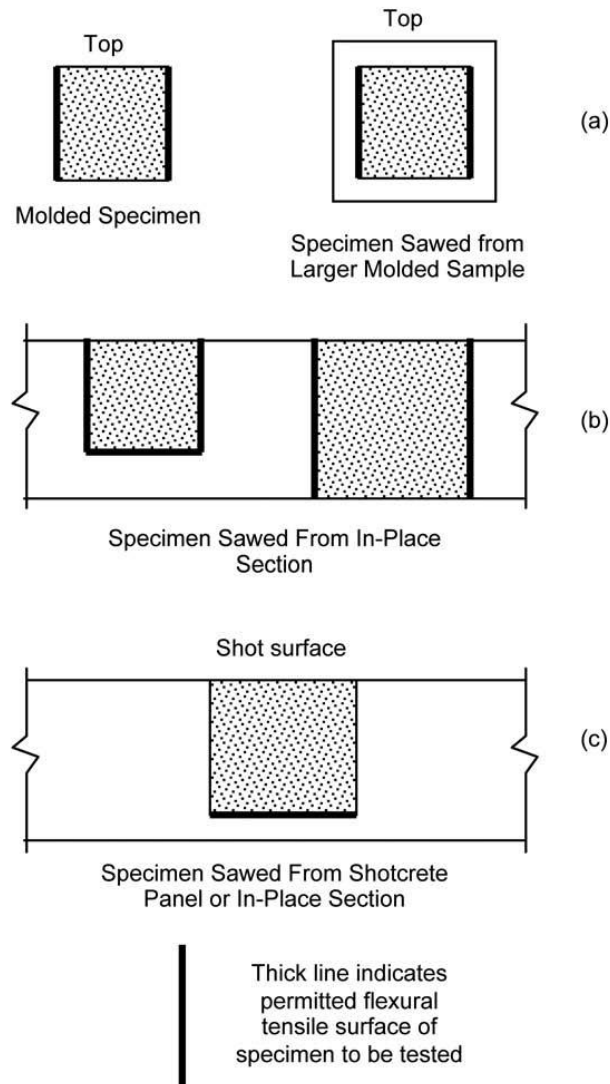
Where:

$k$	= $L/bd^2$ , in <sup>-2</sup> [mm <sup>-2</sup> ]
$ARS$	= average residual strength, psi [MPa]
$P_A + P_B + P_C + P_D$	= sum of recorded loads at specified deflections, lbf [N]
$L$	= span length, in. [mm]
$b$	= average width of beam, in. [mm]
$d$	= average depth of beam, in. [mm]

This test method provides a quantitative measure useful in the evaluation of the performance of fiber-reinforced concrete. Results are intended for comparative analyses of FRC beams and to reflect consistencies or differences among variables used in proportioning the fiber-reinforced concrete to be tested, such as fiber type, fiber size and shape, fiber amount, beam preparation (sawed or molded), and beam conditioning. Results can be used to optimize the proportions of FRC mixtures, to determine compliance with construction specifications, to evaluate FRC which has been in service, and as a research tool. For tests based on studies at ten laboratories on sets of three replicates of four different mixtures, the single-operator coefficient of variation ranged between 13% to 20%, and the multi-laboratory precision was 16% to 44% depending on the fiber content (ASTM C1399 2010).

ASTM C1399 has some advantages over other tests for FRC. Unlike ASTM C496, it is useful for comparing mixtures containing different fiber types and amounts. Also, it uses commonly available equipment, and does not require a servo-controlled machine. In contrast to ASTM 1609, the load-deflection curves that it produces, using the modified steel plate arrangement, agree closely with those obtained using a displacement-controlled, closed-loop

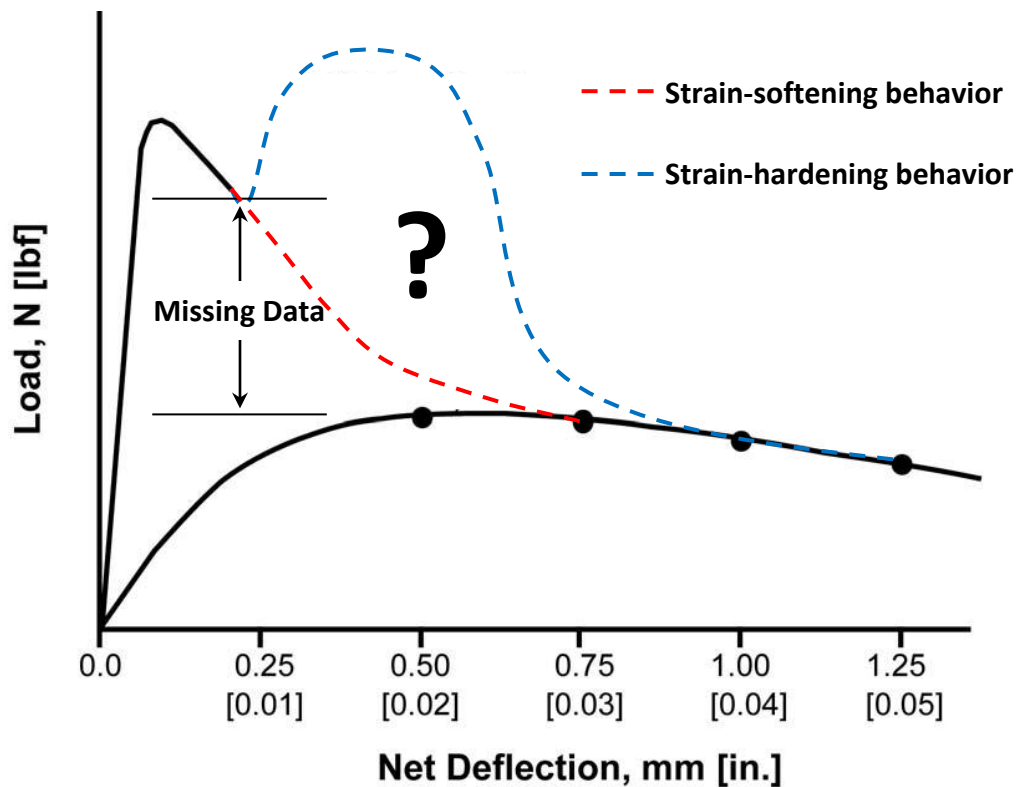
setup (Banthia and Dubey 1999). Therefore, testing can be accomplished using an ordinary universal testing machine. Another benefit of this test method is that preferential fiber alignment is taken into account in a meaningful way. The previously mentioned test methods did not take fiber alignment into account. In ASTM C1399, it is recognized that for molded beams fiber orientation near formed surfaces will be affected by the process of molding. For FRC containing relatively rigid or stiff fibers of length greater than 1.4 in. [35 mm], the use of sawed beams cut from samples with an initial width and depth of at least 3 times the length of the fiber is required to minimize the effects of fiber orientation. When sawed beams are employed, the flexural tensile surface of the beam is required to be a *sawed surface* to avoid the effects of fiber orientation (ASTM C1399 2010). This test condition is shown in the schematic provided in Figure 3-8.



***Figure 3-8: Schematic of Specimen Cross Sections to Indicate Permitted Flexural Tensile Surfaces during Testing (ASTM C1399 2010)***

Although ASTM C1399 addresses some of the difficulties of similar test methods, it has limitations of its own, many of which stem from the application of the steel plate. First, the steel plate adds stiffness to the specimen prior to cracking, which makes it more difficult to estimate the modulus of elasticity (initial slope). Second, the length of the pre-crack obtained prior to the removal of the steel plate is unknown. Thus, for different types of FRC

composites, the pre-cracks obtained with this loading system may be of different lengths, making comparisons of the residual capacities between different specimens more complicated since conditions prior to reloading the specimen could vary considerably. Third, the test is useful only for describing a portion of the load-deflection curve: Because the steel plate is removed and the test is stopped after the “first crack” appears, the effect of the fibers on the performance immediately after the first crack is ignored (Bentur and Mindess 2007). As shown in Figure 3-9, this lack of data means that a strain-softening composite cannot be distinguished from one that exhibits highly ductile, strain hardening behavior (ASTM C1399 2010).



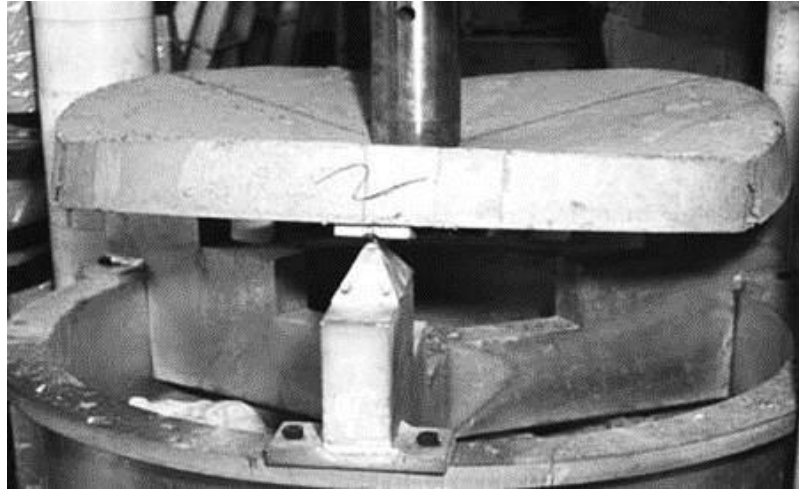
*Figure 3-9: Effect of Steel Plate on Determining Performance Immediately After First Crack – adapted from (ASTM C1399 2010)*

In addition to complexities involving the test arrangement, ASTM C1399 is based on questionable theory related to the determination of the residual strength. Simple beam theory (as required in this method) cannot be used to calculate the strength of a cracked system, so it is unclear what the calculated “residual strengths” mean (Bentur and Mindess 2007). Although sawing the tested surface of the specimen may reduce the effects of fiber orientation, failure is still governed by a *single crack* in a *well-defined* plane, which does not favor any remaining random fiber distribution or alignment.

Although ASTM C1399 is better than its predecessors, the modified test setup (which was originally designed to reduce complexity by eliminating the need for closed-loop operation) presents new drawbacks. The test gives similar precision compared to other bending tests, but does not completely describe the load-deflection behavior of FRC.

#### **3.1.4 ASTM C1550: Standard Test Method for Flexural Toughness of Fiber Reinforced Concrete (Using Centrally Loaded Round Panel)**

ASTM C1550 is intended for determination of the flexural toughness of FRC, expressed as energy absorption in the post-cracking range. Molded round panels of cast fiber-reinforced concrete or fiber-reinforced shotcrete are subjected to a central-point load while supported on three symmetrically arranged pivots. The load is applied through a hemispherical-ended steel piston advanced at a prescribed rate of displacement. Load and deflection are recorded simultaneously up to a specified central deflection. The suggested panel support fixture and test arrangement are shown in Figure 3-10. The nominal dimensions of the panel are 3-in. [75-mm] in thickness and 31.5-in. [800-mm] in diameter. Molded and shotcrete specimens are cast using steel forms. The use of round panels eliminates the sawing that is required to prepare shotcrete beam specimens. Typical molded and shotcrete construction is shown in Figure 3-11 and Figure 3-12, respectively (ASTM C1550 2010).



*Figure 3-10: Testing Arrangement using Suggested Round Panel Support Fixture (ASTM C1550 2010)*



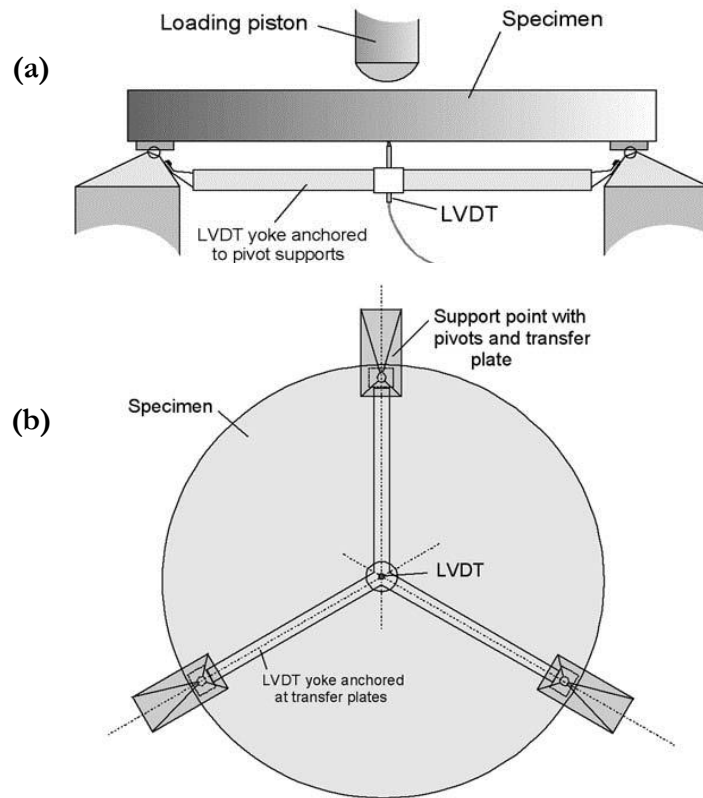
*Figure 3-11: Rolling Steel Form after Molded Specimen Has Gained Sufficient Strength (ASTM C1550 2010)*





*Figure 3-12: Manual Spraying of Shotcrete Panels (ASTM C1550 2010)*

The central deflection of the specimen relative to the support points must be determined in a manner that excludes extraneous deformations of the testing machine and support fixture. This is achieved by one of two methods. As shown in Figure 3-13 (a) and (b), if the displacement of the tensile surface at the center of the panel is measured relative to the pivot supports, then the recorded deflections do not need to be corrected. However, if the movement of the loading piston relative to the crosshead of the testing machine is used to measure deflection, the deflection record must be adjusted to discount extraneous deformations. Regardless of the method of deflection measurement selected, the method requires a servo-controlled testing machine and a displacement transducer with a precision of  $\pm 0.05$ -mm (ASTM C1550 2010).

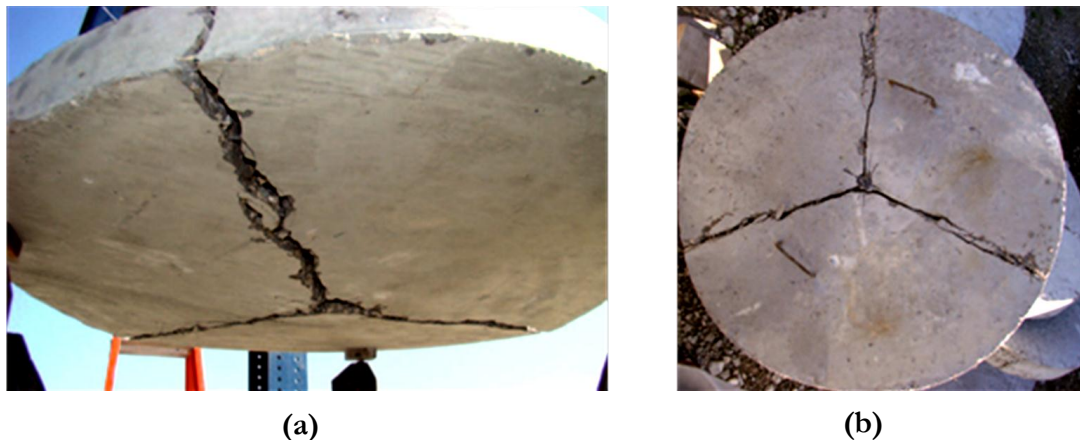


**Figure 3-13: (a) Profile and (b) Plan Views of Suggested Method of Deflection Measurement to Exclude Load-Train Deformations Using an LVDT (ASTM C1550 2010)**

The performance of specimens tested by ASTM C1555 is quantified in terms of the energy absorbed between the onset of loading and selected values of central deflection of the fiber-reinforced concrete panel. Test panels experience bi-axial bending in response to the central point load and exhibit a mode of failure that can be related to the in-situ behavior of structures. The energy absorbed is taken to represent the ability of an FRC to redistribute stress following cracking (ASTM C1550 2010). The single-operator coefficient of variation for peak load and energy absorption are reported as 6.2% and 10.1%, respectively; the multi-laboratory precision is approximately 9% for the same test parameters (ASTM C1550 2010).

The main advantage of ASTM C1550 over other test methods for FRC is that it appears to discriminate reasonably well between different fiber types and volumes, and does so with a higher degree of precision than other tests. Previous studies indicated that the variation in cracking load, peak load, or energy absorbed up to a specified central deflection from this test is generally lower than bending tests, with a COV between 5% and 13% (Bernard 2002, S.-H. Chao 2011). The reduced scatter in the results could be attributed to the following (S.-H. Chao 2011):

1. Location of cracks as well as crack patterns are less constrained: As seen in Figure 3-14 (a) and (b), panels tested by this method almost always split into three segments upon failure, at angles of about 120°.
2. Increased cracked area: the three major cracks give a somewhat average mechanical behavior of the reinforcement that minimizes the influence of non-uniform fiber distribution as well as random fiber orientation.



***Figure 3-14: View from (a) Below and (b) Above Tested Round Panel Specimen Showing Location of Major Cracks (S.-H. Chao 2011)***

The chief disadvantage of ASTM C1550 is that the specimen itself is too large and too heavy to be easily handled, and does not fit into commonly used test machines (Bentur

and Mindess 2007). Each specimen weighs about 200-lb [888-N], and as a result some previous tests were reportedly carried out at 80% scale of the specimen dimensions (S.-H. Chao 2011). Additionally, due to the size of the panel and nature of the test, a closed-loop servo-controlled test machine is required to avoid unstable behavior after cracking (ASTM C1550 2010).

As seen in Figure 3-15, another complication can occur if the crack opening at the center of the panel near the location of the LVDT exceeds the probe width of the LVDT (S.-H. Chao 2011). The probe can slip into the crack, resulting in errors in deflection measurements.



***Figure 3-15: View of Underside of ASTM C1550 Test Specimen showing Crack Width vs. LVDT Probe Width at Location of LVDT (S.-H. Chao 2011)***

In ASTM C1550, it is suggested that using an LVDT with a maximum probe width of 0.8-in. [20-mm] can alleviate this problem. Greater probe widths are not recommended because off-center cracks may induce exaggerated apparent deflections if they occur adjacent to a wide probe (ASTM C1550 2010). However, even if the maximum probe width is used, the opening at the center could be greater than 0.8-in. [20-mm] at large deflections, which may lead to incorrect measurements of displacement (S.-H. Chao 2011).

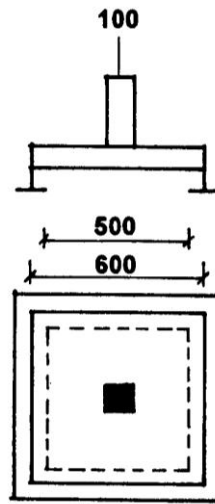
The size of the specimen, the need for a servo-controlled machine, and the intricate support fixtures required by ASTM C1550 combine to make this test method difficult. More effort is required to achieve the same results (with slightly better accuracy) as with other less complicated procedures.

### **3.1.5 Other Test Methods Proposed for Determination of the Toughness of FRC**

Among the many other test methods that have been proposed for the determination of the toughness of FRC, two are worth mentioning here.

#### ***3.1.5.1 EFNARC Panel Tests (Using Square Panel)***

The EFNARC square panel test is possibly the most widely known panel-based assessment procedure. Though often used in Europe as an alternative to beam-based toughness testing, it is rarely used in North America. ASTM C1550, the US alternative, correlates well with results from the EFNARC test (Bernard 2002, Bentur and Mindess 2007). Because shotcrete linings are often required to resist point loads, it is rational in some situations to quantify the performance of competing mix designs by applying a point load to a panel that represents a portion of a continuous lining (Bernard 2002). The EFNARC test involves the application of a central point load to a 4 x 24 x 24-in. [100 x 600 x 600-mm] square panel simply supported on a 20 x 20-in. [500 x 500-mm] flat square base (EFNARC 1996). The test specimen alone weighs about 200-lb. A simple schematic of this test is shown in Figure 3-16.



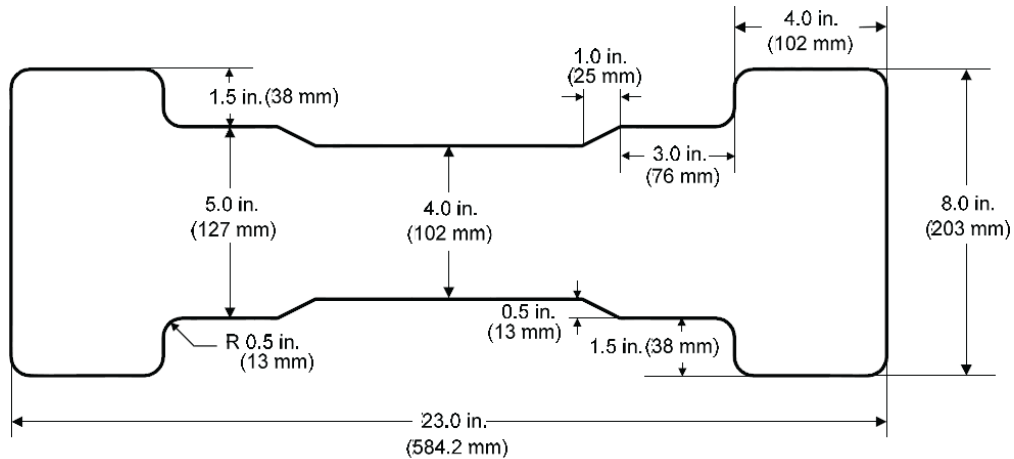
*Figure 3-16: Setup for EFNARC Panel Test (EFNARC 1996)*

Although this test is widely accepted in Europe and elsewhere, it suffers from a number of shortcomings. The most significant is the difficulty entailed in trying to produce a specimen with a perfectly planar base, so that the specimen will have simple and uniform support around the perimeter of the test fixture. Such a flat specimen typically produces a load-displacement curve with a single peak, and maximum possible performance is quantified in terms of energy absorption between the start of loading and a total central deflection of 1-in. [25-mm]. A specimen that is not flat will deform unpredictably, and will often display multiple peaks in load capacity as stress is redistributed around the progressively failing panel. This compromises the usefulness of the test (Bernard 2002).

### ***3.1.5.2 Uniaxial Direct Tensile Test***

A uniaxial direct tensile test can identify the key properties of FRC, such as strain-hardening or strain-softening, elastic modulus, and tensile stress-strain relationships, which are useful for modeling and design of FRC structural members (Naaman 2007). Currently, there is no standard method for this test in the U.S., in part because it is difficult to provide a gripping arrangement that precludes specimen cracking at the grips (S.-H. Chao 2011). Test

specimens have “dog-bone” geometry (Figure 3-17) with an overall length of 23-in. [584-mm], a uniform thickness of 4-in. [102-mm], a flange width of 8-in. [203-mm], and a web width of 4-in. [102-mm].

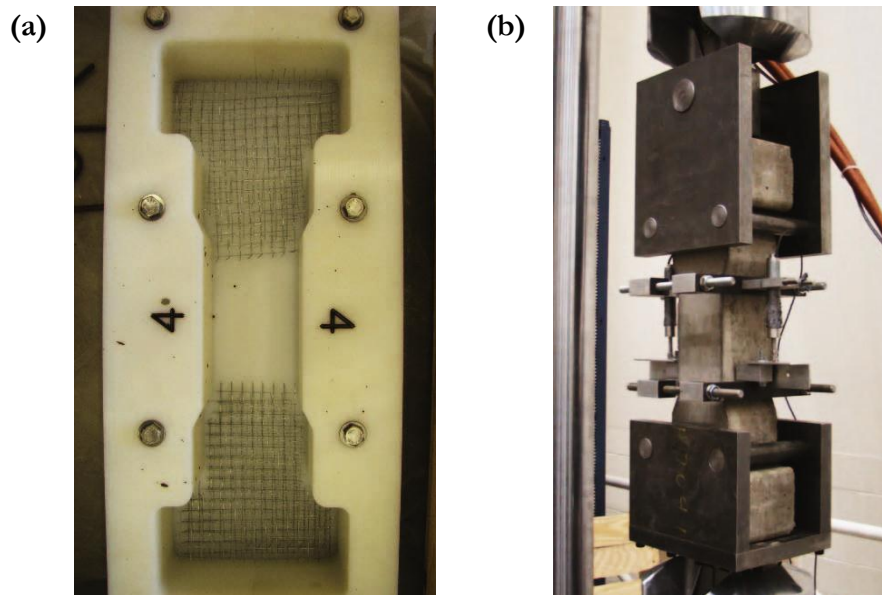


*Figure 3-17: Uniaxial Direct Tensile Test Specimen Dimensions (S.-H. Chao 2011)*

Specimens evaluated by this test method are specifically designed to create a pinned-pinned loading condition at the ends. The advantages of this end condition and specimen geometry are (S.-H. Chao 2011):

1. A pure axial load is applied in tension;
2. No specific treatment such as adhesives is needed to fix the ends to the test setup;
3. Both ends of the specimen are strengthened by steel meshes to ensure that cracking will occur only within the central portion.

Strains are measured by a pair of LVDTs with gauge lengths of about 7-in. [178-mm]. Tests can be facilitated using closed-loop, servo-controlled machine with a loading rate of approximately 0.002 inches per minute [0.05 mm/min] (S.-H. Chao 2011). Figure 3-18 (a) and (b) show the dog-bone mold and typical test arrangement for specimens.

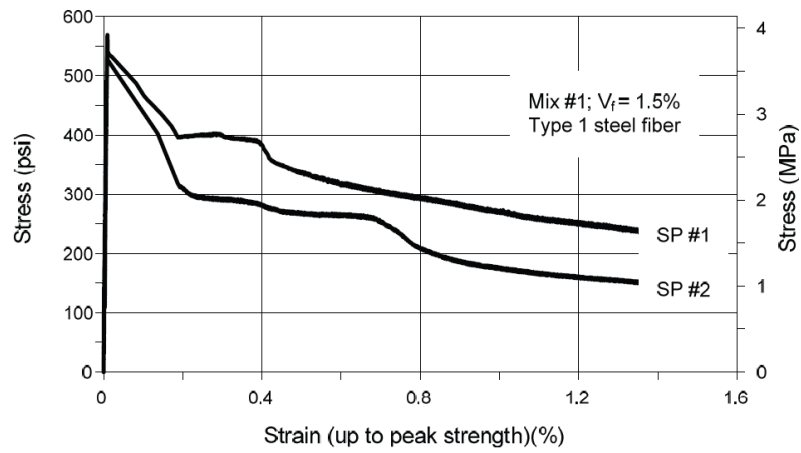


**Figure 3-18: Uniaxial Direct Tensile Test (a) Mold and (b) Testing Arrangement (S.-H. Chao 2011)**

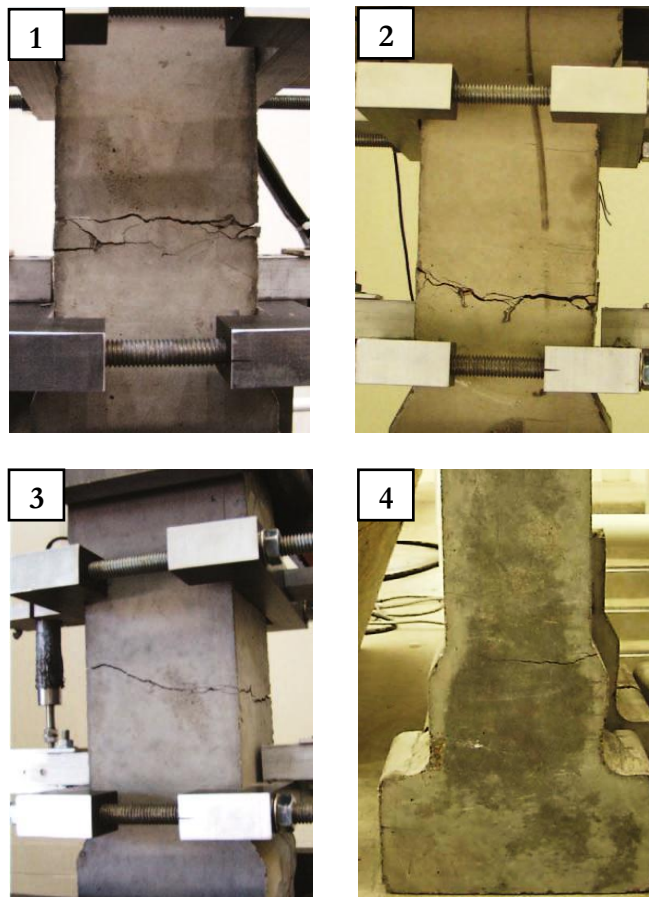
Unfortunately, the major drawback of this test (like others that constrain failure to a single major crack in a well-defined plane) is that it provides only a localized description of the FRC behavior, rather than an average or broad description. Figure 3-19 displays the typical response of two replicate tensile test specimens with 1.5% fiber content. Figure 3-20 shows the various locations of the major cracks in four replicate specimens. These images confirm that the dog-bone geometry and steel-mesh reinforcement at the ends generally do confine the major cracks to the narrow portion of the specimen. Crack locations are inconsistent, however, and crack-propagation paths are not controlled. As shown in Figure 3-19, this results in variable post-cracking response (S.-H. Chao 2011).

The Uniaxial Direct Tensile Test may become a more useful method with future improvements, but currently the large specimen size, requirement for a servo-controlled machine, and variability of crack location are complications.





*Figure 3-19: Replicate Specimen Results for Uniaxial Direct Tensile Test (S.-H. Chao 2011)*



*Figure 3-20: Variability of Uniaxial Tensile Test in Location of Major Cracks for Four Replicate Specimens with 1.5% Fiber Content (S.-H. Chao 2011)*

## 3.2 SUMMARY OF LIMITATIONS OF EXISTING TEST METHODS FOR FRC

Although many test methods are available for evaluating the properties of FRC, none is sufficiently simple, reliable, and reproducible. All current test methods fail to meet one or more of the recommended criteria for testing of FRC listed earlier in this chapter (Bentur and Mindess 2007). Each of the current test methods can be found wanting with respect to one or more of the following basic criteria: simplicity, reliability, and reproducibility.

### 3.2.1 Simplicity

Many existing test methods require test specimens that are difficult to fabricate or handle due to specialized formwork, size, weight (Figure 3-21), or curing regimen. In addition, some test methods require an intricate test arrangement for specimen support fixtures or electronic gauge mountings. Adding to the complexity is the need for a servo-controlled test machine, a rare commodity in many laboratories. Finally, elaborate test procedures, data corrections, and calculations drive other test methods away from simplicity.

### 3.2.2 Reliability

The theoretical basis for evaluating the results of a test method should be consistent with the actual behavior of the test specimen under load. However, this is not the case for some tests, which use elastic theory to evaluate plastic behavior. Furthermore, the high within-batch, single-operator coefficients of variation for key test parameters, which are common to many of the current test methods, suggests the need for more reliable methods.

Also, it is essential to understand that a failure mechanism restricted to a *single major crack* in a *well-defined* plane is disadvantageous. Because fibers are randomly distributed and oriented, the effects that they produce are not well represented by a test in which the failure location is constrained in this way. This disadvantage is amplified if the crack location also

varies between tests. Unfortunately, failures of this type are common to many of the current test methods and result in unreliable data since the load-deflection curves may not adequately describe composite behavior.

### **3.2.3 Reproducibility**

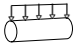
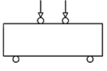
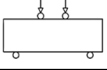
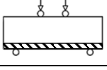
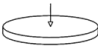

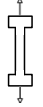
An ideal test method should be reproducible from laboratory to laboratory. Most existing FRC test methods, however, have high or undetermined inter-laboratory, multiple-operator coefficients of variation for key test parameters. In addition, specimen construction and handling as well as test procedures are often time consuming, making it strenuous or uneconomical to test a large number of specimens and obtain sufficient data for inter-laboratory studies.

## **3.3 SIDE-BY-SIDE COMPARISON OF CURRENT TEST METHODS**

As shown in Figure 3-21, over half of the current testing procedures require specimens heavier than 25-lb. Many researchers agree that specimens weighing more than that are difficult to carry and place in position for testing without the use of dollies, cranes, or other special equipment (S. Chao 2012). Manageable specimens are particularly desirable when testing multiple samples.

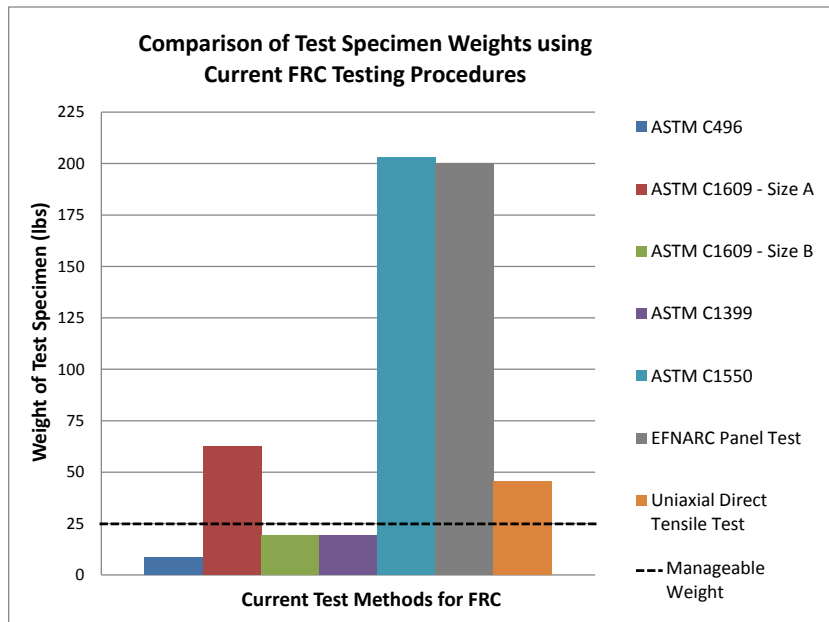
A side-by-side comparison of the test characteristics and factors that affect the simplicity, reliability, and reproducibility of current tests methods for FRC is provided in Table 3-1 and Table 3-2.

**Table 3-1: Test Specimens Required for Current FRC Testing Procedures**

TEST INFORMATION <sup>1</sup>		TEST SPECIMENS <sup>2</sup>			
Designation	Layout	Geometry	Dimensions (in.)	Volume (in. <sup>3</sup> )	Weight (lb)
ASTM C496		Cylinder	4" $\phi$ x 8	101	9
ASTM C1609		Rectangular Prism	6 x 6 x 20	720	63
ASTM C1609		Rectangular Prism	4 x 4 x 14	224	19
ASTM C1399		Rectangular Prism	4 x 4 x 14	224	19
ASTM C1550		Circular Panel	31.5" $\phi$ x 3	2338	203
EFNARC Panel Test		Square Panel	24 x 24 x 4	2304	200
Uniaxial Direct Tensile Test		Dog-bone	Various	524	45

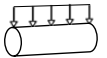
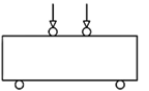
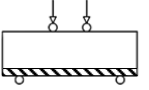
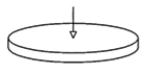
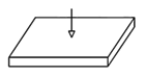
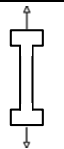
<sup>1</sup> Test layouts modified from (Molins 2006).

<sup>2</sup> Weight of test specimen calculated using average unit weight of FRC = 150 lb/ft<sup>3</sup>.



**Figure 3-21: Graphical Comparison of Specimen Weights for Current FRC Testing Procedures**

Table 3-2: Simplicity, Reliability, and Reproducibility of Current FRC Testing Procedures

TEST INFORMATION <sup>1</sup>		SIMPLICITY <sup>2</sup>				RELIABILITY <sup>3</sup>		REPRODUCIBILITY <sup>3</sup>
Designation	Layout	Specimen Fabrication & Handling	Test Setup & Support Fixtures	Test Procedure	Test Machine	Failure Mechanism	Within-Batch Precision (COV)	Inter-Laboratory Precision (COV)
ASTM C496		Easy	Easy	Easy	Standard	Single Major Crack	± 5% PL	Not Available
ASTM C1609		Moderate	Difficult	Moderate	Closed-Loop	Single Major Crack	± 8% PL ± 20% RS	Not Available
ASTM C1399		Moderate	Difficult	Difficult	Standard	Single Major Crack	± 20% RS	± 40% RS
ASTM C1550		Difficult	Difficult	Difficult	Closed-Loop	Multiple Cracks	± 6% PL ± 10% RS	± 9% PL ± 9% RS
EFNARC Panel Test		Difficult	Difficult	Moderate	Closed-Loop	Multiple Cracks	Not Available	Not Available
Uniaxial Direct Tensile Test		Difficult	Moderate	Moderate	Closed-Loop	Single Major Crack	Not Available	Not Available

<sup>1</sup> Test layouts modified from (Molins 2006).

<sup>2</sup> Complexity levels assigned based on literature and personal communication with researchers who conducted these and other similar tests (S. Chao 2012).

<sup>3</sup> Reliability and reproducibility data obtained from industry standards and research literature (ASTM C496 2011, ASTM C1609 2010, ASTM C1550 2010, ASTM C1399 2010, S.-H. Chao 2011, Bernard 2002). COVs for peak load and residual strength (toughness) are denoted (PL) and (RS), respectively.

### **3.4 RESEARCH SIGNIFICANCE**

Each of the current standardized and non-standardized test methods suffer from one or more limitations that make it impractical, unreliable, or inconsistent for evaluating the performance of FRC composites. This has negatively affected the acceptance of FRC applications into structural design codes. A more practical, reliable, and consistent test method is needed for evaluating the characteristics of FRC with different fiber types, fiber volume fractions, and mixture designs.

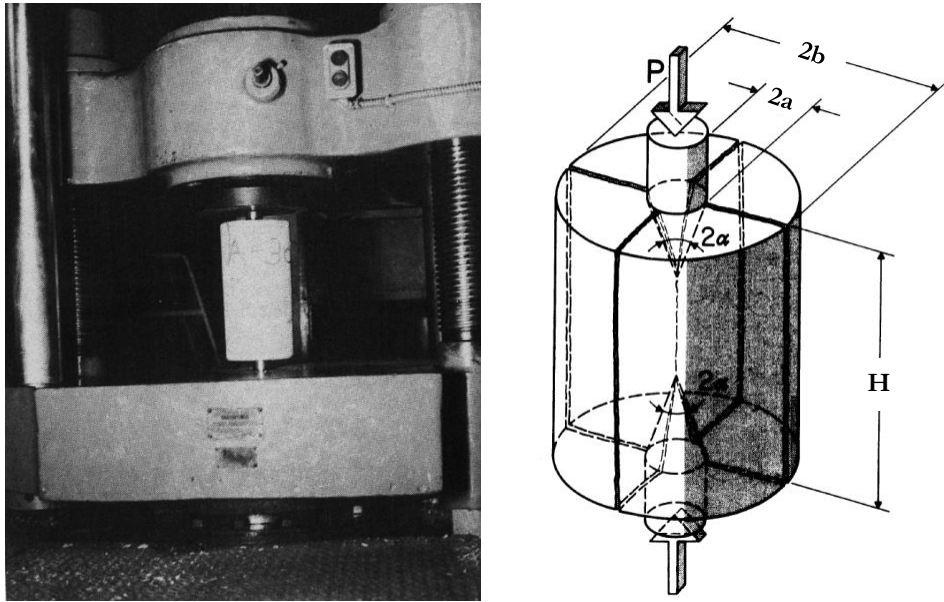
## CHAPTER 4

### DOUBLE-PUNCH TEST (DPT)

#### 4.1 INTRODUCTION

As discussed in the preceding chapter, the tensile strength and toughness of fiber-reinforced concrete can be determined from indirect tensile tests on cylinders (ASTM C496 2011), flexural tests on beams (ASTM C1609 2010, ASTM C1399 2010), centrally load-tested panels (ASTM C1550 2010, EFNARC 1996), or direct pull tests on dog-bone specimens (Chao 2011). Unfortunately, each of these tests suffers from a lack of simplicity, reliability, or reproducibility (alone or in combination). A better test method is needed. That need may be satisfied by the Double-Punch Test (DPT), originally proposed by Chen in 1970.

At the time of its introduction, the DPT was recommended as an alternative to the splitting tensile test for determining the tensile strength of *plain concrete*. As shown in Figure 4-1, in the Double-Punch Test, a concrete cylinder is placed vertically between the loading platens of the test machine and compressed by two steel punches located concentrically on the top and bottom surfaces of the cylinder (W. Chen 1970). It is hypothesized that the simplicity, procedure, and fracture mechanics of this test method make it a prime candidate for evaluating the tensile strength and inelastic behavior of *fiber-reinforced concrete*.

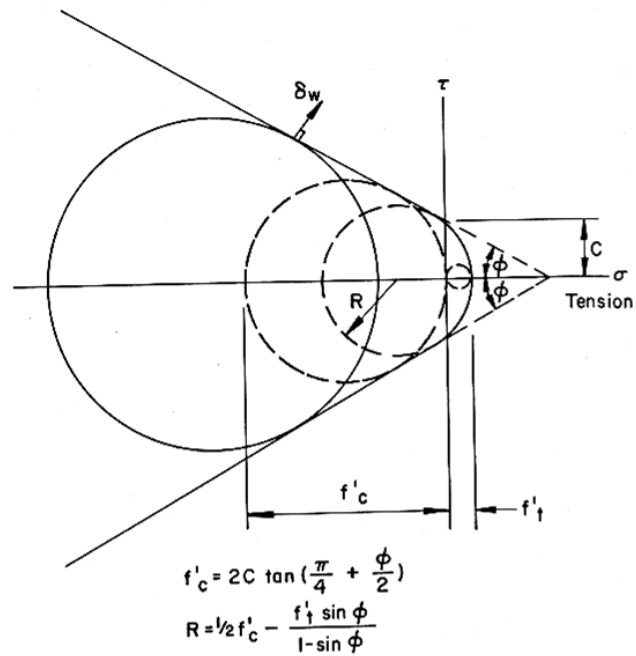


*Figure 4-1: Apparatus (W. Chen 1970) and Loading Schematic (Marti 1989) for the Double-Punch Test*

#### 4.1.1 Theory and Mechanics of the Double-Punch Test

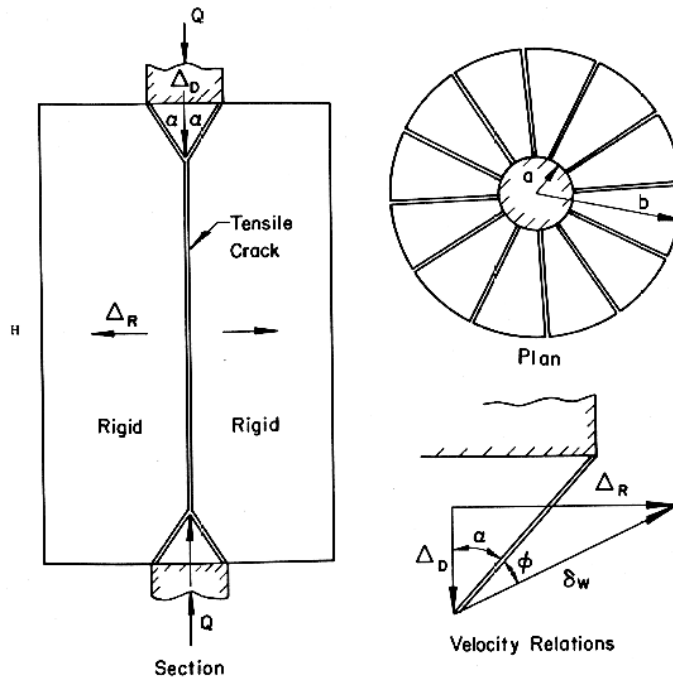
The fundamental theory and mechanics of the Double-Punch Test are based on the bearing capacity of concrete blocks (W. Chen 1969). A formula for computing the tensile strength of indirect tensile tests was obtained from the theory of linear elasticity and combined with a plasticity approach for concrete. This approach was based on the assumption that sufficient local deformability of concrete in tension and in compression existed such that generalized theorems of limit analysis could be applied to concrete idealized as a perfectly plastic material (W. Chen 1970). As shown in Figure 4-2, a Mohr-Coulomb failure surface in compression and a small but non-zero tension cut-off was used. Here  $f_c'$  and  $f_t'$  denote the simple compression and simple tension strength respectively,  $c$  is cohesion, and  $\phi$  is the symbol of internal friction of the concrete.





*Figure 4-2: Modified Mohr-Coulomb Criterion for Concrete (W. Chen 1970)*

Figure 4-3 shows a schematic of an ideal failure mechanism for a double-punch test on a cylinder specimen. It consists of many simple, radially oriented tension cracks and two conical rupture surfaces, each located directly beneath a steel punch. The conical shapes defined by those rupture surfaces move towards each other as rigid bodies, displacing the surrounding material radially. The relative velocity vector  $\delta w$  at each point along the conical rupture surface is inclined at an angle  $\phi$  to the surface of the cylinder (W. Chen 1970, Bortolotti 1988).



*Figure 4-3: Bearing Capacity of a Double-Punch Test (W. Chen 1970)*

Because the behavior of a concrete block during a bearing capacity test is closely related to the behavior of a double-punch test, the formula for the DPT was obtained directly from a simple modification of results reported for concrete blocks (W. Chen 1969, Bortolotti 1988). The working formula for computing the tensile strength in a Double-Punch Test was given by (W. Chen 1970):

$$f_t' = \frac{Q}{\pi(1.20 bH - a^2)} \quad \text{Equation 4-1}$$

Where:

- $f_t'$  = tensile strength, psi [kgf/cm<sup>2</sup>]
- $Q$  = ultimate load, lb. [kg]
- $H$  = cylinder height, in [cm]
- $b$  = cylinder radius, in [cm]
- $a$  = punch radius, in [cm]

It is important to note that earlier bearing capacity tests indicate that when the ratio  $\frac{b}{a}$  or  $\frac{H}{2a}$  is greater than approximately 4, the local deformability of concrete in tension is not sufficient to permit the application of limit analysis (W. Chen 1969). Consequently, for any ratio  $\frac{b}{a} > 4$  or  $\frac{H}{2a} > 4$ , the limiting value  $b = 4a$  or  $H = 8a$  should be used in Equation 2-1 for the computation of the tensile strength in a double-punch test. Equation 2-1 is also valid for the case of circular punches on a *square block* specimen. However, the restrictions on the limiting value of the ratio  $\frac{b}{a} = 4$  (specimen width/punch diameter) or  $\frac{H}{2a} = 4$  should be taken into account in a similar manner (W. Chen 1970).

The following example shows a typical Double-Punch Test calculation for the tensile strength of a plain concrete cylinder specimen:  $Q = 26,500\text{-lb}$  [12-kg],  $2a = 1.5\text{-in.}$  [3.80-cm],  $2b = 6\text{-in.}$  [15.30-cm], and  $H = 6\text{-in.}$  [15.30-cm].

$$f_t' = \frac{26,500}{\pi[1.20 \times 3 \times 6 - (0.75)^2]} = 402 \text{ psi } (\approx \frac{1}{11} f_c')$$

Table 4-1 shows the tensile strength computed from the results of a several Double-Punch Tests on 6-in. [15.30-cm] plain concrete cylinders with 1.5-in. [3.80-cm] diameter punches.

**Table 4-1: Tensile Strength Computed from Double-Punch Tests on Plain Concrete Cylinders – modified from (W. Chen 1970)**

Set	Make	Cylinder Height H, in. (cm)	Ultimate Load Q, kip (kg)	Tensile Strength $f_t'$ , psi (kgf/cm <sup>2</sup> )	$\frac{f_c'}{f_t'}$
1	Concrete	12 (30.60)	36.5 (16.6)	553 (38.8)	11.6
2		12 (30.60)	30.6 (13.9)	464 (32.5)	12.0
3		6 (15.30)	32.2 (14.6)	487 (34.1)	13.2
4		6 (15.30)	29.8 (13.5)	452 (31.7)	12.3
5		4 (10.2)	27.0 (12.3)	620 (43.4)	10.4
6		4 (10.2)	25.3 (11.5)	582 (40.8)	9.6

## **4.2 EXTENSION OF THE DOUBLE-PUNCH TEST TO EVALUATE THE MECHANICAL PROPERTIES OF FRC**

The extension of the Double-Punch Test for testing of FRC is a novel application of this test method. At the time of writing, the earliest use of DPT for FRC was reported in 2007 by Molins *et al.* in Barcelona, Spain. Previous research showed that the Double-Punch Test resulted in lower coefficients of variation compared to beam tests on FRC (Molins and Aguado 2009). However, further experimental and theoretical work was recommended to determine the extent of this test to the characterization of tensile properties of fiber-reinforced concrete.

The Double-Punch Test is thought to be easily applied and advantageous to testing FRC based on the following test characteristics:

1. Test Setup & Procedure
2. Cracking Pattern & Damage
3. Correlation with FRC Structure

Each of these will be discussed separately in the following sections.

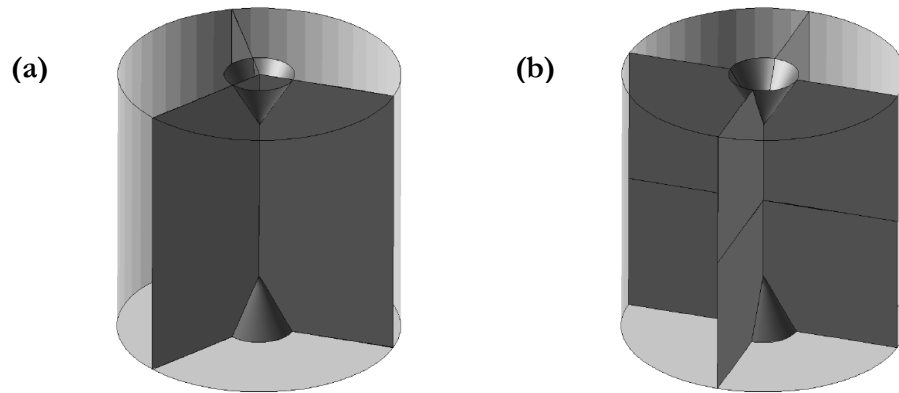
### **4.2.1 Test Setup & Procedure**

One of the primary reasons the Double-Punch Test was thought to be a reasonable substitution for the split-cylinder test was its simple testing arrangement and procedure. Indirect tensile tests enable similar specimens and the same testing machine to be used for both tensile and compressive strength tests. Many of the drawbacks of direct pull tests, such as the difficulty in eliminating eccentricity and complicated gripping devices, are overcome by loading the specimen in compression. In addition, indirect tensile tests give more consistent results with the measured strengths lying between those measured using bending and direct tensile tests (W. Chen 1970).

Many of the current test methods for FRC require specialized formwork, heavy specimens, or intricate testing supports and arrangements. Moreover, a closed-loop, servo-controlled testing machine is often necessary. The Double-Punch Test is conducted using an easily handled 6 x 6-in. [15.30 x 15.30-cm] cylinder specimen weighing about 15-lb [6.80-kg]. Since specimens are tested in compression (indirect tension), any universal testing machine (UTM) can be used to facilitate the test: UTMs of some type (screw-gear or hydraulic) are available at most, if not all, testing laboratories. Simple mounting of LVDTs of appropriate gauge lengths on the UTM is sufficient for recording deflection measurements. The simplified testing arrangement and straightforward procedure of the DPT makes this method attractive for testing of fiber-reinforced concrete.

#### **4.2.2 Cracking & Damage**

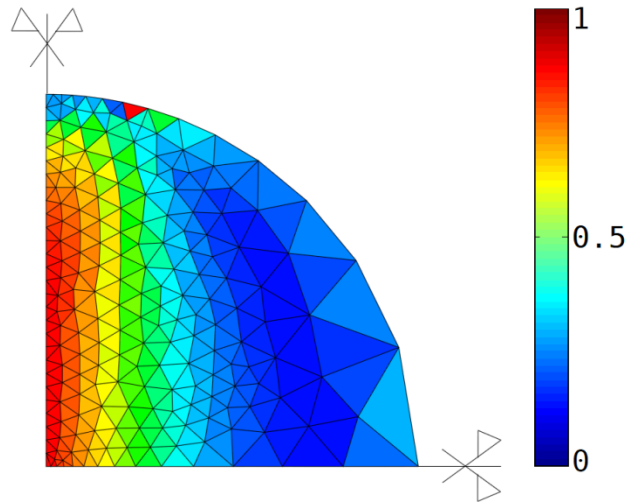
Similar to the split-cylinder test, the DPT is an indirect tension test but does not confine failure to a predetermined plane (Pros, Diez and Molins 2010, W. Chen 1970). Typically, three to four radial cracks occur as indicated in Figure 4-4. The applied load gives rise to an almost uniform tensile stress over the planes containing the cylinder axis, and the specimen splits across these planes similar to the split-cylinder test. Ultimately, an average mechanical behavior is obtained due to the multiple crack surfaces that develop from the DPT.



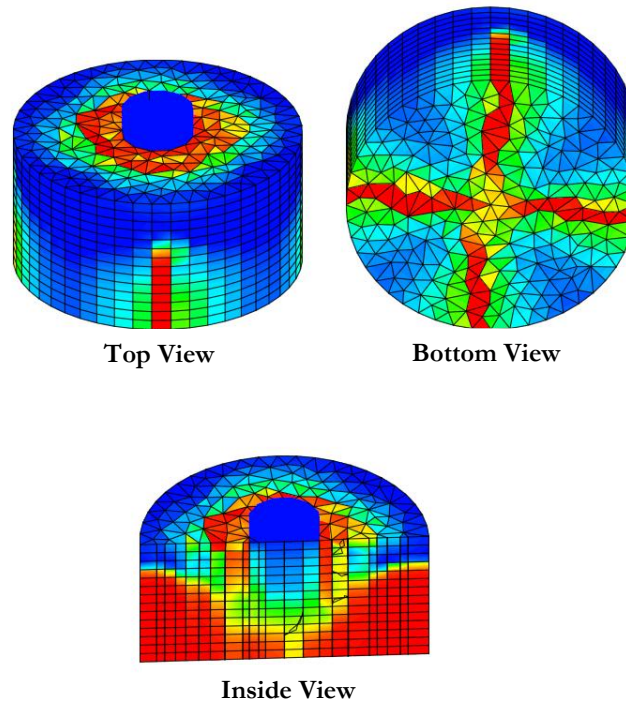
**Figure 4-4: Two Possible DPT Collapse Mechanisms with (a) Three and (b) Four Radial Fracture Planes (Pros, Diez and Molins 2010)**

The difference between a *single major crack* and the *multiple cracking* pattern of the DPT can be seen in Figure 4-5 (a) and (b) which compare the damage profiles for split-cylinder and double-punch loading on plain concrete cylinders, respectively. The damage profile of the split-cylinder test is similar to current test methods for FRC that result in a single plane of failure. In the damage scale, for  $D = 0$ , the material is considered healthy and if  $D = 1$ , the material is completely damaged (Pros, Diez and Molins 2010). It is clear that the DPT results in intense damage at discrete locations.

(a) Split-Cylinder Test



(b) Double-Punch Test



*Figure 4-5: Damage Profiles for (a) Split-Cylinder Test and (b) Double-Punch Test Loading on Plain Concrete Cylinders (Pros, Diez and Molins 2010)*

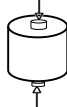
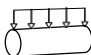
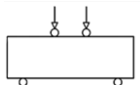
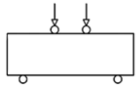
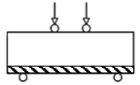
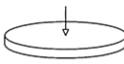
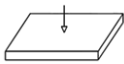
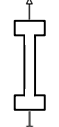
### 4.2.3 Correlation with FRC Structure

The cracking pattern of the Double-Punch Test is preferred over a *single crack* in a *well-defined* plane which is common to many of the current testing methods for FRC. Since the fiber dispersion and orientation is random, increasing the number of fracture planes, and more importantly the specific failure surface of a test specimen, increases the probability that fibers will indeed intersect crack planes. Thus, the effect of the fiber-reinforcement, which distinguishes FRC from other concrete mixtures, is more likely to be captured.

The specific failure surface  $\beta$  can be defined as the total failure surface area per unit volume of a test specimen. Numerically, it represents the fractured plane or planes that manifest when a specimen reaches failure for a given test method. As shown in Table 4-2, a specimen tested using the DPT has a higher specific failure surface ( $\beta$ ) than specimens tested by any other test method for FRC. The ratio  $\beta_{\text{DPT}}/\beta_{\text{TEST}}$  is provided in the last column of Table 4-2 to compare the specific failure surface of the DPT to that of current testing procedures. It is shown that the Double-Punch Test can result in a specific failure surface up to an order of magnitude higher than other test methods. This data supports the idea that the failure mechanism of the DPT should result in reliable data for fiber-reinforced concrete specimens, particularly in the post-cracking region where fiber performance dominates the composite behavior.

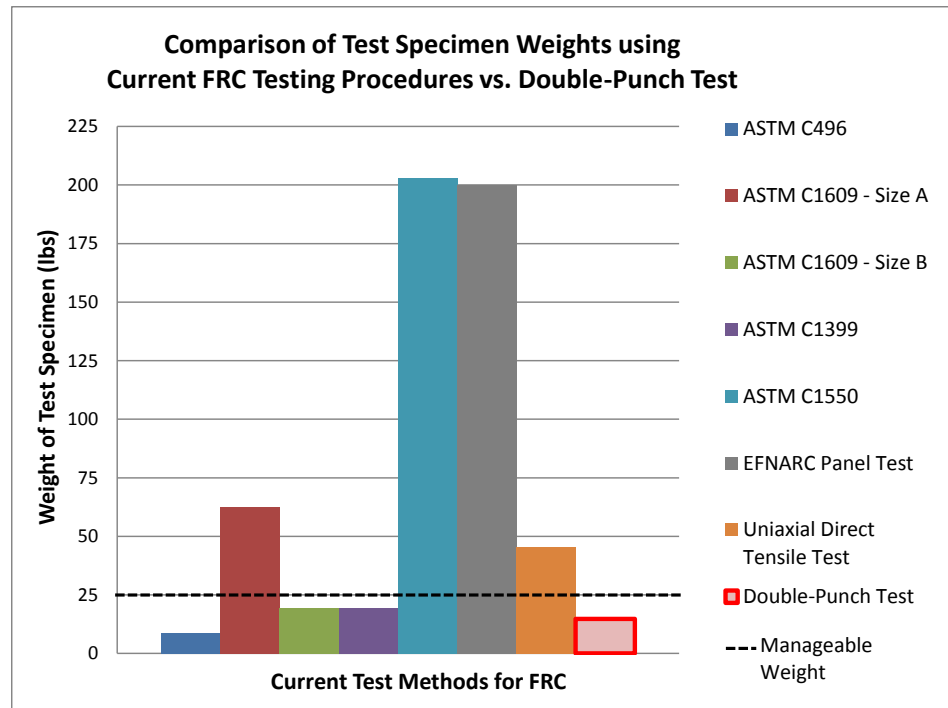


*Table 4-2: Comparison of the Specific Failure Surface of Test Specimens for Current FRC Test Methods vs. Double-Punch Test*

TEST INFORMATION <sup>1</sup>		TEST SPECIMENS				
Designation	Layout	Volume (in. <sup>3</sup> )	Number of Failure Planes	Failure Surface Area (in. <sup>2</sup> )	Specific Failure Surface, $\beta$	$\beta_{DPT} / \beta_{TEST}$
Double-Punch Test		170	3	54.0	0.318	1
ASTM C496		101	1	12.6	0.125	3
ASTM C1609		720	1	36.0	0.050	6
ASTM C1609		224	1	16.0	0.071	4
ASTM C1399		224	1	16.0	0.071	4
ASTM C1550		2338	3	141.8	0.061	5
EFNARC Panel Test		2304	3	144.0	0.063	5
Uniaxial Direct Tensile Test		524	1	16.0	0.031	10

<sup>1</sup> Test layouts modified from (Molins 2006).

In addition to the fact that the DPT produces a higher specific failure surface area than any of the current test methods for FRC, the weight of the specimen required to conduct the test is manageable. As shown in Figure 4-6, the 6 x 6 in. DPT cylinder specimen weighs less than all of the specimens required for current test methods for FRC. It very similar to the cylinder specimen required for the Split Cylinder Test (ASTM C496).



*Figure 4-6: Comparison of Test Specimen Weights for Current FRC Testing Procedures vs. Double-Punch Test*

### 4.3 SUMMARY

Based on previous research on both plain and fiber-reinforced concrete, the test arrangement, procedure, specimen size and cracking pattern of the DPT method clearly indicate that the test should be useful for evaluating the elastic and plastic behavior of FRC. The DPT will, by nature, result in a large failure surface area which correlates better with the random distribution and orientation of fibers in FRC composites. Furthermore, it is speculated that the DPT may prove to be more convenient and reliable than current test methods for fiber-reinforced concrete. In order to confirm these hypotheses, the DPT Research and Testing Program was organized at the University of Texas at Austin to determine the effectiveness of the double-punch method for evaluating the mechanical properties of FRC.

## CHAPTER 5

### DPT RESEARCH AND TESTING PROGRAM OUTLINE

#### 5.1 INTRODUCTION

The main objectives of *this portion* of Study 6348, previously stated in Chapter 1, include the following:

1. Quantify the influence of mix compositions, fiber types, and fiber volume fractions on the mechanical characteristics of FRC;
2. Develop test protocols for comparing the effectiveness of steel fiber-reinforced concrete mixtures with different fiber types and volume fractions;
3. Supply intra- and inter-laboratory data and observations useful for comparing the Double-Punch Test with current test methods for FRC.

Again, the central focus of the DPT Research and Testing Program at UT Austin is to produce sufficient within-batch, intra-laboratory data to make conclusions and recommendations regarding the simplicity, reliability, and reproducibility of the Double-Punch Test when applied to steel fiber-reinforced concrete.

#### 5.2 DPT PROGRAM ORGANIZATION

The experimental program was conducted in two phases. Test variables include fiber manufacturer and type, fiber volume fraction, specimen surface preparation, and testing machine. As shown in the testing matrix provided in Figure 5-1, the most significant difference between **PHASE 1** and **PHASE 2** is the fiber manufacturer. Royal™ (domestic) steel fibers are used in the first series of tests, whereas Bekaert Dramix® (foreign) steel fibers are used in the second round of testing. Also, in **PHASE 2**, the specimen surface preparation

variable was eliminated based on results obtained from **PHASE 1** which indicated that surface preparation was not a distinguishing factor in the experiment. Thirty 6 x 12-in. cylinders were cast in each phase.

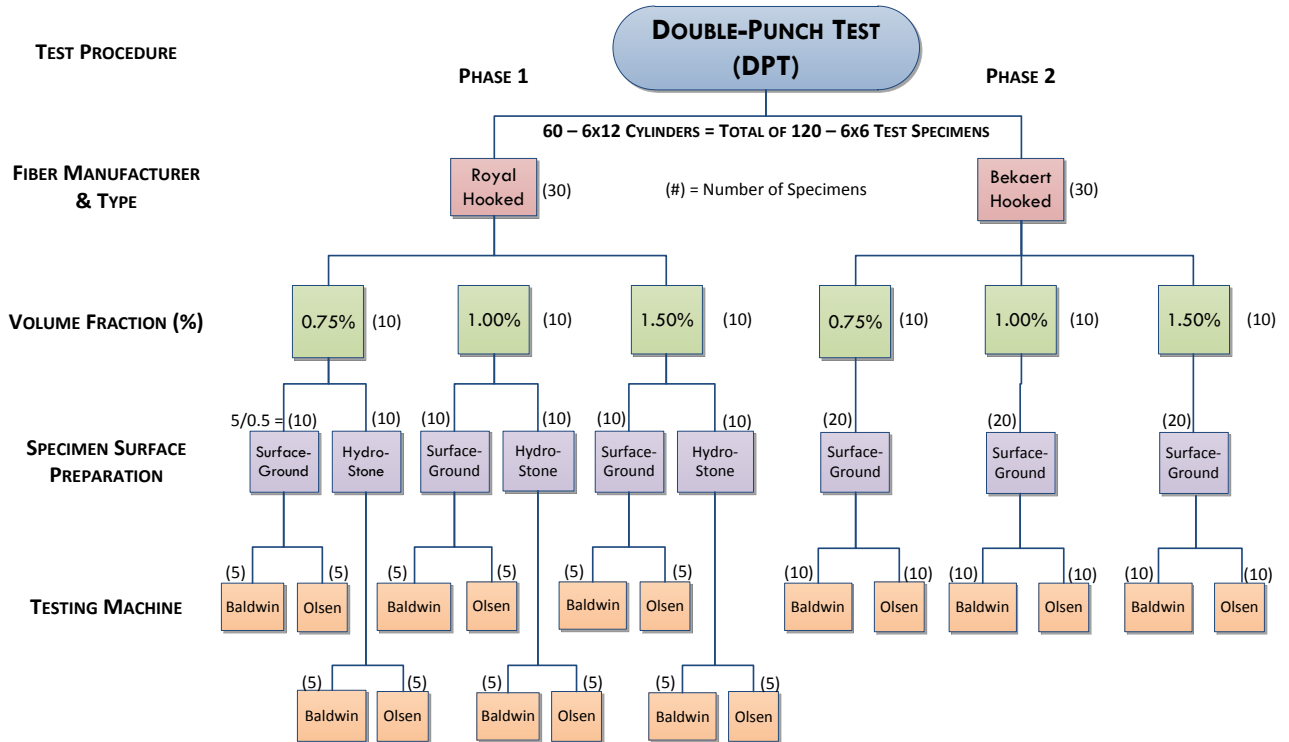
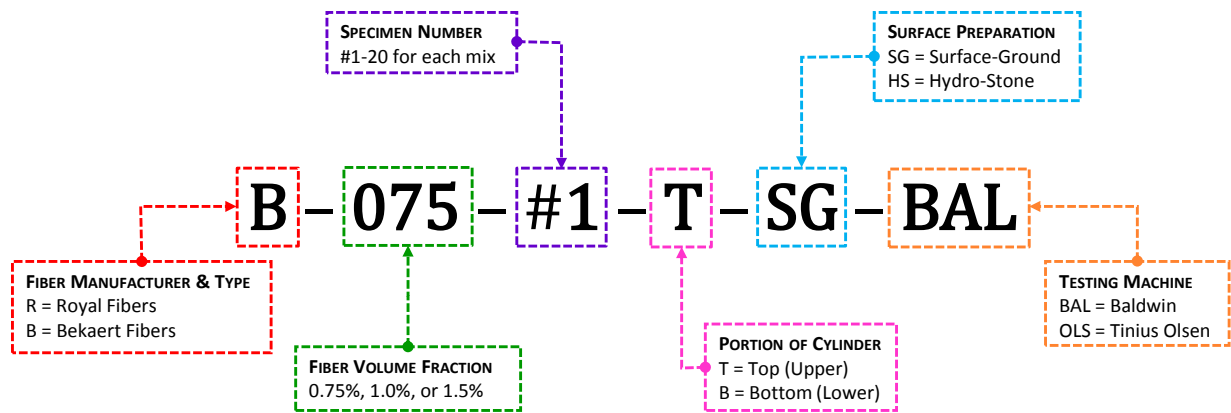


Figure 5-1: Testing Matrix for DPT Research and Testing Program

### 5.2.1 Nomenclature used to Identify Test Specimens

The thirty 6 x 12-in. steel fiber-reinforced concrete cylinders that were cast in each phase were cut in half to obtain 120, 6 x 6-in. specimens for the DPT Research and Testing Program. Because of the large number of test variables, each 6 x 6-in. test specimen was uniquely identified according to the nomenclature provided in Figure 5-2.

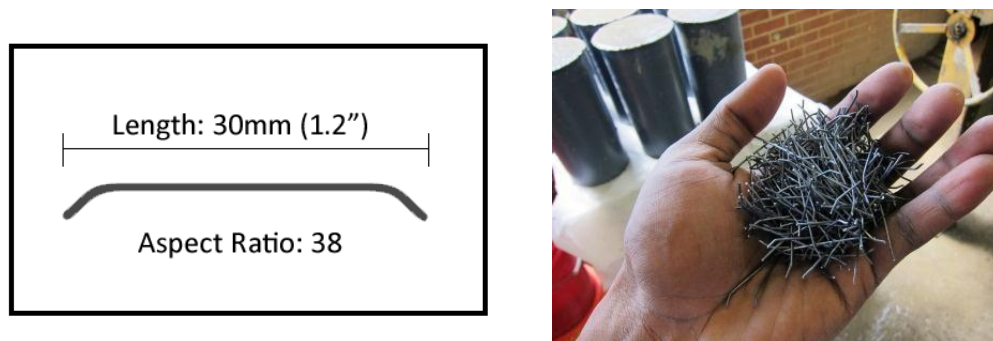


*Figure 5-2: Nomenclature used to Identify Specimens for DPT Research and Testing Program*

### 5.3 DPT PROGRAM MATERIALS

#### 5.3.1 Steel Fibers

Both US-made (domestic) and foreign steel fibers were used in the testing program. Royal™ fibers are commonly used in SFRC applications in the United States and were selected as the domestic fiber in **PHASE 1** of this study. These fibers are manufactured from cold-drawn, low-carbon steel wire, and are designed to enhance concrete performance such as average residual strength, toughness, and impact resistance. As shown in Figure 5-3, the Royal™ fibers have a hooked geometry, are 1.2-in. [30-mm] long, and have an aspect ratio of 38.



*Figure 5-3: Royal™ Steel Fibers*

Bekaert is a major international fiber manufacturer, and is recognized as a leader in fiber technology. Bekaert Dramix® fibers were employed in **PHASE 2** of the current study. Similar to the Royal™ fibers, Bekaert Dramix® fibers are cold-drawn steel wire with hooked ends for optimum anchorage. As shown in Figure 5-4, these fibers are approximately 1.37-in. [35-mm] long, and have an aspect ratio of 65.



*Figure 5-4: Bekaert Dramix® Steel Fibers*

Figure 5-1 provides a side-by-side visual comparison of the two fiber types used in this study.



*Figure 5-5: Royal vs. Bekaert Fiber Type*

The fiber volume fraction, or fiber content, is denoted as a percentage of the total volume of freshly mixed concrete. The weight of fibers added to the concrete mix was calculated using the given fiber content, total volume of concrete, and the unit weight of steel as shown in Equation 5-1:

$$\text{Steel Fiber (lb)} = \frac{\text{Fiber VF (\%)}}{100} * \text{Total Volume of Concrete (ft}^3\text{)} * 490 \frac{\text{lb}}{\text{ft}^3} \quad \text{Equation 5-1}$$

*Note 5-1: The DPT Research and Testing Program is meant to evaluate the DPT method. It is **not intended** to compare the performance of the different fibers used in this study. Royal™ and Bekaert Dramix® fibers were chosen arbitrarily to determine the ability of the Double-Punch Test to distinguish between FRC composed of different fiber types and volume fractions.*

### 5.3.2 Concrete Mix Design & Procedure

To produce the number of specimens required for the DPT Research and Testing Program, six separate concrete mixtures were batched and mixed using a standard drum mixer. Although batches varied by fiber type and fiber content, the mixture proportions shown in Table 5-1 were used throughout. The cement, sand, and coarse aggregate used were Alamo Type I/II, Colorado River Sand, and Martin Marietta crushed limestone, respectively. Prior to mixing, the sand and coarse aggregate were lightly coated with water in the drum mixer. Samples were removed from these constituents and oven dried. The moisture content was determined, and adjustments were made to the mix quantities to satisfy saturated-surface-dry (SSD) conditions.

**Table 5-1: Concrete Mixture Proportions**

Cement	Sand	Coarse Aggregate	Water	Total
1.00	2.00	2.25	0.50	5.75

\* Proportions based on 2.5 ft<sup>3</sup> of concrete.

Mixture proportions and mixing procedure affect the microstructure of the final SFRC produced. Fiber performance can be maximized by using well-graded aggregates and high fines content; however this was not done in the DPT Research and Testing Program because this research is focused on evaluating the test method itself. In this case, the aggregate gradation is not important as long as each batch is proportioned identically. To ensure consistency between mixes, quantities were corrected based on SSD and the concrete was mixed using the following sequence recommended by researchers at UT Arlington.

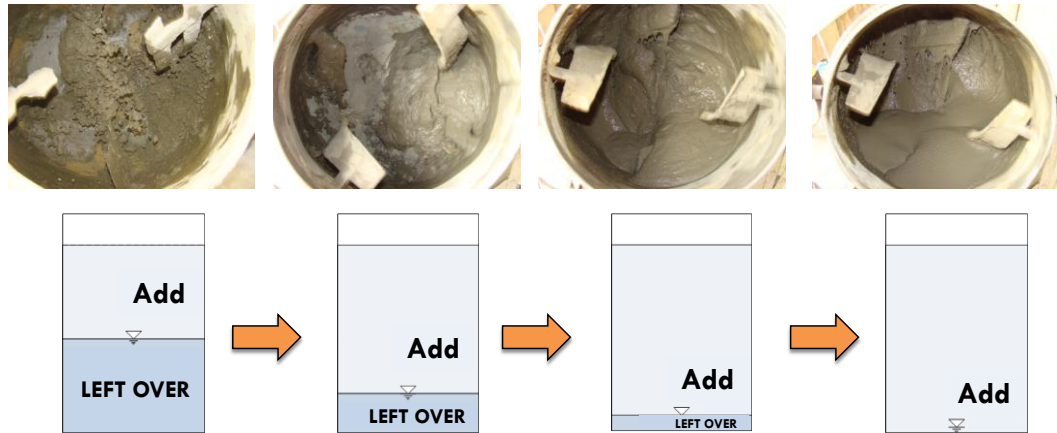
- **Step 1:** Calculate weight of materials based on concrete mix proportions and correct for SSD conditions.
- **Step 2:** Place cement and sand into mixer. Mix for about 3 minutes.



*Figure 5-6: SFRC Mixing Sequence, Step 2*

- **Step 3:** Add water in phases, mixing for about 30 seconds between each addition.





*Figure 5-7: SFRC Mixing Sequence, Step 3*

- **Step 4:** Add coarse aggregate. Mix for about 3 minutes and visually inspect mixing status.



*Figure 5-8: SFRC Mixing Sequence, Step 4*

- **Step 5:** Add steel fibers. Mix for about 3 minutes and visually inspect mixing status. Ensure uniform mixing by breaking up “clumped” or “balled” fibers (Figure 5-10).



*Figure 5-9: SFRC Mixing Sequence, Step 5*



*Figure 5-10: Example of “Clumping” and “Balling” of Fibers Observed During Mixing*

- **Step 6:** Measure concrete fresh properties (slump and unit weight).



*Figure 5-11: SFRC Mixing Sequence, Step 6*

- **Step 7:** Place concrete into 6 x 12-in. cylinder molds, consolidate concrete by tapping with steel rod and placing on vibrating table for 1 to 2 minutes.



*Figure 5-12: SFRC Mixing Sequence, Step 7*

- **Step 8:** Cap cylinder specimens. Cure in mixing room at 73°F for first 24 hours, strip cylinder molds, and place in curing chamber (fog room) at 73°F and 100% relative humidity until testing date.



*Figure 5-13: SFRC Mixing Sequence, Step 8*

Table 5-2 (a) and (b) provides the batch quantities and fresh and hardened concrete properties of the SFRC mixtures used to create the DPT test specimens.

**Table 5-2: (a) Batch Quantities and (b) Fresh and Hardened Concrete Properties of SFRC Mixtures used in DPT Experiments**

(a)

Mix Number	Mix ID	Cement (lbs/ft <sup>3</sup> )	Coarse Aggregate (lbs/ft <sup>3</sup> )	Sand (lbs/ft <sup>3</sup> )	Water <sup>1</sup> (lbs/ft <sup>3</sup> )	Steel Fiber (lbs/ft <sup>3</sup> )
1	R-075	67.3	154.5	138.0	31.8	9.2
2	R-100	67.3	154.8	137.0	26.3	12.6
3	R-150	67.3	156.2	139.9	28.6	18.9
4	B-075	94.7	218.7	194.7	43.8	11.4
5	B-100	90.8	209.2	185.7	43.2	14.4
6	B-150	90.8	208.7	186.7	42.7	21.6

<sup>1</sup> Water content was adjusted for SSD conditions

(b)

Mix Number	Mix ID	w/cm	Slump (in)	Unit Weight (lbs/ft <sup>3</sup> )	28-Day Strength <sup>2</sup> (psi)	Modulus of Elasticity (psi)
1	R-075	0.47	10.50	147	5531	4.38E+06
2	R-100	0.39	3.25	149	6635	4.88E+06
3	R-150	0.42	5.00	150	6439	4.85E+06
4	B-075	0.46	8.25	146	5634	4.37E+06
5	B-100	0.48	7.50	146	5164	4.20E+06
6	B-150	0.47	5.50	147	4753	4.05E+06

<sup>2</sup> Avg. 28-day Compressive Strength reported was back-calculated using ACI-209 equations for mix-IDs R-075, R-100, and R-150. Actual cylinders were tested at 35-days for these mixes.

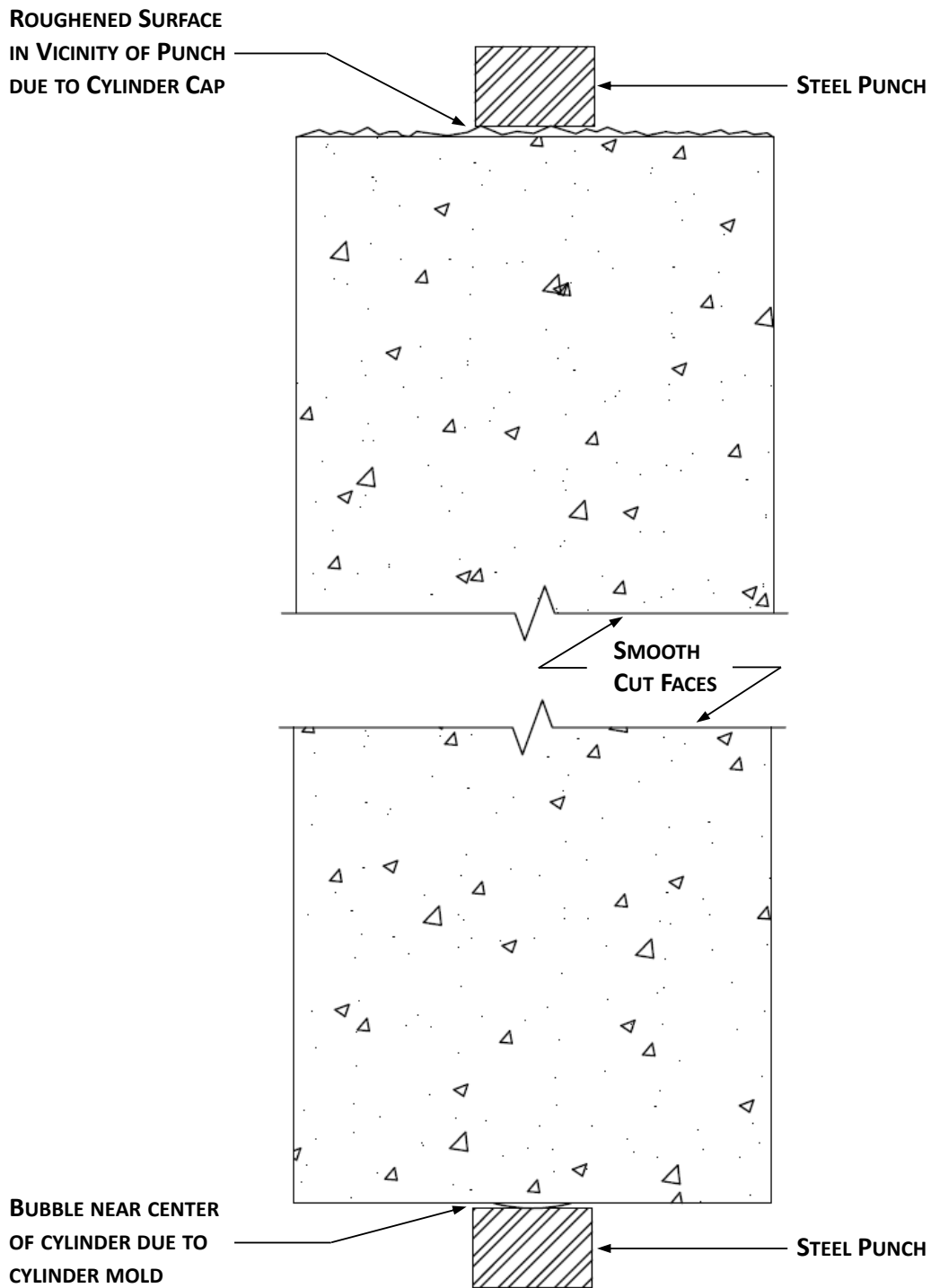
### 5.3.3 Specimen Preparation

In the Double-Punch Test, specimens are loaded in concentric axial compression through two steel punches. It is important that the steel punches lay flat against the test machine and concrete cylinder surfaces, because smooth contact between these surfaces will generate the most uniform loading possible.



*Figure 5-14: Using Wet-Saw to Cut 6 x 12-in. Cylinder in Half*

As seen in Figure 5-14, 6 x 6-in. test specimens were prepared by cutting the cast 6 x 12-in. cylinders in half using a heavy-duty concrete wet-saw. Once cut in half, only the cut face of the specimen is guaranteed to be smooth in the area where the steel punch will be located. As shown in Figure 5-15, the top and bottom faces of the cast 6 x 12-in. concrete cylinder have uneven surfaces due to the cylinder cap and cylinder mold, respectively.



*Figure 5-15: Schematic showing Surface Roughness on Top and Bottom Surfaces of Cylinder due to Mold*

This can cause an uneven distribution of stress under the area of the punch. Furthermore, the net effect of the defect on the stress distribution could vary between specimens, and result in increased variation in experimental measurements. For this reason, the surfaces of the test specimens were refinished to provide a smooth contact area in the vicinity of the steel punches. Two methods were employed: (1) surface grinding the top and bottom faces, and (2) applying a thin layer of Hydro-Stone to the rough faces prior to testing. The latter was selected to determine if satisfactory results could be obtained without grinding, since some laboratories may not have equipment capable of surface grinding the ends of 6-in. diameter cylinders.

Specimens refinished by surface grinding were milled using a Gilson Concrete Cylinder End Grinding machine. As shown in Figure 5-16, this machine is capable of producing a smooth testing surface for cylinders up to 6 in. in diameter.



***Figure 5-16: Surface-Grinding (SG) Uneven Faces of Test Specimens***

Other specimens were refinished by applying Hydro-Stone to the uneven area under the punch location as illustrated in Figure 5-17. A small amount of Hydro-Stone was placed on the steel punch and the cylinder was carefully placed on top using a guide. Upon

hardening, the Hydro-Stone produces a smooth layer that allows for uniform contact with the steel punches.

1. Hydro-Stone mixture placed on steel punch surface area.



2. Cylinder gently placed on steel punch using constructed guide to ensure punch location coincides with centroidal axis of test specimen.



3. Cylinder removed from guide and set aside to allow thin layer of Hydro-Stone to solidify. Process repeated for other side of test specimen.



*Figure 5-17: Process of Applying Hydro-Stone to Rough Faces of Test Specimen*



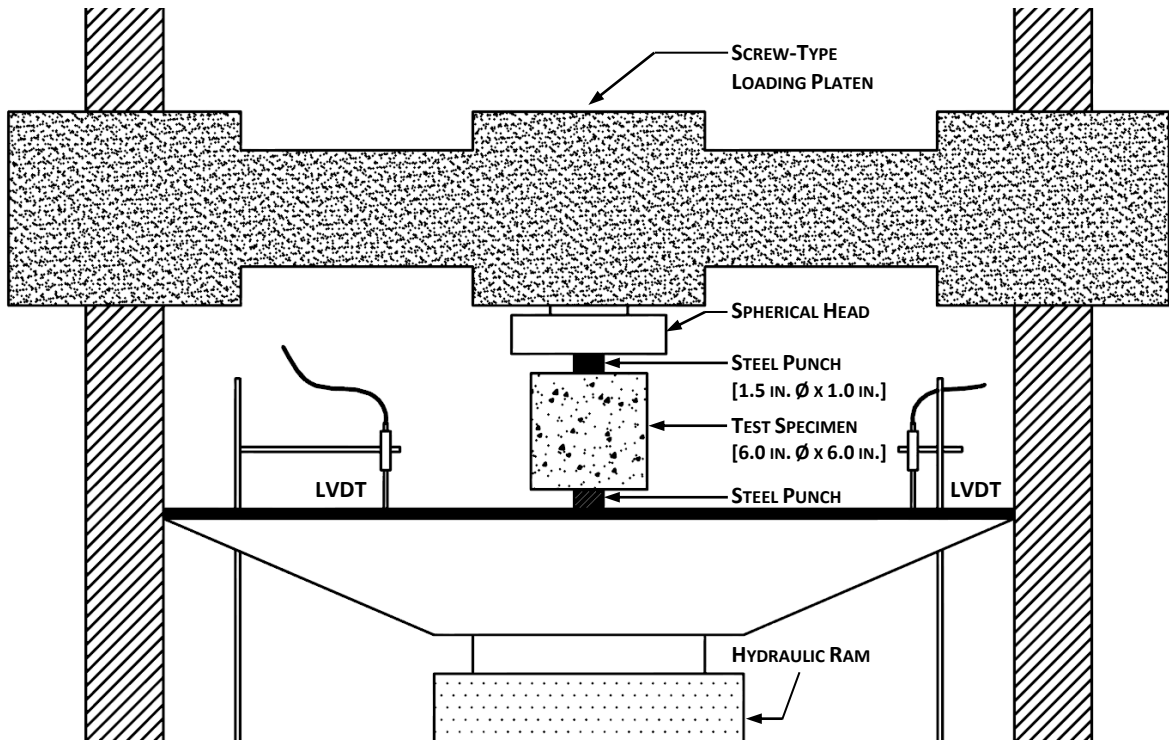
## 5.4 DPT PROGRAM TESTING

### 5.4.1 Test Setup & Equipment

After the test specimens were cut to size and refinished using Hydro-Stone or surface grinding, they were ready to be placed in the test frame for the Double-Punch Test. To assess the reliability of the DPT for different testing equipment, two universal test machines (UTM) were used: (1) 60-kip capacity Baldwin UTM and (2) 120-kip capacity Tinius Olsen UTM. Half of the test specimens from each batch were tested using the Baldwin machine, and the other half were tested on the Olsen machine. The same basic setup was used in each arrangement. Each setup consisted of the following:

- *Spherical Head* - to compensate for any unevenness of the specimen cut, ground, or Hydro-Stone faces;
- *Steel Punches* - two 1.0 x 1.5-in. diameter steel punches cut from a section of 75 ksi tool steel;
- *LVDTs* - two linear variable differential transducers (LVDTs) of 2.0-in. stroke to measure vertical displacement of the DPT test specimen. Displacement was taken as the average of the two measurements;
- *PDAQ* - load and deflection data was recorded using a data acquisition system and LabView software.

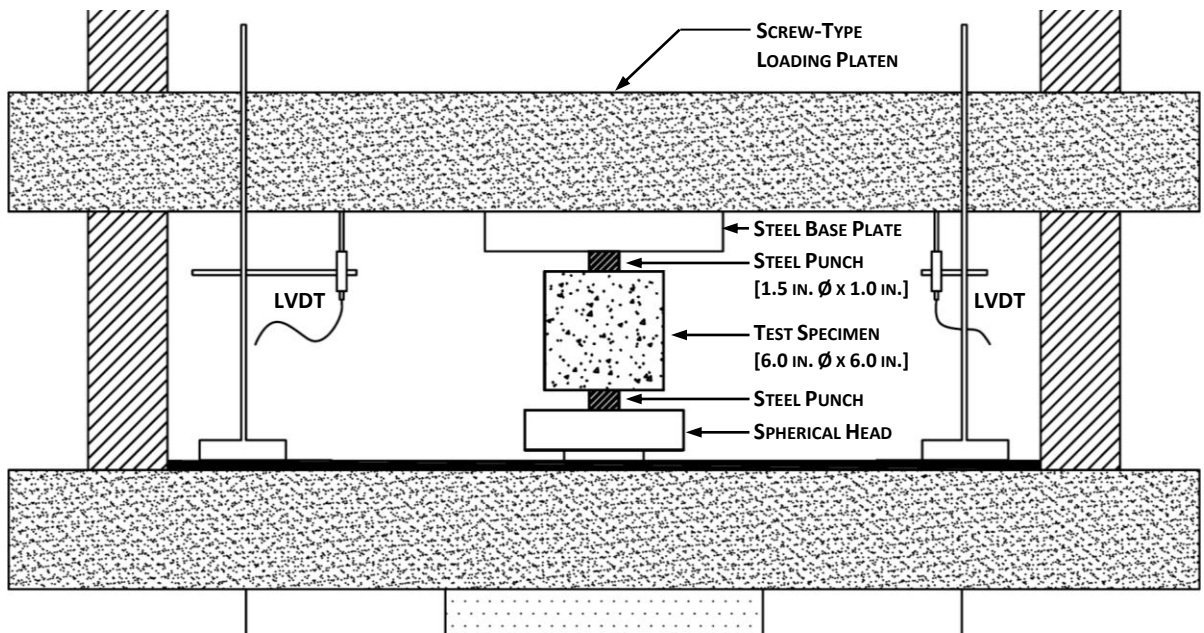
Schematics and photographs of the testing arrangements used on the Baldwin and Olsen UTMs are provided in the following figures.



*Figure 5-18: Schematic of DPT Arrangement on 60-kip Baldwin UTM (Hydraulic)*



*Figure 5-19: DPT Setup on 60-kip Baldwin UTM (Hydraulic)*



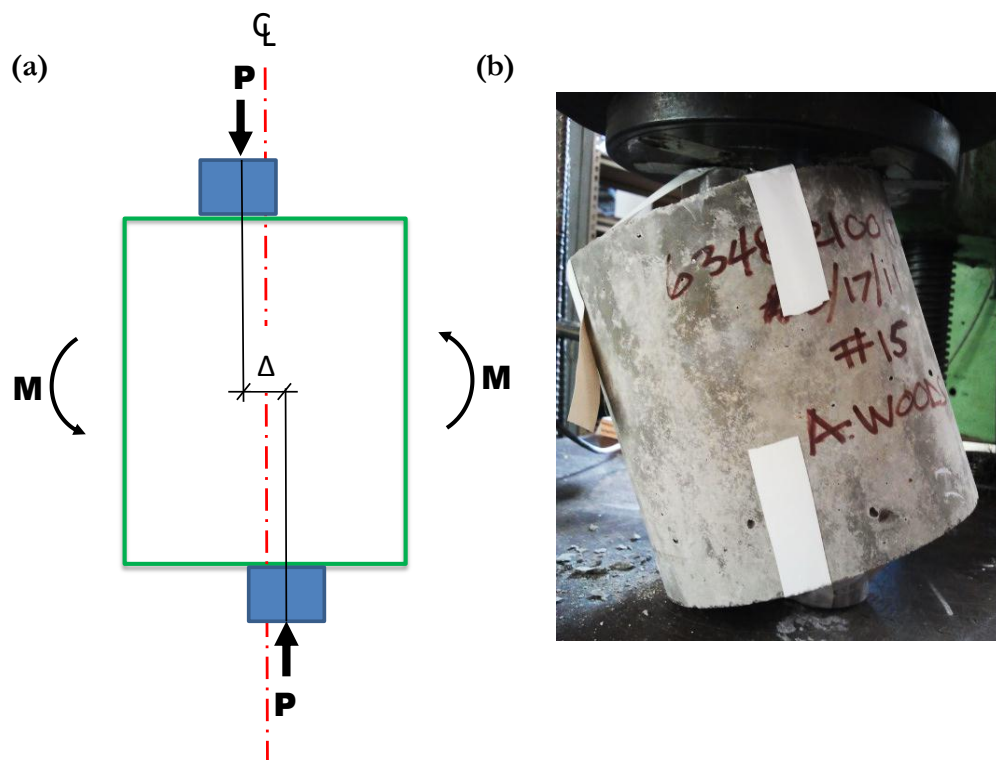
*Figure 5-20: Schematic of DPT Arrangement on 120-kip Olsen UTM (Screw-Type)*



*Figure 5-21: DPT Setup on 120-kip Olsen UTM (Screw-Type)*

### 5.4.2 Testing Procedure for DPT

As described in Chapter 4, in the Double-Punch Test, a 6 x 6-in. cylindrical concrete specimen is placed vertically between the loading platens of the test machine and compressed by two steel punches located concentrically on the top and bottom surfaces of the specimen. This loading produces radial transverse tension in the specimen. Although the DPT is simple, centering and seating of the steel punches prior to taking load-deflection measurements is critical. Centering of the punches is necessary to avoid placing a moment on the specimen due to eccentric load. As shown in Figure 5-22, if the punches are misaligned, the specimen can topple during loading due to the overturning force. Results obtained under these conditions are meaningless, and are disregarded.



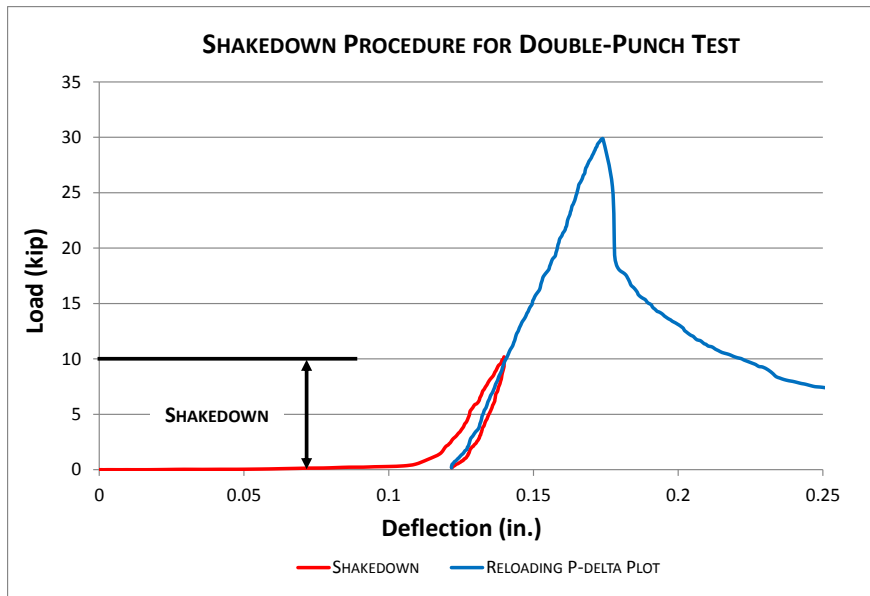
*Figure 5-22: Effect of Misaligned Steel Punches in DPT shown (a) Schematically and (b) for Trial Specimen*

Even a small degree of misalignment can result in this behavior, and simple measures were used to guard against the effects of eccentric loading. For one, a punch centering guide was constructed to ensure adequate placement of the punches on the DPT specimen. Secondly, the punches were strapped to the specimen using masking tape for additional security against slipping or sliding of the steel punches during placement and loading. Finally, a spherical loading head was used to compensate for any unevenness of the DPT specimen produced from cutting, grinding, or Hydro-Stone.



**Figure 5-23: Steel Punch Centering Guide and Masking Tape Used to Secure Against Eccentric Loading Effects**

In addition to alignment, the steel punches must be seated into the specimen. As shown in Figure 5-24, during the initial loading stage, the effect of the steel punches seating into the concrete can be seen in the curved ascending branch of the load-deflection plot. This initial non-linearity indicates the *seating process*. To correct for the seating of the punches, a “shakedown” loading sequence was employed: DPT specimens were loaded up to 10 kips, unloaded, and then reloaded to failure. In this way, the steel punches are set into the concrete and the appropriate *linear-elastic* behavior up to first crack was obtained by using a corrected zero reading corresponding to the end of the shakedown.



**Figure 5-24: Schematic of Shakedown Procedure for DPT Experiments**

All specimens were carefully prepared and placed into the loading apparatus. Once positioned, each DPT specimen was tested according to the following sequence:

1) *Shakedown (Initial Loading and Unloading to Seat Punches)*

- Load the specimen at a rate of 100 lb/sec [445 N/sec]  $\pm$  25 lb/sec [ $\pm$  111 N/sec] up to a load of 10 kips [44.5 kN].
- Unload the specimen at a rate between 100 and 300 lb/sec [445 and 1334 N/sec] to a load between 100 lb [445 N] and 200 lb [890 N].
- The deflection at that final load is termed the “initial deflection offset.”

2) *Reloading*

- Load the specimen at a rate of 100 lb/sec [445 N/sec]  $\pm$  25 lb/sec [ $\pm$  111 N/sec].
- Note the corresponding rate of applied deformation.
- Load at that deformation rate until the first radial crack appears in the top or bottom face of the specimen.

3) *End Point*

- Continue loading at a rate between 1.0 and 3.0 times the pre-cracking deformation rate until the deformation reaches or exceeds 0.5 in. [13 mm], or the steel punches are almost fully penetrated into the specimen.
- Do not permit the loading head of the testing machine to contact the specimen.

4) *Data Recording*

- Record the applied load and the deflection of the loading head at approximately 1-second time intervals.

### 5.4.3 Calculation of Key Test Parameters

The corrected load-deflection plot was obtained, and key test parameters were assigned in order to determine how the fiber type, volume fraction, surface preparation, and test machine affect the DPT results. This was done by the following process:

1) *Correct Deflections*

- Subtract the “initial deflection offset” from each deflection reading during the reloading phase. The resulting deflections are termed “corrected deflections.”

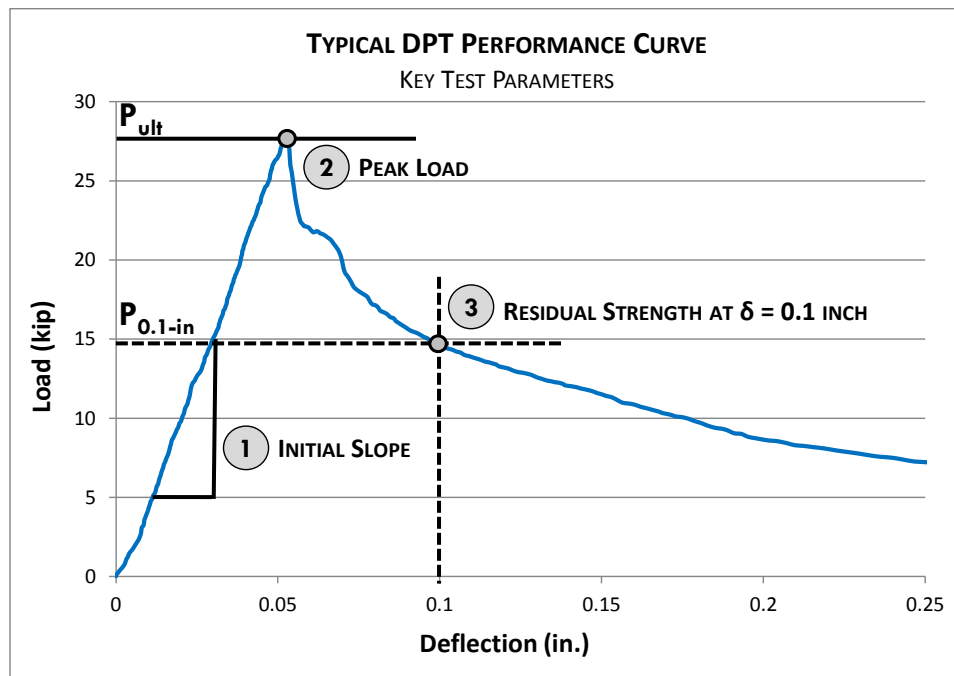
2) *Calculate Key Test Parameters*

Using the recorded loads and the corrected deflections, calculate and report the initial slope, peak load, and residual strength, as follows:

- **Initial Slope:** Evaluate the initial slope as the slope between applied loads of approximately 5 kips [22 kN] and 15 kips [67 kN].
- **Peak Load:** Evaluate the maximum load directly.

- **Residual Strength:** Evaluate the residual load at a corrected deflection of 0.1 in.  $\pm 0.01$  in. [ $2.5 \text{ mm} \pm 0.025 \text{ mm}$ ].

The key parameters are shown graphically in Figure 5-25: (1) initial slope, (2) peak load, and (3) the residual strength at a deflection of 0.1 in. With these values, the elastic modulus, ultimate tensile strength, and toughness can be calculated, respectively, and the performance of mixtures with different fiber types and volume fractions can be compared. Ultimately, these parameters summarize the behavior of steel fiber-reinforced concrete.



*Figure 5-25: Typical DPT Performance Curve showing Key Test Parameters*

The initial slope was calculated between 5 and 15 kips because this range represents the most stable portion of the ascending branch. It was very difficult to control the rate of loading up to 5 kips and beyond about 20 kips due to sensitive dials on the testing equipment. The initial slope represents a tangent stiffness, and was taken in the specified region to avoid potential errors introduced by variations in loading rate.



The key test parameters were evaluated statistically to assess the reliability and reproducibility of the Double-Punch Test, as well as its ability to accurately describe the performance of steel fiber-reinforced concrete. This information is presented in the following chapter.

## CHAPTER 6

### DPT RESEARCH AND TESTING PROGRAM RESULTS

#### 6.1 OVERVIEW OF RESULTS

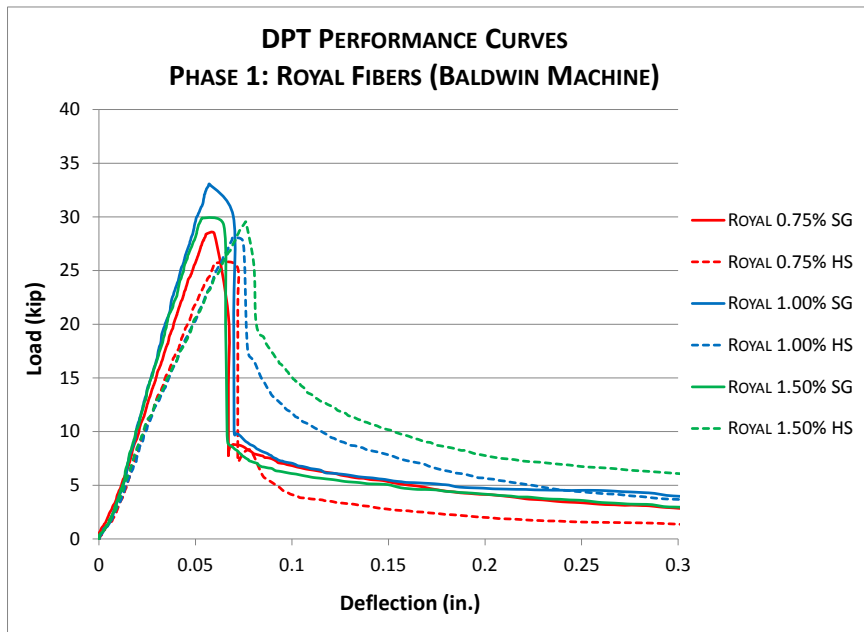
The goal of the DPT Research and Testing Program was to produce sufficient within-laboratory data to make conclusions and recommendations regarding the Double-Punch Test for evaluating FRC. In this chapter, the results of 120 tests on steel fiber-reinforced concrete specimens are summarized. *Selected* DPT Performance Curves from experiments will be presented to show the range of behavior observed during testing. *Typical* statistical analysis results will also be provided to explain the effects of test variables on DPT results. The complete set of (120) DPT Performance Curves as well as Phase 1 and 2 statistical analysis results are available in Appendix A and B, respectively.

#### 6.2 DPT PHASE 1 RESULTS

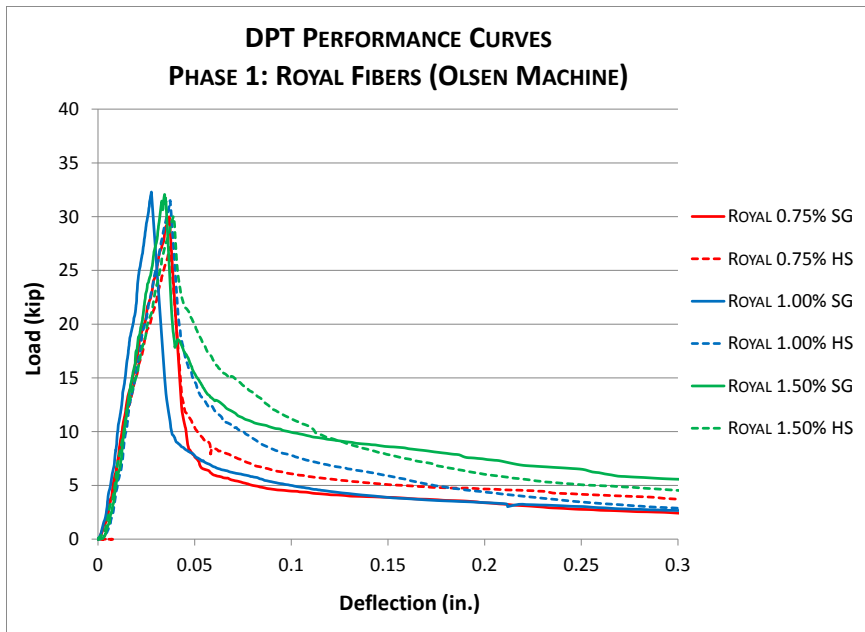
The age at the time of testing was 54 days on average for the 60 specimens tested during Phase 1 of the program. Averages for key test parameters are provided in Table 6-1, and selected performance curves for specimens tested on the Baldwin and Olsen machines are displayed in Figure 6-1 and Figure 6-2, respectively. Photographs of typical cracking and damage of specimens are also provided in Figure 6-3.

**Table 6-1: Phase 1 – Royal Fibers**

Test Machine	Testing Group	Number of Tests	Avg. Initial Slope (kips/in)	Avg. Peak Load (kips)	Avg. Residual Strength at $\delta=0.1$ in. (kips)
<i>Baldwin</i>	R-075	10	534	27	7
	R-100	10	788	30	9
	R-150	10	532	30	14
<i>Olsen</i>	R-075	10	1106	29	6
	R-100	10	1042	30	7
	R-150	10	1051	31	14



**Figure 6-1: Phase 1 - Selected DPT Performance Curves for Royal Fibers on Baldwin Machine**



*Figure 6-2: Phase 1 - Selected DPT Performance Curves for Royal Fibers on Olsen Machine*



*Figure 6-3: Phase 1 - Typical Damage and Cracking Pattern of DPT Specimens with Royal Fibers*

### 6.2.1 Discussion of Results

The averages of the key parameters as well as the selected performance curves for specimens tested in Phase 1 agree with the expected behavior of SFRC. As the fiber volume fraction increases, the initial slope and peak load are unaffected; however, the residual strength increases noticeably. There is also an unexpected difference in the initial slope

(stiffness) for specimens tested on the Baldwin versus Olsen UTMs. In general, specimens with surface-ground (SG) and Hydro-Stone (HS) surfaces performed similarly, but there is a change in initial slope for HS specimens after about 10 kips; this result will be explained in the forthcoming statistical analysis.

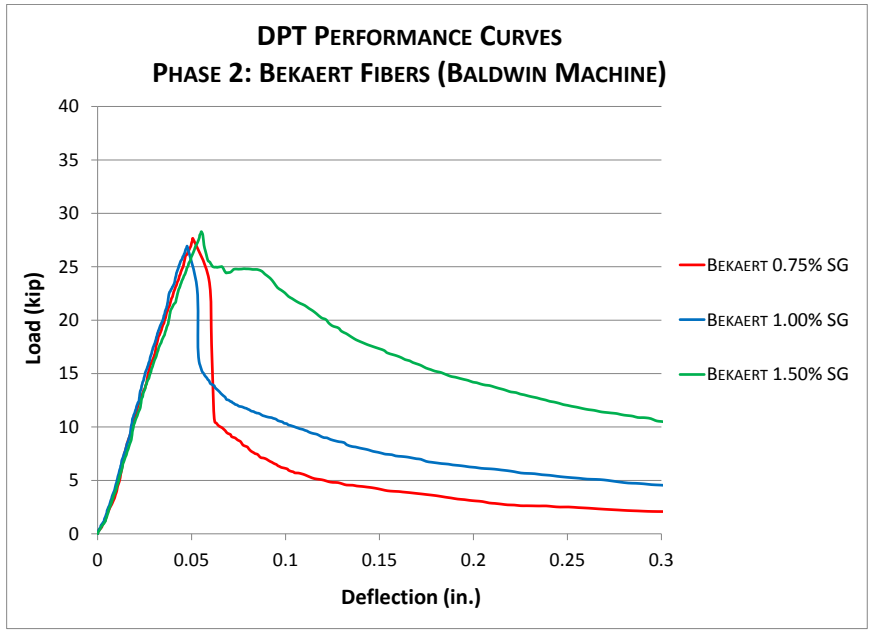
As shown in Figure 6-3, typical failure of SFRC specimens containing Royal™ fibers agreed with the fracture mechanics approach previously mentioned for DPT loading. Cracks formed along three or four radial planes.

### 6.3 DPT PHASE 2 RESULTS

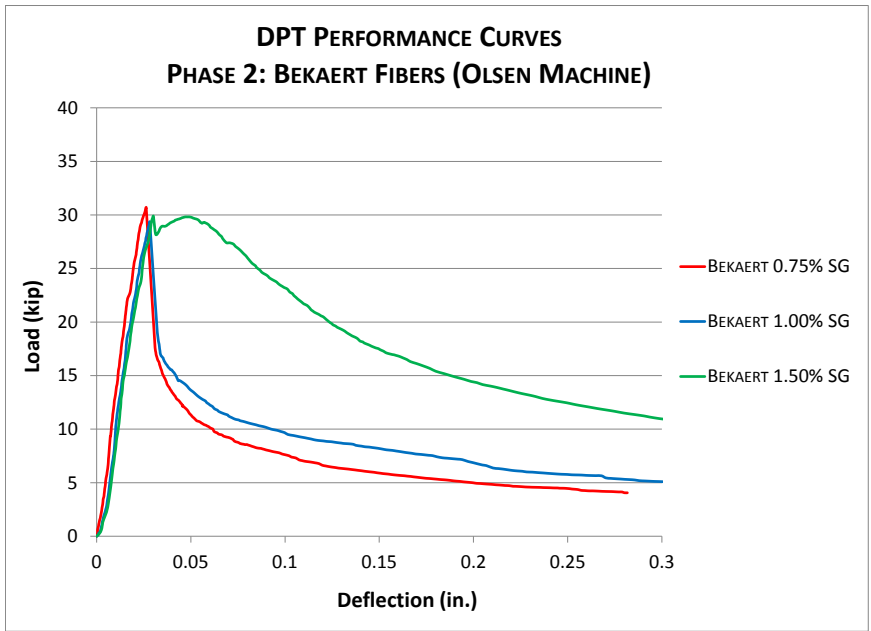
The average age at the time of testing was 63 days for the 60 specimens tested during Phase 2 of the program. Averages for key test parameters are provided in Table 6-2, and selected performance curves for specimens tested on the Baldwin and Olsen machines are displayed in Figure 6-4 and Figure 6-5, respectively. Photographs of typical cracking and damage of specimens tested in Phase 2 are shown in Figure 6-6.

*Table 6-2: Phase 2 – Bekaert Fibers*

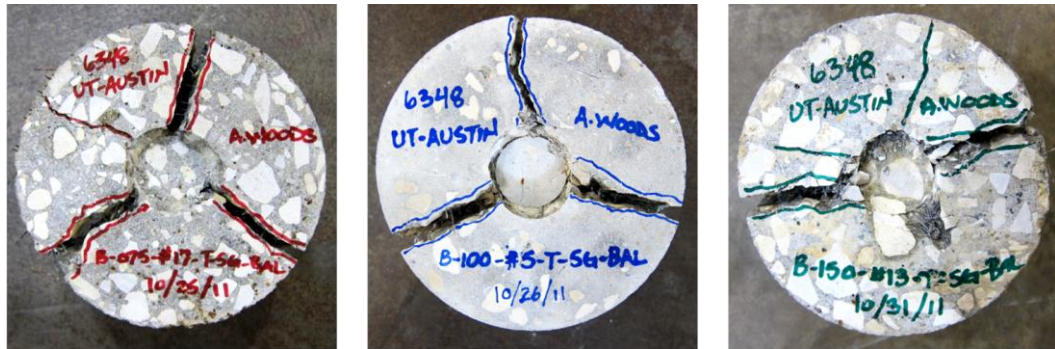
Test Machine	Testing Group	Number of Tests	Avg. Initial Slope (kips/in)	Avg. Peak Load (kips)	Avg. Residual Strength at $\delta=0.1$ in. (kips)
<i>Baldwin</i>	B-075	10	632	28	10
	B-100	10	644	27	11
	B-150	10	647	28	22
<i>Olsen</i>	B-075	10	1292	30	10
	B-100	10	1316	28	11
	B-150	10	1313	29	19



*Figure 6-4: Phase 2 - Selected DPT Performance Curves for Bekaert Fibers on Baldwin Machine*



*Figure 6-5: Phase 2 - Selected DPT Performance Curves for Bekaert Fibers on Olsen Machine*



*Figure 6-6: Phase 2 - Typical Damage and Cracking Pattern of DPT Specimens with Bekaert Fibers*

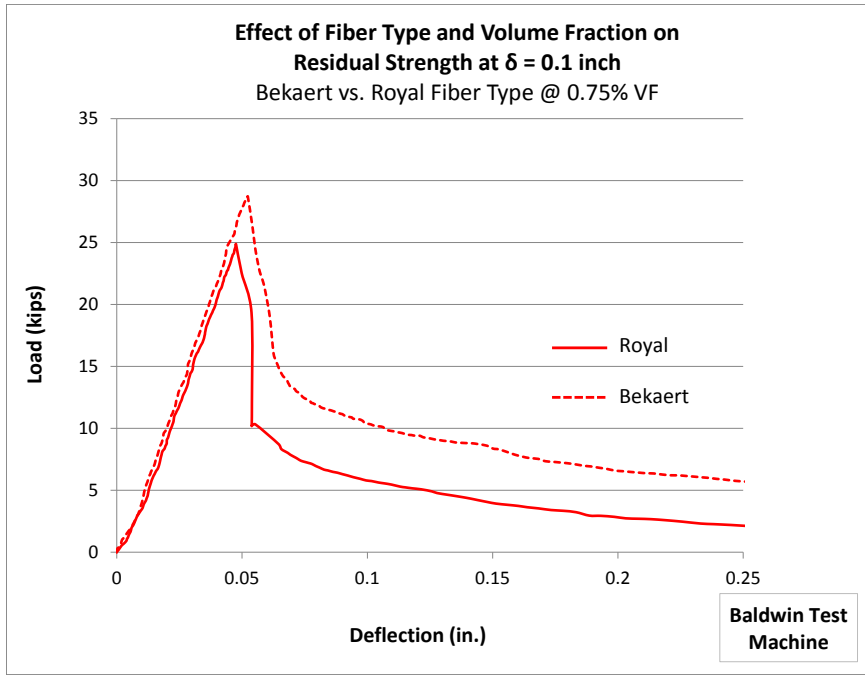
### 6.3.1 Discussion of Results

Similar to the findings reported for Phase 1, the averages of the key test parameters as well as the typical performance curves for specimens tested in Phase 2 agree with the expected behavior of SFRC; residual strength increases with increasing fiber content. However, Phase 2 specimens, composed of Bekaert Dramix® fibers, had higher residual strengths at 0.1 in. deflection than Phase 1 specimens containing Royal™ fibers. The same relative difference in the initial stiffness (slope) for different test machines found in Phase 1 was observed in Phase 2; specimens tested on the Olsen machine appear to be about twice as stiff as those tested on the Baldwin machine. The effects of test machine will be mentioned in more detail in the statistical analysis section of this chapter.

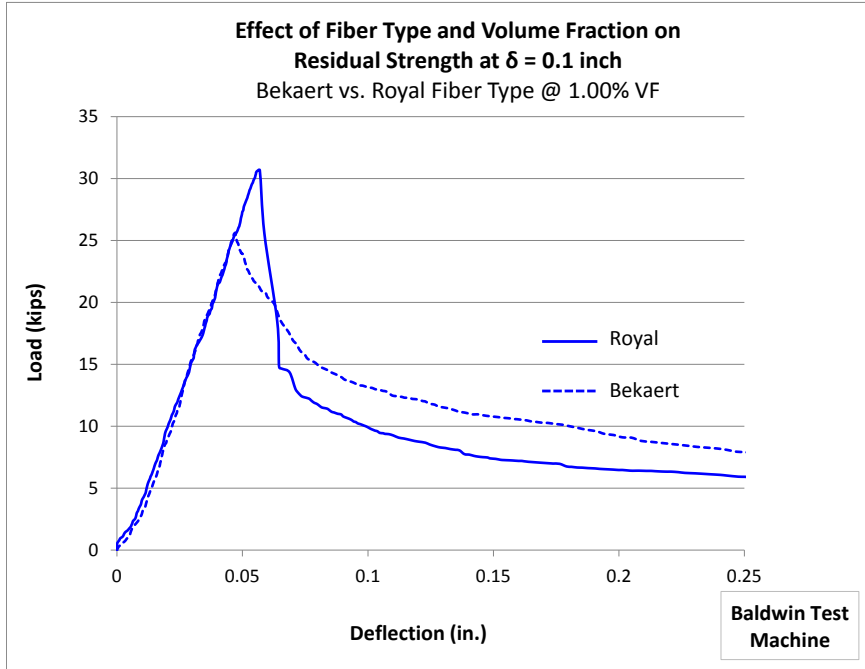
As shown in Figure 6-6, typical failures of SFRC specimens containing Bekaert Dramix® fibers were consistent with the fracture mechanics of DPT loading.

## 6.4 COMBINED RESULTS

Selected performance curves for both Phase 1 and Phase 2 specimens tested on the Baldwin machine are provided in Figure 6-7, Figure 6-8 and Figure 6-9, which compare Royal and Bekaert fibers at 0.75%, 1.00% and 1.50% volume fractions, respectively.

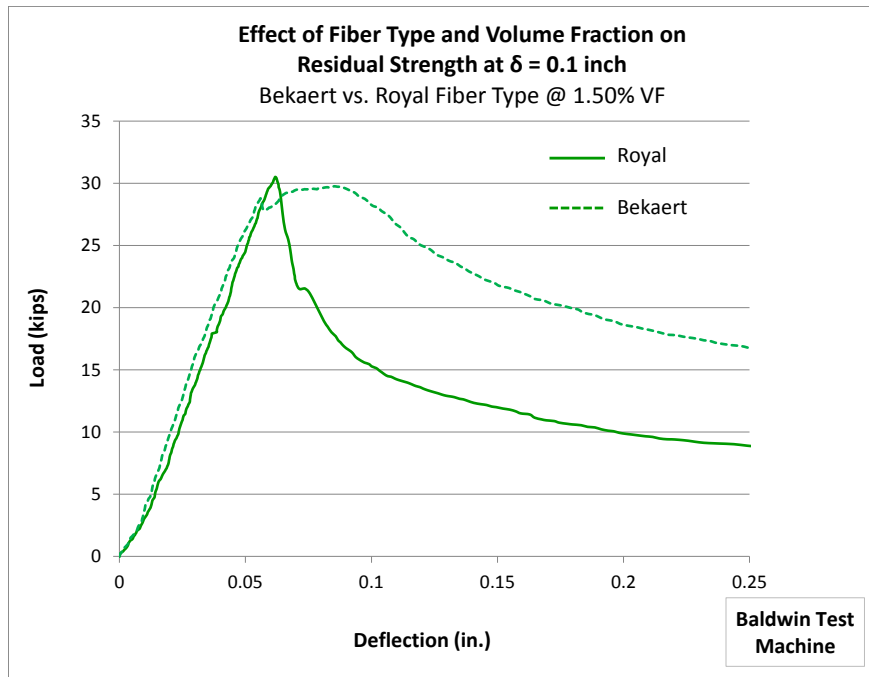


*Figure 6-7: Combined Results - Selected DPT Performance Curves showing Effect of Fiber Type and Volume Fraction at 0.75% Fiber Content*



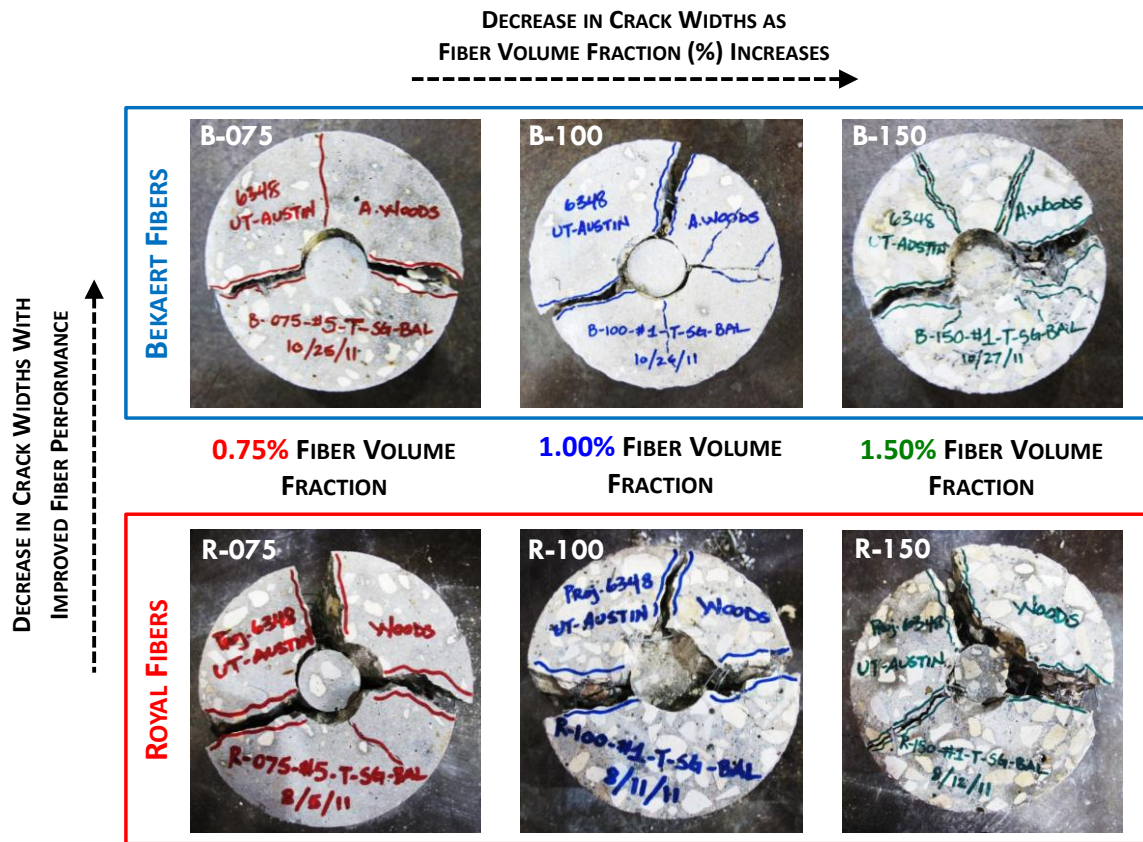
*Figure 6-8: Combined Results - Selected DPT Performance Curves showing Effect of Fiber Type and Volume Fraction at 1.00% Fiber Content*





*Figure 6-9: Combined Results - Selected DPT Performance Curves showing Effect of Fiber Type and Volume Fraction at 1.50% Fiber Content*

The performance of DPT specimens with different fiber types and volume fractions was also observed in the cracking pattern of test specimens. This comparison is provided in Figure 6-10.



*Figure 6-10: Effect of Fiber Type and Volume Fraction on Crack Widths and Cracking Pattern*

#### 6.4.1 Discussion of Results

The combined selected performance curves for Phase 1 and Phase 2 show that it is possible to compare different fiber types and volume fractions using the load-deflection curves obtained from the Double-Punch Test. The performance of different mixtures can also be compared using the cracked specimen. As shown in Figure 6-10, cracks were smaller for Bekaert specimens than for Royal specimens, indicating that the Bekaert fibers did not deform as much as the Royal fibers. As expected, crack widths also decreased as the fiber volume fraction increased.

## 6.5 DPT STATISTICAL ANALYSIS

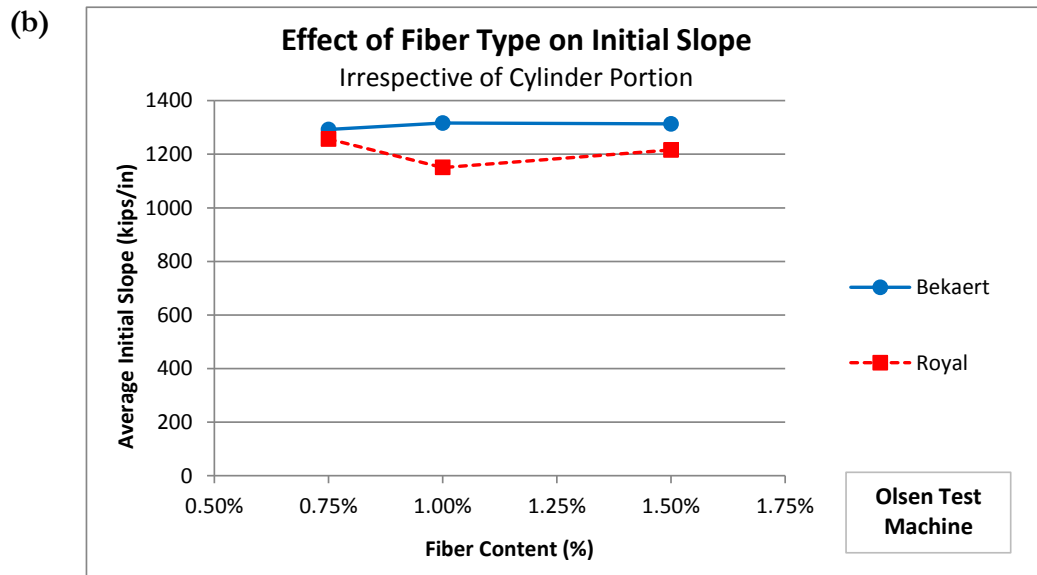
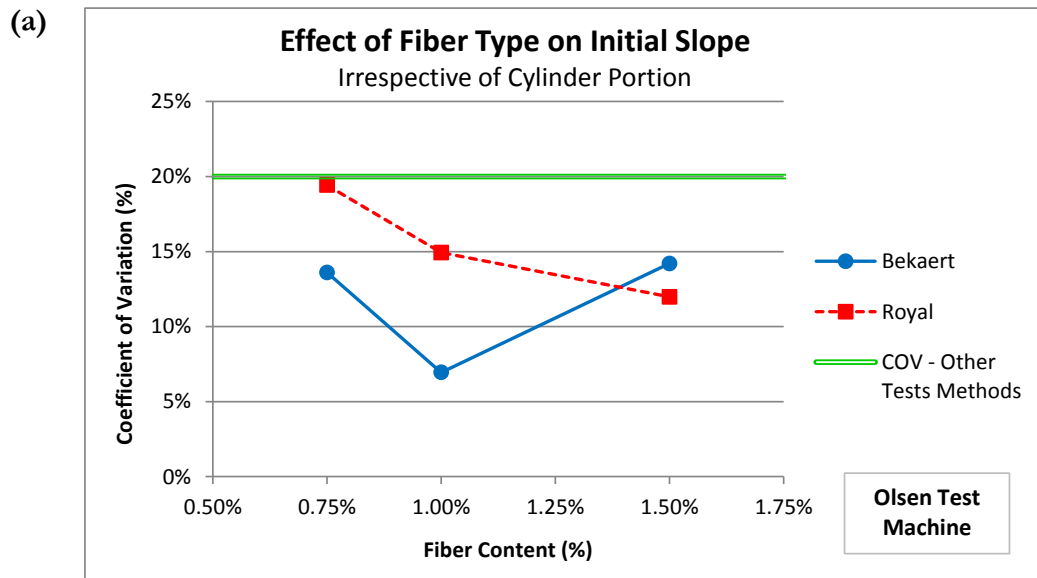
The DPT performance curves and cracking patterns are useful for comparing general trends and performance, but cannot be strictly relied upon to make conclusions and recommendations regarding the potential of the Double-Punch Test to replace current test methods for FRC. Thus, the data from the two-phase study was combined and a pivot table was constructed to analyze the effects of several variables. A statistical analysis was conducted to evaluate the reliability and reproducibility of the Double-Punch Test, as well as its ability to accurately describe the performance of steel fiber-reinforced concrete. Each variable was analyzed in terms of how it affected the key test parameters (Figure 5-25): initial slope, peak load, and residual strength at 0.1 inch deflection.

In the following sections, Phase 1 (Royal fibers) and Phase 2 (Bekaert fibers) analysis results will be shown for the investigation of fiber type and volume fraction. Only Phase 1 analysis results will be shown for the surface preparation variable since this variable was eliminated in Phase 2. Statistics for all other test variables in Phase 1 and Phase 2 were similar, and only results from Phase 2 will be discussed. Comprehensive statistical analysis results for Royal and Bekaert fibers are provided in Appendix B.

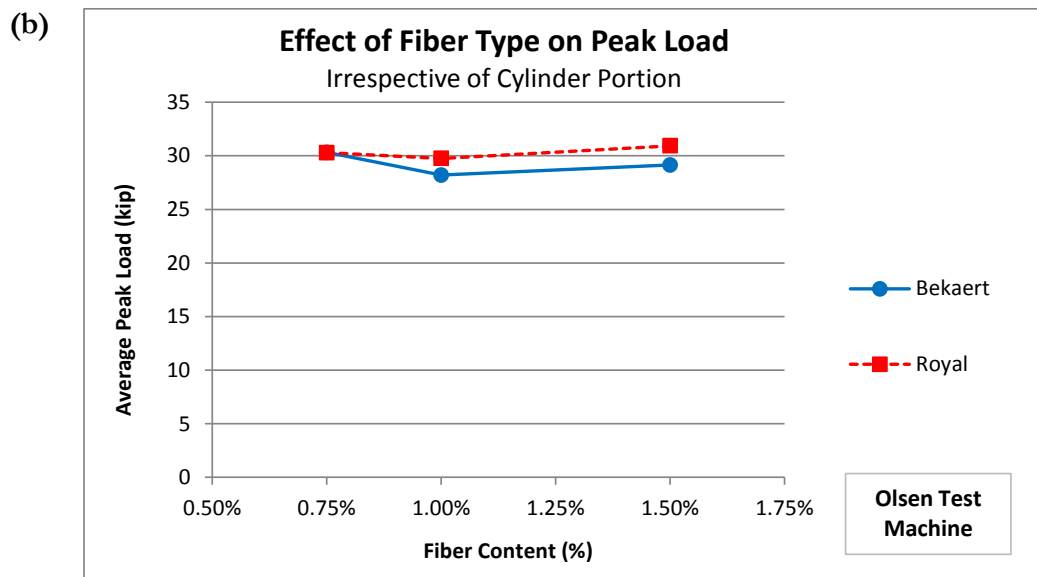
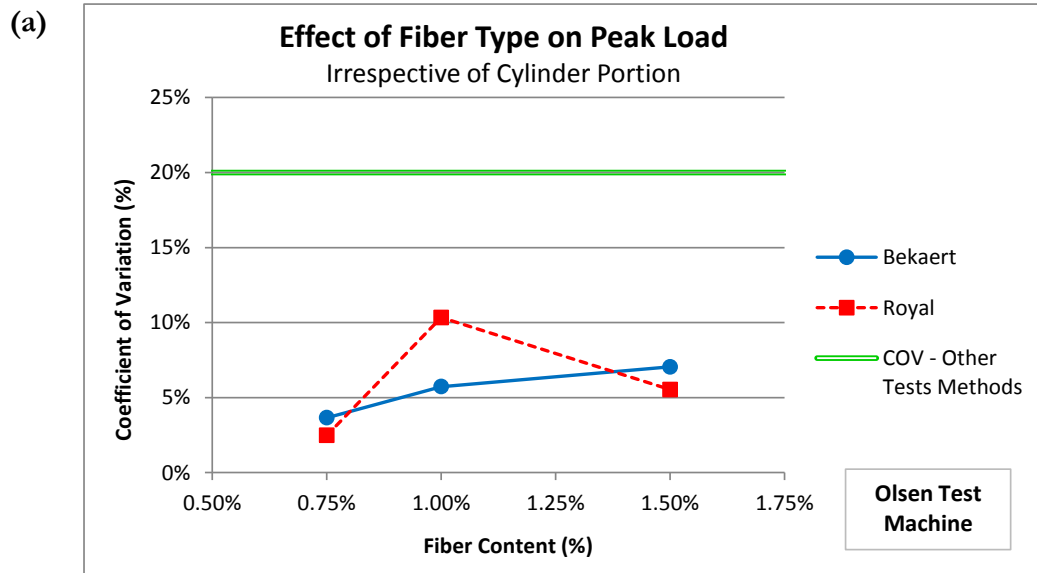
The analysis results presented in this thesis are “irrespective of cylinder portion.” This means that specimens from both the top and the bottom of cast cylinders were used to calculate the averages and coefficient of variations of key test parameters. Although the cylinder portion (top versus bottom) is technically another variable in the experiment, results for top and bottom specimens were fairly similar and were grouped for simplification. A separate analysis of the effects of cylinder portion (casting) was conducted to identify any key differences between the results from top and bottom specimens.

### **6.5.1 Analyzing the Effects of Fiber Type & Volume Fraction**

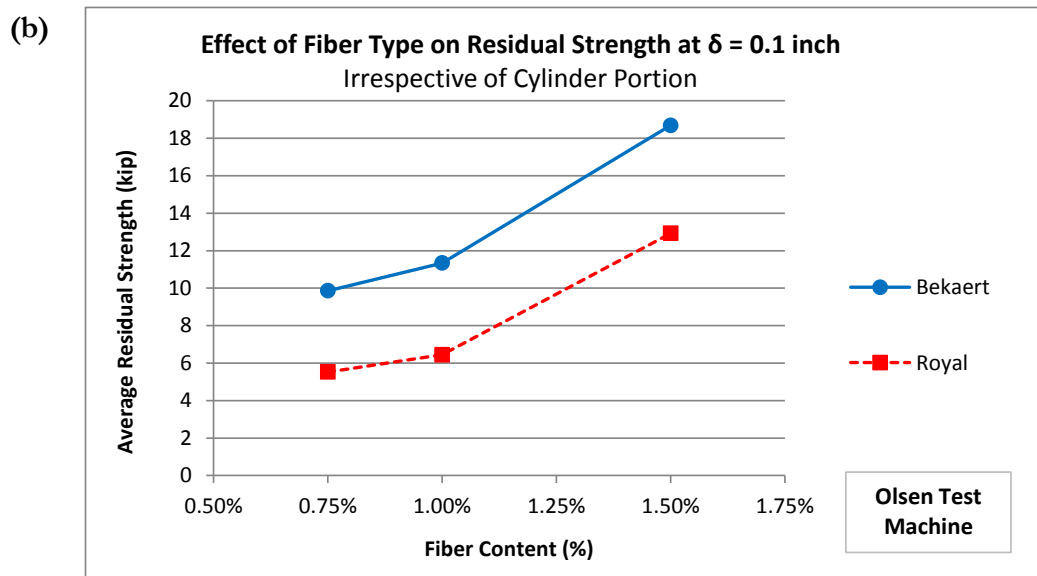
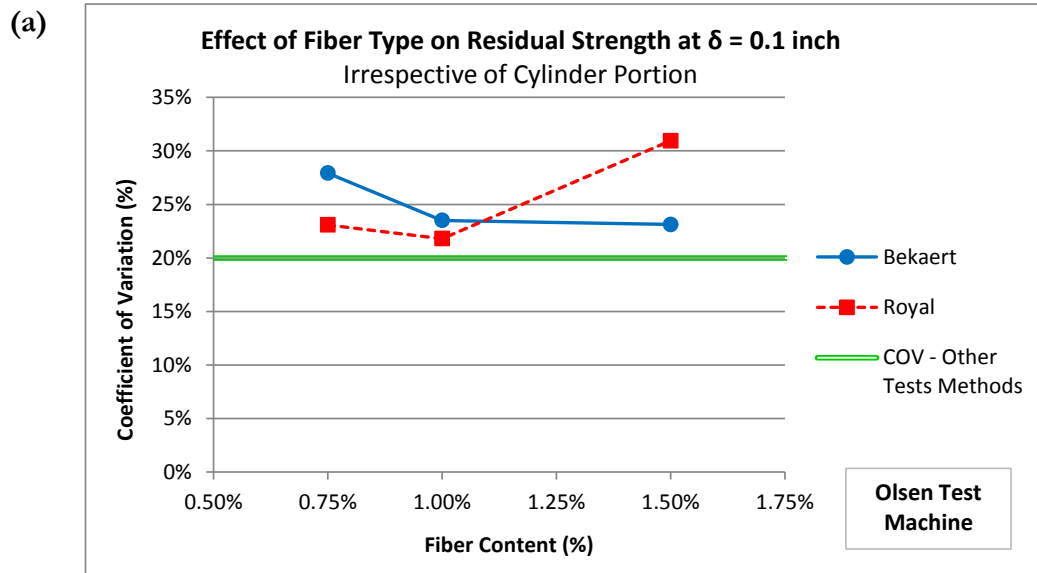
As shown in the selected DPT Performance Curves, it is evident that the Double-Punch Test is sensitive to both fiber type and volume fraction. In order to determine to what extent the DPT is able to detect changes in fiber geometry and content, a statistical analysis was conducted. Figure 6-11, Figure 6-12, and Figure 6-13 show the effects of fiber type and volume fraction on the (a) coefficient of variation and (b) average value of key parameters of the DPT. These statistics are based on ten tests.



*Figure 6-11: Effect of Fiber Type and Volume Fraction on (a) Coefficient of Variation and (b) Average Value of Initial Slope*



*Figure 6-12: Effect of Fiber Type and Volume Fraction on (a) Coefficient of Variation and (b) Average Value of Peak Load*



*Figure 6-13: Effect of Fiber Type and Volume Fraction on (a) Coefficient of Variation and (b) Average Value of Residual Strength*

### 6.5.1.1 Analysis Summary

The coefficient of variation is generally low for key test parameters (less than 20%), but variation in the residual strength parameter is high compared to the initial slope and peak

load variation. The coefficients of variation are similar for Royal and Bekaert fiber types; results from both fiber types have similar statistical dispersions.

The average value of initial slope and peak load are independent of fiber type and content. With increasing fiber volume fraction, or different fiber type, the initial slope and peak load do not change. This agrees with the expected behavior of steel fiber-reinforced concrete, because reinforcement in general is not effective until the concrete cracks.

On the other hand, the residual strength is highly dependent on the fiber volume fraction and fiber type. Increased fiber content means an increased number of fibers potentially crossing crack planes, and hence increased strength after cracking. As shown in Figure 6-13 (b), this aspect of SFRC behavior is adequately captured by the DPT, in that the residual strength increases as the fiber volume fraction increases.

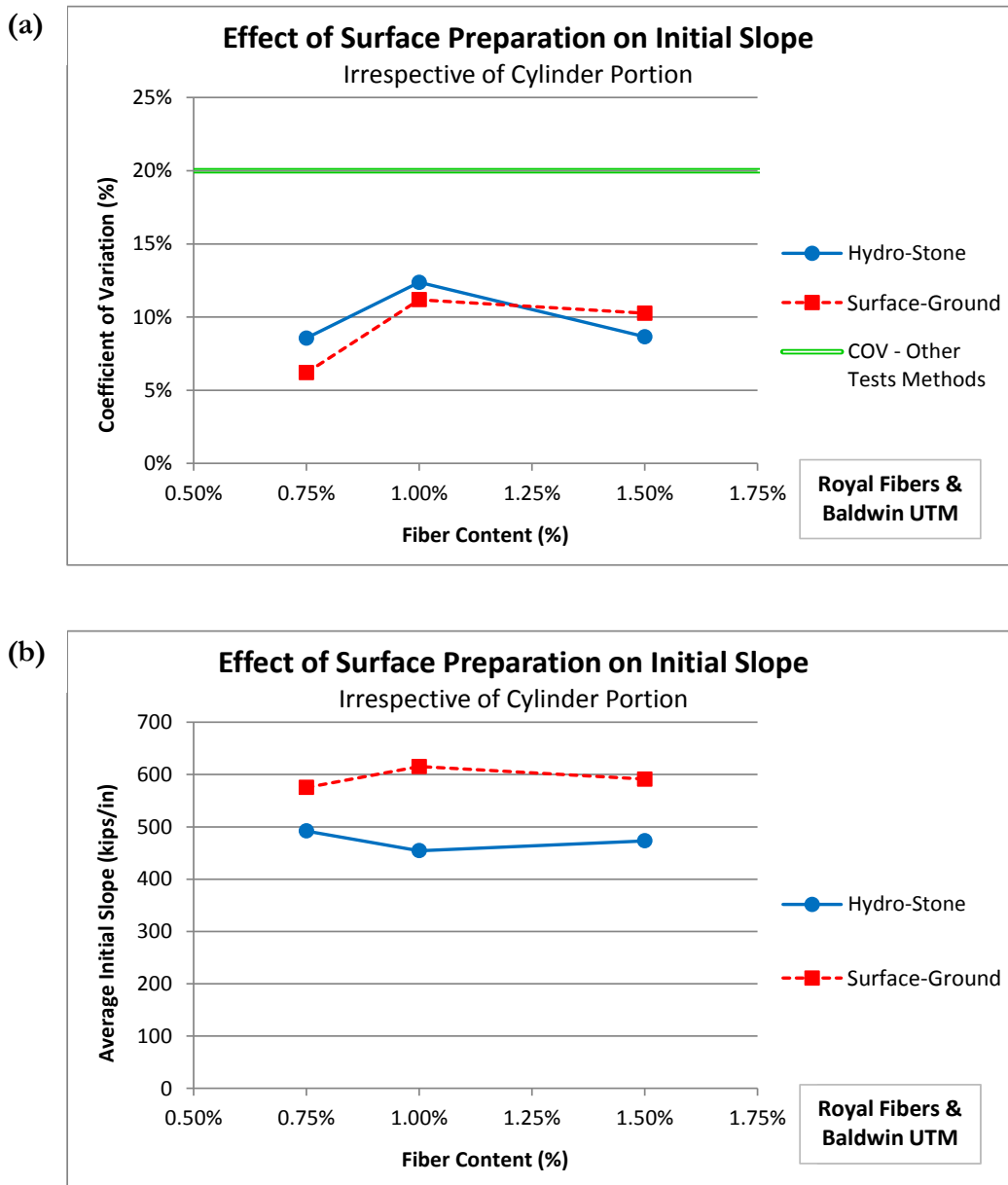
It is also clear from Figure 6-13 (b) that the DPT is able to distinguish between different fiber types. For instance, the average value of the residual strength is 20-50% higher for *Bekaert* specimens than for *Royal* specimens. This superiority in reserve capacity indicates that the Bekaert Dramix® fibers perform better than the Royal™ fibers. Thus, information obtained from the DPT can be useful for comparing different fiber-reinforcement options, and determining the appropriate fiber type(s) and relative volume fraction(s) needed for SFRC applications.

This analysis confirms the trends obtained from DPT performance curves and verifies that the DPT is effective at comparing post-cracking ductility and fiber performance.

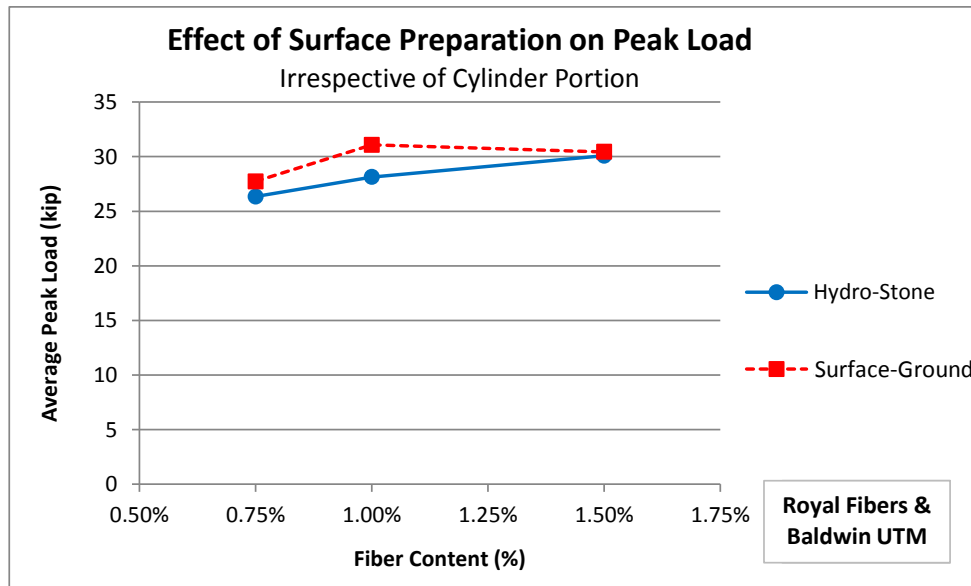
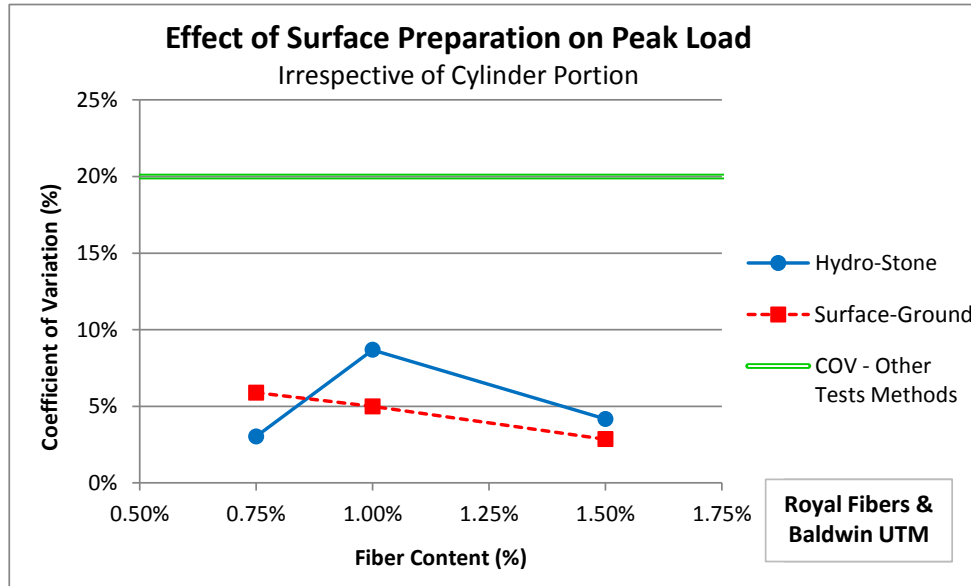


### 6.5.2 Analyzing the Effects of Surface Preparation

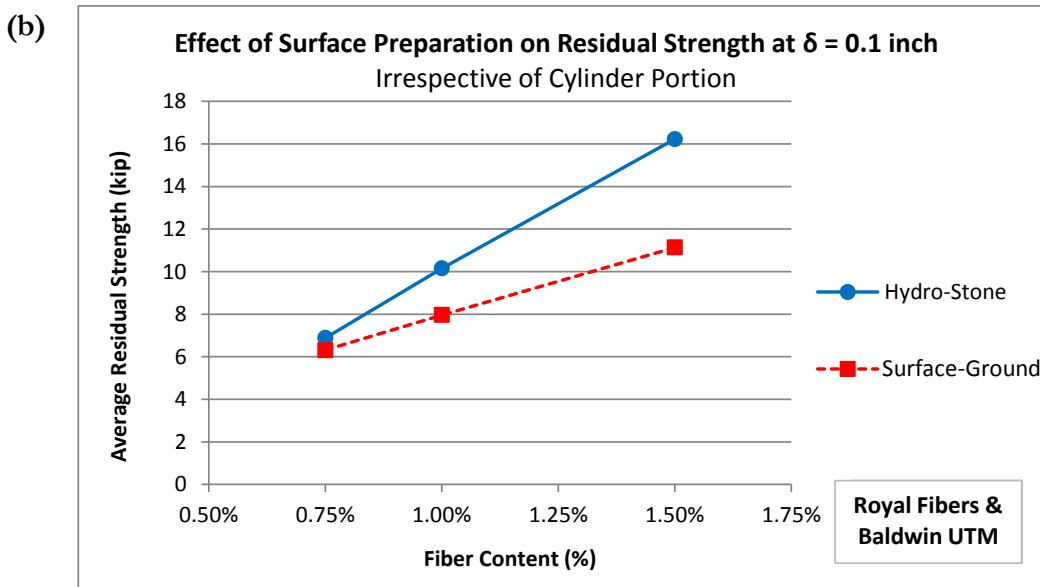
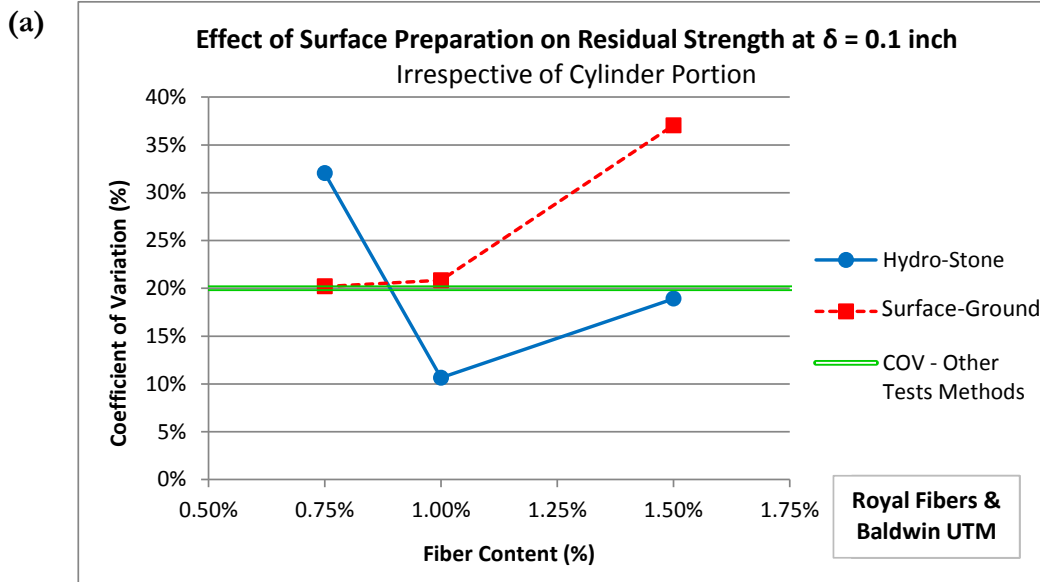
Figure 6-14, Figure 6-15, and Figure 6-16 show the effects of surface preparation on the (a) coefficient of variation and (b) average value of key parameters of the DPT. These statistics are based on five tests.



**Figure 6-14: Effect of Surface Preparation on (a) Coefficient of Variation and (b) Average Value of Initial Slope for Royal Fiber Type**



*Figure 6-15: Effect of Surface Preparation on (a) Coefficient of Variation and (b) Average Value of Peak Load for Royal Fiber Type*

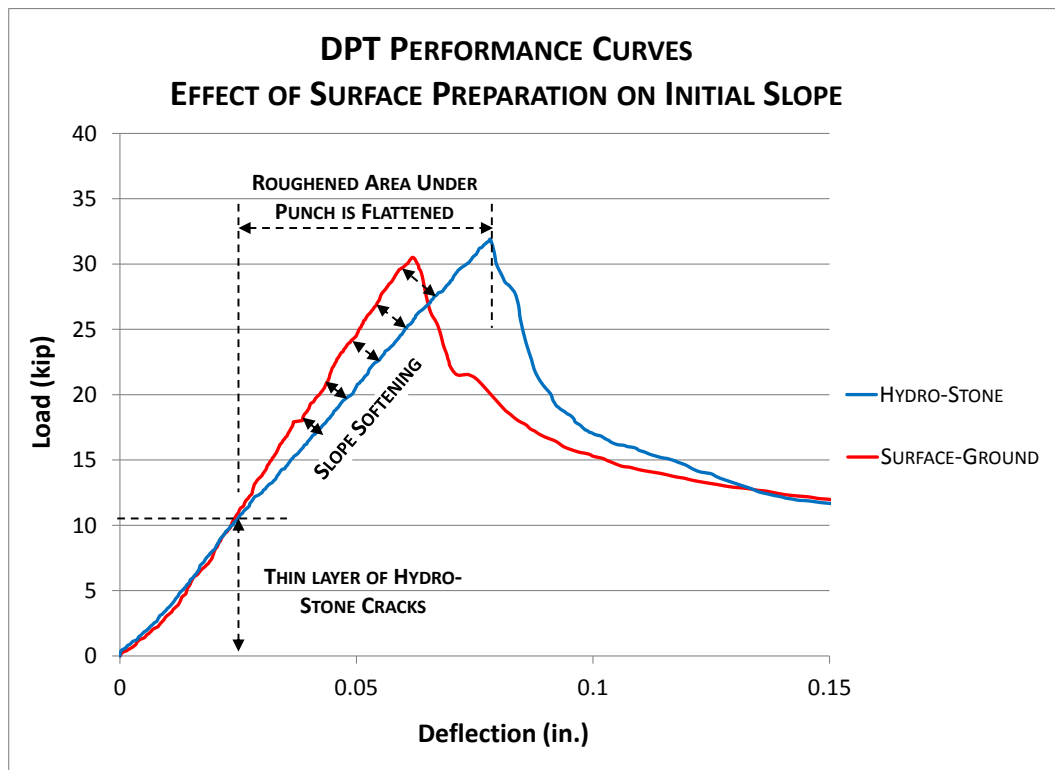


*Figure 6-16: Effect of Surface Preparation on (a) Coefficient of Variation and (b) Average Value of Residual Strength for Royal Fiber Type*

### 6.5.2.1 Analysis Summary

The coefficient of variation is generally low for key test parameters (less than 20%), but variation in residual strength parameter is high compared to initial slope and peak load

variation. Surface-ground and Hydro-Stone specimens exhibited similar COV. On average, Hydro-Stone specimens had a smaller initial slope (less stiff) and higher residual strength than Surface-Ground specimens, probably due to stress concentrations under the steel punches. As shown in Figure 6-17, this is most noticeable at loads beyond about 10 kips, as the brittle layer of Hydro-Stone fails and the steel punches flatten the roughened concrete surface underneath prior to rupture of the specimen.



*Figure 6-17: DPT Performance Curves showing Effect of Surface Preparation on Initial Slope Parameter*

In general, end grinding the surfaces of specimens is preferred over using Hydro-Stone for two reasons: (1) surface grinding specimens provides a smoother surface between the punch and concrete, and does not produce stress concentrations; and (2) the reduction in initial stiffness resulting from Hydro-Stone application may result in an error in the value of

residual strength at a specified deflection, leading to a perceived increase in performance. Because Hydro-Stone is a surface application only, it would be unreasonable to conclude that it is able to increase the residual strength or ductility of the specimen. When the peak load is reached, the Hydro-Stone and surface concrete crack, and do not provide additional internal resistance. It is evident from other results that improved *post-peak* performance is only related to the fiber type, content, and distribution.

Although refinishing the DPT specimen by end grinding is preferred, it is possible that some laboratories may not have the necessary equipment to grind 6-in. diameter cylinders. In this case, a thin layer of Hydro-Stone can be applied to the area beneath the punch location to provide a relatively smooth contact surface between the steel punches and DPT specimen. However, specimens with different surface finishes should not be compared directly.

Similar results are obtained for surface-ground and Hydro-Stone finishes, and either method is acceptable for the Double-Punch Test for means of comparing mixtures with different fiber types and volume fractions.

### 6.5.3 Analyzing the Effects of Test Machine

The data from test conducted in Phase 1 and Phase 2 indicate that some results from the DPT may be dependent on the test machine. Figure 6-18, Figure 6-19, and Figure 6-20 show the effects of test machine on the (a) coefficient of variation and (b) average value of key parameters of the DPT. These statistics are based on ten Double-Punch Tests.

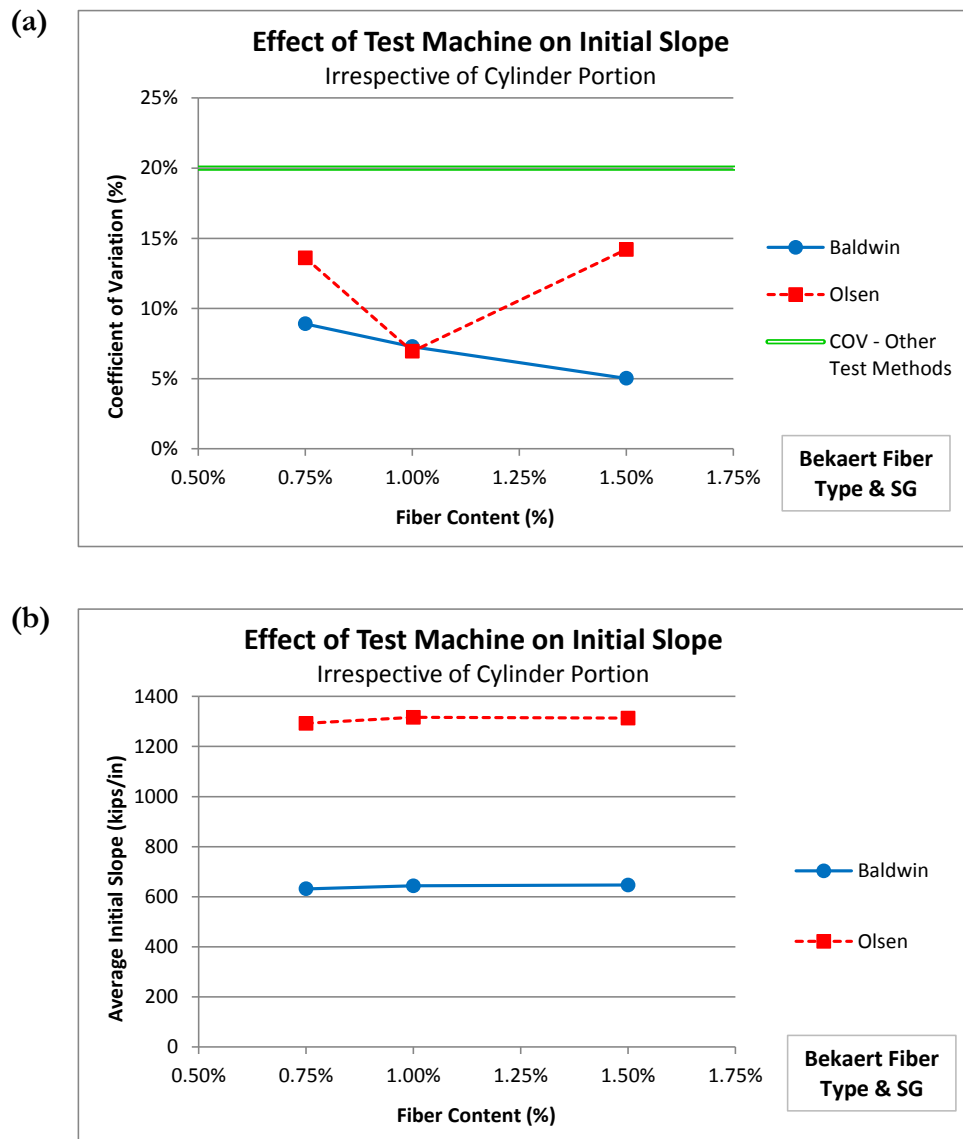
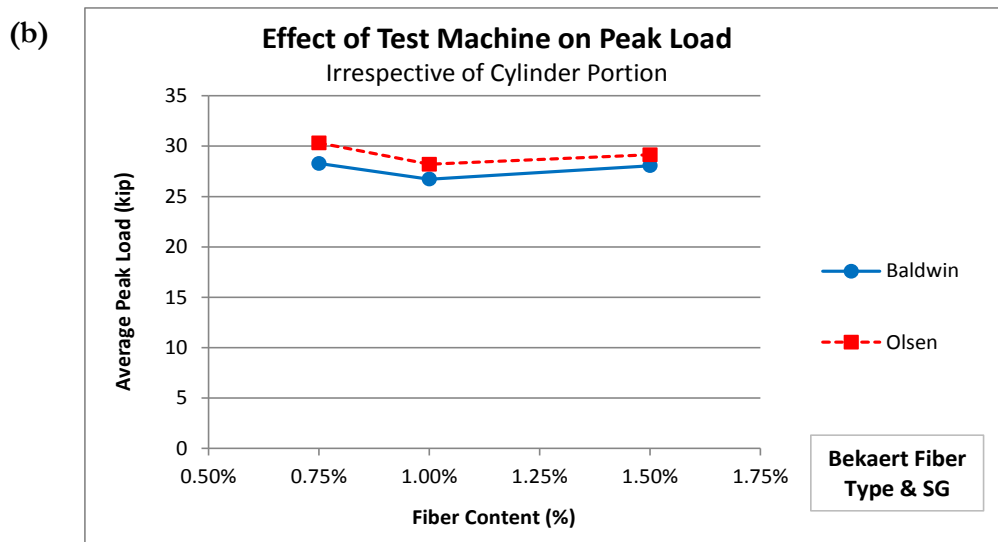
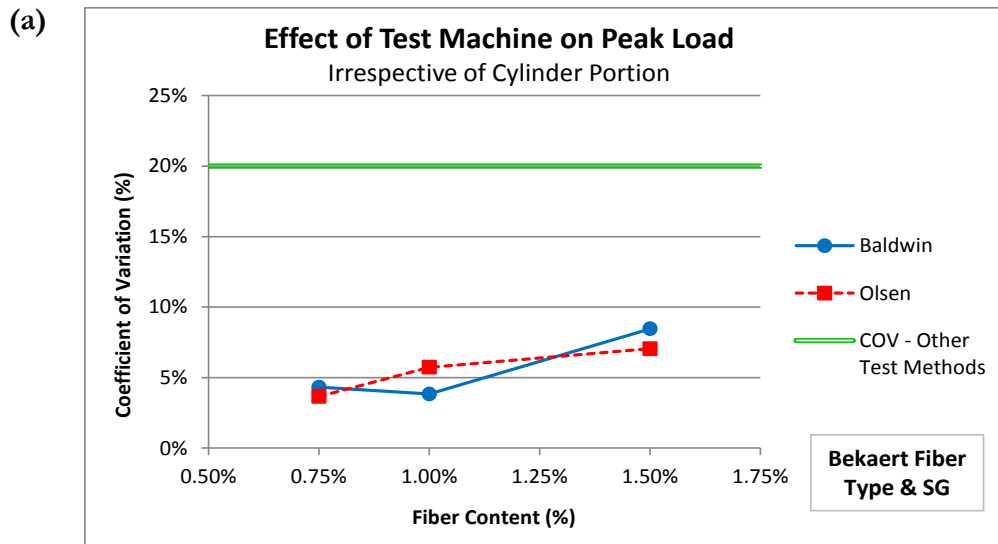
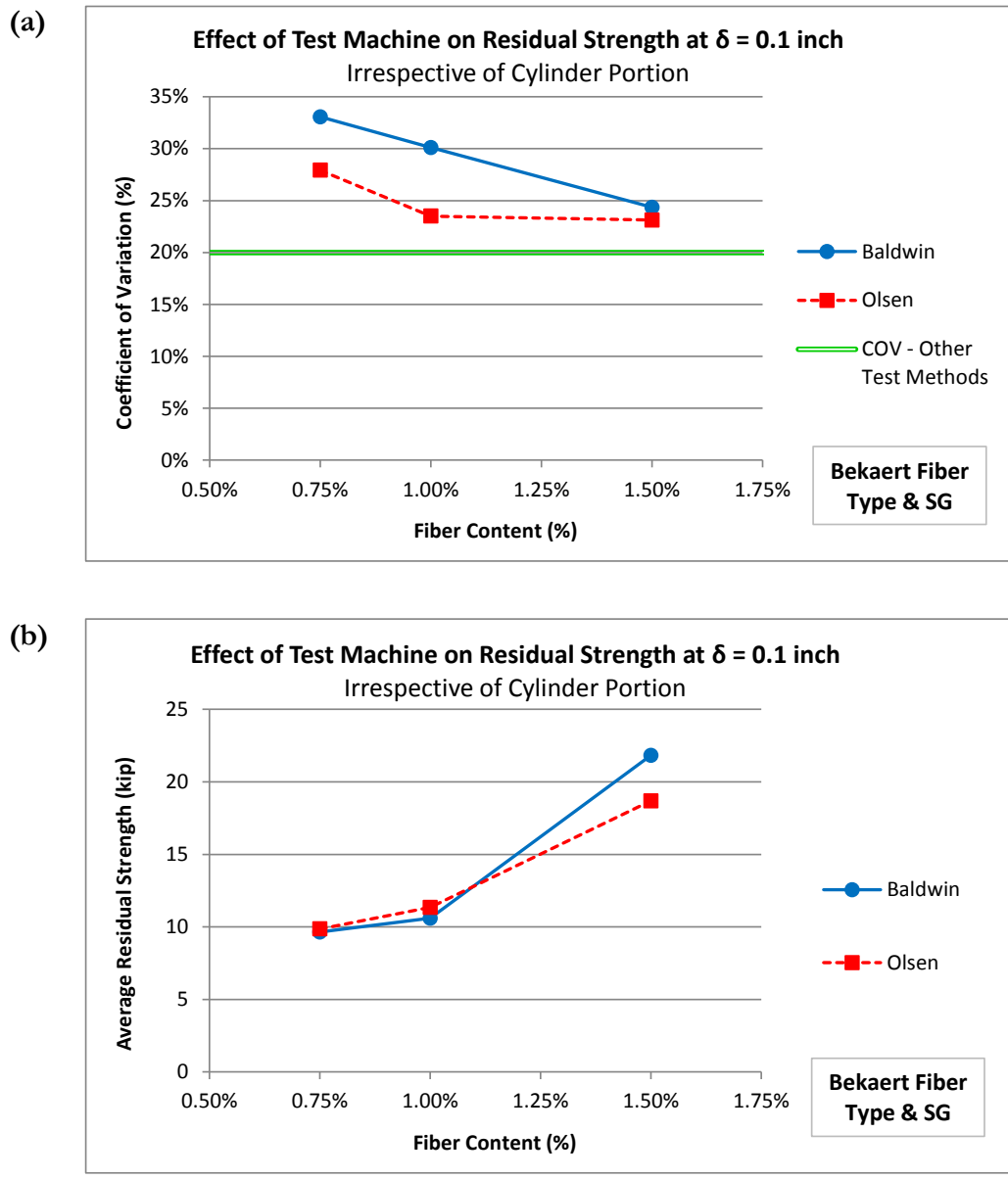


Figure 6-18: Effect of Test Machine on (a) Coefficient of Variation and (b) Average Value of Initial Slope for Bekaert Fiber Type



*Figure 6-19: Effect of Test Machine on (a) Coefficient of Variation and (b) Average Value of Peak Load for Bekaert Fiber Type*



**Figure 6-20: Effect of Test Machine on (a) Coefficient of Variation and (b) Average Value of Residual Strength for Bekaert Fiber Type**

As shown in the previous figures, the effect of the test machine is significant only for the initial slope parameter for both Royal and Bekaert fibers. The average value of the initial slope of specimens tested on the Olsen UTM is about 1½ to 2 times that of otherwise identical specimens tested on the Baldwin UTM. This difference was unexpected, because



the specimens tested on the two machines were from identical batches of concrete and tested beyond 28 days (concrete strength has leveled off). The elastic modulus of the specimens should not differ by a factor of 2. Thus, a calibration, independent of DPT specimens and measuring devices, was conducted to determine the stiffness of the two test machines in order to evaluate the effects of the test machine on DPT results.

The machines were checked simply, using a dial gage and load cell. The load cell was used to confirm the load displayed by the UTMs was correct. Next, readings of load (from machine) and displacement (from dial gage) were taken for a concrete cylinder loaded in compression. The calibration setups are shown in Figure 6-21.

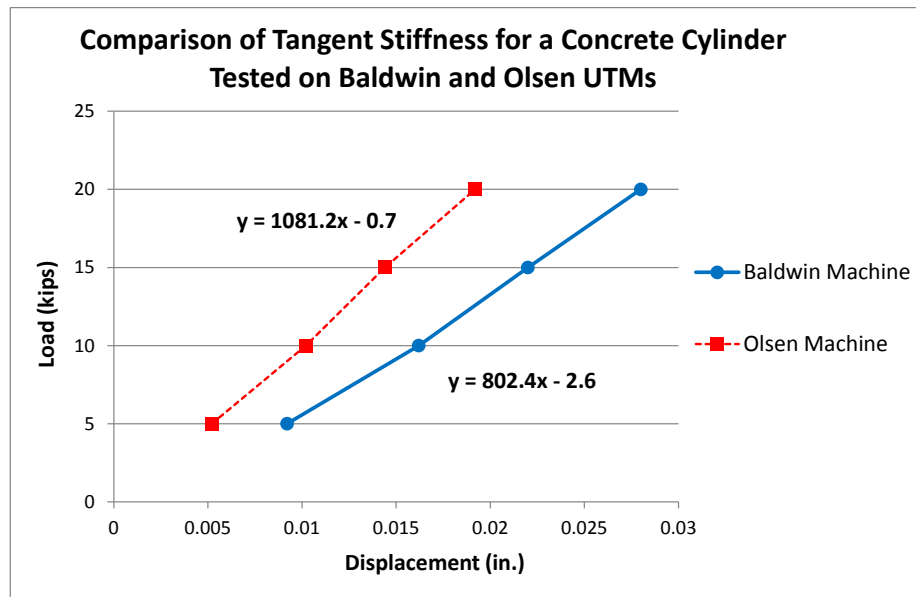


*Figure 6-21: Calibration Setup for Baldwin (left) and Olsen (right) UTMs*

Finally, a small portion of the initial loading curve was constructed to determine the tangent stiffness of the same cylinder tested on the Baldwin and Olsen UTMs. In Table 6-3, this data is compared to the averages for initial slope found in the DPT. The tangent stiffness calibration curves for the Baldwin and Olsen are shown in Figure 6-22.

*Table 6-3: Comparison between Initial Slopes from DPT and Calibration Test*

Machine	Avg. Initial Slope from DPT Data	Measured Initial Slope from Calibration
<i>Baldwin</i>	587	781
<i>Olsen</i>	1187	1087
<b>Olsen/Baldwin</b>	<b>2.02</b>	<b>1.39</b>



*Figure 6-22: Tangent Stiffness Calibration Curves*

The calibration curves and test data show that the test setup can have some effect on the measured initial stiffness. Similar to DPT data, the calibration experiment suggests the Olsen machine is about twice as stiff as the Baldwin machine. This is explained by the fact that the Olsen UTM (120-kip) has twice the load capacity as the Baldwin UTM (60-kip); thus, the stiffness of the connecting rods on the Olsen UTM are twice that of the Baldwin UTM.

Due to these effects, the initial stiffness of the test specimen itself does not correspond to the measured stiffness from the DPT. The actual stiffness of the specimen can only be determined if strains are measured directly on the test cylinder using an extensometer, strain gauge, or other methods. Thus, the measured initial stiffness from the DPT should only be used to provide further evidence of the repeatability of the DPT on the same machine; it should not be used as an estimate of the actual stiffness of the DPT test specimen due to flexibilities observed in the DPT setup.

#### ***6.5.3.1 Analysis Summary***

The coefficient of variation is generally low for key test parameters (less than 20%), but variation in the residual strength parameter is high compared to initial slope and peak load variation. Results did not show that the test machine has an effect on the coefficients of variation for the key test parameters. However, the test machine was found to effect the average values (or performance) of DPT specimens. These effects varied based on the test parameter:

##### *1. Initial Slope*

- The value of the initial slope differed by a factor of approximately 2 between the two test machines used in this study. This difference can be attributed to the differences in the stiffness of the *testing equipment* used and not the DPT *specimens* themselves;
- The measured initial slope is only valuable for analyzing the statistical variation of DPT results obtained on a single test machine.

##### *2. Peak Load*

- The peak load is not influenced by the stiffness of the machine;

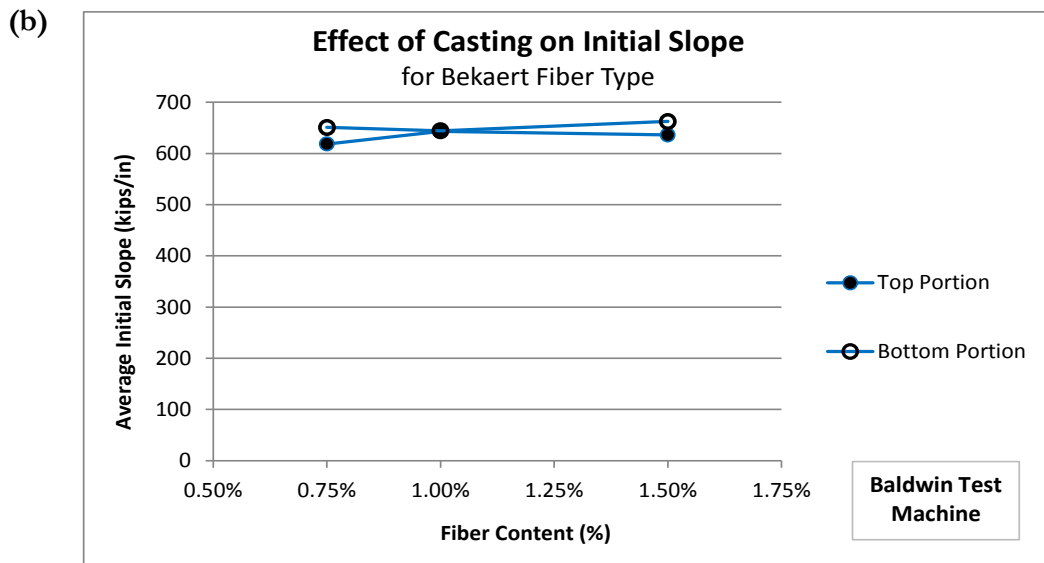
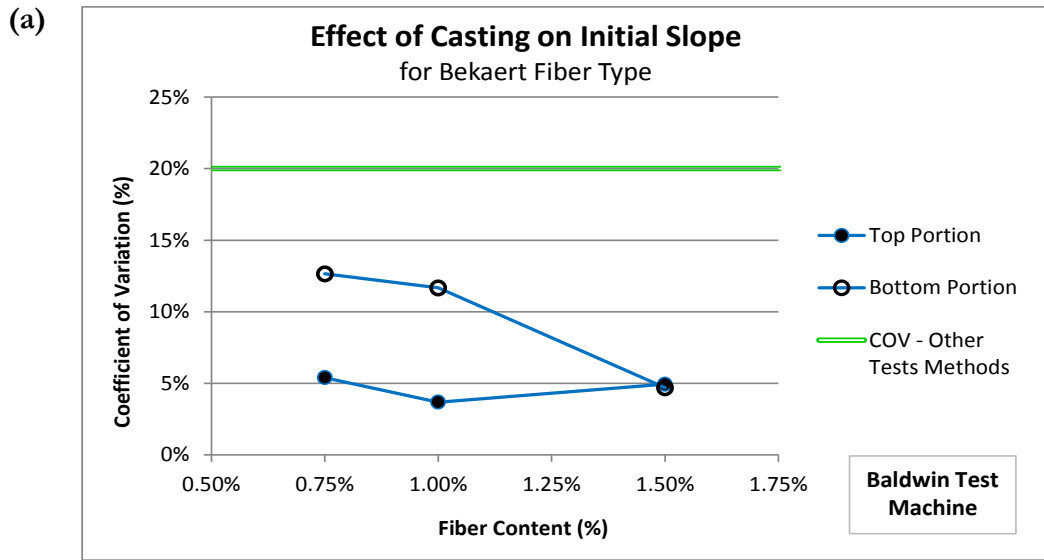
### 3. *Residual Strength at 0.1 inch Deflection*

- The measure of ductility may be slightly influenced, but because the specimens are sufficiently less stiff after cracking, the differences in machine stiffness are not as apparent in results for the residual strength. Also, the shallow slope of the post-peak curve is much flatter so the net effect of machine stiffness is not as significant.

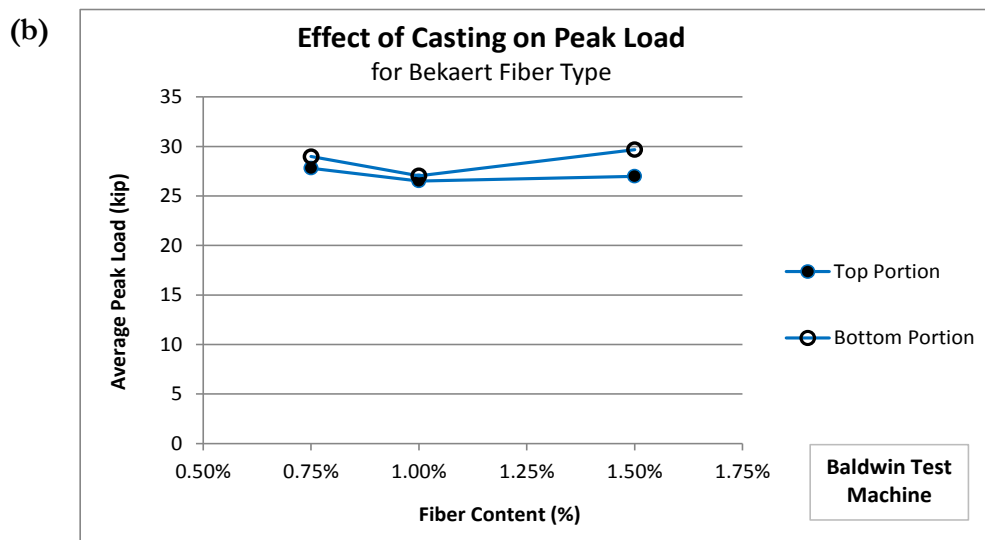
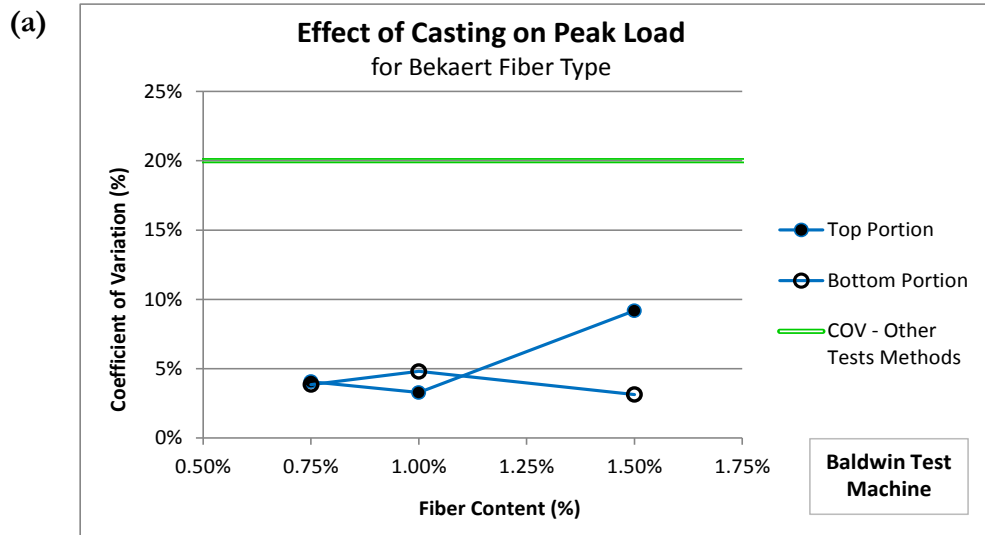
Nevertheless, since many test methods for FRC require the use of closed-looped, servo-controlled test machines, the DPT presents an immediate advantage over current tests since any common universal test machine can be used to conduct the test.

#### **6.5.4 Analyzing the Effects of Cylinder Portion (Casting)**

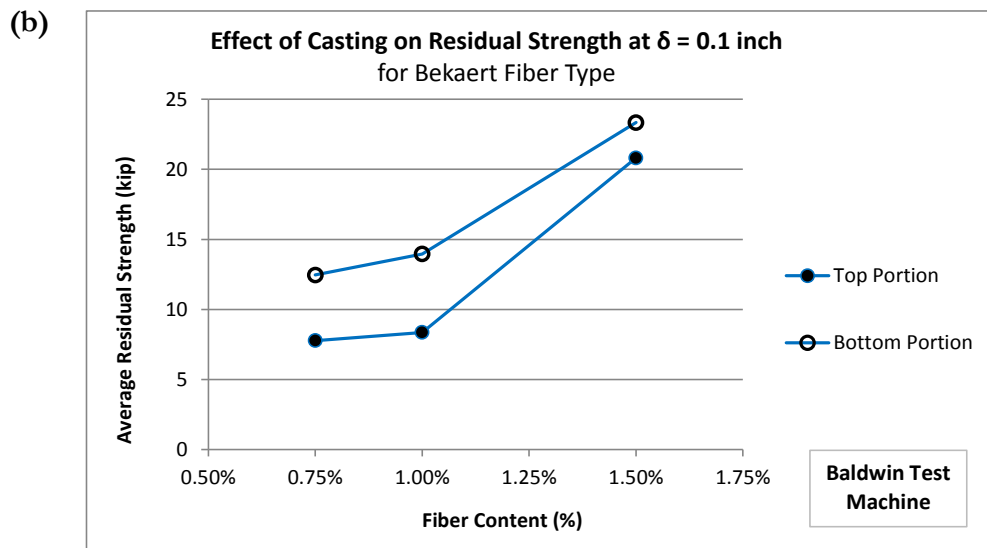
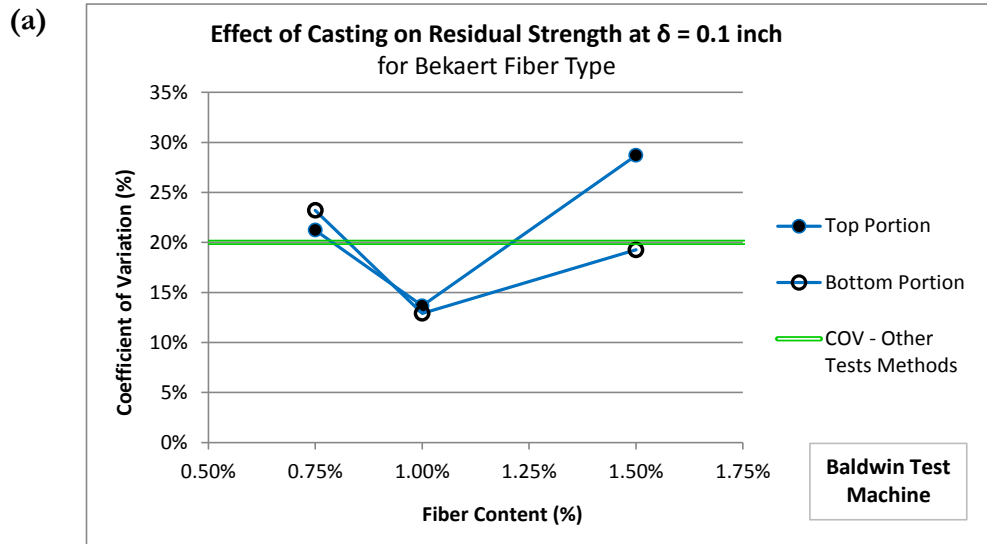
Figure 6-23, Figure 6-24, and Figure 6-25 show the effects of cylinder portion (casting) on the (a) coefficient of variation and (b) average value of key parameters of the DPT. These statistics are based on ten Double-Punch Tests.



*Figure 6-23: Effect of Cylinder Portion (Casting) on (a) Coefficient of Variation and (b) Average Value of Initial Slope for Bekaert Fiber Type*



*Figure 6-24: Effect of Cylinder Portion (Casting) on (a) Coefficient of Variation and (b) Average Value of Peak Load for Bekaert Fiber Type*



*Figure 6-25: Effect of Cylinder Portion (Casting) on (a) Coefficient of Variation and (b) Average Value of Residual Strength for Bekaert Fiber Type*

#### 6.5.4.1 Analysis Summary

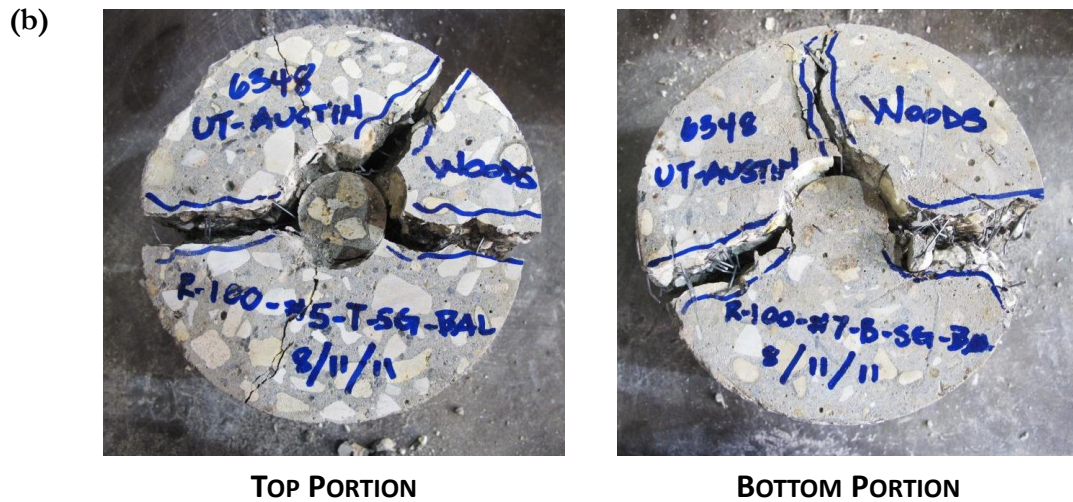
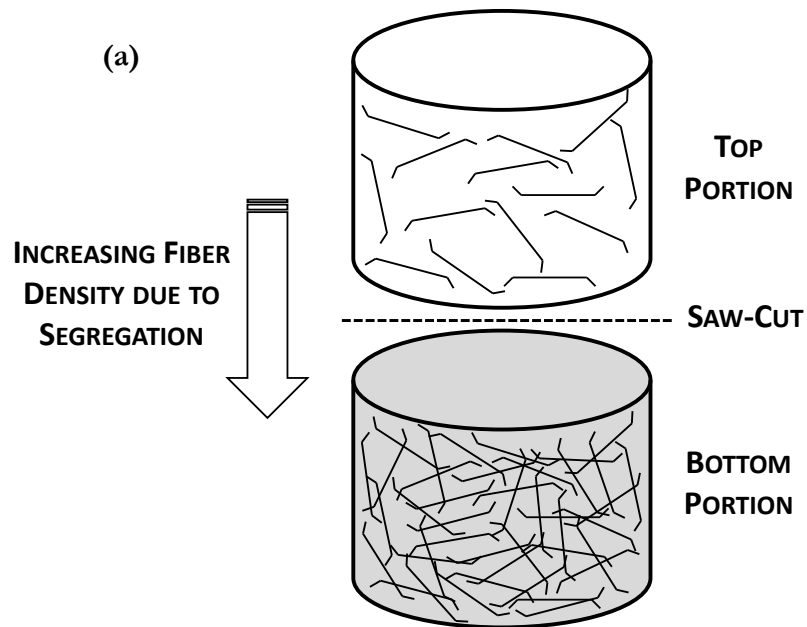
The coefficient of variation is generally low for key test parameters (less than 20%), but the variation in the residual strength is higher than that of the initial slope and peak load. The coefficients of variation for are similar for Top and Bottom specimens, indicating that

the scatter is not dependent on the portion of cylinder used in the DPT. The average values of initial slope and peak load are also independent of the cylinder portion.

However, the average value of residual strength is greatly dependent on the cylinder portion. As shown in Figure 6-25 (b), the bottom portion of the cylinder has additional reserve capacity for a given fiber content. This is directly associated with the distribution of fibers. As shown in Figure 6-26 (a), the distribution of fibers in the bottom portion of the cylinder is denser due to segregation during casting. This is corroborated by the appearance of the cracked specimens from DPT experiments as seen in Figure 6-26 (b).

The number of fibers bridging the cracks of failed specimens was much greater for specimens taken from the bottom portion of the original 6 x 12-in. cylinders. Thus, residual strengths are generally higher for bottom specimens because they have more fibers crossing the radial cracks.





*Figure 6-26: Effect of Casting on (a) the Fiber Distribution and (b) the Number of Fibers Crossing Crack Planes in Top and Bottom Test Specimens*

## **CHAPTER 7**

### **CONCLUSIONS AND RECOMMENDATIONS**

#### **7.1 RESEARCH SUMMARY**

It was found that the Double-Punch Test (DPT) provided data for comparing fiber-reinforcement options for use in various applications and for evaluating fiber-reinforced concrete (FRC) in general. The DPT Research and Testing Program was organized to produce sufficient within-laboratory data to make conclusions and recommendations regarding the simplicity, reliability, and reproducibility of the DPT for evaluating the performance of steel fiber-reinforced concrete. In this chapter, key results are discussed and protocols for the effective application of the Double-Punch Test to FRC are recommended.

#### **7.2 CONCLUSIONS**

The DPT Performance Curves (raw data) show that the Double-Punch Test can reliably distinguish between the effects of different fiber types and volume fractions on steel fiber-reinforced concrete (SFRC); indicating that the DPT is useful for comparing SFRC mixtures. The statistical analysis (derived data), substantiates the validity of the DPT for such comparison purposes. The Double-Punch Test can also be used to characterize other aspects of the mechanical performance of SFRC, such as resistance to cracking, residual strength, and toughness.

The following conclusions are based on the results of the DPT Research and Testing Program and statistical analysis described in this thesis. Conclusions are categorized based on their relation to the simplicity, reliability, and reproducibility of the Double-Punch Test.

### 7.2.1 Simplicity of the DPT

- The *specimens* required to conduct the Double-Punch Test can be fabricated using basic cylinder molds, are lightweight, and can be placed into the testing apparatus without the need for special fixtures.
  - a) The specimens can be prepared using the same type of cylinder molds used to determine the compressive strength of concrete (ASTM C39/C39M).
  - b) Because DPT specimens are cylindrical, cores from existing structures can easily be extracted and tested using the DPT to determine in-place properties. This can be useful in forensic investigations involving fiber-reinforced concrete.
- The *test setup* and *support conditions* are simple and it is very easy to ensure concentric load is applied to the specimen through the steel punches by using dimensional guides and masking tape.
- As for *test machine*, any Universal Testing Machine can be used to conduct the DPT; a closed-loop, servo-controlled machine is not required as is the case for other tests to determine FRC characteristics.
- The *test procedure* is quick and simple; the average Double-Punch Test takes less than 20 minutes to perform.

### 7.2.2 Reliability of the DPT

- The *test results* show that the DPT is an effective way to compare the post-cracking ductility and performance of mixtures containing different fiber types (manufacturer and geometry) as well as different fiber volume fractions (% fiber).
- The *failure mechanism* produced by the DPT occurs along multiple planes; typical damage is concentrated along three or four radial planes, thus test results represent an averaged mechanical behavior.



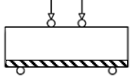



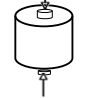
- The *within-batch, single-laboratory precision (COV)* for key test parameters is generally low and comparable to or better than other current test methods for FRC:  $\pm 10\%$  Initial Slope;  $\pm 5\%$  Peak Load; and  $\pm 20\%$  Residual Strength at 0.1 in. deflection.
  - a) The test setup can have some effect on the measured initial stiffness depending on the stiffness of the machine. For this reason, specimens should be tested on the same test machine if compared directly.
  - b) The measured initial stiffness is tabulated to provide further evidence of the repeatability of the DPT on the same machine; it should not be used as an estimate of the actual stiffness of the DPT test specimen due to flexibilities observed in the DPT setup.

### 7.2.3 Reproducibility of the DPT

- The *inter-laboratory precision (COV)* for key test parameters was not determined in this study.

In Table 7-1, the DPT is compared with the complexity, reliability, and reproducibility of other current test methods for FRC. It is clear that the Double-Punch Test can be extended to SFRC with similar precision and less complexity compared to other tests.

*Table 7-1: Simplicity, Reliability, and Reproducibility of Current FRC Testing Procedures vs. Double-Punch Test*

TEST INFORMATION <sup>1</sup>		SIMPLICITY <sup>2</sup>				RELIABILITY <sup>3</sup>		REPRODUCIBILITY <sup>3</sup>
Designation	Layout	Specimen Fabrication & Handling	Test Setup & Support Fixtures	Test Procedure	Test Machine	Failure Mechanism	Within-Batch Precision (COV)	Inter-Laboratory Precision (COV)
ASTM C496		Easy	Easy	Easy	Standard	Single Major Crack	± 5% PL	Not Available
ASTM C1609		Moderate	Difficult	Moderate	Closed-Loop	Single Major Crack	± 8% PL ± 20% RS	Not Available
ASTM C1399		Moderate	Difficult	Difficult	Standard	Single Major Crack	± 20% RS	± 40% RS
ASTM C1550		Difficult	Difficult	Difficult	Closed-Loop	Multiple Cracks	± 6% PL ± 10% RS	± 9% PL ± 9% RS
EFNARC Panel Test		Difficult	Difficult	Moderate	Closed-Loop	Multiple Cracks	Not Available	Not Available
Uniaxial Direct Tensile Test		Difficult	Moderate	Moderate	Closed-Loop	Single Major Crack	Not Available	Not Available
<b>Double-Punch Test</b>		<b>Easy</b>	<b>Easy</b>	<b>Easy</b>	<b>Standard</b>	<b>Multiple Cracks</b>	<b>± 10% Initial Slope ± 5% Peak Load ± 20% Residual Strength</b>	<b>Not Available</b>

<sup>1</sup> Test layouts modified from (Molins 2006).

<sup>2</sup> Complexity levels assigned based on literature and personal communication with researchers who conducted these and other similar tests (S. Chao 2012).

<sup>3</sup> Reliability and reproducibility data obtained from industry standards and research literature (ASTM C496 2011, ASTM C1609 2010, ASTM C1550 2010, ASTM C1399 2010, S.-H. Chao 2011, Bernard 2002). COVs for peak load and residual strength (toughness) are denoted (PL) and (RS), respectively.

## 7.3 RECOMMENDATIONS

The following recommendations were developed based on the results of the DPT Testing Program and statistical analysis conducted in this thesis:

### 7.3.1 Recommended DPT Protocols for Effective Application to FRC

After conducting more than 120 tests on steel fiber-reinforced concrete specimens, it has been determined that the DPT is effective for evaluating the performance of SFRC. For optimal results, the following protocols are recommended:

#### *Calibration*

- 1) LVDTs of appropriate stroke (2 in. or less) should be used and calibrated with gage blocks to ensure that small deflections are recorded accurately.

#### *Specimen Size*

- 2) The top or bottom 6 x 6-in. portion of a 6 x 12-in. cylinder specimen can be used for testing.
- 3) Top and bottom specimens should not be compared directly, as bottom portions have a greater fiber density for a given fiber volume fraction due to segregation during casting.

#### *Specimen Surface Preparation*

- 4) Specimen surfaces should be smooth so that the steel punches make uniform (flat) contact with the top and bottom faces of the specimen.
- 5) End grinding cylinders is the preferred method of obtaining a smooth surface; however, a thin layer of Hydro-Stone can be used to provide an even surface beneath the steel punches if grinding equipment is unavailable.
- 6) Results obtained from specimens with different surface finishes should not be compared directly.

#### *Punch Alignment*

- 7) To avoid eccentric loading, use a dimensional guide and masking tape to center the punches and secure them to the cylinder specimen.

#### *Shakedown Procedure*

- 8) Follow shakedown procedure and corresponding load rates presented in Chapter 5 to obtain the DPT Performance Curve (load-deflection plot).

### **7.3.2 Recommendations for Future Research**

In this thesis, fundamental data was reported that showed the Double-Punch Test is useful for evaluating SFRC. However, the fiber types and volume fractions needed for specific performance requirements have not been quantified in this study. Research that correlates field stresses in bridge decks (or other applications of interest) with stresses from a Double-Punch Test will be useful for determining if the DPT can be used in this way. Other applications of interest may include using steel fibers as a replacement of secondary reinforcement in the end regions of reinforced concrete beams and girders.

The DPT appears to be less complex and at least or more reliable than current test methods for FRC. However, additional intra- and inter-laboratory studies are needed before this method can be widely accepted by researchers or standardized by testing agencies. In anticipation of future experiments that verify the DPT for FRC, a proposal for standardization has been drafted and is included in Appendix C.

## APPENDIX A

### DPT PERFORMANCE CURVES

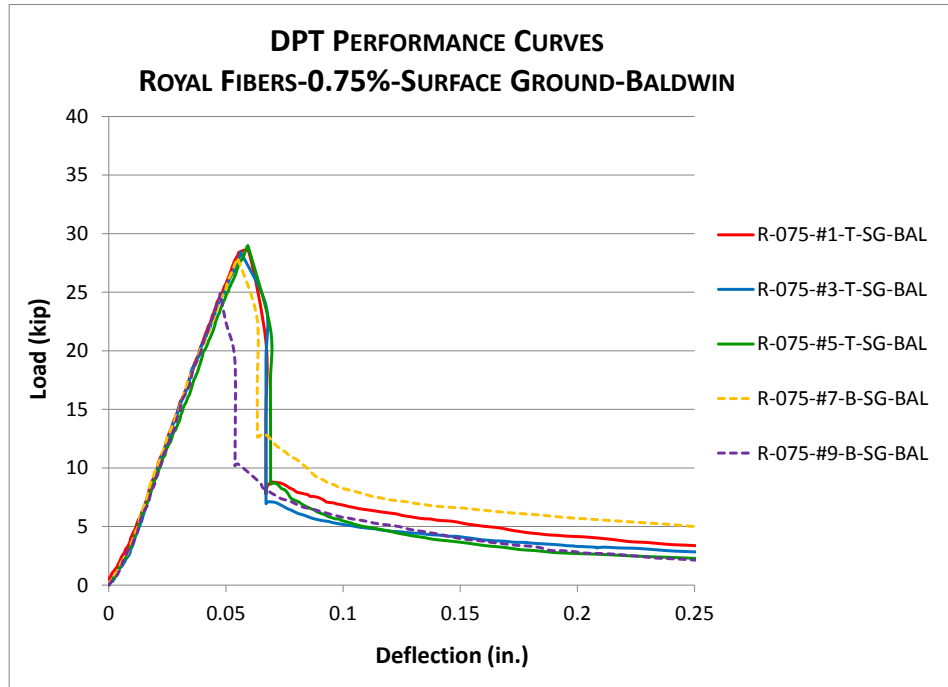
#### A.1 DPT PERFORMANCE CURVES FOR PHASE 1 TESTING

A total of sixty (60) Double-Punch Tests were conducted in Phase 1 of this study using Royal™ fibers. Performance curves were developed for each specimen and are displayed in the following figures. Note that top and bottom specimens are displayed on the same charts and are differentiated by line-type: top specimen – solid line; bottom specimen – dashed line. Also, for easy reading, only five (5) DPT Performance Curves are plotted on a given graph.

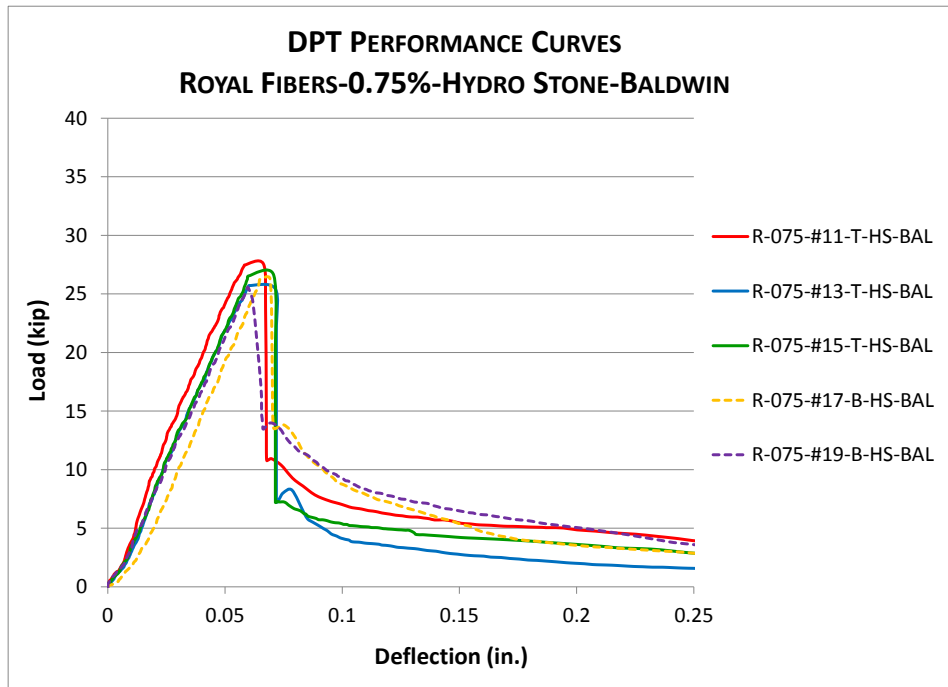
*Note A-1: Analysis results are meant to evaluate the DPT method. They are **not intended** to compare the performance of the different fibers used in this study. Royal™ and Bekaert Dramix® fibers were chosen arbitrarily to determine the ability of the Double-Punch Test to distinguish between FRC composed of different fiber types and volume fractions.*



**SURFACE-GROUND**

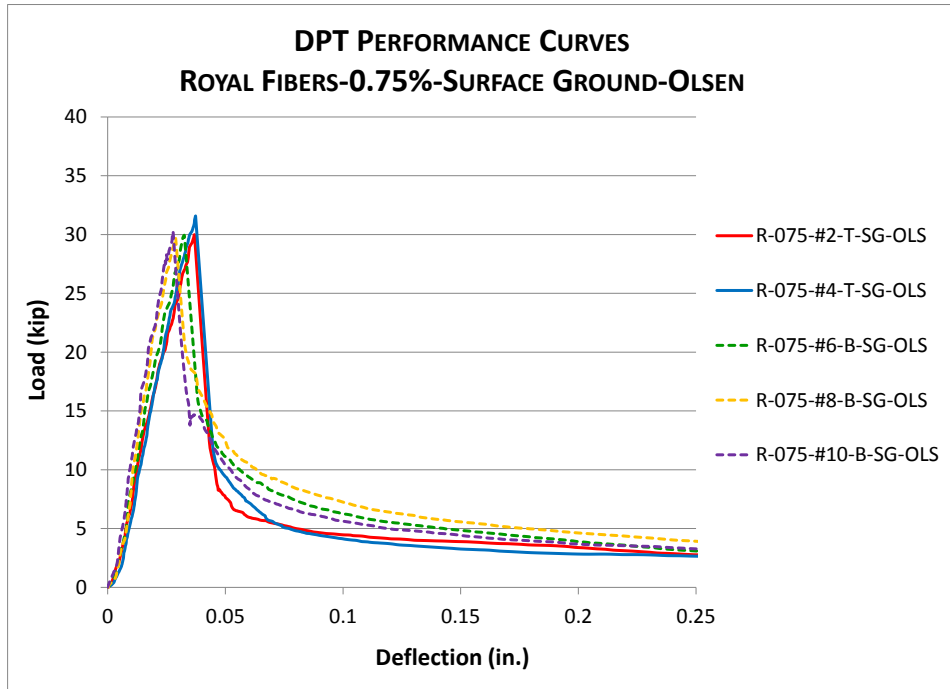


**HYDRO-STONE**

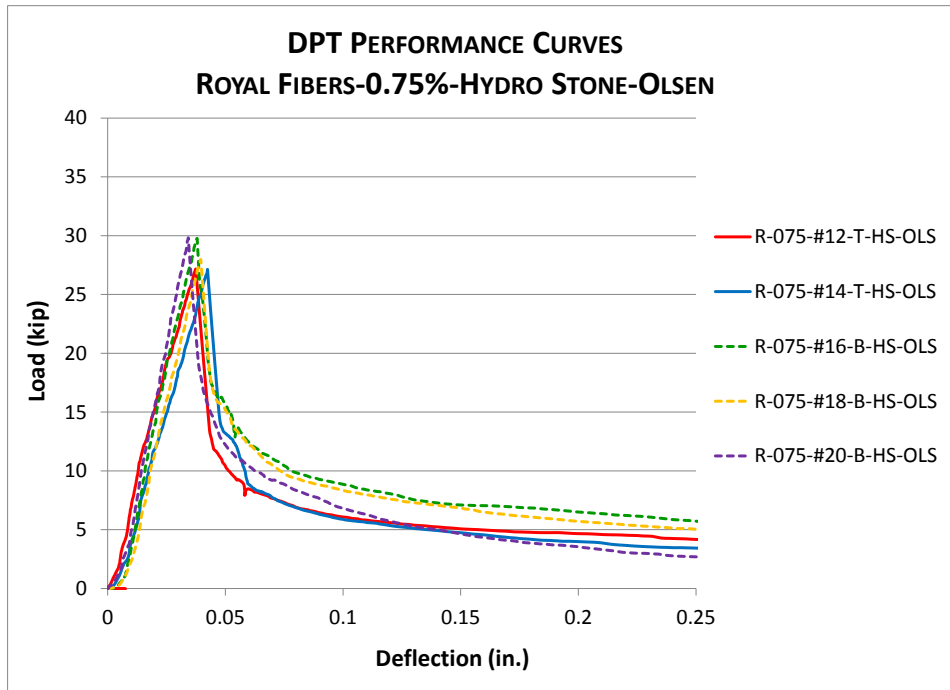


*Figure A-1: DPT Performance Curves for Phase 1 - Royal Fibers @ 0.75% Fiber Volume Fraction Tested on Baldwin Machine*

**SURFACE-GROUND**

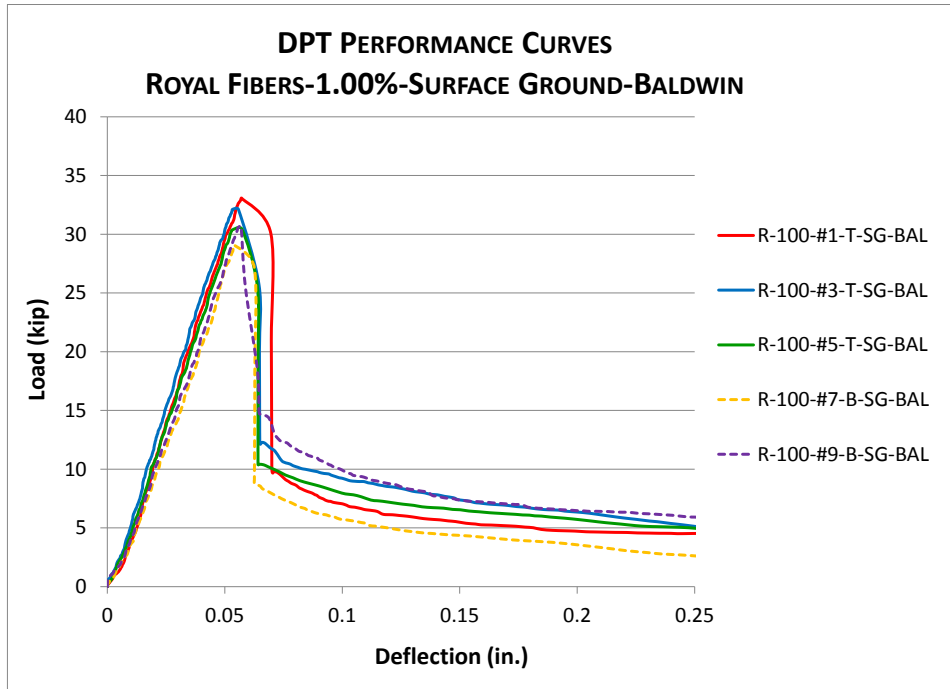


**HYDRO-STONE**

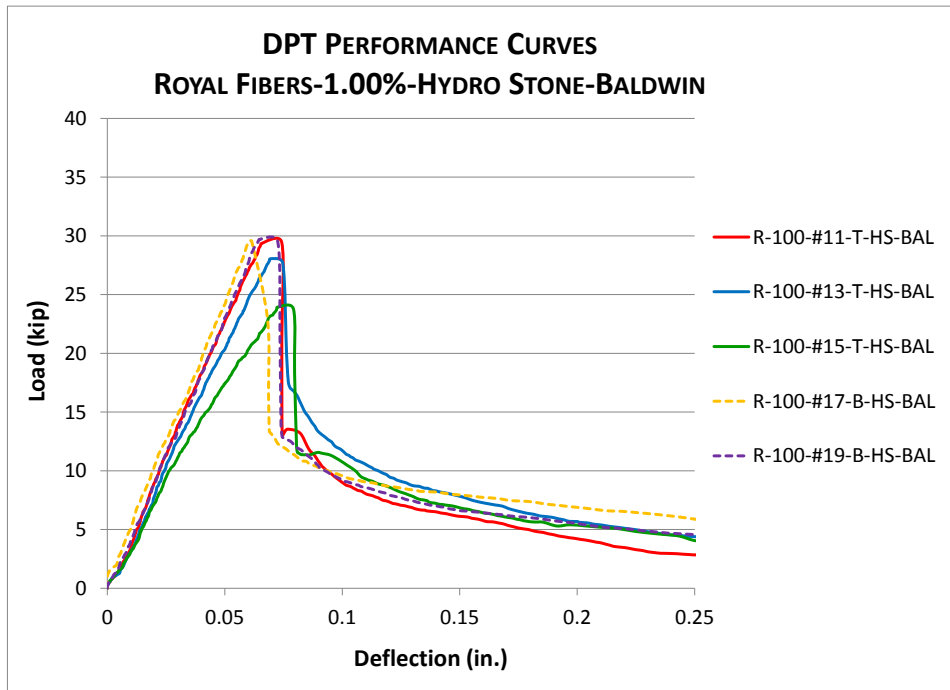


*Figure A-2: DPT Performance Curves for Phase 1 - Royal Fibers @ 0.75% Fiber Volume Fraction Tested on Olsen Machine*

**SURFACE-GROUND**

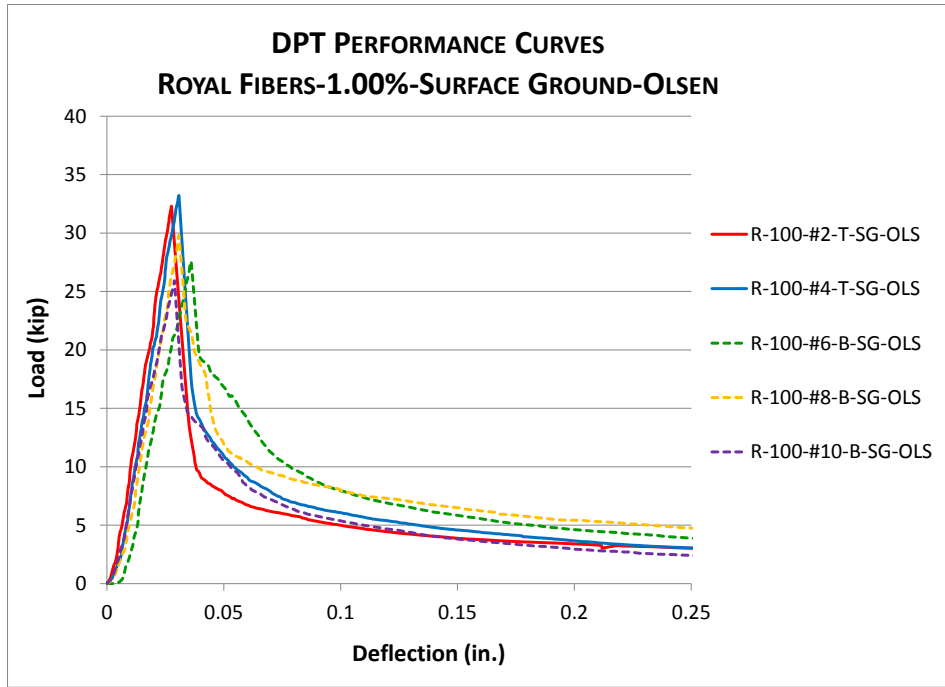


**HYDRO-STONE**

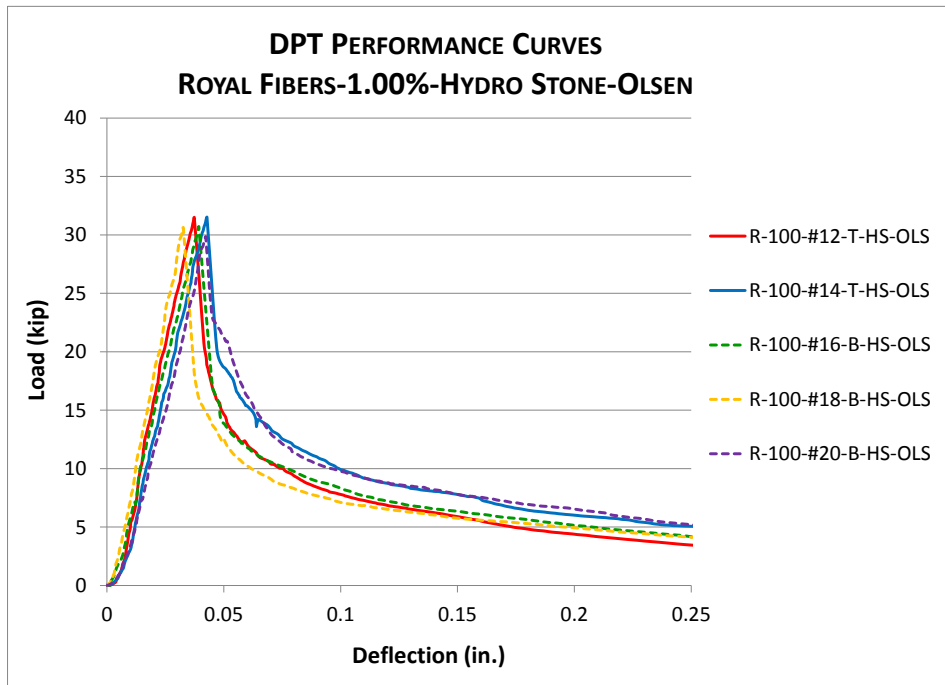


*Figure A-3: DPT Performance Curves for Phase 1 - Royal Fibers @ 1.00% Fiber Volume Fraction Tested on Baldwin Machine*

**SURFACE-GROUND**

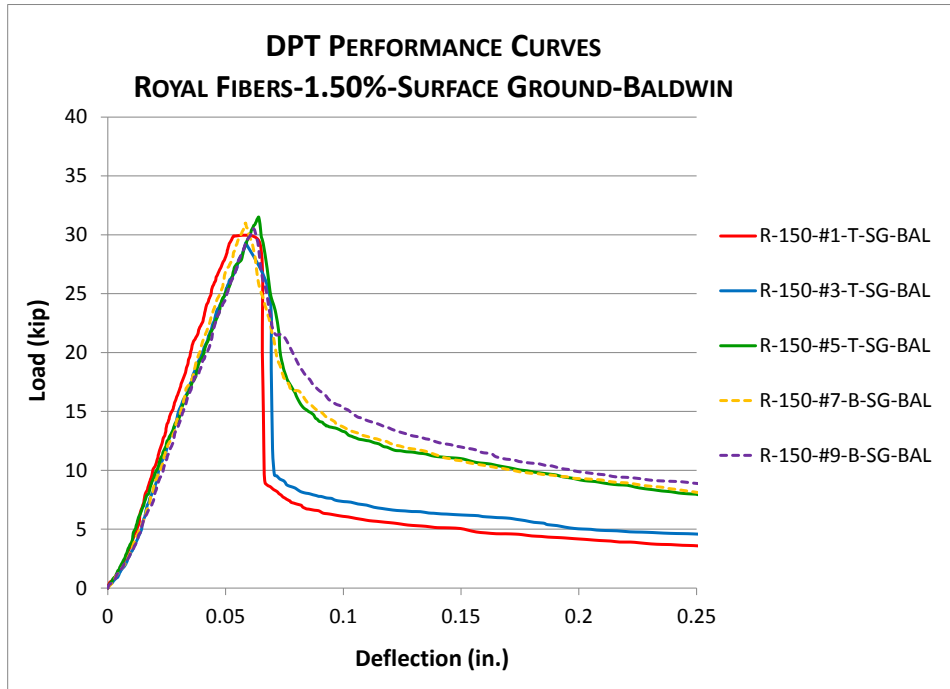


**HYDRO-STONE**

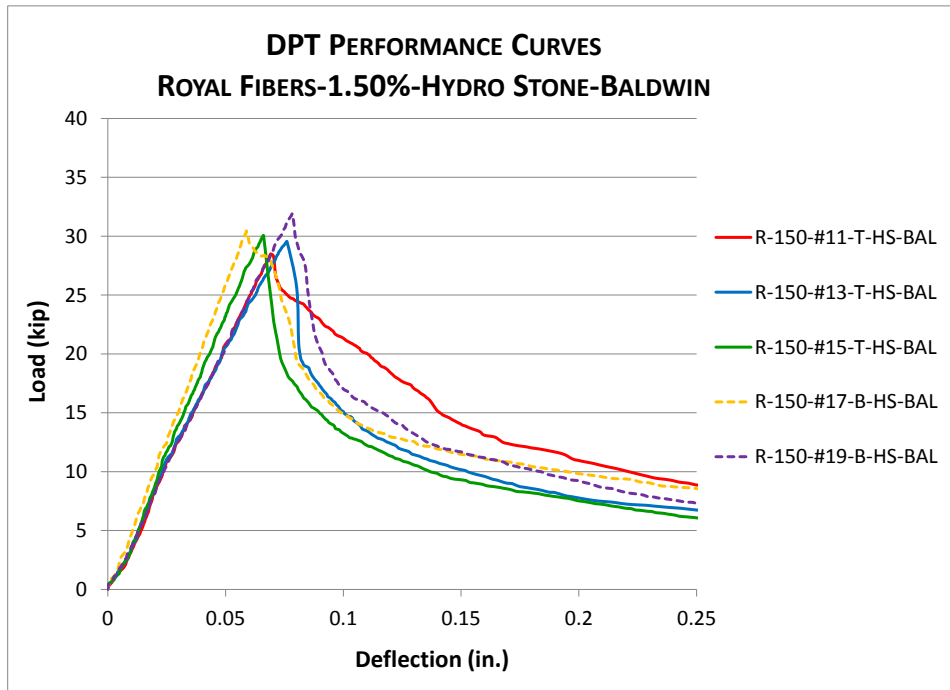


*Figure A-4: DPT Performance Curves for Phase 1 - Royal Fibers @ 1.00% Fiber Volume Fraction Tested on Olsen Machine*

**SURFACE-GROUND**

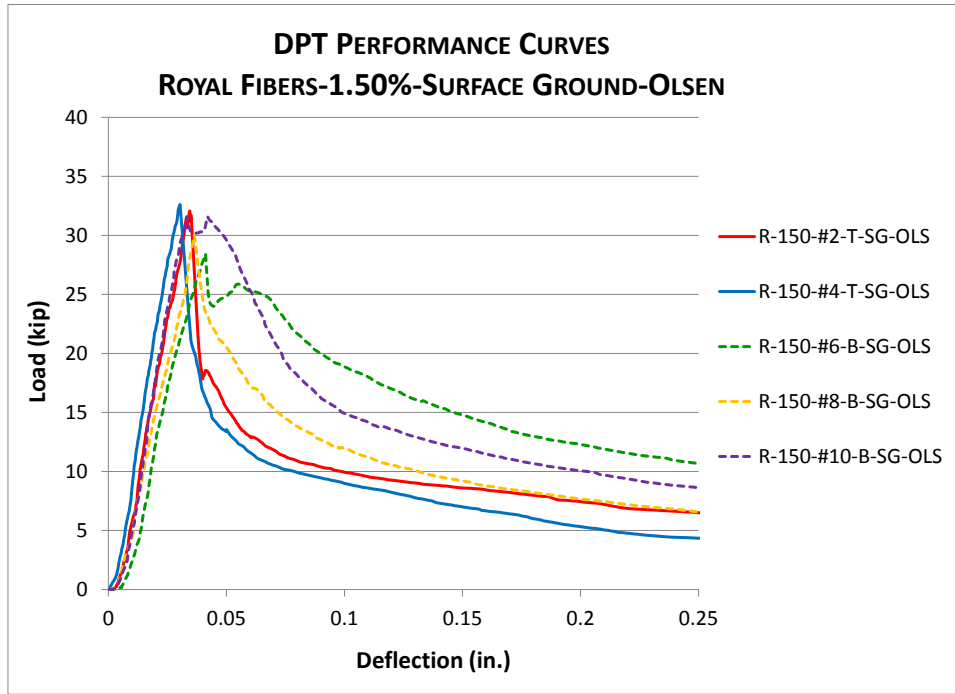


**HYDRO-STONE**

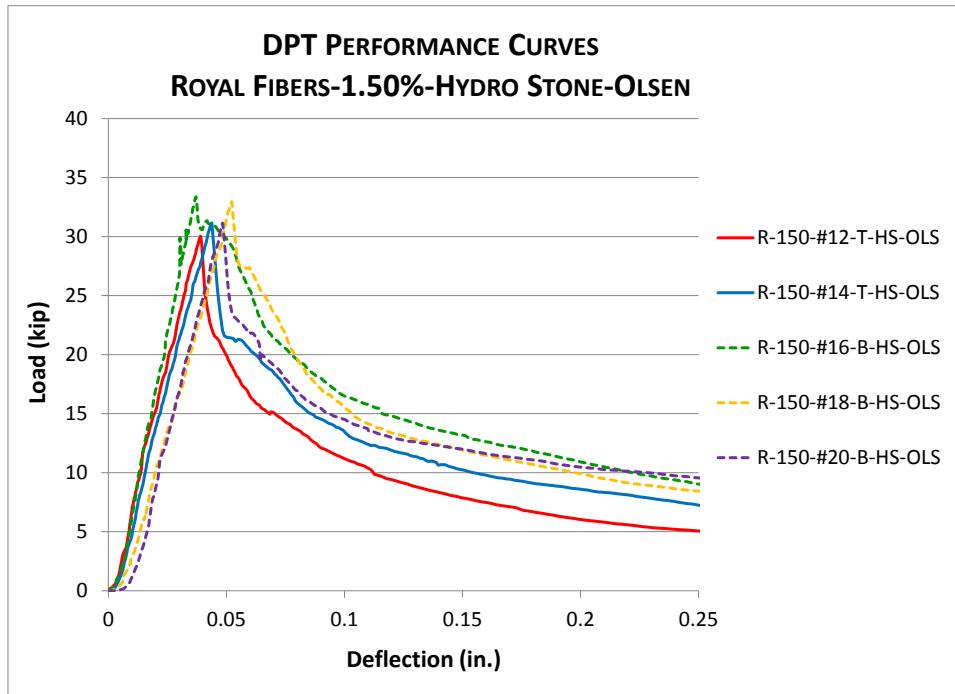


*Figure A-5: DPT Performance Curves for Phase 1 - Royal Fibers @ 1.50% Fiber Volume Fraction Tested on Baldwin Machine*

**SURFACE-GROUND**



**HYDRO-STONE**



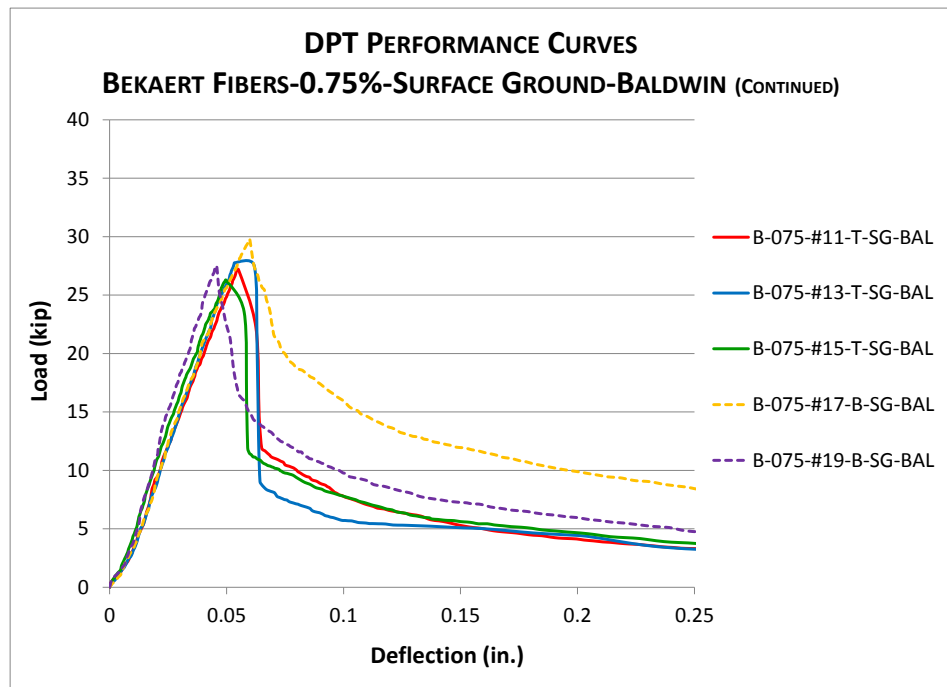
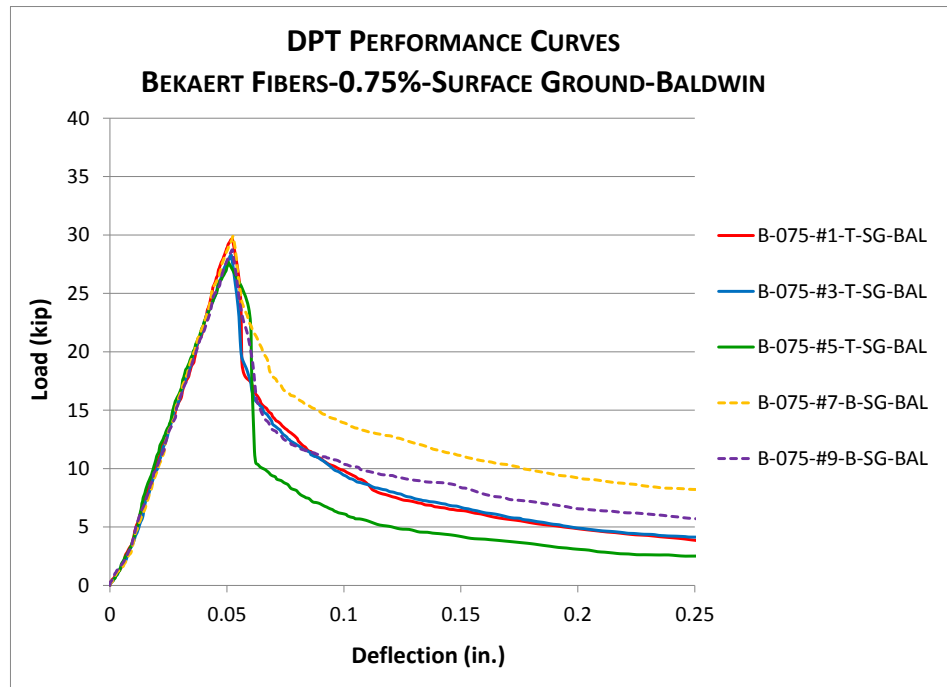
*Figure A-6: DPT Performance Curves for Phase 1 - Royal Fibers @ 1.50% Fiber Volume Fraction Tested on Olsen Machine*

## A.2 DPT PERFORMANCE CURVES FOR PHASE 2 TESTING

Another sixty (60) Double-Punch Tests were conducted in Phase 2 of this study using Bekaert Dramix® fibers. Performance curves were developed for each specimen and are displayed in the following figures. Note that top and bottom specimens are displayed on the same charts and are differentiated by line-type: top specimen – solid line; bottom specimen – dashed line. Also, for easy reading, only five (5) DPT Performance Curves are plotted on a given graph.

*Note A-2: Analysis results are meant to evaluate the DPT method. They are **not intended** to compare the performance of the different fibers used in this study. Royal™ and Bekaert Dramix® fibers were chosen arbitrarily to determine the ability of the Double-Punch Test to distinguish between FRC composed of different fiber types and volume fractions.*

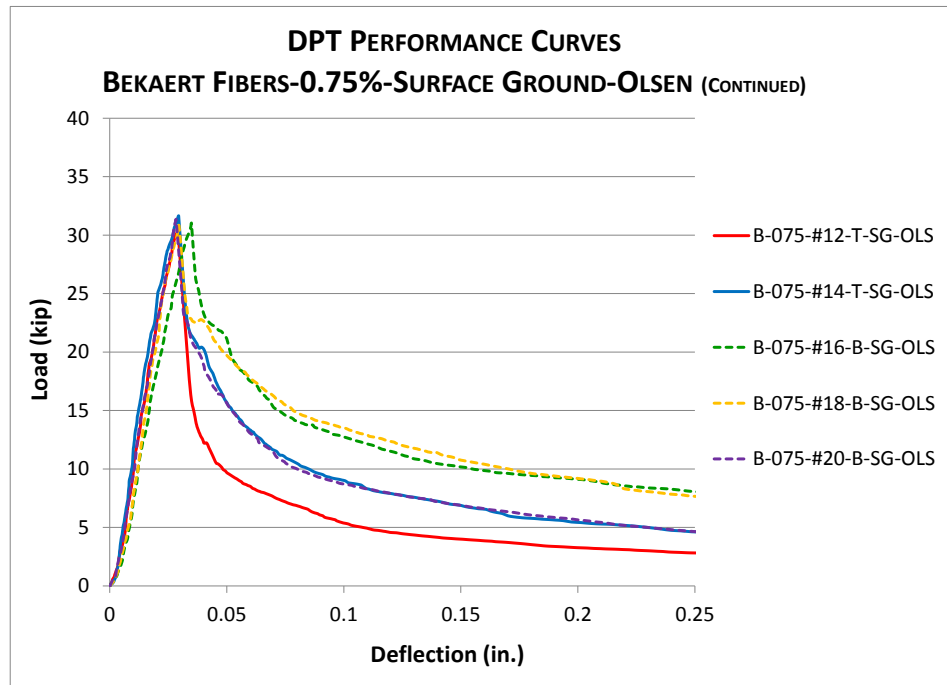
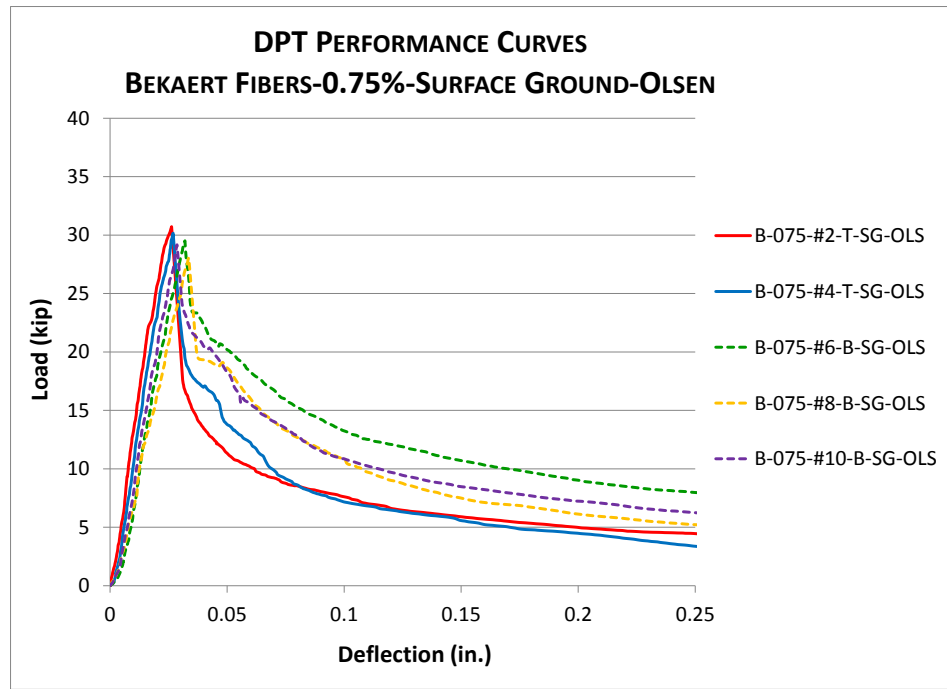
**SURFACE-GROUND ONLY**  
(NO HYDRO-STONE IN PHASE 2)



*Figure A-7: DPT Performance Curves for Phase 2 – Bekaert Fibers @ 0.75% Fiber Volume Fraction Tested on Baldwin Machine*

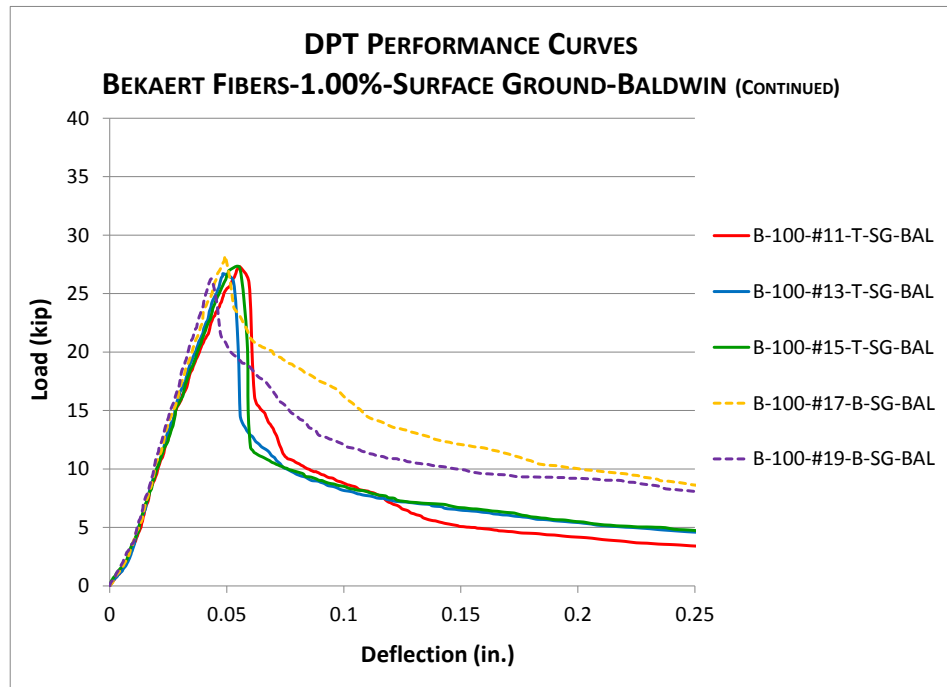
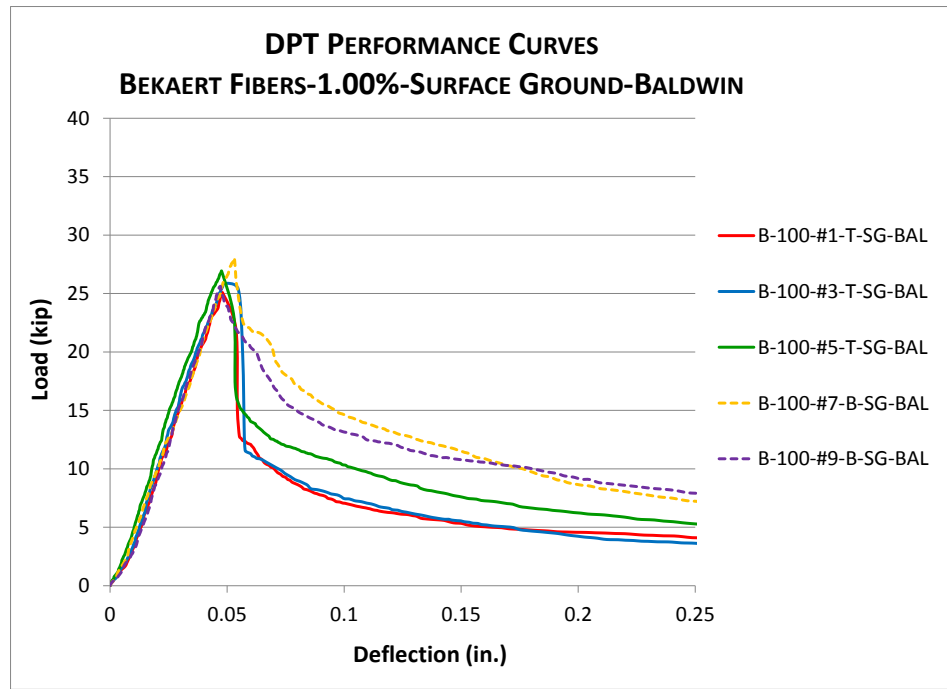


**SURFACE-GROUND ONLY**  
(NO HYDRO-STONE IN PHASE 2)



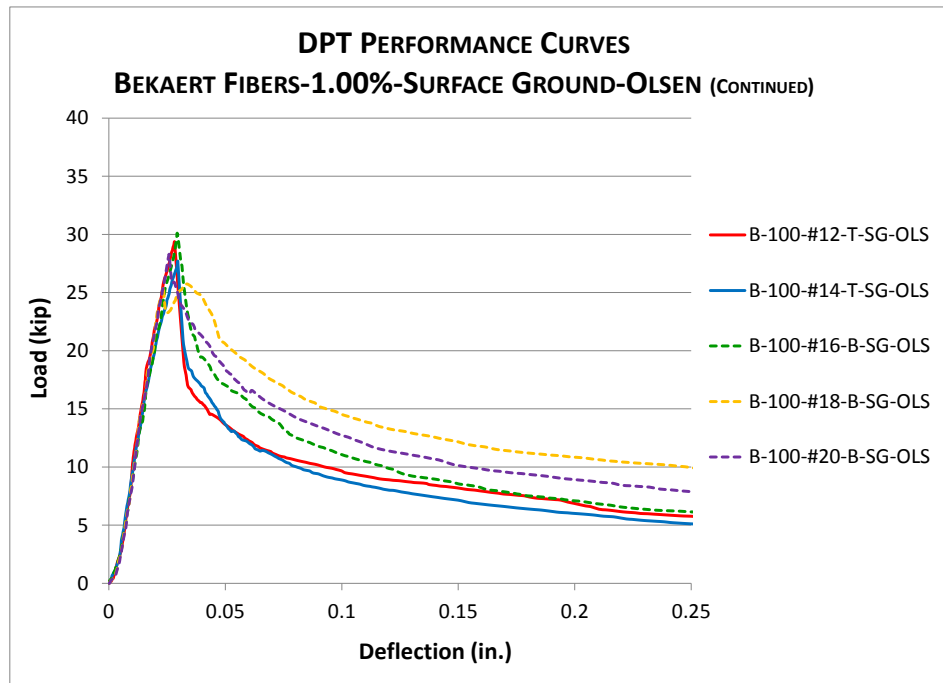
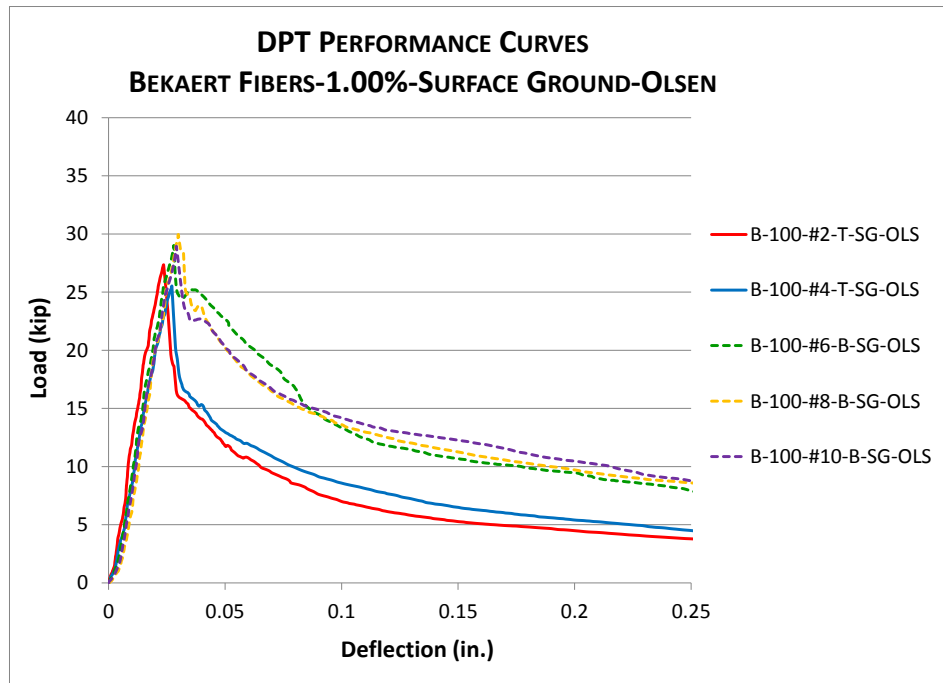
*Figure A-8: DPT Performance Curves for Phase 2 – Bekaert Fibers @ 0.75% Fiber Volume Fraction Tested on Olsen Machine*

**SURFACE-GROUND ONLY**  
(NO HYDRO-STONE IN PHASE 2)



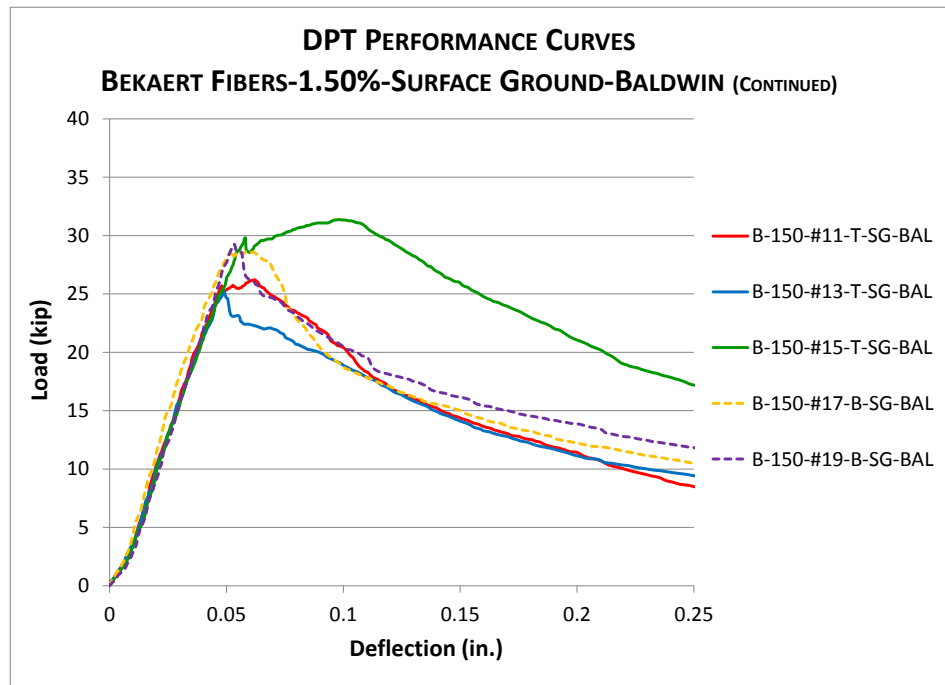
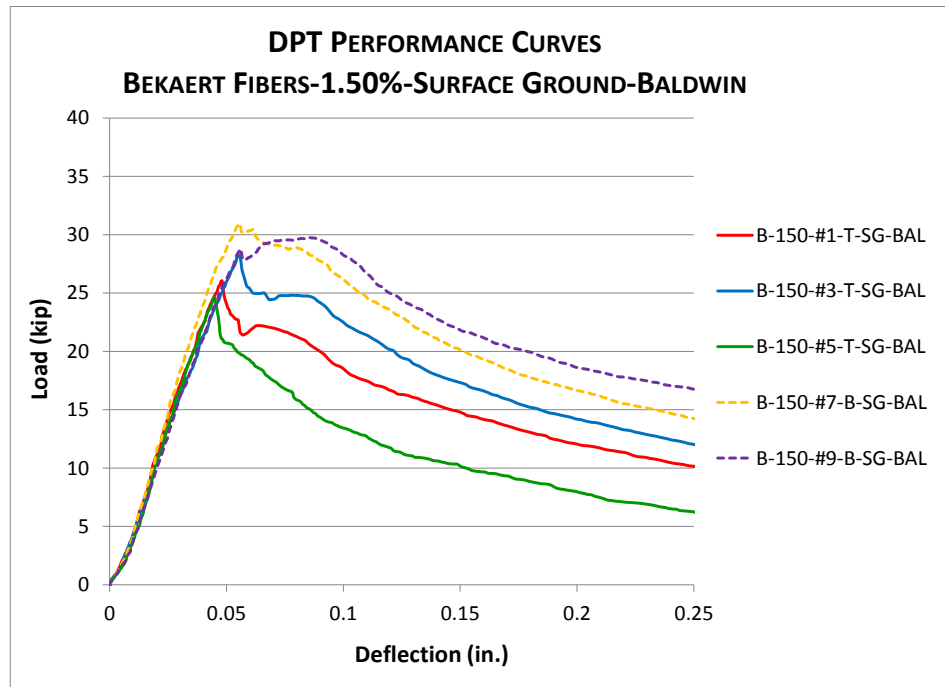
*Figure A-9: DPT Performance Curves for Phase 2 – Bekaert Fibers @ 1.00% Fiber Volume Fraction Tested on Baldwin Machine*

**SURFACE-GROUND ONLY**  
 (NO HYDRO-STONE IN PHASE 2)



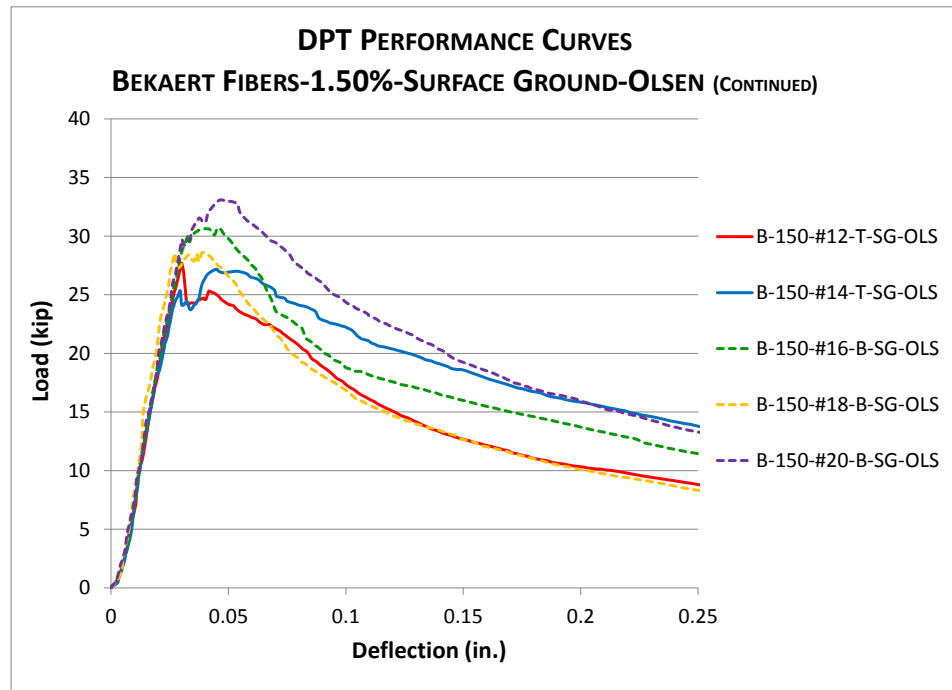
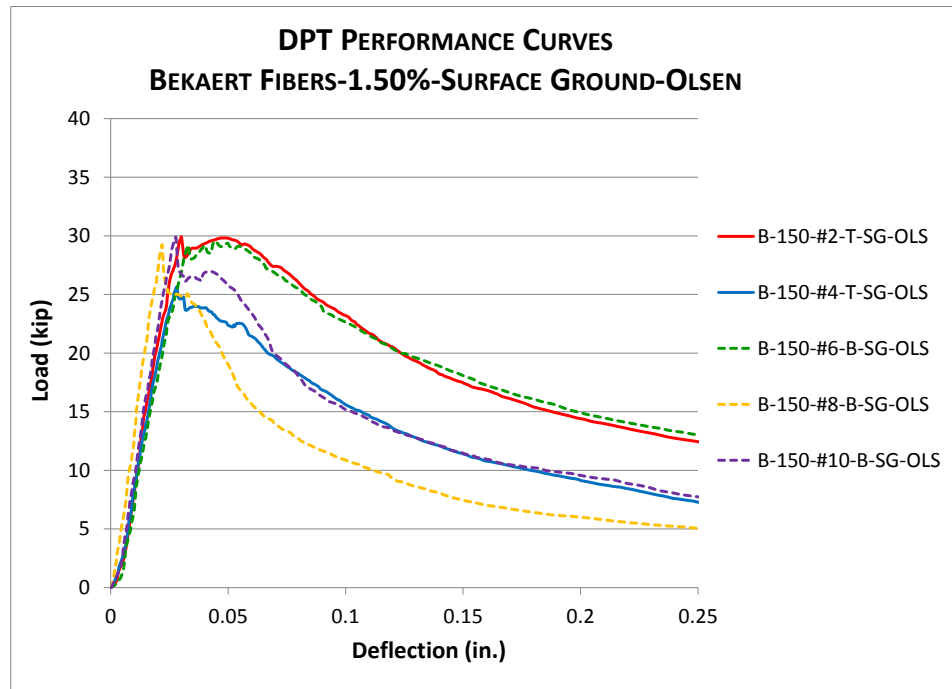
*Figure A-10: DPT Performance Curves for Phase 2 – Bekaert Fibers @ 1.00% Fiber Volume Fraction Tested on Olsen Machine*

**SURFACE-GROUND ONLY**  
(NO HYDRO-STONE IN PHASE 2)



*Figure A-11: DPT Performance Curves for Phase 2 – Bekaert Fibers @ 1.50% Fiber Volume Fraction Tested on Baldwin Machine*

**SURFACE-GROUND ONLY**  
(NO HYDRO-STONE IN PHASE 2)



*Figure A-12: DPT Performance Curves for Phase 2 – Bekaert Fibers @ 1.50% Fiber Volume Fraction Tested on Olsen Machine*

## APPENDIX B

### STATISTICAL ANALYSIS OF KEY DPT PARAMETERS

#### B.1 ANALYZING THE EFFECTS OF FIBER TYPE & VOLUME FRACTION

In Chapter 5, the key parameters of the DPT were stated. Figure 5-25 is repeated below for easy reference.

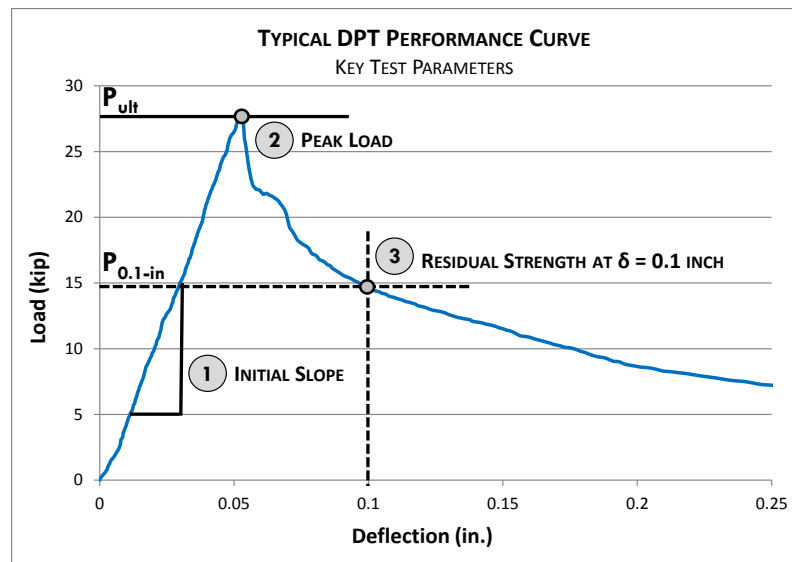


Figure 5-25: Typical DPT Performance Curve showing Key Test Parameters

Note B-1: Analysis results are meant to evaluate the DPT method. They are **not intended** to compare the performance of the different fibers used in this study. Royal™ and Bekaert Dramix® fibers were chosen arbitrarily to determine the ability of the Double-Punch Test to distinguish between FRC composed of different fiber types and volume fractions.

The following analyses were conducted to analyze the effects of fiber type and volume fraction on the initial slope, peak load, and residual strength at 0.1 in. deflection, respectively:

*Table B-1: Analyzing the Effects of Fiber Type & Volume Fraction on the Initial Slope*

**Analysis #1**

**Bekaert vs. Royal**

Test Criteria

Initial Slope

Constants

Surface Grinded, Baldwin Machine

Variable

Fiber Manufacturer & Type, Portion of Cylinder

Analysis #1	Bekaert			Royal		
	0.75%	1.00%	1.50%	0.75%	1.00%	1.50%
Test Criteria Initial Slope Top & Bot-SG-BAL	657	667	681	522	600	516
	660	637	593	604	679	634
	590	604	654	612	693	669
	620	640	622	571	570	558
	597	641	648	568	535	579
	586	668	618			
	582	655	625			
	629	536	693			
	771	707	651			
	622	679	682			
Mean	632	644	647	575	615	591
Std. Deviation	56.2	46.8	32.4	35.6	68.8	60.7
COV	8.9%	7.3%	5.0%	6.2%	11.2%	10.3%

**Analysis #2**

**Bekaert vs. Royal**

Test Criteria

Initial Slope

Constants

Surface Grinded, Olsen Machine

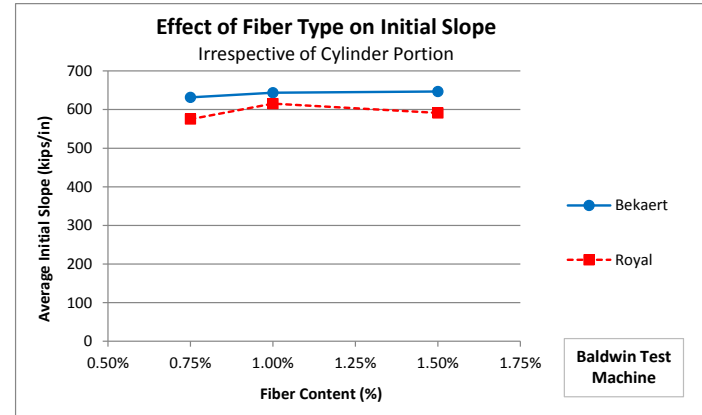
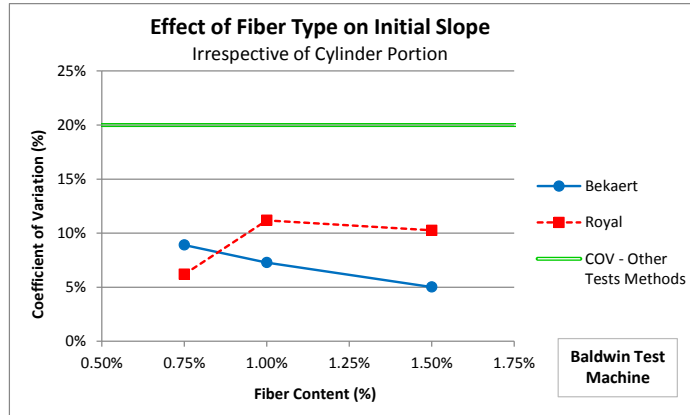
Variable

Fiber Manufacturer & Type, Portion of Cylinder

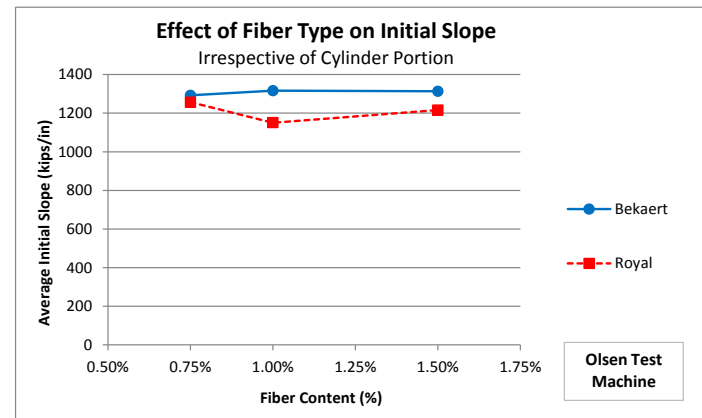
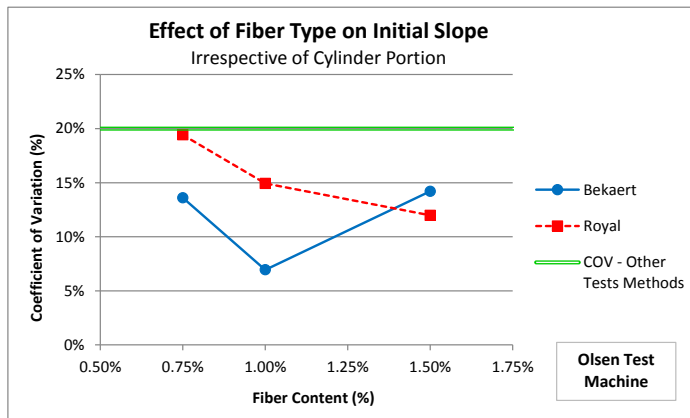
Analysis #2	Bekaert			Royal		
	0.75%	1.00%	1.50%	0.75%	1.00%	1.50%
Test Criteria Initial Slope Top & Bot-SG-OLS	1376	1444	1154	981	1323	1190
	1511	1238	1274	1085	1296	1350
	1509	1382	1437	1335	1156	1384
	1342	1208	1141	1271	1073	1084
	1251	1264	1400	1613	903	1072
	1184	1222	1192			
	1322	1398	1645			
	1311	1443	1127			
	1216	1279	1201			
	901	1284	1561			
Mean	1292	1316	1313	1257	1150	1216
Std. Deviation	175.8	91.4	186.4	244.2	171.7	145.6
COV	13.6%	6.9%	14.2%	19.4%	14.9%	12.0%

<sup>1</sup> See Note B-1.

**BALDWIN TEST MACHINE**



**OLSEN TEST MACHINE**



**COEFFICIENT OF VARIATION**

**AVERAGE PERFORMANCE**

*Figure B-1: Effect of Fiber Type & Volume Fraction on the Coefficient of Variation and Average Value of Initial Slope*



**Table B-2: Analyzing the Effects of Fiber Type & Volume Fraction on the Peak Load**

**Analysis #3**

**Bekaert vs. Royal**

Test Criteria

Peak Load

Constants

Surface Grinded, Baldwin Machine

Variable

Fiber Manufacturer & Type, Portion of Cylinder

Analysis #3	Bekaert			Royal		
	0.75%	1.00%	1.50%	0.75%	1.00%	1.50%
Test Criteria Peak Load Top & Bot-SG-BAL	27	27	26	28	33	30
	28	27	25	28	32	29
	26	27	31	29	30	32
	30	25	26	28	29	31
	28	26	28	25	31	31
	28	27	25			
	30	28	29			
	28	26	29			
	30	28	31			
	29	26	30			
Mean	28	27	28	28	31	30
Std. Deviation	1.2	1.0	2.4	1.6	1.6	0.9
COV	4.3%	3.8%	8.5%	5.9%	5.0%	2.9%

**Analysis #4**

**Bekaert vs. Royal**

Test Criteria

Peak Load

Constants

Surface Grinded, Olsen Machine

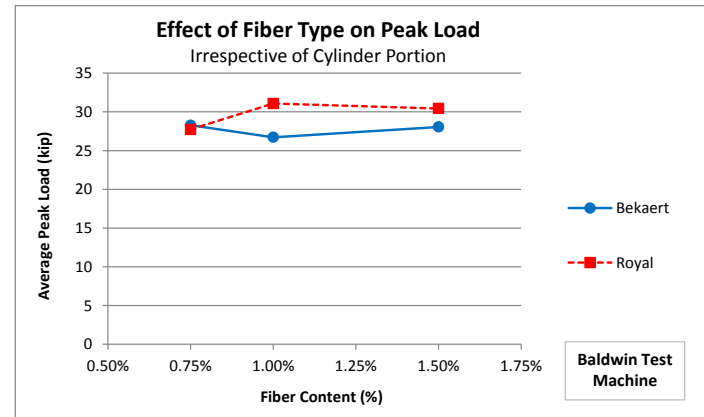
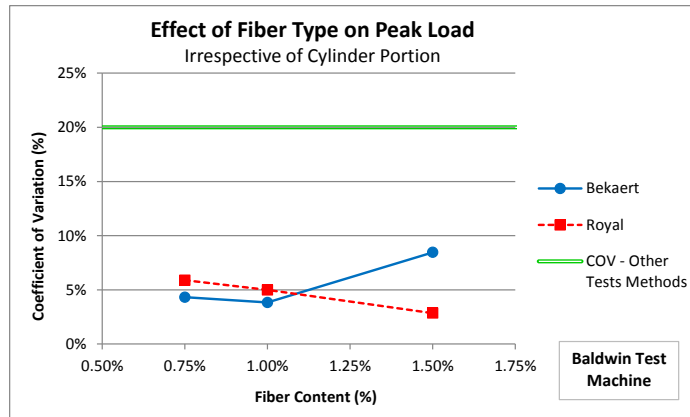
Variable

Fiber Manufacturer & Type, Portion of Cylinder

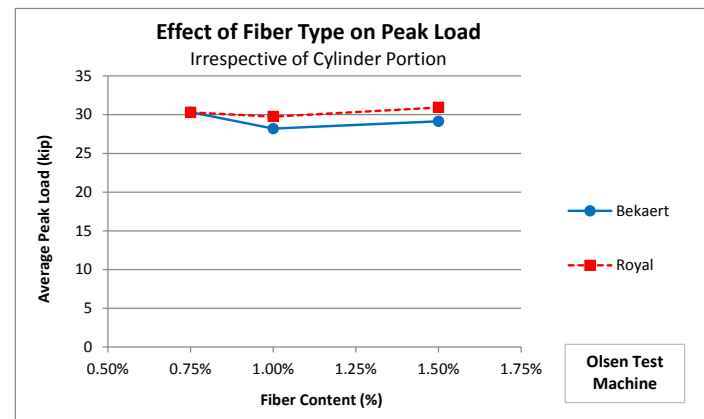
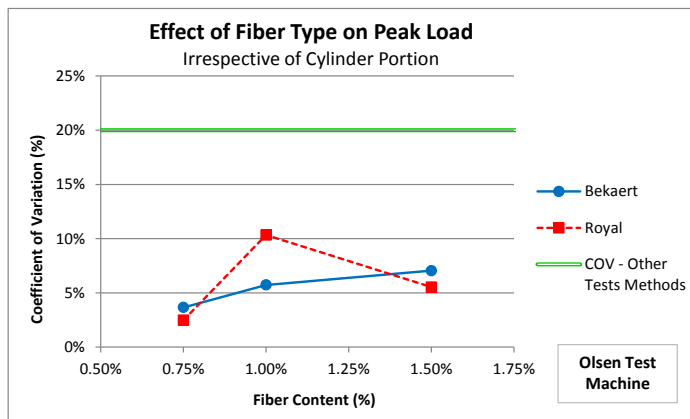
Analysis #4	Bekaert			Royal		
	0.75%	1.00%	1.50%	0.75%	1.00%	1.50%
Test Criteria Peak Load Top & Bot-SG-OLS	31	29	28	30	32	32
	32	28	27	32	33	33
	31	27	30	30	26	32
	30	26	26	30	28	28
	29	29	30	30	30	30
	31	30	31			
	31	26	29			
	31	28	33			
	30	29	30			
	28	30	29			
Mean	30	28	29	30	30	31
Std. Deviation	1.1	1.6	2.1	0.8	3.1	1.7
COV	3.7%	5.7%	7.0%	2.5%	10.3%	5.5%

<sup>1</sup> See Note B-1.

**BALDWIN TEST MACHINE**



**OLSEN TEST MACHINE**



**COEFFICIENT OF VARIATION**

**AVERAGE PERFORMANCE**

*Figure B-2: Effect of Fiber Type & Volume Fraction on the Coefficient of Variation and Average Value of Peak Load*

**Table B-3: Analyzing the Effects of Fiber Type & Volume Fraction on the Residual Strength**

**Analysis #5**

**Bekaert vs. Royal**

Test Criteria

Residual Strength

Constants

Surface Grinded, Baldwin Machine

Variable

Fiber Manufacturer & Type, Portion of Cylinder

Analysis #5	Bekaert			Royal		
	0.75%	1.00%	1.50%	0.75%	1.00%	1.50%
Test Criteria Residual Strength Top & Bot-SG-BAL	8	9	20	7	7	6
	6	8	19	5	9	7
	8	8	31	5	8	13
	10	7	18	8	6	14
	9	7	23	6	10	15
	6	10	13			
	16	16	19			
	10	12	20			
	14	15	26			
	10	13	28			
Mean	10	11	22	6	8	11
Std. Deviation	3.2	3.2	5.3	1.3	1.7	4.1
COV	33.1%	30.1%	24.4%	20.2%	20.8%	37.0%

**Analysis #6**

**Bekaert vs. Royal**

Test Criteria

Residual Strength

Constants

Surface Grinded, Olsen Machine

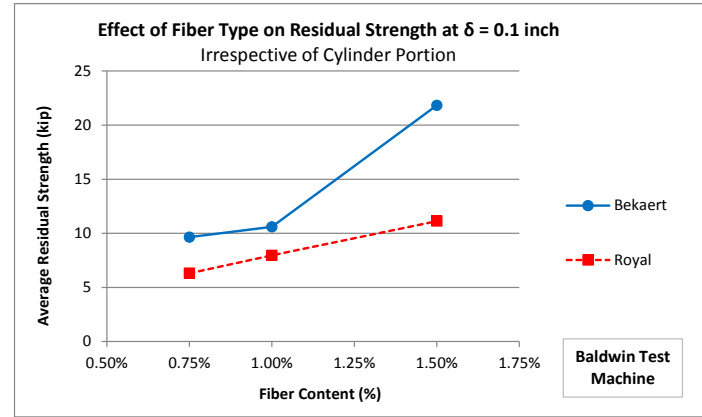
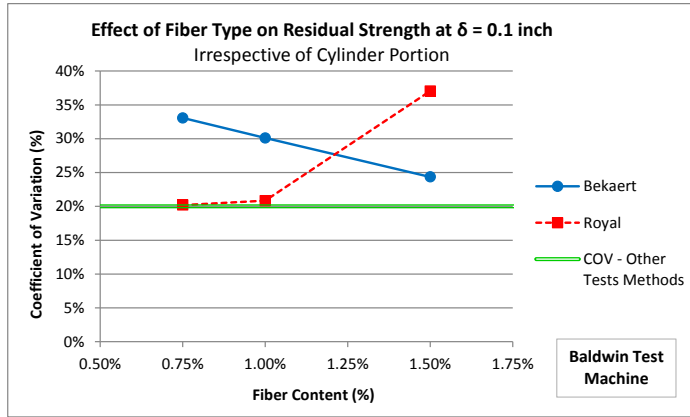
Variable

Fiber Manufacturer & Type, Portion of Cylinder

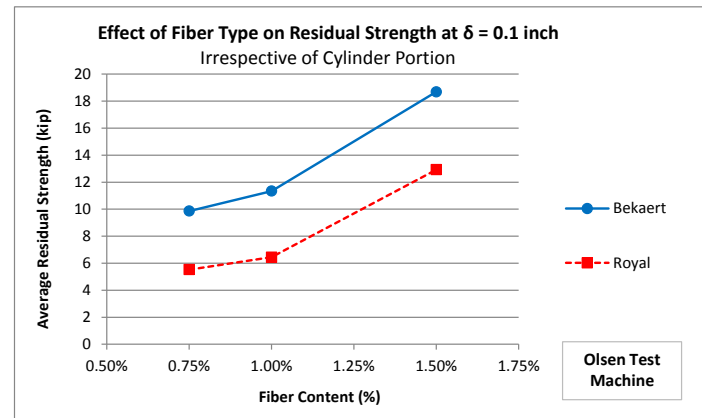
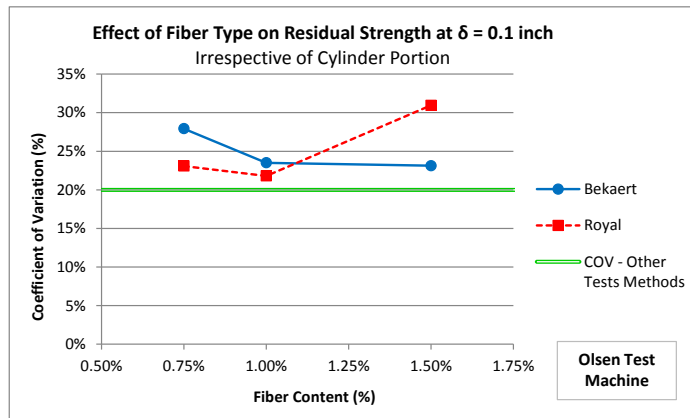
Analysis #6	Bekaert			Royal		
	0.75%	1.00%	1.50%	0.75%	1.00%	1.50%
Test Criteria Residual Strength Top & Bot-SG-BAL	5	10	17	4	5	10
	9	9	22	4	6	9
	8	7	23	6	5	15
	7	9	16	6	8	19
	11	14	15	7	8	12
	13	11	19			
	13	14	17			
	9	13	24			
	13	13	23			
	11	14	11			
Mean	10	11	19	6	6	13
Std. Deviation	2.8	2.7	4.3	1.3	1.4	4.0
COV	27.9%	23.5%	23.1%	23.1%	21.8%	30.9%

<sup>1</sup> See Note B-1.

**BALDWIN TEST MACHINE**



**OLSEN TEST MACHINE**



**COEFFICIENT OF VARIATION**

**AVERAGE PERFORMANCE**

*Figure B-3: Effect of Fiber Type & Volume Fraction on the Coefficient of Variation and Average Value of Residual Strength*

## **B.2 ANALYZING THE EFFECTS OF SPECIMEN SURFACE PREPARATION**

The following analyses were conducted to analyze the effects of specimen surface preparation on the initial slope, peak load, and residual strength at 0.1 in. deflection, respectively:

*Table B-4: Analyzing the Effects of Surface Preparation on the Initial Slope*

**Analysis #7**                      **Hydro-Stone vs. Surface Grinded**

Test Criteria                      *Initial Slope*  
 Constants                          *Royal Fibers, Baldwin Machine*  
 Variable                            *Surface Preparation, Portion of Cylinder*

Analysis #7	Hydro-Stone			Surface Grinded		
	0.75%	1.00%	1.50%	0.75%	1.00%	1.50%
Test Criteria Initial Slope Royal-Top & Bot-BAL	557	502	454	612	693	669
	501	449	441	604	679	634
	485	360	521	522	600	516
	476	489	514	568	535	579
	443	471	436	571	570	558
Mean	492	454	473	575	615	591
Std. Deviation	42.1	56.2	40.9	35.6	68.8	60.7
COV	8.6%	12.4%	8.7%	6.2%	11.2%	10.3%

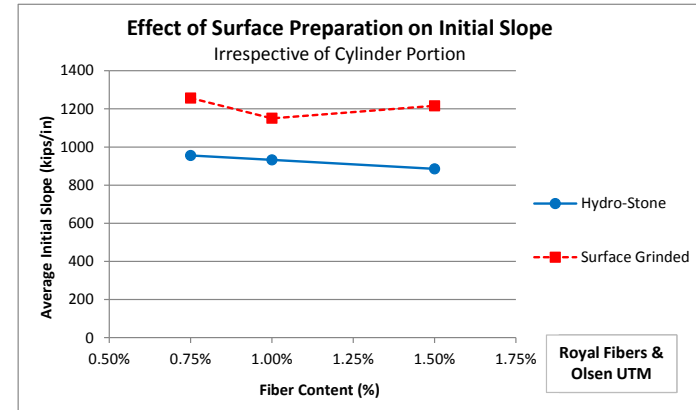
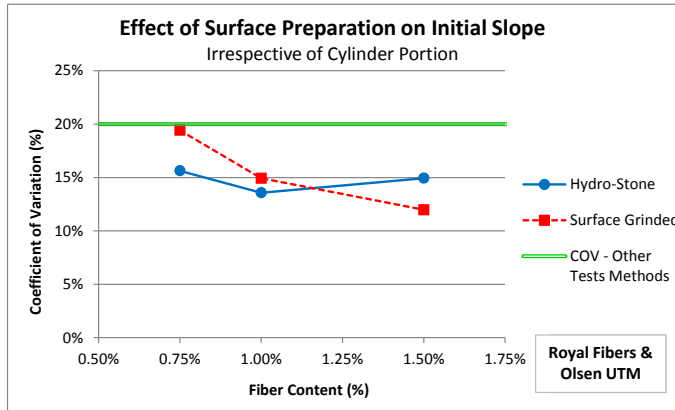
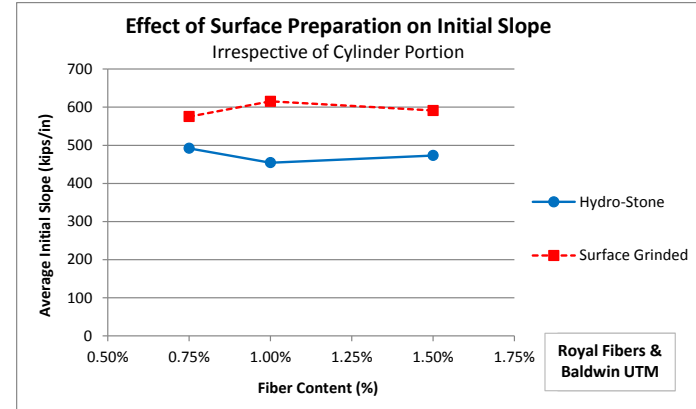
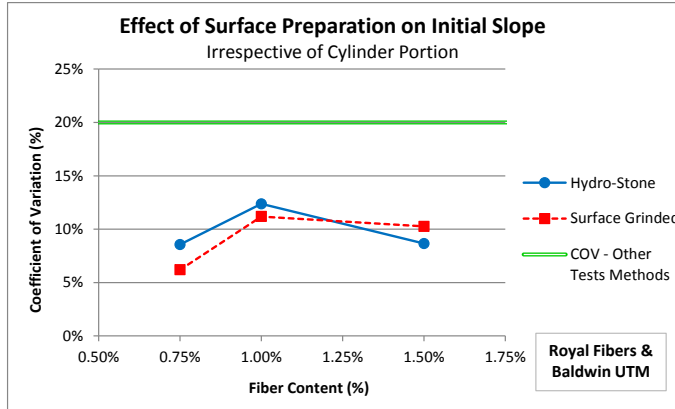
**Analysis #8**                      **Hydro-Stone vs. Surface Grinded**

Test Criteria                      *Initial Slope*  
 Constants                          *Royal Fibers, Olsen Machine*  
 Variable                            *Surface Preparation, Portion of Cylinder*

Analysis #8	Hydro-Stone			Surface Grinded		
	0.75%	1.00%	1.50%	0.75%	1.00%	1.50%
Test Criteria Initial Slope Royal-Top & Bot-OLS	889	1078	919	981	1323	1190
	737	912	847	1085	1296	1350
	1093	873	1073	1335	1156	1384
	968	1036	706	1271	1073	1084
	1089	764	882	1613	903	1072
Mean	955	933	885	1257	1150	1216
Std. Deviation	149.3	126.6	132.3	244.2	171.7	145.6
COV	15.6%	13.6%	14.9%	19.4%	14.9%	12.0%

<sup>1</sup> See Note B-1.

**PHASE 1**  
**ROYAL FIBERS TESTED ON BALDWIN AND OLSEN UTMS**



**COEFFICIENT OF VARIATION**

**AVERAGE PERFORMANCE**

*Figure B-4: Effect of Surface Preparation on the Coefficient of Variation and Average Value of Initial Slope*

*Table B-5: Analyzing the Effects of Surface Preparation on the Peak Load*

**Analysis #9**                      **Hydro-Stone vs. Surface Grinded**

Test Criteria                      *Peak Load*  
 Constants                          *Royal Fibers, Baldwin Machine*  
 Variable                            *Surface Preparation, Portion of Cylinder*

Analysis #9	Hydro-Stone			Surface Grinded		
	0.75%	1.00%	1.50%	0.75%	1.00%	1.50%
<b>Test Criteria</b> Peak Load Royal-Top & Bot-BAL	28	29	28	28	33	30
	26	28	30	28	32	29
	27	24	30	29	30	32
	26	30	30	28	29	31
	26	30	32	25	31	31
<b>Mean</b>	26	28	30	28	31	30
<b>Std. Deviation</b>	0.8	2.4	1.3	1.6	1.6	0.9
<b>COV</b>	3.0%	8.7%	4.2%	5.9%	5.0%	2.9%

**Analysis #10**                      **Hydro-Stone vs. Surface Grinded**

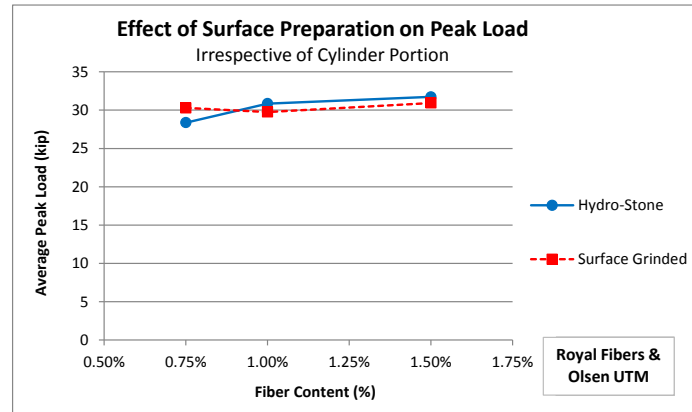
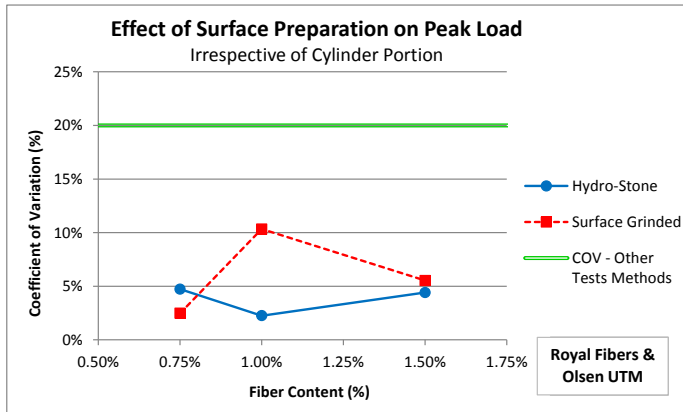
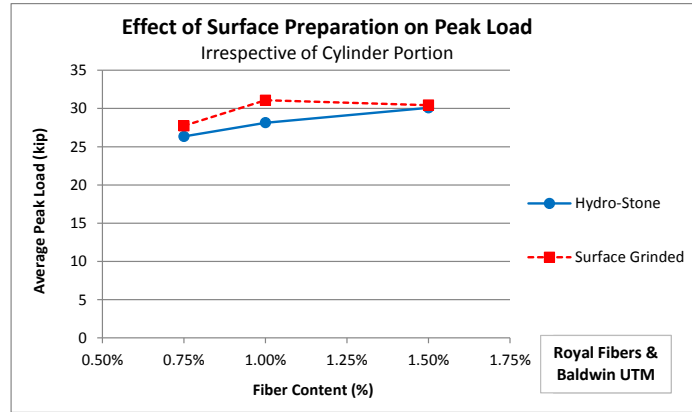
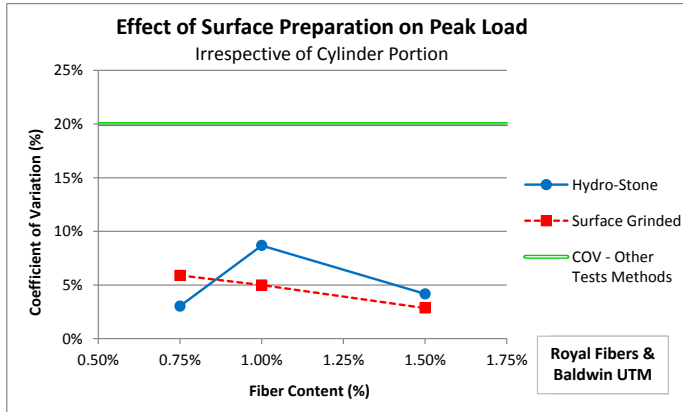
Test Criteria                      *Peak Load*  
 Constants                          *Royal Fibers, Olsen Machine*  
 Variable                            *Surface Preparation, Portion of Cylinder*

Analysis #10	Hydro-Stone			Surface Grinded		
	0.75%	1.00%	1.50%	0.75%	1.00%	1.50%
<b>Test Criteria</b> Peak Load Royal-Top & Bot-OLS	27	32	30	30	32	32
	27	32	31	32	33	33
	30	31	33	30	26	32
	28	31	33	30	28	28
	30	30	31	30	30	30
<b>Mean</b>	28	31	32	30	30	31
<b>Std. Deviation</b>	1.3	0.7	1.4	0.8	3.1	1.7
<b>COV</b>	4.7%	2.3%	4.4%	2.5%	10.3%	5.5%

<sup>1</sup> See Note B-1.



**PHASE 1  
ROYAL FIBERS TESTED ON BALDWIN AND OLSEN UTMS**



**COEFFICIENT OF VARIATION**

**AVERAGE PERFORMANCE**

*Figure B-5: Effect of Surface Preparation on the Coefficient of Variation and Average Value of Peak Load*

*Table B-6: Analyzing the Effects of Surface Preparation on the Residual Strength*

**Analysis #11**      **Hydro-Stone vs. Surface Grinded**

Test Criteria      *Residual Strength*  
 Constants      *Royal Fibers, Baldwin Machine*  
 Variable      *Surface Preparation, Portion of Cylinder*

Analysis #11	Hydro-Stone			Surface Grinded		
	0.75%	1.00%	1.50%	0.75%	1.00%	1.50%
<b>Test Criteria</b> Residual Strength Royal-Top & Bot-BAL	7	10	21	7	7	6
	4	12	15	5	9	7
	5	11	13	5	8	13
	9	10	15	8	6	14
	9	9	17	6	10	15
Mean	7	10	16	6	8	11
Std. Deviation	2.2	1.1	3.1	1.3	1.7	4.1
COV	32.0%	10.6%	18.9%	20.2%	20.8%	37.0%

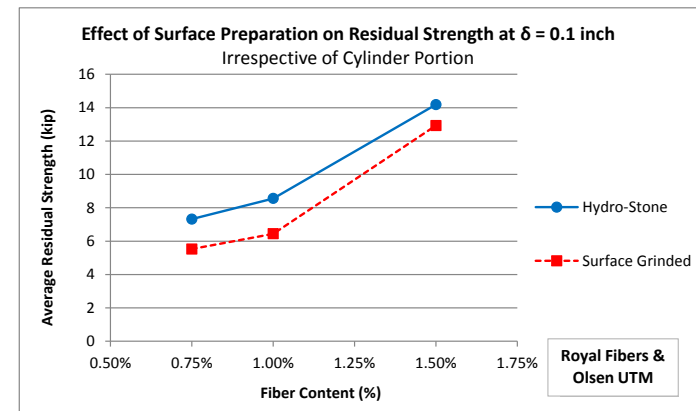
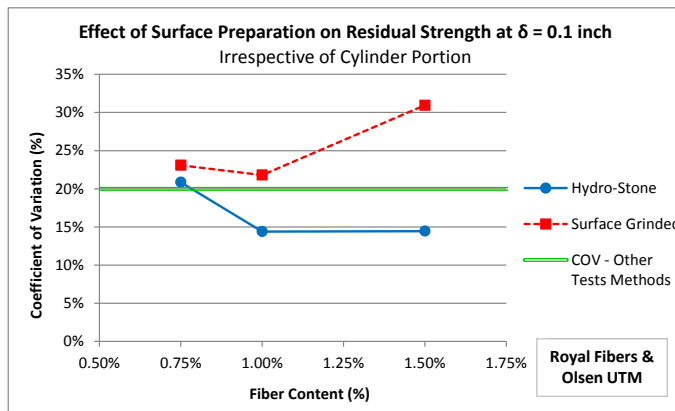
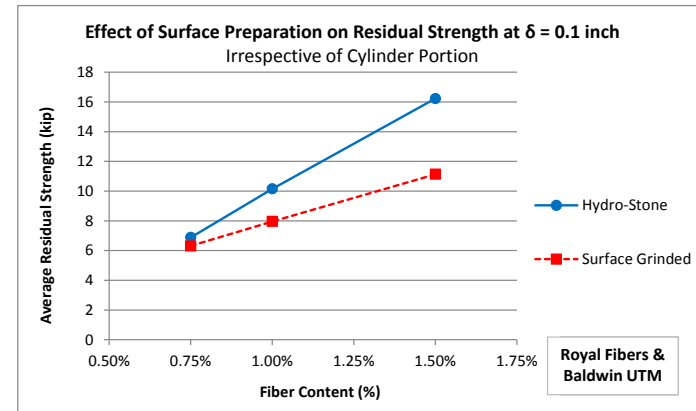
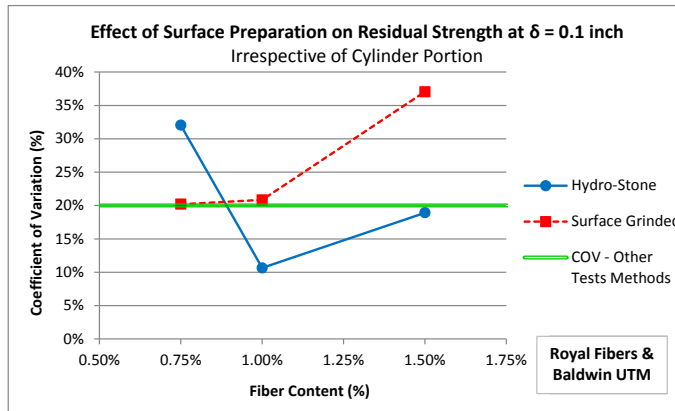
**Analysis #12**      **Hydro-Stone vs. Surface Grinded**

Test Criteria      *Residual Strength*  
 Constants      *Royal Fibers, Baldwin Machine*  
 Variable      *Surface Preparation, Portion of Cylinder*

Analysis #12	Hydro-Stone			Surface Grinded		
	0.75%	1.00%	1.50%	0.75%	1.00%	1.50%
<b>Test Criteria</b> Residual Strength Royal-Top & Bot-OLS	6	8	11	4	5	10
	6	10	13	4	6	9
	9	8	16	6	5	15
	9	7	16	6	8	19
	7	10	14	7	8	12
Mean	7	9	14	6	6	13
Std. Deviation	1.5	1.2	2.0	1.3	1.4	4.0
COV	20.9%	14.4%	14.5%	23.1%	21.8%	30.9%

<sup>1</sup> See Note B-1.

**PHASE 1**  
**ROYAL FIBERS TESTED ON BALDWIN AND OLSEN UTMS**



**COEFFICIENT OF VARIATION**

**AVERAGE PERFORMANCE**

*Figure B-6: Effect of Surface Preparation on the Coefficient of Variation and Average Value of Residual Strength*

### **B.3 ANALYZING THE EFFECTS OF TEST MACHINE**

The following analyses were conducted to analyze the effects of different test machines on the initial slope, peak load, and residual strength at 0.1 in. deflection, respectively:

*Table B-7: Analyzing the Effects of Test Machine on the Initial Slope*

**Analysis #13**

**Baldwin Machine vs. Olsen Machine**

Test Criteria

*Initial Slope*

Constants

*Royal Fibers, Surface Grinded*

Variable

*Test Machine, Portion of Cylinder*

Analysis #13	Baldwin			Olsen		
	0.75%	1.00%	1.50%	0.75%	1.00%	1.50%
Test Criteria Initial Slope Royal-Top & Bot-SG	612	693	669	981	1323	1190
	604	679	634	1085	1296	1350
	522	600	516	1335	1156	1384
	568	535	579	1271	1073	1084
	571	570	558	1613	903	1072
Mean	575	615	591	1257	1150	1216
Std. Deviation	35.6	68.8	60.7	244.2	171.7	145.6
COV	6.2%	11.2%	10.3%	19.4%	14.9%	12.0%

**Analysis #14**

**Baldwin Machine vs. Olsen Machine**

Test Criteria

*Initial Slope*

Constants

*Bekaert Fibers, Surface Grinded*

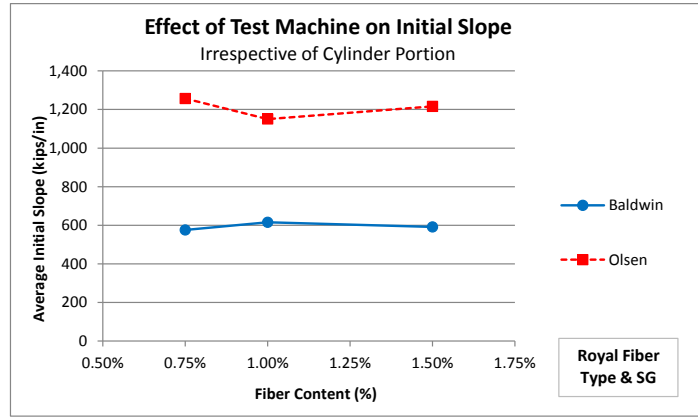
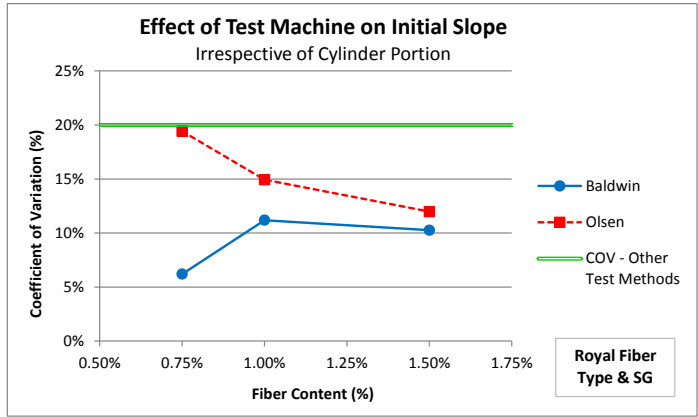
Variable

*Test Machine, Portion of Cylinder*

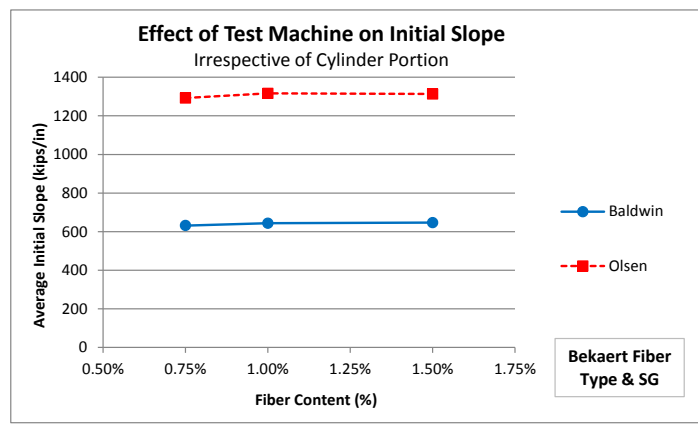
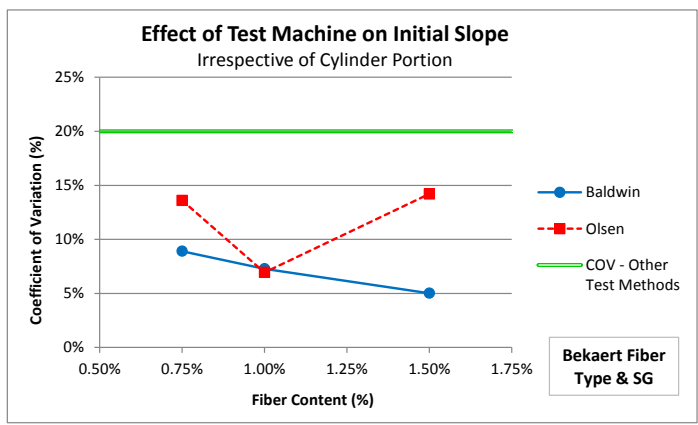
Analysis #14	Baldwin			Olsen			
	0.75%	1.00%	1.50%	0.75%	1.00%	1.50%	
Test Criteria Initial Slope Bekaert-Top & Bot-SG	590	604	654	1509	1382	1437	
	660	637	593	1342	1208	1141	
	657	667	681	1376	1444	1154	
	586	668	618	1511	1238	1274	
	597	641	648	1216	1279	1201	
	620	640	622	901	1284	1561	
	629	536	693	1251	1264	1400	
	582	655	625	1184	1222	1192	
	622	679	682	1322	1398	1645	
	771	707	651	1311	1443	1127	
	Mean	632	644	647	1292	1316	1313
	Std. Deviation	56.2	46.8	32.4	175.8	91.4	186.4
COV	8.9%	7.3%	5.0%	13.6%	6.9%	14.2%	

<sup>1</sup> See Note B-1.

**PHASE 1  
ROYAL FIBERS**



**PHASE 2  
BEKAERT FIBERS**



**COEFFICIENT OF VARIATION**

**AVERAGE PERFORMANCE**

*Figure B-7: Effect of Test Machine on the Coefficient of Variation and Average Value of Initial Slope*

*Table B-8: Analyzing the Effects of Test Machine on the Peak Load*

**Analysis #15**

**Baldwin Machine vs. Olsen Machine**

Test Criteria

Peak Load

Constants

Royal Fibers, Surface Grinded

Variable

Test Machine, Portion of Cylinder

Analysis #15	Baldwin			Olsen		
	0.75%	1.00%	1.50%	0.75%	1.00%	1.50%
Test Criteria Peak Load Royal-Top & Bot-SG	28	33	30	30	32	32
	28	32	29	32	33	33
	29	30	32	30	26	32
	28	29	31	30	28	28
	25	31	31	30	30	30
Mean	28	31	30	30	30	31
Std. Deviation	1.6	1.6	0.9	0.8	3.1	1.7
COV	5.9%	5.0%	2.9%	2.5%	10.3%	5.5%

**Analysis #16**

**Baldwin Machine vs. Olsen Machine**

Test Criteria

Peak Load

Constants

Bekaert Fibers, Surface Grinded

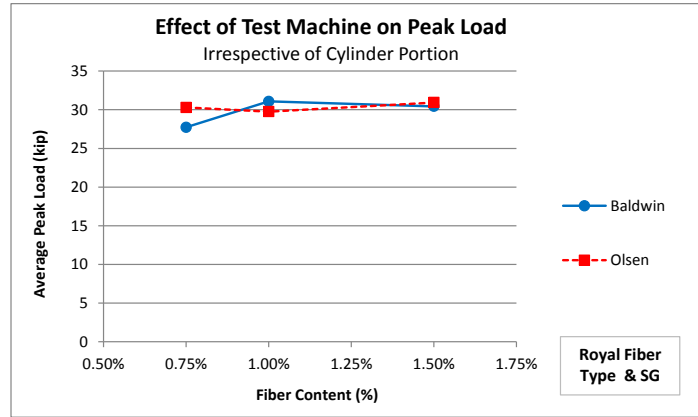
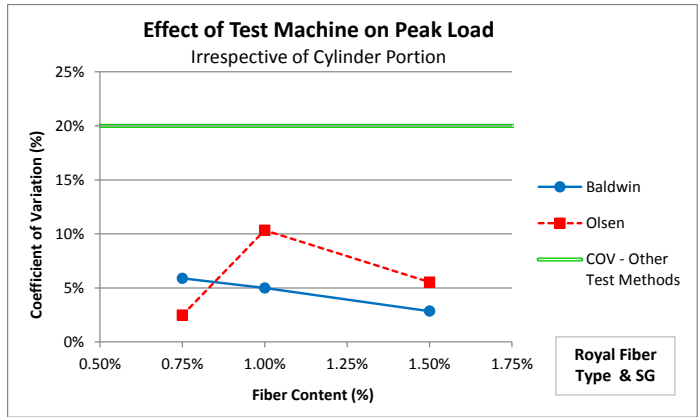
Variable

Test Machine, Portion of Cylinder

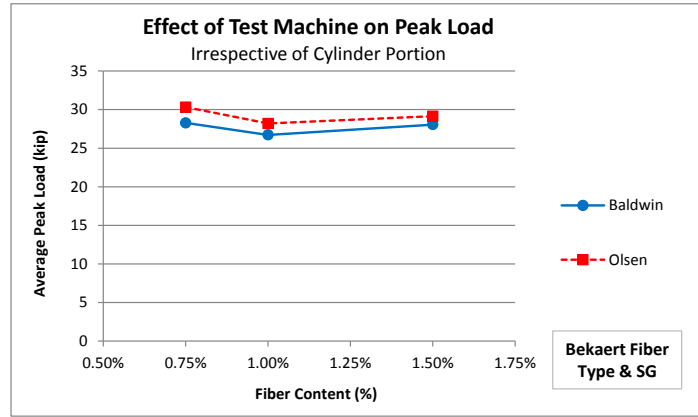
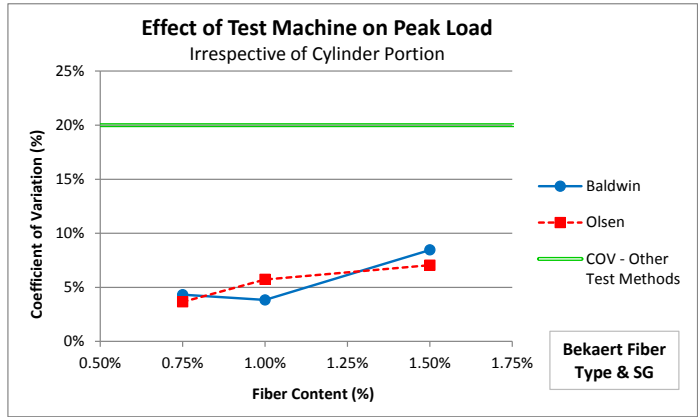
Analysis #16	Baldwin			Olsen		
	0.75%	1.00%	1.50%	0.75%	1.00%	1.50%
Test Criteria Peak Load Bekaert-Top & Bot-SG	30	25	26	31	27	30
	28	26	28	30	26	26
	28	27	25	31	29	28
	27	27	26	32	28	27
	28	27	25	30	29	30
	26	27	31	28	30	29
	30	28	31	29	29	30
	29	26	30	31	30	31
	30	28	29	31	26	29
	28	26	29	31	28	33
Mean	28	27	28	30	28	29
Std. Deviation	1.2	1.0	2.4	1.1	1.6	2.1
COV	4.3%	3.8%	8.5%	3.7%	5.7%	7.0%

<sup>1</sup> See Note B-1.

**PHASE 1  
ROYAL FIBERS**



**PHASE 2  
BEKAERT FIBERS**



**COEFFICIENT OF VARIATION**

**AVERAGE PERFORMANCE**

*Figure B-8: Effect of Test Machine on the Coefficient of Variation and Average Value of Peak Load*



*Table B-9: Analyzing the Effects of Test Machine on the Residual Strength*

**Analysis #17**

**Baldwin Machine vs. Olsen Machine**

Test Criteria

Residual Strength

Constants

Royal Fibers, Surface Grinded

Variable

Test Machine, Portion of Cylinder

Analysis #17	Baldwin			Olsen		
	0.75%	1.00%	1.50%	0.75%	1.00%	1.50%
Test Criteria Residual Strength Royal-Top & Bot-SG	7	7	6	4	5	10
	5	9	7	4	6	9
	5	8	13	6	5	15
	8	6	14	6	8	19
	6	10	15	7	8	12
Mean	6	8	11	6	6	13
Std. Deviation	1.3	1.7	4.1	1.3	1.4	4.0
COV	20.2%	20.8%	37.0%	23.1%	21.8%	30.9%

**Analysis #18**

**Baldwin Machine vs. Olsen Machine**

Test Criteria

Residual Strength

Constants

Bekaert Fibers, Surface Grinded

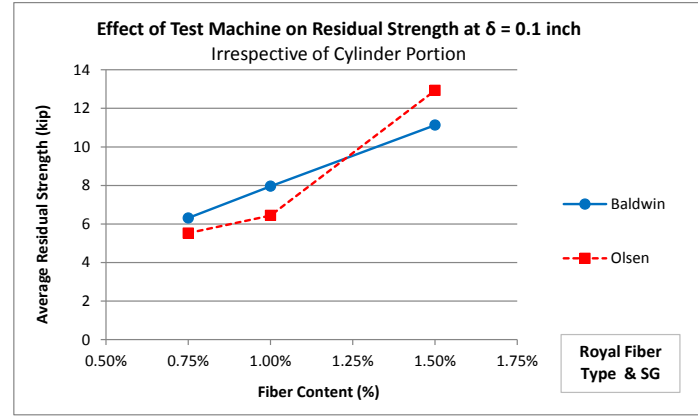
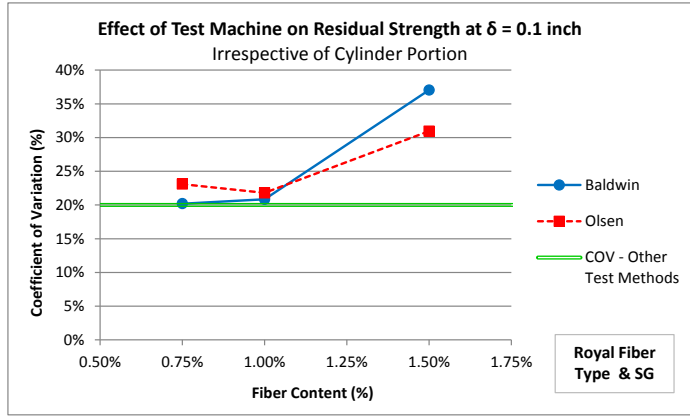
Variable

Test Machine, Portion of Cylinder

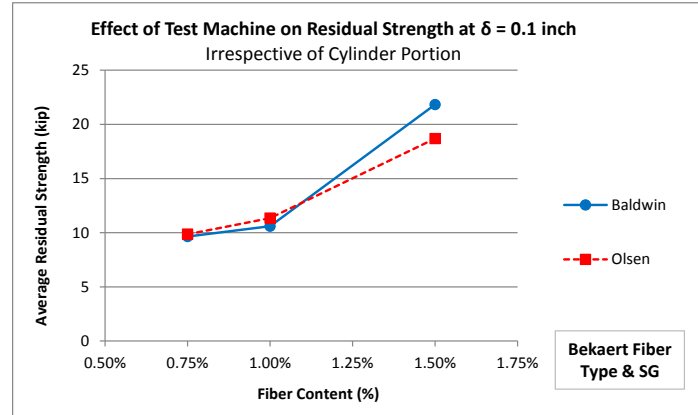
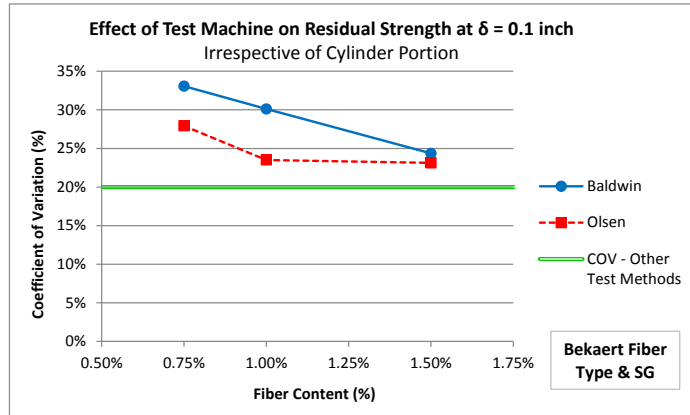
Analysis #18	Baldwin			Olsen		
	0.75%	1.00%	1.50%	0.75%	1.00%	1.50%
Test Criteria Residual Strength Bekaert-Top & Bot-SG	10	7	18	8	7	23
	9	7	23	7	9	16
	6	10	13	5	10	17
	8	9	20	9	9	22
	6	8	19	13	13	23
	8	8	31	11	14	11
	14	15	26	11	14	15
	10	13	28	13	11	19
	16	16	19	13	14	17
	10	12	20	9	13	24
	Mean	10	11	22	10	11
Std. Deviation	3.2	3.2	5.3	2.8	2.7	4.3
COV	33.1%	30.1%	24.4%	27.9%	23.5%	23.1%

<sup>1</sup> See Note B-1.

**PHASE 1  
ROYAL FIBERS**



**PHASE 2  
BEKAERT FIBERS**



**COEFFICIENT OF VARIATION**

**AVERAGE PERFORMANCE**

*Figure B-9: Effect of Test Machine on the Coefficient of Variation and Average Value of Residual Strength*

#### **B.4 ANALYZING THE EFFECTS OF CYLINDER PORTION (CASTING)**

The following analyses were conducted to analyze the effects of the cylinder portion (or casting) on the initial slope, peak load, and residual strength at 0.1 in. deflection, respectively:

*Table B-10: Analyzing the Effects of Cylinder Portion (Casting) on the Initial Slope*

**Analysis #19**

**Bekaert vs. Royal**

Test Criteria

*Initial Slope*

Constants

*Top Portion, Surface Grinded, Baldwin Machine*

Variable

*Fiber Manufacturer & Type*

Analysis #19	Bekaert			Royal		
	0.75%	1.00%	1.50%	0.75%	1.00%	1.50%
Test Criteria Initial Slope Top-SG-BAL	657	667	681	522	600	516
	660	637	593	604	679	634
	590	604	654	612	693	669
	620	640	622			
	597	641	648			
	586	668	618			
Mean	619	643	636	579	657	606
Std. Deviation	33.4	23.6	31.4	49.8	50.2	79.9
COV	5.4%	3.7%	4.9%	8.6%	7.6%	13.2%

**Analysis #20**

**Bekaert vs. Royal**

Test Criteria

*Initial Slope*

Constants

*Bottom Portion, Surface Grinded, Baldwin Machine*

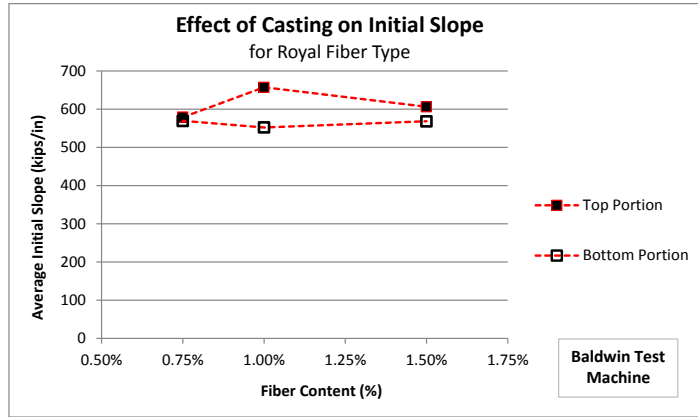
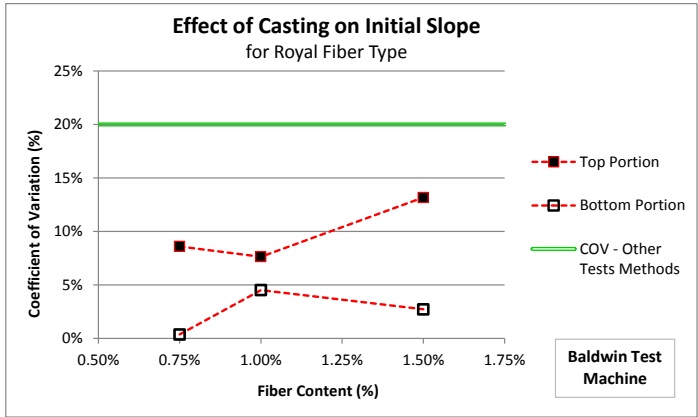
Variable

*Fiber Manufacturer & Type*

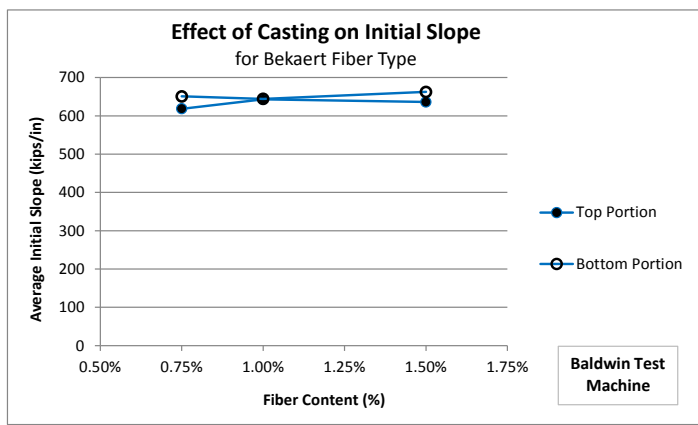
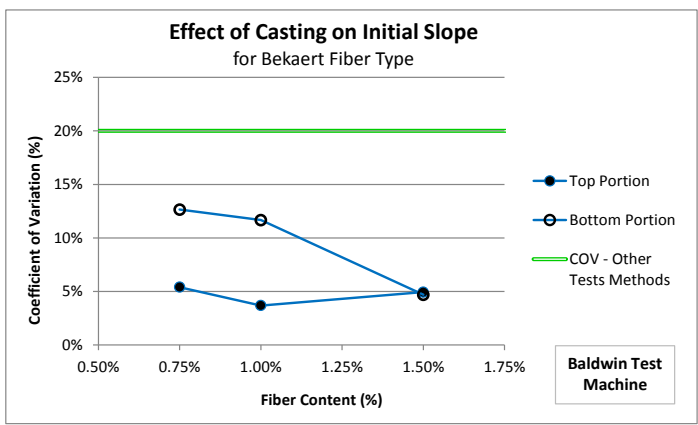
Analysis #20	Bekaert			Royal		
	0.75%	1.00%	1.50%	0.75%	1.00%	1.50%
Test Criteria Initial Slope Bot-SG-BAL	582	655	625	571	570	558
	629	536	693	568	535	579
	771	707	651			
	622	679	682			
Mean	651	644	662	570	552	569
Std. Deviation	82.3	75.2	31.1	2.1	24.9	15.4
COV	12.6%	11.7%	4.7%	0.4%	4.5%	2.7%

<sup>1</sup> See Note B-1.

**PHASE 1  
ROYAL FIBERS**



**PHASE 2  
BEKAERT FIBERS**



**COEFFICIENT OF VARIATION**

**AVERAGE PERFORMANCE**

*Figure B-10: Effect of Cylinder Portion (Casting) on the Coefficient of Variation and Average Value of Initial Slope*

*Table B-11: Analyzing the Effects of Cylinder Portion (Casting) on the Peak Load*

**Analysis #21**

**Bekaert vs. Royal**

Test Criteria

Peak Load

Constants

Top Portion, Surface Grinded, Baldwin Machine

Variable

Fiber Manufacturer & Type

Analysis #21	Bekaert			Royal		
	0.75%	1.00%	1.50%	0.75%	1.00%	1.50%
Test Criteria Peak Load Top-SG-BAL	27	27	26	28	33	30
	28	27	25	28	32	29
	26	27	31	29	30	32
	30	25	26			
	28	26	28			
	28	27	25			
Mean	28	27	27	29	32	30
Std. Deviation	1.1	0.9	2.5	0.3	1.3	1.1
COV	4.1%	3.3%	9.2%	1.1%	4.2%	3.8%

**Analysis #22**

**Bekaert vs. Royal**

Test Criteria

Peak Load

Constants

Bottom Portion, Surface Grinded, Baldwin Machine

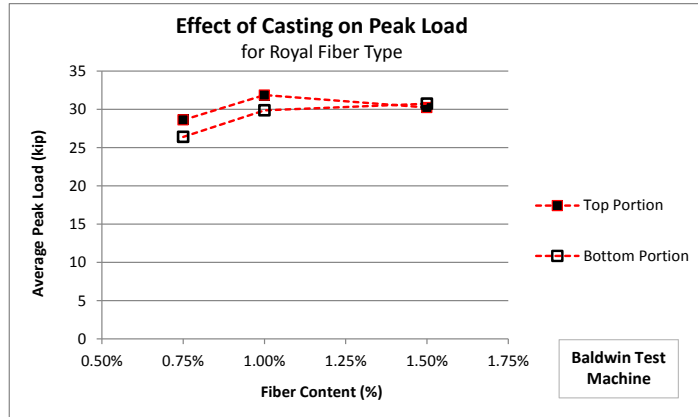
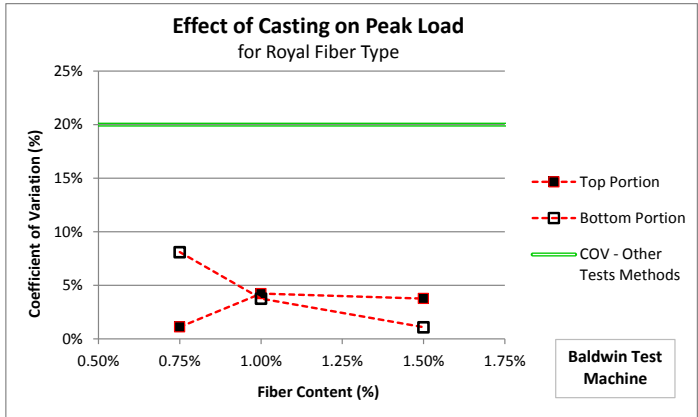
Variable

Fiber Manufacturer & Type

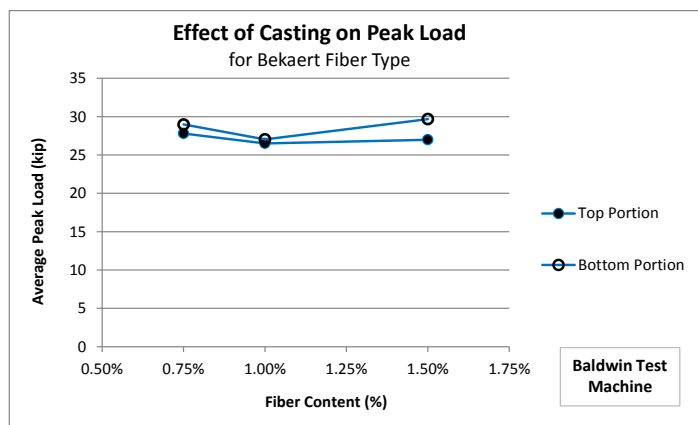
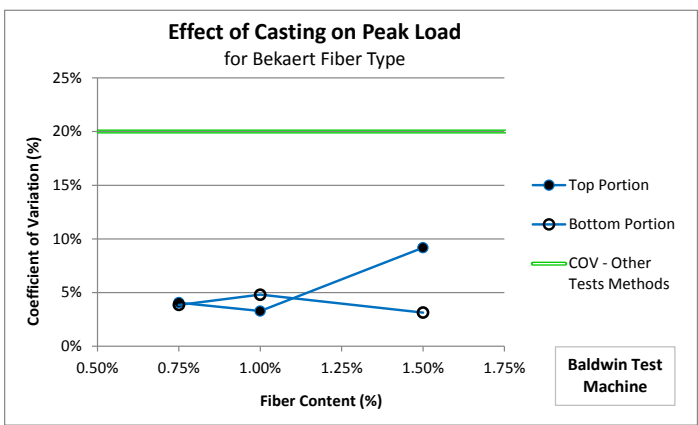
Analysis #22	Bekaert			Royal		
	0.75%	1.00%	1.50%	0.75%	1.00%	1.50%
Test Criteria Peak Load Bot-SG-BAL	30	28	29	28	29	31
	28	26	29	25	31	31
	30	28	31			
	29	26	30			
Mean	29	27	30	26	30	31
Std. Deviation	1.1	1.3	0.9	2.1	1.1	0.3
COV	3.8%	4.8%	3.1%	8.1%	3.7%	1.1%

<sup>1</sup> See Note B-1.

**PHASE 1  
ROYAL FIBERS**



**PHASE 2  
BEKAERT FIBERS**



**COEFFICIENT OF VARIATION**

**AVERAGE PERFORMANCE**

*Figure B-11: Effect of Cylinder Portion (Casting) on the Coefficient of Variation and Average Value of Peak Load*

*Table B-12: Analyzing the Effects of Cylinder Portion (Casting) on the Residual Strength*

**Analysis #23**

**Bekaert vs. Royal**

Test Criteria

*Residual Strength*

Constants

*Top Portion, Surface Grinded, Baldwin Machine*

Variable

*Fiber Manufacturer & Type*

Analysis #23	Bekaert			Royal		
	0.75%	1.00%	1.50%	0.75%	1.00%	1.50%
Test Criteria Residual Strength Top-SG-BAL	8	9	20	7	7	6
	6	8	19	5	9	7
	8	8	31	5	8	13
	10	7	18			
	9	7	23			
	6	10	13			
Mean	8	8	21	6	8	9
Std. Deviation	1.6	1.1	6.0	0.9	1.1	3.8
COV	21.2%	13.7%	28.7%	15.2%	13.8%	42.9%

**Analysis #24**

**Bekaert vs. Royal**

Test Criteria

*Residual Strength*

Constants

*Bottom Portion, Surface Grinded, Baldwin Machine*

Variable

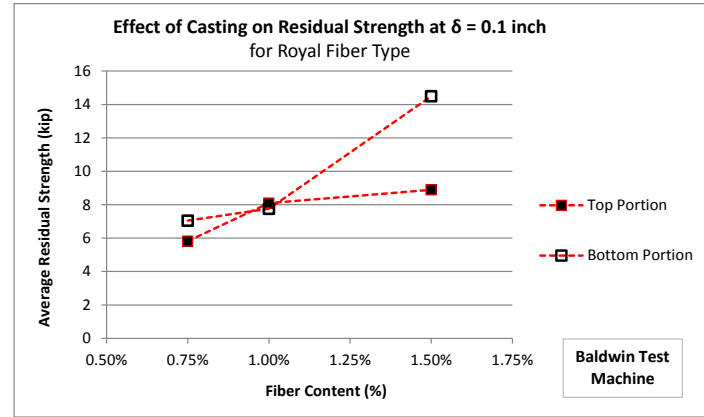
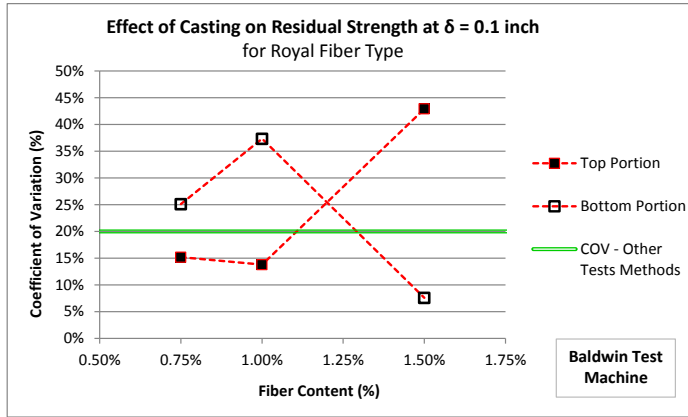
*Fiber Manufacturer & Type*

Analysis #24	Bekaert			Royal		
	0.75%	1.00%	1.50%	0.75%	1.00%	1.50%
Test Criteria Residual Strength Bot-SG-BAL	16	16	19	8	6	14
	10	12	20	6	10	15
	14	15	26			
	10	13	28			
Mean	12	14	23	7	8	14
Std. Deviation	2.9	1.8	4.5	1.8	2.9	1.1
COV	23.2%	12.9%	19.3%	25.1%	37.3%	7.6%

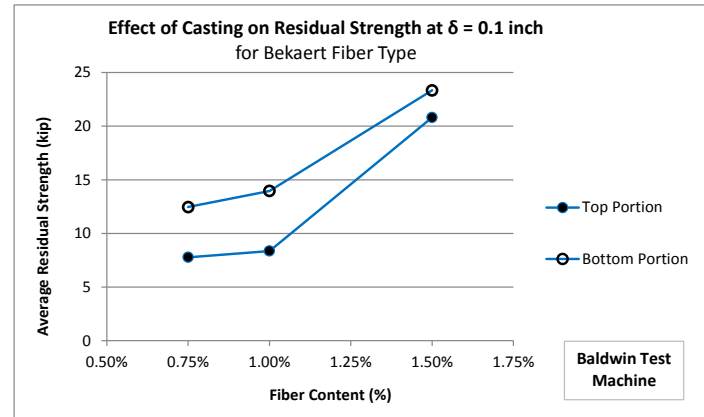
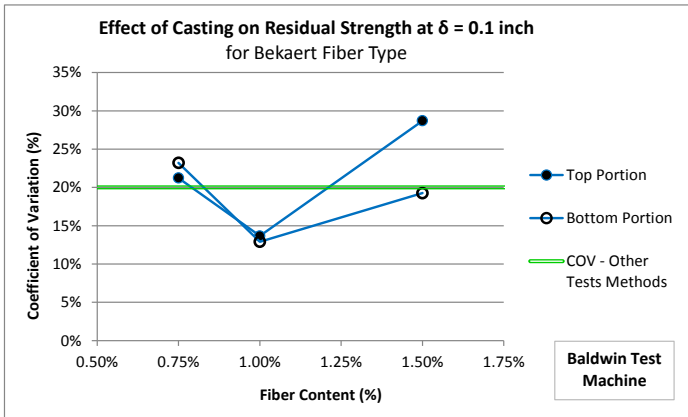
<sup>1</sup> See Note B-1.



**PHASE 1  
ROYAL FIBERS**



**PHASE 2  
BEKAERT FIBERS**



**COEFFICIENT OF VARIATION**

**AVERAGE PERFORMANCE**

*Figure B-12: Effect of Cylinder Portion (Casting) on the Coefficient of Variation and Average Value of Residual Strength*

## **APPENDIX C**

### **ASTM STANDARDIZATION OF DOUBLE-PUNCH TEST**

#### **C.1 ASTM STANDARDIZATION PROCESS**

The formal process of standardization requires that a proposed test method be submitted to the appropriate technical committee within an ANSI-accredited standardization organization such as ASTM. The test method, as approved by that organization, can then be widely cited, required, conducted, and reported. To that end, the following standard test ballot for the Double-Punch Test was drafted using the ASTM template.



C.2 ASTM DRAFT BALLOT FOR STANDARDIZATION OF DOUBLE-PUNCH TEST

1 **Standard Test Method for**  
2 **Evaluating the Performance of Fiber-Reinforced Concrete (Using**  
3 **Cylindrical Specimens with Double-Punch Loading)<sup>1</sup>**

4 This standard is issued under the fixed designation X XXXX; the number immediately following the  
5 designation indicates the year of original adoption or, in the case of revision, the year of last revision. A  
6 number in parentheses indicates the year of last reapproval. A superscript epsilon ( $\epsilon$ ) indicates an editorial  
7 change since the last revision or reapproval.

8  
9 **1. Scope**

10 1.1 This test method can be applied to plain concrete or fiber-reinforced concrete (FRC)  
11 cylindrical specimens, such as molded cylinders and drilled cores.

12 1.2 This test method covers the determination of the ultimate tensile strength and residual  
13 capacity (toughness) up to a specified deflection. In this test, commonly referred to as the  
14 “Double-Punch Test (DPT),” a concrete cylinder is placed vertically between the loading platens  
15 of a universal test machine and compressed by two steel punches located concentrically on the  
16 top and bottom surfaces of the cylinder. The applied compression results in uniformly  
17 distributed, indirect tension along radial planes of the cylindrical specimen. The performance of  
18 specimens tested by this method is quantified in terms of the initial stiffness, peak load, and  
19 residual strength at a specified deflection.

20 *1.3 The values stated in either SI units or inch-pound units are to be regarded separately as*  
21 *standard. The values stated in each system may not be exact equivalents; therefore, each system*  
22 *shall be used independently of the other. Combining values from the two systems may result in*  
23 *non-conformance with the standard.*

---

<sup>1</sup> This test method is under the jurisdiction of ASTM Committee and is the direct responsibility of Subcommittee.  
Current edition approved XXX. XX, XXXX. Published XX XXXX. DOI:10.1520/XXXXX-XX

24 1.4 *This standard does not purport to address all of the safety concerns, if any, associated*  
25 *with its use. It is the responsibility of the user of this standard to establish appropriate safety and*  
26 *health practices and determine the applicability of regulatory limitations prior to use.*

## 27 **2. Referenced Documents**

### 28 2.1 *ASTM Standards:*

29 **C31/C31M Practice for Making and Curing Concrete Test Specimens in the Field**

30 **C39/C39M Test Method for Compressive Strength of Cylindrical Concrete Specimens**

31 **C42/C42M Test Method for Obtaining and Testing Drilled Cores and Sawed Beams of**  
32 **Concrete**

33 **C172 Practice for Sampling Freshly Mixed Concrete**

34 **C192/C192M Practice for Making and Curing Concrete Test Specimens in the Laboratory**

35 **C496/C496M Test Method for Splitting Tensile Strength of Cylindrical Concrete Specimens**

36 **C823 Practice for Examination and Sampling of Hardened Concrete in Constructions**

37 **C1609/C1609M Test Method for Flexural Performance of Fiber-Reinforced Concrete (Using**  
38 **Beam with Third-Point Loading)**

39 **C1399/C1399M Test Method for Obtaining Average Residual-Strength of Fiber-Reinforced**  
40 **Concrete**

## 41 **3. Terminology**

42 3.1 *Definitions:* This test method has no definitions unique to this standard.

## 43 **4. Summary of Test Method**

44 4.1 This test method consists of loading molded cylinders or cores, at a rate that is within a  
45 prescribed range, through cylindrical steel punches at each end, until a prescribed deflection is  
46 reached. Test results are the initial stiffness of the specimen, its maximum strength, and its  
47 residual strength at a deflection of 0.1 in. (2.5 mm).

## 48 **5. Significance and Use**

49 5.1 The test provides the entire load-deflection curve, before and after cracking, for a  
50 concrete or fiber-reinforced concrete cylinder specimen loaded axially through cylindrical steel  
51 punches at each end. Key parameters (initial stiffness, peak load, and residual strength at 0.1 in.

52 [2.5 mm] deflection) are obtained from the load-deflection curve, and are useful for evaluating  
53 the elastic and plastic behavior of FRC with different fiber types and volume fractions (% fiber  
54 content). The test is particularly appropriate for comparing the behavior of concrete reinforced  
55 with high-performance steel fibers.

56 5.2 The motivation for using the “Double-Punch Test (DPT)” setup is based on the within-  
57 batch, intra-laboratory repeatability and consistency of the failure mode that arises through the  
58 use of steel punches.<sup>2</sup>

## 59 **6. Apparatus**

60 6.1 *Testing Machine* -- The testing machine shall meet the requirements of Sections 5.1  
61 through 5.4 of Specification C 39.

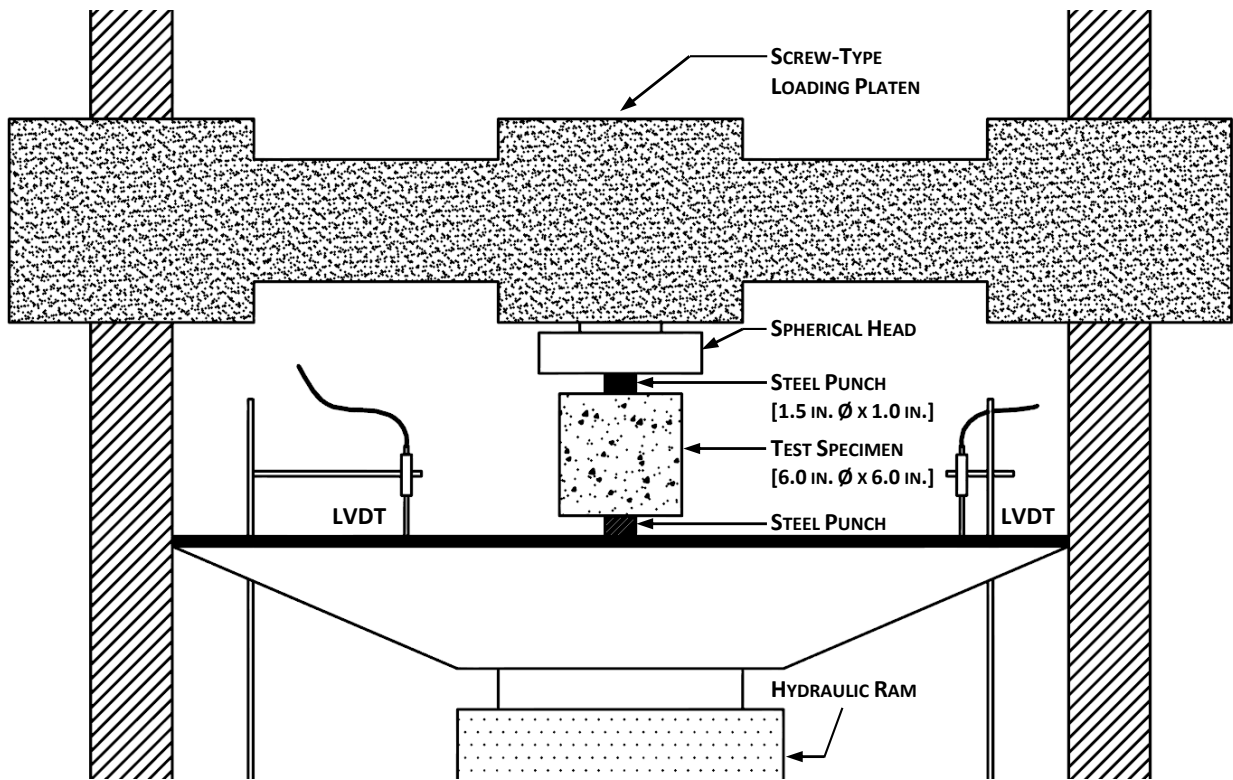
62 6.2 *Steel Punches* -- The steel punches shall be cylindrical in shape, with a diameter of 1.5  
63 in. (38 mm)  $\pm$  0.1 in. ( $\pm$ 2.5 mm) and a height of 1.0 in. (25 mm)  $\pm$  0.1 in. ( $\pm$ 2.5 mm). The  
64 punches shall be cut from tool steel with a yield strength between 75 ksi [517 MPa] and 90 ksi  
65 [620 MPa].

66 6.3 *Instrumentation for Measuring Deflections* -- Measure the deflection of the loading head  
67 using a dial indicator or linear potentiometer with a range of at least 1 in. (25 mm) and a  
68 precision of at least 1% of that range.

69  
70  
71  
72  
73  
74  
75  
76  
77  
78

79 <sup>2</sup> Woods, A.P. “Double-Punch Test for Evaluating the Performance of Steel Fiber-Reinforced Concrete.” MS Thesis,  
80 Department of Civil Engineering, University of Texas at Austin, 2012.

81



82

83

*Figure 6-1: Schematic of Double-Punch Test Arrangement*

84 **7. Specimens**

85 7.1 Specimens shall be prepared by cutting molded concrete cylinders having a nominal  
 86 diameter of 6 in. (150 mm) and a nominal height of 12 in. (300 mm), into two cylinders, each  
 87 having a nominal diameter of 6 in. (150 mm) and a nominal height of 6 in. (150 mm).

88 7.2 The top or bottom 6 x 6 in. portion can be used for testing. However, specimens obtained  
 89 from the bottom portion have a greater fiber density than those from the top portion, due to  
 90 segregation during casting. Thus, top and bottom specimens should not be compared directly.

91 7.3 Specimen surfaces shall be smoothed so that the steel punches make uniform (flat)  
 92 contact with the top and bottom faces of the specimen. Smooth contact surfaces can be obtained  
 93 by grinding the ends of the cylinder using a milling machine, or by applying a thin layer of  
 94 Hydro-Stone to the rough concrete at the location of the steel punches. End grinding is preferred;

95 however, Hydro-Stone application is acceptable should grinding equipment be unavailable.  
96 Results obtained from specimens with different surface finishes should not be compared directly.

## 97 **8. Procedure**

98 8.1 Using masking tape, affix steel punches concentrically to the top and bottom of the  
99 specimen. To avoid eccentricity of load, the centroid of each steel punch should align with the  
100 centroid of the cylinder surface within  $\pm 0.1$  in. [ $\pm 2.5$  mm]. A plywood dimensional guide may  
101 be used to help ensure this.

102 8.2 Place the specimen concentrically in the testing machine.

103 8.3 Load the specimen using the following sequence:

104 8.3.1 *Shakedown (Initial Loading and Unloading to Seat Punches)* -- Load the specimen at a  
105 rate of 100 lb/sec (445 N/sec)  $\pm$  25 lb/sec ( $\pm$  111 N/sec) up to a load of 10 kips (44.5 kN).  
106 Unload the specimen at a rate between 100 and 300 lb/sec (445 and 1334 N/sec) to a load  
107 between 100 lb (445 N) and 200 lb (890 N). The deflection at that final load is termed the  
108 “initial deflection offset.”

109 8.3.2 *Reloading* -- Load the specimen at a rate of 100 lb/sec (445 N/sec)  $\pm$  25 lb/sec ( $\pm$  111  
110 N/sec). Note the corresponding rate of applied deflection. Load at that deflection rate until the  
111 first radial crack appears in the top or bottom face of the specimen. Continue loading at a rate  
112 between 1.0 and 3.0 times that deflection rate until the deflection reaches or exceeds 0.5 in. (13  
113 mm), or the steel punches are almost fully seated into the specimen. Do not permit the loading  
114 head of the testing machine to contact the specimen.

115 8.4 *Data Recording* -- Record the applied load and the deflection of the loading head at 1-  
116 second time intervals.

117 **9. Evaluation and Reporting of Results**

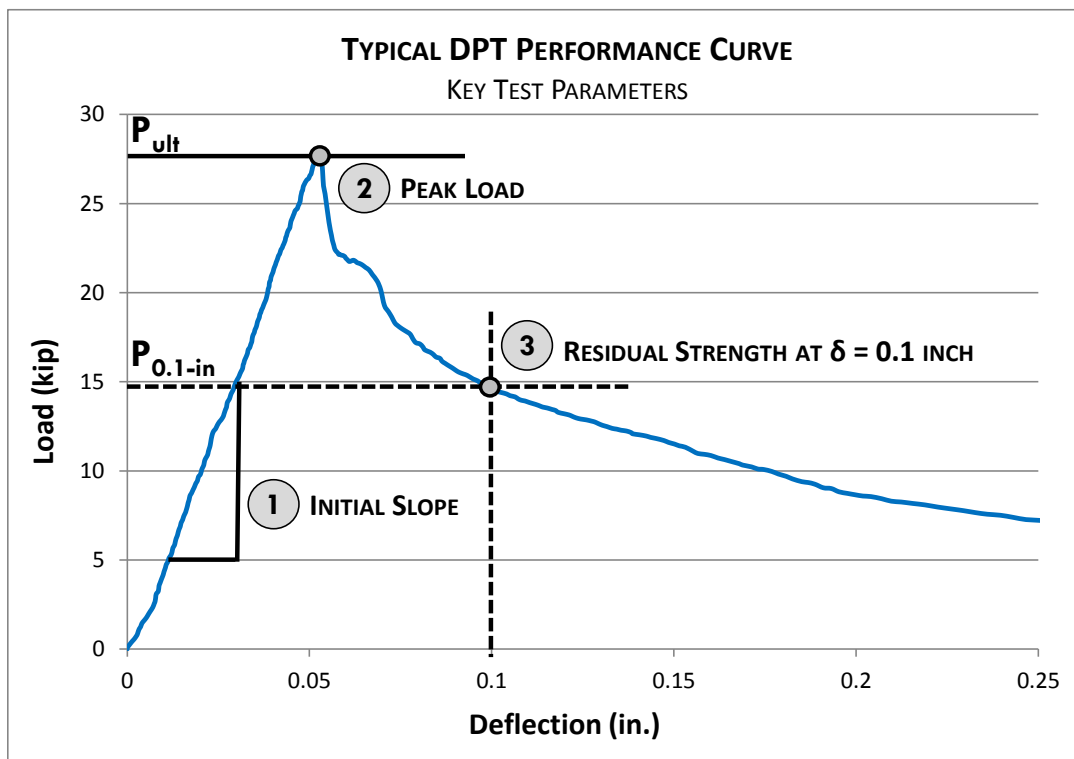
118 9.1 Subtract the initial deflection offset from each deflection reading during the reloading  
 119 phase. The resulting deflections are termed “corrected deflections.”

120 9.2 Using the recorded loads and the corrected deflections, calculate and report the initial  
 121 slope, maximum load, and residual load, as follows:

122 9.2.1 Evaluate the initial slope as the slope between applied loads of approximately 5 kips  
 123 (22 kN) and 15 kips (67 kN).

124 9.2.2 Evaluate the maximum load directly.

125 9.2.3 Evaluate the residual load at a corrected deflection of 0.1 in.  $\pm 0.01$  in. (2.5 mm  $\pm$  0.025  
 126 mm).



127

128 *Figure 9-1: Typical Double-Punch Test (DPT) Load-Deflection Plot*  
 129 *(Performance Curve) showing Key Test Parameters*

130



131 **10. Precision and Bias**

132 10.1 Because the specific testing protocol of this standard is relatively new, an inter-  
133 laboratory study of this test method has not been performed to quantify its precision and bias.  
134 Available research data, however, suggests that the within-batch, intra-laboratory coefficients of  
135 variation for key test parameters is generally low and comparable to other current test methods  
136 for FRC:  $\pm 10\%$  Initial Slope;  $\pm 5\%$  Peak Load; and  $\pm 20\%$  Residual Strength at 0.1 in.  
137 deflection.<sup>2</sup> A precision and bias statement will be prepared as more data becomes available.

138 **11. Keywords**

139 11.1 double-punch test; cylindrical concrete specimens; fiber-reinforced concrete; peak  
140 tensile strength; residual strength; toughness

141

142 <sup>2</sup> Woods, A.P. "Double-Punch Test for Evaluating the Performance of Steel Fiber-Reinforced Concrete." MS Thesis,  
143 Department of Civil Engineering, University of Texas at Austin, 2012.

## REFERENCES

- ACI. *Building Code Requirements for Structural Concrete (ACI 318-08) and Commentary*. Farmington Hills, MI: American Concrete Institute, 2011.
- ASTM C1399. *Standard Test Method for Obtaining Average Residual-Strength of Fiber-Reinforced Concrete*. American Society of Testing and Materials, 2010.
- ASTM C1550. *Standard Test Method for Flexural Toughness of Fiber Reinforced Concrete (Using Centrally Loaded Round Panel)*. American Society of Testing and Materials, 2010.
- ASTM C1609. *Standard Test Method for Flexural Performance of Fiber-Reinforced Concrete (Using Beam with Third-Point Loading)*. American Society of Testing and Materials, 2010.
- ASTM C496. *Standard Test Method for Splitting Tensile Strength of Cylindrical Concrete Specimens*. American Society of Testing and Materials, 2011.
- Azimov, Umid. *Controlling Cracking in Precast Concrete Panels*. MS Thesis, Austin, TX: University of Texas at Austin, 2012.
- Banthia, N., and A. Dubey. "Measurement of Flexural Toughness of Fiber Reinforced Concrete Using a Novel Technique, Part I: Assessment and Calibration." *Materials Journal* (American Concrete Institute), 1999: 651-656.
- Bentur, A., and S. Mindess. "Cracking Process in Steel Fiber Reinforced Cement Paste." *Cement Concrete Research* 15 (1985): 331-342.
- Bentur, A., and S. Mindess. *Fibre Reinforced Cementitious Composites*. 2nd. New York, NY: Taylor & Francis, 2007.
- Bernard, E. S. "Correlations in the Behaviour of Fibre Reinforced Shotcrete Beam and Panel Specimens." *Materials and Structures (RILEM)* 35 (April 2002): 156-164.
- Bortolotti, Lionello. "Double-Punch Test for Tensile and Compressive Strengths in Concrete." *ACI Materials Journal* (American Concrete Institute), January-February 1988: 26-32.
- Callister, William D. *Materials Science and Engineering, An Introduction*. 6th. New York: John Wiley & Sons, 2003.
- Chao, Shih-Ho, interview by Aaron P. Woods. *Assistant Professor in Structural Engineering* (March 14, 2012).

- Chao, Shih-Ho. *Evaluation of Mechanical Properties of Steel Fiber Reinforced Concrete for TxDOT Project 0-6368*. Progress Report, Department of Civil Engineering, Arlington, TX: University of Texas at Arlington, 2009.
- Chao, Shih-Ho. "FRC Performance Comparison: Uniaxial Direct Tensile Test, Third-Point Bending Test, and Round Panel Test." *ACI Special Publication 276: Durability Enhancements in Concrete with Fiber Reinforcement*, 2011: 5.1-5.20.
- Chao, Simon, interview by Aaron P. Woods. *Assistant Professor in Structural Engineering* (March 14, 2012).
- Chen, L., and S. Mindess. "Comparative Toughness Testing of Fiber Reinforced Concrete." *ACI SP-155* (American Concrete Institute), 1995: 45, 59.
- Chen, W.F. "Bearing Capacity of Concrete Blocks or Rock." *ASCE Proceedings*. American Society of Civil Engineers, 1969. 955-978.
- Chen, W.F. "Double Punch Test for Tensile Strength of Concrete." *ACI Journal* (American Concrete Institute), December 1970: 993-995.
- Cooke, Tony. "Formation of Films on Hatschek Machines." *Inorganic Bonded Wood and Fibre Composites*. 2002.
- Coskun, Hilmi. *Construction of SIMCON Retrofitted Reinforced Concrete Columns*. PhD Dissertation, North Carolina State University, 2002.
- De Vekey, R.C, and A.J. Majumdar. "Determining Bond Strength in Fiber Reinforced Composites." *Magazing of Concrete Research*, 1968: 229-234.
- EFNARC. *European Specification for Sprayed Concrete*. European Federation of National Associations of Specialist Representing Concrete, 1996.
- Folliard, K., C Smith, and J.E. Breen. *Evaluation of Alternative Materials to Control Drying Shrinkage in Concrete Bridge Decks*. TX-DOT Project 0-4098-4 Report, Texas Department of Transportation, 2003.
- Folliard, Kevin, and C. Smith. "Evaluation of Alternative Materials to Control Drying-Shrinkage Cracking in Concrete Bridge Decks." Technical Report, Texas Department of Transportation, Austin, TX, 2003, 44-45.
- Foreman, J. *Controlling Cracking in Prestressed Concrete Panels*. MS Thesis, Austin, TX: University of Texas at Austin, 2010.
- Foster, Stephen. *Reducing Top Mat Reinforcement in Bridge Decks*. MS Thesis, Austin, TX: The University of Texas at Austin , 2010.

- Frangky, Welly W. *How To Make Fiber Cement on Hatschek Machine*. 2010.  
<http://fibercementprocess.blogspot.com/2010/11/httpgreenmyplace.html> (accessed March 23, 2012).
- Gopalaratnam, and S.P. Shah. "Failure Mechanisms and Fracture of Fiber Reinforced Concrete." *American Concrete Institute SP105-1*, 1987: 2-11.
- Igarashi, S., and A. Bentur. "The Effect of Processing on the Bond and Interfaces in Steel Fiber Reinforced Concrete Composites." *Cement Concrete Composites* 18 (1996): 313-322.
- Johnston, C. D. "Deflection Measurement Considerations in Evaluating FRC Performance Using ASTM C1018." *ACI SP-155* (American Concrete Institute), 1995: 1-11.
- Krenchel, H. *Fibre Reinforcement*. Copenhagen: Akademick Forlag, 1964.
- Krstulovic, and LaFave. "Seismic Retrofit with Discontinuous Slurry Infiltrated Mat Concrete (SIMCON) Jackets." *ACI SP 185-2: High-Performance Fiber-Reinforced Concrete in Infrastructural Repair and Retrofit* (American Concrete Institute), 2000: 142-160.
- Lankard, D.R. "Slurry Infiltrated Fiber Concrete (SIFCON): Properties and Applications." *Very High Strength Cement-Based Materials*. Pittsburgh, PA: Materials Research Society, 1985. 277-286.
- Maage, M. "Fibre Bond and Friction in Cement and Concrete." In *Testing and Test Methods of Fibre Cement Composites*, by R.N. Swamy, 329-336. Lancaster: The Construction Press, 1978.
- Marti, Peter. "Size Effect in Double-Punch Tests on Concrete Cylinders." *ACI Materials Journal* (American Concrete Institute), November-December 1989: 597-601.
- Merrill, B.D. "Texas' Use of Precast Concrete Stay-In-Place Forms for Bridge Decks." *Concrete Bridge Conference*. Skokie, IL: National Concrete Bridge Council, 2002.
- Mindess, S., J. F. Young, and D. Darwin. *Concrete*. 2nd. Upper Saddle River: Prentice Hall, 2003.
- MKTJ. *The Great Ziggurat of Dur-Kurigalzu, Aqar-Quf*. May 15, 2009.  
<http://www.skyscrapercity.com/showthread.php?t=871190> (accessed March 15, 2012).
- Molins, C. "Quality Control Test for SFRC to be used in Precast Segments." *Tunneling and Underground Space Technology* 21, 2006: 423-424.
- Molins, Climent, and A. Aguado. "Double Punch Test to Control the Energy Dissipation in Tension of FRC (Barcelona Test)." *Materials and Structures*, 2009: 415-425.

- Naaman, A. E. "Measurement of Tensile Properties of Fiber Reinforced Concrete: Draft Submitted to ACI Committee 544." High Performance Fiber Reinforced Cement Composites (HPFRCC5), Mainz, Germany, 2007, 3-12.
- Naaman, A. E., and et al. "Measurement of Tensile Properties of Fiber Reinforced Concrete: Draft Submitted to ACI Committee 544." High Performance Fiber Reinforced Cement Composites (HPFRCC5), Mainz, Germany, 2007, 3-12.
- Naaman, A. "SIFCON: Tailored Properties for Structural Performance." *High Performance Fiber Reinforced Cement Composites*. London, UK: E & FN Spon, 1992. 18-38.
- Pros, Alba, Pedro Diez, and Climent Molins. "Numerical Modeling of the Double Punch Test for Plain Concrete." *Internation Journal of Solids and Structures*, November 2010: 1-32.
- Ramakrishnan, V. "Flexural Fatigue Strength of Steel Fiber Reinforced Concrete." *ACI-SP 105-13: Fiber Reinforced Concrete Properties and Applications* (American Concrete Institute), 1987: 225-245.
- Romualdi, J.P., and G. Batson. *Mechanics of Crack Arrest in Concrete*. Vol. 89. ASCE, J. Eng. Mech., 1963.
- Stroeven, P., and S.P. Shah. "Use of Radiography-Image Analysis for Steel Fibre Reinforced Concrete." In *Testing and Test Methods for Fibre Cement Composites*, by R.N. Swamy, 275-288. Lancaster, England: The Construction Press, 1978.
- Tepfers, R. *A Theory of Bond applied to Overlapped Tensile Reinforcement Splices for Deformed Bars*. Gotenborg, Sweden: Chalmers University of Technology, 1973.
- Wecharatana, M., and S.P. Shah. "A Model for Predicting Fracture Resistance of Fiber Reinforced Concrete." *Cement Concrete Research* 13 (1983): 819-829.
- Zondervan. *New Living Translation Study Bible*. Grand Rapids, MI: Zondervan, 2002.

## VITA

Aaron Paul Woods was born to Verdun and Vanessa Woods; He is the third eldest of seven children and has two older sisters (Angela and Danielle), two younger brothers (Joshua and Timothy), and two younger sisters (Amanda and Johanna). Although born in St. Louis, he grew up in Jacksonville, FL and graduated from Ridgeview High School in Orange Park in May 2004.

He began college at Jacksonville University (JU) on a football and academic scholarship, and played free-safety for the JU Dolphins while enrolled in a three-year, dual-degree physics and engineering program. In 2007, Aaron received his Bachelor of Science in Physics degree from JU with Cum Laude honors and transferred to the University of Florida (UF) to complete the civil engineering portion of the dual program. He graduated from UF with Summa Cum Laude honors and received his Bachelor of Science in Civil Engineering degree in December 2009. While in “The Swamp” he met his wife, Tania, and they married in April 2010.

In August 2010, Aaron enrolled in the civil engineering graduate program at the University of Texas at Austin and worked as a research assistant at the Phil M. Ferguson Structural Engineering Laboratory. In the first year of the program his wife gave birth to their first child, Elijah. In May 2012, Aaron graduated with a Master of Science in Civil Engineering and plans to continue working as a forensic structural engineer.

This thesis was typed by the author: Aaron P. Woods ([aaron.p.woods@gmail.com](mailto:aaron.p.woods@gmail.com))

Permanent address: 135 Ridgefield Ct.  
Orange Park, FL 32065